

Autoantibodies as biomarkers in autoimmune diseases

Inauguraldissertation

Zur

Erlangung der Würde eines Doktors der Philosophie
vorgelegt der Philosophisch-Naturwissenschaftlichen Fakultät
der Universität Basel
von

Giulio Macchiarella

2023

Originaldokument gespeichert auf dem Dokumentenserver der Universität Basel
edoc.unibas.ch

Genehmigt von der Philosophisch-Naturwissenschaftlichen Fakultät
auf Antrag von

Erstbetreuer: Dr. Alexandre Avrameas

Zweitbetreuer: Prof. Jean Pieters

Externer Experte: Prof. Davide F. Robbiani

Basel, 02-Mar-2021

Prof. Dr. Marcel Mayor

The Dean of Faculty

“It is better to be lucky.
But I would rather be exact.
Then when luck comes you are ready.”

*Ernest Hemingway,
The Old Man and The Sea*

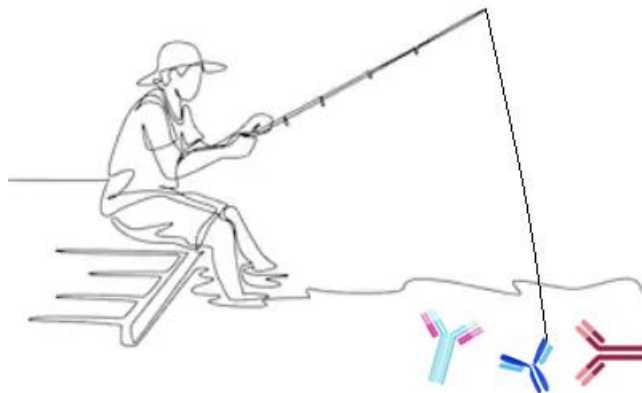


Image modified from Shutterstock.com

Abstract

The immune system plays a critical role in the homeostasis and protection of our body, but its dysregulation is often associated with the pathogenesis of autoimmune diseases. The cellular and molecular components of the immune system have been explored as therapeutic targets or biomarkers with the aim of curing autoimmunity. Although studied since decades, autoantibodies' use as biomarker in clinical trials is still limited to a handful of well-known markers. The aim of the thesis was to test autoantibody profiling as an exploratory tool to identify new biomarkers in the context of clinical trials conducted in three autoimmune diseases.

In the first part of the PhD, I tested a large set of autoantibodies on baseline serum samples from a phase III anti-IL17 clinical trial of Psoriatic Arthritis, with the aim of identifying a group of biomarkers that could discriminate between responders and non-responders to the treatment. Numerous autoantibodies of either IgG, IgM and IgA isotype were found more expressed in clinical non-responders when compared to responders. Such autoantibodies were directed against molecules related to IL17 pathway, a commensal bacterium (*Lachnospiraceae*) and antigens linked to Rheumatoid Arthritis. Overall, these markers allowed a discrimination of 40% of non-responders from responders population, which was judged as a too low sensitivity in order to start the development of a companion diagnostic. However, the technical knowledge acquired during this first project was fundamental for the rest of the PhD. In the second part of the PhD, I applied autoantibody profiling, using a targeted set of antigens, on serum samples from a phase II anti-IL17 treatment clinical trial of Hidradenitis Suppurativa (HS). The aim of this project was to demonstrate the presence of autoantibodies that could support the hypothesis of an autoimmune component of HS pathogenesis. We found IgG anti-Carboxyethyl-lysine (CEL) autoantibodies with specific high levels in HS when compared to healthy volunteers and other comorbidities such as Crohn's disease and Ulcerative Colitis. B-cells producing anti-CEL antibodies were detected in HS lesional skin as well. Sera with high levels of anti-CEL autoantibodies activated macrophages and complement pathway in presence of CEL-BSA. The majority of IgG anti-CEL antibodies was of IgG2 subclass and no cross-reactivity with similar molecules such as Carboxymethyl-lysine and Octopine was found. Overall, these results suggested a role for oxidative stress and advanced glycation events in the pathogenesis of HS. In the third part of the PhD, I detected anti-FcεR1a autoantibodies in serum from Chronic Spontaneous Urticaria (CSU) from a phase II clinical trial of anti-IgE treatment. It was hypothesized that patients expressing anti-FcεR1a autoantibodies may activate mast cells degranulation in an IgE-free manner, which would make them resistant to anti-IgE treatment. The results showed no correlation between the presence of anti-FcεR1a autoantibodies and clinical response to IgE treatment. The detection of the soluble form of FcεR1a (sFcεR1a) at different time-points throughout the treatment showed a dose-dependent decrease of sFcεR1a concentration, similarly to what already published for FcεR1a expression on basophils surface. The data showed in this thesis suggested that sFcεR1a might be a substitute mechanistic marker of cell-bound FcεR1a.

In conclusion, although autoantibody profiling did not allow identifying specific markers for anti-IL17 treatment response in PsA, the knowledge acquired during this project was critically important. Indeed, the same approach allowed the finding of anti-CEL autoantibodies abundance and specificity in HS and the testing of anti-FcεR1a autoantibodies and sFcεR1a in CSU, which gave new insights in these diseases. The results presented in this thesis show the potential and limitations of autoantibodies profiling when applied to clinical trials of autoimmune diseases.

Table of Contents

Abstract.....	2
Abbreviations list	6
Figures list	9
Tables list	9
Acknowledgement	10
Introduction	11
Immune system.....	11
Innate immunity.....	12
Adaptive immunity.....	12
Autoimmunity	24
Autoimmunity development.....	24
Autoimmunity prevention	29
Autoantibodies.....	31
Autoantibodies dualism: pathogenicity and immune system regulation.....	31
Natural Autoantibodies.....	32
Biomarkers	34
Biomarker’s definition.....	34
Clinical trials	35
Autoantibodies as biomarkers	38
Aim of the thesis	41
Autoantibodies profiling in an anti-IL17 clinical trial of Psoriatic Arthritis.....	41
Autoantibodies profiling in Hidradenitis Suppurativa	41
Anti-FcεR1a autoantibodies and sFcεR1a detection in Chronic Spontaneous Urticaria	42
Results part I: Autoantibodies profiling in an anti-IL17 clinical trial of PsA.....	43
Introduction	43
Results.....	48
Discussion.....	56
Results Part II: Manuscript Hidradenitis Suppurativa.....	62
Results part III: Autoantibodies and sFcεR1a in Chronic Urticaria	86
Introduction	86
Results.....	88
Discussion.....	92

Discussion.....	95
Methods.....	100
Bibliography	114
Curriculum Vitae Giulio Macchiarella	132

Abbreviations list

AD	Alzheimer Disease
AGEs	Advanced Glycation Events
AICD	Activation-Induced Cell Death
AID	Activation-Induced cytidine Deaminase
APC	Antigen Presenting Cell
AS	Ankylosing Spondylitis
BCR	B Cell Receptor
BM	Bone Marrow
BSA	Bovine Serum Albumin
CCP	Cyclic Citrullinated Peptides
CEL	Carboxyethyl-lysine
CML	Carboxymethyl-lysine
CSR	Class Switch Recombination
CSU	Chronic Spontaneous Urticaria
DCIS	Ductal Carcinoma In Situ
DMARD	Disease Modifying Antirheumatic Drug
EAE	Encephalomyelitis
FBS	Fetal Bovine Serum
GC	Germinal Center
H&E	Hematoxylin and Eosin
H1-AH	H1-Antihistamines
H2-AH	H2-Antihistamines
HAV	Hepatitis A Virus
HERVs	Human Endogenous Retroviruses
HLA	Human Leukocyte Antigen

HS	Hidradenitis Suppurativa
HSP	Heat Shock Protein
IFN- γ	Interferon γ
IgA	Immunoglobulin A
IgE	Immunoglobulin E
IgG	Immunoglobulin G
IgM	Immunoglobulin M
IL17	Interleukin 17
LTRA	Leukotriene Receptor Antagonist
MBC	Memory B Cell
MGO	Methylglyoxal
MHC	Major Histocompatibility Complex
MS	Multiple Sclerosis
MTX	Methotrexate
MZ	Marginal Zone
NAAs	Natural AutoAntibodies
NETs	Neutrophils Extracellular Traps
NO	Nitric Oxide
NSAIDS	Non-Steroidal Anti-Inflammatory Drugs
PAMPs	Pathogen Associated Molecular Patterns
PBS	Phosphate Buffered Saline
PBS T	Phosphate Buffered Saline Tween20
PC	Plasma Cell
PD	Parkinson Disease
PsA	Psoriatic Arthritis
RA	Rheumatoid Arthritis

RF	Rheumatoid factor
SHM	Somatic Hyper Mutation
SLE	Systemic Lupus Erythematosus
SS	Sjögren Syndrome
SSc	Systemic Sclerosis
TAAAs	Tumor Associated Antigens
TBS	Tris Buffered Saline
TBS T	Tris Buffer Saline Tween20
Tc	Cytotoxic T cell
TCR	T Cell Receptor
Th	T helper cell
TLR	Toll-Like Receptor
TNFa	Tumor Necrosis Factor alpha

Figures list

Figure 1:	11
Figure 2:	13
Figure 3:	16
Figure 4:	17
Figure 5:	19
Figure 6:	20
Figure 7:	22
Figure 8:	23
Figure 9:	27
Figure 10:	29
Figure 11:	37
Figure 12:	45
Figure 13:	47
Figure 14:	49
Figure 15:	50
Figure 16:	53
Figure 17:	54
Figure 18:	55
Figure 19:	87
Figure 20:	88
Figure 21:	89
Figure 22:	90
Figure 23:	91
Figure 24:	92

Tables list

Table 1:	46
Table 2:	51
Table 3:	52
Table 4:	113

Acknowledgement

First of all, I would like to thank my mentor and manager Alexandre Avrameas, to whom I own a debt for all the trust he put in me and the knowledge I acquired during those years working together. Working with you was an honor and I hope that you will continue finding new biomarkers.

I would like to thank Jean Pieters for accepting to be my academic supervisor and helping me in continuing my PhD. Thanks for your kindness and professionalism. I would also like to thank Sai Reddy for accepting to be a member of the committee and for his precious comments and advices throughout the PhD. A lot of my gratitude goes to Roxane Tussiwand, grazie mille for your help and for your enthusiastic support and guidance during my PhD. Another grazie mille to Davide Robbiani for accepting to be the external referee for my thesis. A big thank must also go to the late Antonius Rolink, who sadly passed away, as he was the first one to see the potential of this PhD project and agreed to take me as PhD student.

I would also like to thank my colleagues at Novartis, that helped me directly or indirectly during my years in this company. Thank you Anita for being a great mentor and solving most of my technical doubts. Thank you Stephane and Thierry for helping me with MS, you also taught me a lot. Thank you to Stephanie, Ines, H el ene, Agnieszka, Marie-Anne and Julie for being great colleagues. A big thank to Alessandra and Scott for allowing me to work in MCS and BMD. I hope that my results can contribute to the success of the department.

I would also like to thank the people that I collaborated with during my projects, hoping not to forget anyone. Thanks to Reinhold, Christoph, Till, Christian and Bruno for your collaboration. It was truly an honor to work with great professionals like you and I learned a lot from all of you. A big thank to Vanessa, Elisabetta, Ben, Joachim and Genevieve for collaborating and producing such nice results with HS.

I would like to thank all of my friends at Novartis, who made those years unforgettable. From the PhD students group, to the football team, I made many dear friends.

A big grazie to my family, for always being there even though they were far away and for reminding me where my roots are.

Last but not least I would like to thank my Scompiez for being by my side in the bad and good times, making the bad times less sad and the good times happier.

Introduction

Immune system

The immune system is classically considered as a complex and fundamental defensive structure whose role is to constantly shield the host from aggressions by external pathogens, such as virus, bacteria, fungi and parasites. The different components of the immune system are able to recognize those entities through the targeting of specific structures or stimuli and react with the goal of neutralizing the aggression. The immune system strategies put in place to deal with pathogens are generally grouped in two categories: innate and adaptive response. These two components of the immune system present different approaches to protect the body from microbial aggressions, and interact with each other to optimize the immune response (Figure 1).

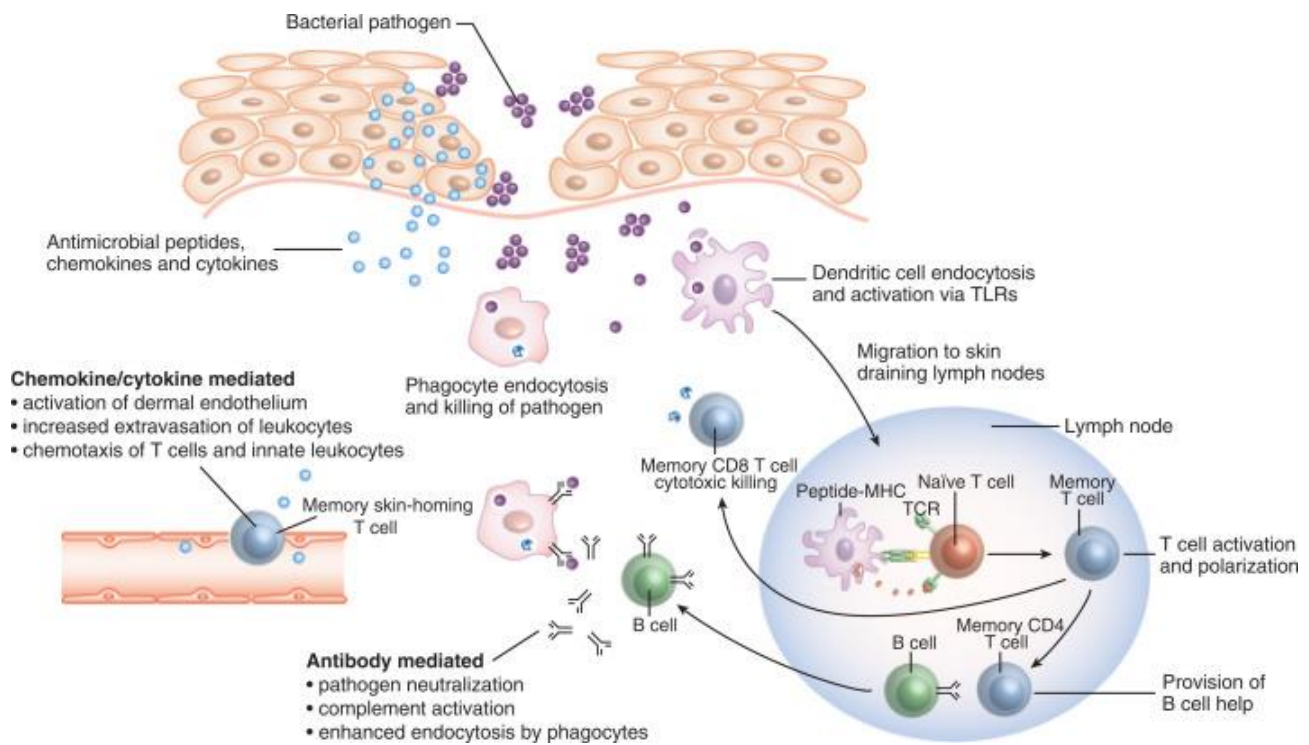


Figure 1:

Interactions between the innate and acquired immune systems in response to bacterial infection of the skin. In response to bacteria that have breached the epithelial barrier, keratinocytes synthesize anti-microbial peptides, chemokines, and cytokines. These factors lead to activation of the dermal endothelium, inducing the migration of innate leukocytes and memory T cells into the skin and additionally guiding these cells via chemotactic gradients. These factors and bacterial antigens activate innate phagocytes to kill ingested organisms and activate dendritic cells to migrate to the skin-homing lymph nodes. In the lymph nodes, dendritic cells present bacterial antigens to naïve and central memory T cells, leading to stimulation of pathogen-specific cells. Effector CD8 cells exit the lymph node, home to inflamed skin and kill pathogens. Helper CD4 T cells provide help to B cells, inducing the production of antibodies that directly neutralize pathogens and lead to additional targeting of innate responses. Antibody-directed phagocytosis by innate cells leads to enhanced antigen presentation, further enhancing acquired responses. Figure published by Clark et al, "Old meets new: the interaction between innate and adaptive immunity", J Invest Dermatol. 2005 [1].

Innate immunity

The innate immunity is based on the recognition of conserved molecular patterns that are targeted by a limited number of germline-encoded receptors present on specific immune cells types. These receptors evolved to recognize pathogen associated molecular patterns (PAMPs) such as proteins, DNA, lipids and carbohydrates produced by microbial pathogens, but not by the host. Recognition of these molecular structures allows the immune system to distinguish infectious non-self from non-infectious self and to neutralize pathogens [2]. The innate immune system has a variety of components: physical and anatomical barriers, cells (lysozyme, macrophages, neutrophils, mast cells, natural killer cells), pro-inflammatory proteins (such as C-reactive protein and lectins) and antimicrobial peptides (defensins, cathelicidin) [3]. From an evolutionary point of view, the innate immunity is an ancient mechanism that is present in most multicellular organisms, from plants to insects and mammals [4, 5]. Its role is to be the first barrier against unwelcomed microbes and parasites, and to use its components to rapidly react to and neutralize pathogens infections.

Adaptive immunity

The purpose of adaptive immunity is to react to microbial aggressions that bypassed innate immunity. This is achieved by detecting the microbes and instruct the immune cells from the innate immunity to recognize and attack the new targets. Therefore, the main role of adaptive immunity is to continuously screen for potential foreign antigens and produce the molecular tools to specifically target and regulate or suppress the corresponding pathogenic activities. Adaptive immunity is based on numerous genetic and cellular processes that generate favorable somatic variants of antigen-binding receptors under evolutionary selection pressure by pathogens and other factors [6]. Adaptive immunity involves a tightly regulated interplay between antigen-presenting cells and T and B lymphocytes, which facilitate pathogen-specific immunologic effector pathways, generation of immunologic memory and regulation of host immune homeostasis [7]. T and B lymphocytes action is carried on by their molecular products: cytokines and antibodies. Those proteins play a pivotal role in activating and directing cells from the innate immunity in order to suppress microbial infections. The main role of B lymphocytes is the production of immunoglobulins, also called antibodies, whose role is to bind to molecules recognized as non-self and activate innate immunity effectors cells like macrophages and mast cells through binding with specific receptors on the cells surface. The production of antibodies directed against a specific antigen requires an interaction between T and B lymphocytes that both recognized the antigen as non-self through their T cell receptor (TCR) and B cell receptor (BCR). This double recognition step is necessary for ensuring the targeting of foreign antigens and prevent cross-reacting against molecules from the body. Cytokines are regulatory proteins with pro-inflammatory or inhibiting properties, whose role is to modulate the activity and development of immune cells.

T-cells

The establishment and maintenance of immune responses, homeostasis, and memory depends on T cells. T cells express a receptor with the potential to recognize diverse antigens from pathogens, tumors and the

environment, while also maintaining immunological memory and self-tolerance [8, 9]. T cells roles are numerous, with specialized subsets that deal with specific tasks. T cells are usually classified in two groups, depending on the expression of CD4 or CD8 on their surface. Each group is further divided in different T cells subsets, particularly for CD4+: T-helper (Th)1, Th2, Th9, Th17, Th22, and CD4+ regulatory T cells; for CD8+ T: cytotoxic T lymphocyte (Tc)1, Tc2, Tc9, Tc17, and CD8+ regulatory T cells [10]. T lymphocytes originate from hematopoietic cells that migrate from the bone marrow to the thymus, where they go through different development phases (Figure 2). T cells differentiation steps are typically defined based on the cell-surface expression of CD4 and CD8, with thymocytes first starting as CD4–CD8– double negative (DN), then becoming CD4+CD8+ double positive (DP), and lastly maturing into single-positive (SP) CD4+ or CD8+ T cells [11]. This last maturation step happens after positive and negative selection of T cells. The purpose of the positive selection is to guarantee that only T-cells whose TCR can bind to the Major Histocompatibility Complex (MHC) are selected for further development [12]. The negative selection is performed in order to avoid TCR cross-reactivity with antigens from self [13].

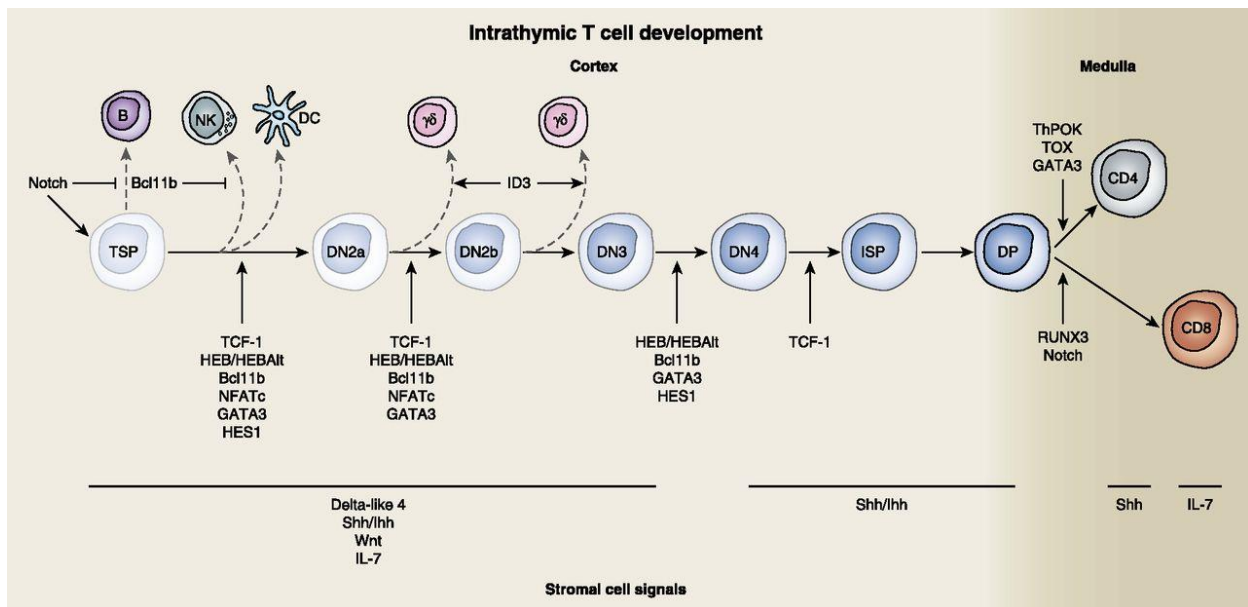


Figure 2:

Overview of thymocyte development, highlighting role of key transcription factors and signaling molecules at specific developmental points. The main stages of thymocyte development are depicted, with transcription factors marked with arrows and signals provided by thymic stromal cells, including receptor–ligand interactions, shown at the bottom (see text for details). Notch–Dl4 signaling is required for specification of TSPs to the T cell lineage and for instructing transcription factors to adopt and commit to the T cell pathway at specific stages during differentiation. Thymic epithelial signals, such as those from the Hh- (Shh and lhh), Wnt-, and IL-7–signaling pathways, aid in the commitment to the T cell lineage and continued proliferation and survival of developing thymocytes. Figure published by Shah et al, “An overview of the intrathymic intricacies of T cell development”, *J Immunol*, 2014 [14].

After maturation, T cells leave the thymus and become peripheral, starting their role as circulating immune cells. Peripheral T cells have a variety of roles and are divided in several categories, from naive T cells ready to bind new antigens and start immune reactions, to memory T cells that maintain long-term immune

response capacity after antigen activation, and regulatory T cells (Tregs) that modulate the magnitude of immune responses to different antigens [8]. Naive T cells are in a quiescent state, with their survival depending on the antiapoptotic signaling of IL7 and tonic signals from TCR low affinity bindings with self-antigens, with CD4⁺ SP cells also needing IL2 and CD8⁺ SP needing IL2 and IL15 [15]. When a naive T cell binds to a peptide with high affinity through its TCR, it starts to rapidly clonally expand and develop effector capacities [16, 17]. Activated CD4⁺ SP T cells differentiate into distinct T helper subsets that produce lineage-specific cytokines. The most studied subsets are type 1 T helper (Th1) and type 2 T helper (Th2) cells that preferentially produce interferon γ (IFN- γ) and IL4 respectively [18]. Those two T cells subsets define a dualism in immune response. Th1 pathway leads to the activation of macrophages, while Th2 pathways activation causes the production of antibodies and the involvement of mast cells and eosinophils [19]. This difference allows the application of a variety of responses to different pathogenic aggressions. Th1 response is more adapted to dealing with intracellular pathogens such as bacterial and viral infection, while Th2 response is designed for dealing with extracellular pathogens, like parasites and worms [18, 20]. This difference is particularly relevant in autoimmune diseases, as Th1 is linked organ specific disorders, such as Crohn's disease and type 1 diabetes, while Th2 is more relevant in atopic and IgE-driven diseases [19, 21]. Another relevant CD4⁺ SP T cells subset is Th17, which is characterized by the production of IL17 and is specialized in dealing with extracellular bacteria and fungi [22]. Th17 are involved in the development of several autoimmune disease, such as Psoriasis, and IL17 is a therapeutic target [22, 23]. Activated CD8⁺ SP T cells, also called cytotoxic T lymphocytes or killer T cells, are critically important in dealing with intracellular viral infections and tumors [24, 25]. The most studied CD8⁺ SP T cells subset is Tc1. Tc1 are capable of killing cells bearing the target antigen by releasing cytotoxic molecules, such as granzymes and perforin, into the immunological synapse and to secrete cytokines, such as IFN- γ and TNF- α , which further accelerate the innate and adaptive immune response against intracellular pathogens [26]. After pathogens clearance, both CD8⁺ SP and CD4⁺ SP T cells populations rapidly decline and only long-living memory T cells survive. The memory T cells compartment consists of both CD4⁺ and CD8⁺ T cells that can rapidly acquire effector functions to kill infected cells and/or secrete inflammatory cytokines that inhibit replication of the pathogen [27]. Memory T cells role is to maintain long-term immune response capacity against pathogens, in order to quickly react to new infections, which is one of the most important perks of adaptive immunity. A subset of T cells, called T regulatory (Tregs) and expressing CD4, CD25 and FoxP3, has an immuno-suppressing role that is fundamental in preventing autoimmunity [28, 29]. Tregs inhibit the activation of naive T cells and action of B cells with a series of mechanisms [30]. Tregs can hinder the activation of effector T cells by modulating dendritic cells (DCs) activity and inducing poor T cell proliferation [31]. Tregs release TGF- β , IL-10, and IL-35, which are cytokines involved in the direct suppression of effector T cell signaling, regulation of IFN- γ , induction of Tregs, and maintenance of FoxP3 expression [32]. Tregs are able to kill and suppress B cells and possibly hinder effector T cell function by inducing apoptosis [33]. CD8⁺ regulatory T cells have also been described, with similar roles, although more focused on memory cells targeting, compared to CD4⁺ Tregs [34]. Overall, T cells can be considered

as a variegated family of immuno-modulating and effector cells, with common cellular ancestors but different roles and mechanisms of action. These cells can be considered the key operators of adaptive immunity through Th and Tc cells and immune response homeostasis through Tregs.

B-cells

B cells are the second part of the cellular compartment of adaptive immunity. They work in close contact with T cells, especially Th, and their main role is to produce immunoglobulins with the aim of binding to specific antigens targeted by the immune response. Similarly to T cells, B cell development is segmented in several steps defined by the expression of different receptors and markers (Figure 3). B cells originate in the bone marrow (BM), from hematopoietic stem cells (HSC), where they develop in pro- and pre-B cells. Phenotypically, the main stages of early B cell development, the pro-B, pre-B and immature B cells, are characterized by the expression of specific cell surface markers and by successive rearrangements of the immunoglobulin (Ig) heavy (H) and light (L) gene segments [35]. The genetic shuffling during the rearrangements of Ig gene segments is at the core of the adaptive immunity ability to react to virtually any number of antigens [36]. A fundamental step is the expression of the pre-BCR on the surface of pre-B cells, which, if functional, initiates the development into immature B-cells expression IgM on their surface [37]. Immature B cells undergo a negative selection step, where the autoreactivity potential of their BCR is tested. Cells expressing autoreactive BCRs are either deleted by induced apoptosis or selected for secondary L-chain rearrangements, while all other B cells are able to migrate from the BM to the spleen as transitional B cells [38]. Throughout life, these gene rearrangements continuously generate B cell repertoires capable of recognizing an extremely diverse number of antigens. This refinement of the B cells repertoire directly contributes to immunity, and defects in the process contribute to autoimmune disease [39]. There, they complete maturation by developing into either follicular or marginal zone (MZ) B cells. MZ B cells carry BCRs that bind preferentially to blood-borne antigens like cell wall components of bacteria. Combined with Toll-like receptor (TLR) signals induced by recognition of PAMPs, MZ B cells rapidly develop into IgM-secreting plasma cells and form a first line defense against pathogens that reach the spleen [35]. Activation of follicular B cells requires the transport of antigens into the B cell follicles of secondary lymphoid organs, where they encounter and respond to foreign antigens bound to follicular DCs [40]. B cells express MHC class II and serve as antigen-presenting cells (APCs) for CD4+ T cells [41]. Upon antigen recognition and activation, follicular B cells present their antigens on MHC II to T helper cells to receive additional activation signals provided by T helper cells, which are also critical for B cell activation, proliferation, and differentiation [42]. After T cell-dependent activation, B cells proliferate and either differentiate into plasma cells or enter germinal center (GC) reactions [40]. GC originate within spleen, lymph nodes and tonsils, forming secondary follicles inhabited mostly by activated B cells. In these structures, B cells compete for an array of signals that are delivered in an affinity-dependent manner, so that B cells with higher-affinity BCRs are expected to progressively outcompete lower-affinity B cells [43]. Whereas higher-affinity cells are selectively expanded, lower-affinity cells are eliminated by apoptosis, resulting in a GC in which B cell clones have an increasingly higher average affinity for the immunizing antigen [44].

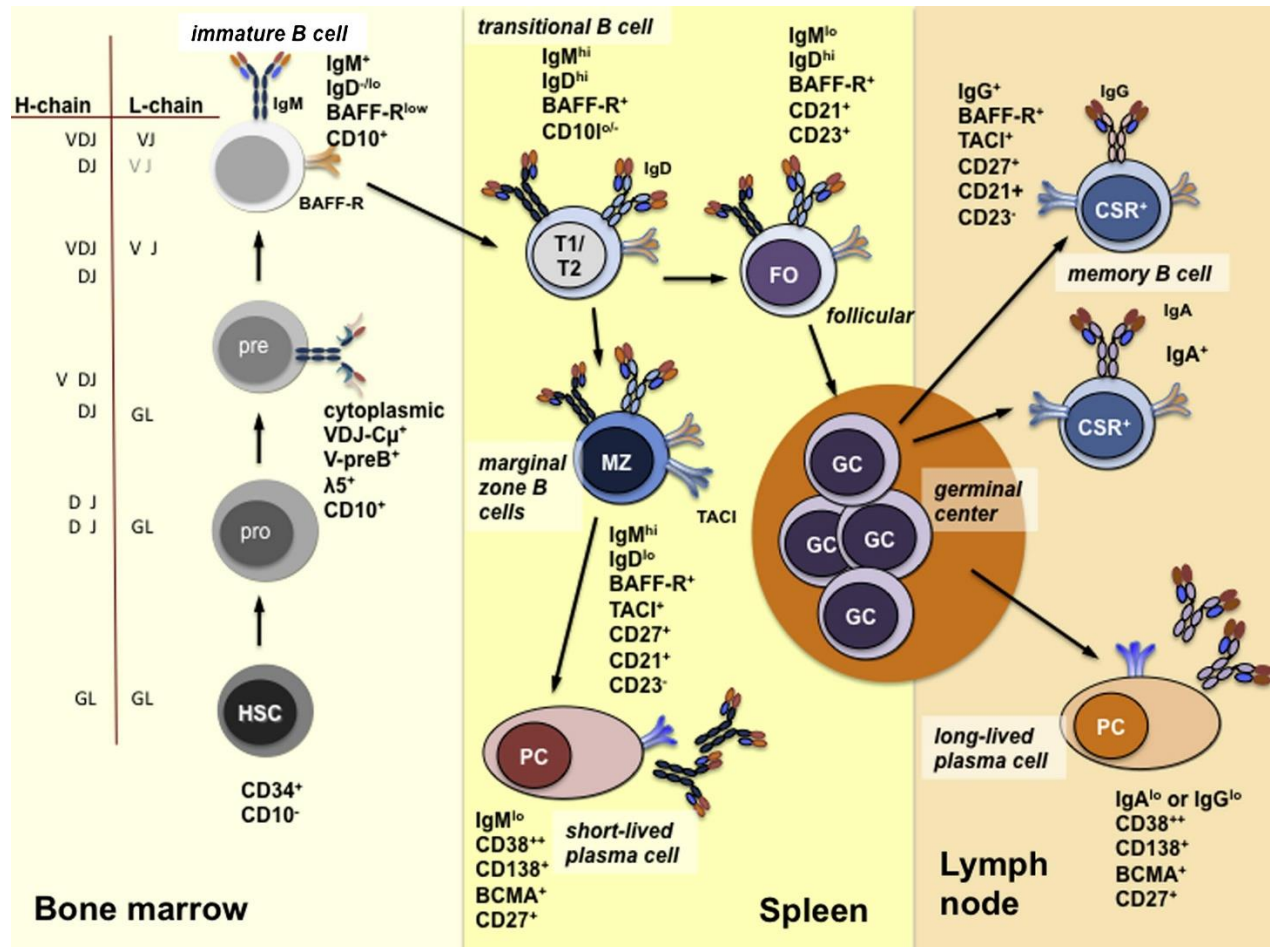


Figure 3:

B-cell development and B-cell subsets. B cells develop in the BM from hematopoietic precursor cells (HSC). Recombination-activating gene (RAG) 1/2-dependent rearrangement of the H-chain, D-gene, and J-gene segments from germline (GL) starts at the pro-B-cell stage. V-gene segment rearrangement follows in the early pre-B cell stage. In CD10+ CD19+ pre-B cells, functional H-chains (VDJ-C μ) pair with V-preB and λ -like, forming the pre-BCR, which is expressed within a cell and not detected on the surface. Pre-BCR-induced signals shut down RAG expression, preventing the rearrangement of the second H-chain allele and inducing proliferation. Next, RAG genes are re-expressed to initiate V-J rearrangement of L-chains. Successfully rearranged κ or λ L-chains replace V-preB/ λ 5 of the pre-BCR pair with the H-chain and form IgM. IgM expressed by immature B cells changes the expression pattern of many genes and initiates egress into the circulation. Immature B cells enter the spleen as transitional B cells, where they receive survival signals through BAFF-R and complete the first stage of development as MZ B cells or follicular B cells, depending on the specificity of their BCR. On contact with antigen and supported by NBH cells, MZ B cells develop into short-lived plasma cells. Follicular B cells are activated by antigen binding and develop in GCs supported by TH cells into memory B cells (CSR+) or plasma cells (PC). Activation of B cells induces AID and other components of the SHM/class-switch machinery, thus changing the affinity of the BCR and the isotype (IgM to IgG, IgA, or IgE). Figure published by Piper et al, "B-cell biology and development", J Allergy Clin Immunol, 2013 [45].

Iterations of this process will lead to affinity maturation, replicating Darwinian evolution on the cellular level. GC B-cell selection can lead to four different outcomes: further expansion and evolution, apoptosis (non-selection), or output from the GC with differentiation into memory B cells (MBCs) or short-lived plasma blasts that further develop into long-lived plasma cells (PCs) [46]. MBCs and PCs are the final output of GCs and provide effective long-lived humoral immunity [47]. PCs are the terminally differentiated, non-

dividing effector cells of the B-cell lineage. They are cellular factories devoted to the task of synthesizing and secreting of clonospecific antibodies [48]. Although long-lived PCs exist in multiple lymphoid organs in the body and in non-lymphoid organs in disease states, the bone marrow houses the majority of plasma cells in healthy individuals [49]. Antibodies produced by long-lived PCs are the first component of long-term humoral immunity, with the second one being MBCs (Figure 4), which are pathogen-experienced memory B cells able to be rapidly reactivated to produce antibodies [50]. Compared with the primary antibody response, the reactive humoral memory response is typically faster, of greater magnitude and consists of antibodies of switched isotypes and higher affinity [51].

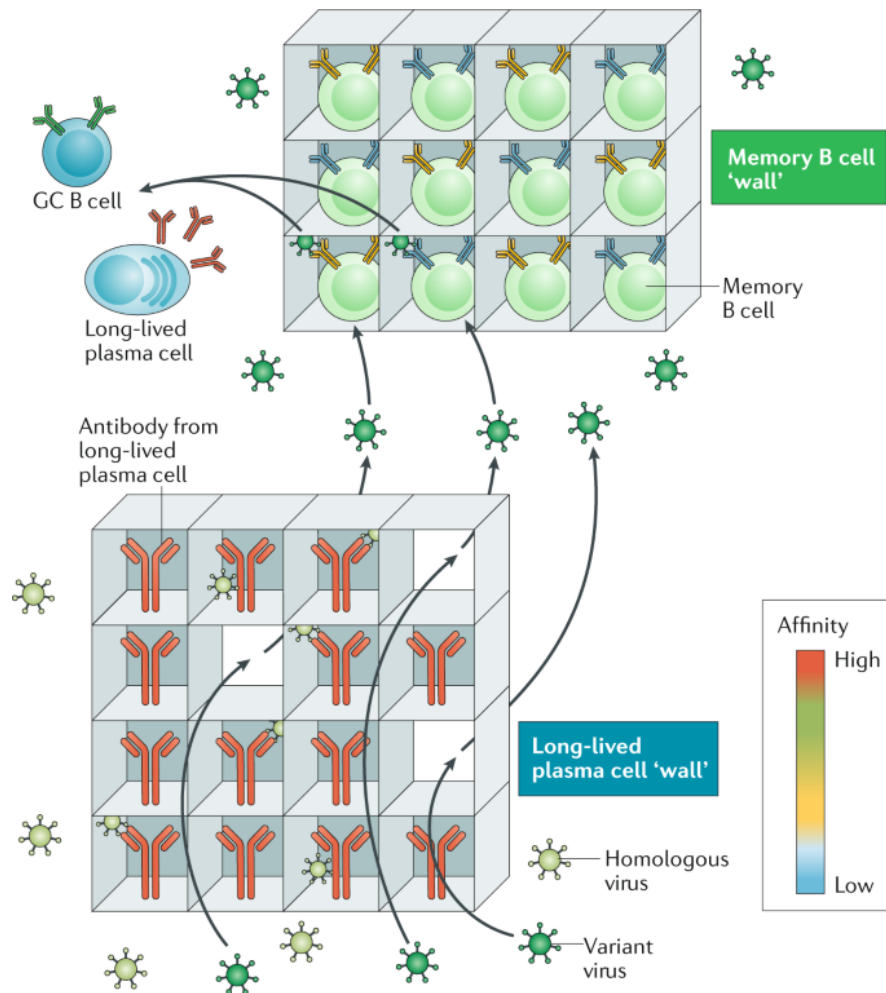


Figure 4:

Long-lived plasma cells in the bone marrow secrete highly selected, highly specific antibodies (depicted in red) that form a first 'wall' (bottom) against reinfection by homologous pathogens. Variant pathogens can find holes in this wall; however, having escaped the antibodies from the long-lived plasma cells, the variant pathogens encounter a second wall (top) formed by memory B cells that were less highly selected and therefore maintain a broader range of antigen affinities and specificities. The memory B cells are activated by the variant pathogen to differentiate into long-lived plasma cells or to re-enter the germinal centers (GCs) to replenish the memory B cell pool. Figure published by Akkaya et al, "B cell memory: building two walls of protection against pathogens", Nat Rev Immunol, 2020 [52].

The current model of B cell memory suggests that the highly-selected, high-affinity antibodies produced by long-lived PCs form the first line of defense against pathogenic challenges and that MBCs provide a second layer of defense against able to build an even stronger secondary humoral immune response [52]. Although B cells mainly augment immune response, a subset of B cells has regulatory and immuno-suppressive capacities. Such subset is called B10, because of the characteristic production of IL10, which is a potent inhibitory cytokine [53]. Once generated, B10 cells respond to both innate and adaptive immune signals, with a requirement for antigen-specific local interactions with T cells to induce IL-10 production, thus providing an antigen-specific mechanism for delivering IL-10 locally to sites of immune activation and inflammation [54]. B10 cells populations are small under physiological conditions but expand substantially in both human patients and murine models of chronic inflammatory diseases, autoimmune diseases, infection, transplantation, and cancer [55]. Their ability to reduce inflammation and immune response represent a potential therapeutic approach to autoimmune and inflammatory diseases [56]. Overall, B cells are central effector and mediators of adaptive immunity, following a complex development process requiring multiple activation steps. They are critically important in maintaining long-term immune response through long-lived plasma cells and memory cells, but they also have an immuno-suppressing action through a small subset of B10 regulatory cells.

Antibodies

The basic unit of an antibody is composed of two identical light and two identical heavy chains (Figure 5). Each chain contains two functionally and structurally distinct regions: an amino-terminal variable or antigen-binding site, and a carboxy-terminal constant region responsible for immunological effector functions [57, 58]. The ability to produce antibodies able to specifically bind to virtually any foreign antigen is at the base of adaptive immunity efficacy and long-term protection. The number of different antibodies that a human can produce during lifetime greatly exceeds the coding capacity of the inherited genome. Indeed, the size of the expressed antibody repertoire owes much to somatic gene diversification processes [59]. This genetic diversification happens mainly during pre-B cells stage and GCs reactions. During pre-B cells stage, in the bone marrow, developing BCRs diversity is due to the so called V(D)J recombination. The genes that encode BCR are highly unusual in that they exist in a non-functional state with gene's portions arranged as arrays of variable (V), diversity (D) and joining (J) gene segments [60]. Assembly of these genes by V(D)J recombination generates antigen receptor diversity and is the central process around which early lymphocyte development is organized [61].

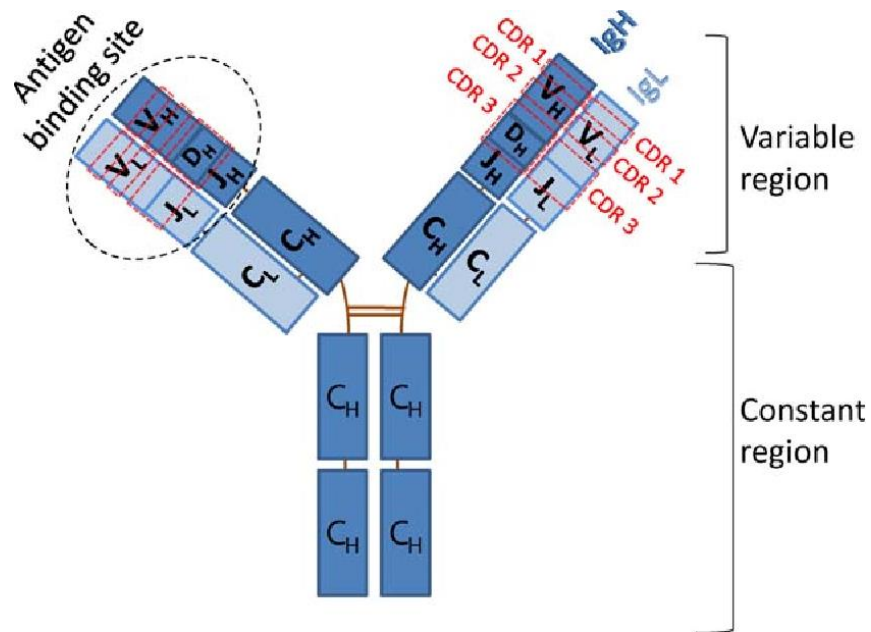


Figure 5:

*Antibody structure. The BCR is comprised of two immunoglobulin (Ig) heavy (IgH) chains encoded by the IgH heavy chain locus and two Ig light (IgL) chains. The rectangles represent Ig domains that constitute the structural units of the immunoglobulin heavy and light chains. The variable regions are assembled through V(D)J recombination of VH, DH, and JH gene segments on the heavy chain and VL and JL gene segments on the light chain. Complementarity-determining regions (CDRs) are indicated as regions in dashed red boxes: CDR 1 and 2 are encoded in the VH or VL gene segments, and CDR 3 is encoded by the VH DH JH junctional region or VL and JL junctional region. The heavy and light chain variable regions form the antigen-binding site. The constant region determines the class and effector function of the antibody molecule. Figure published by Hwang et al, "Related Mechanisms of Antibody Somatic Hypermutation and Class Switch Recombination", *Microbiol Spectr*, 2015 [58].*

V(D)J recombination can be considered as a "cut and paste" DNA rearrangement process, consisting in gene segments selection, introduction of double-strand breaks adjacent to each segment and ligation of the segments together [62, 63]. V(D)J recombination is controlled by RAG1 and RAG2 genes (recombination activating gene-1 and 2) [64]. The diversity of BCRs is tremendously amplified by the characteristic variability at the segments junctions, with loss or gain of small numbers of nucleotides, between the various segments, and this process leverages a relatively small investment in germline coding capacity into an almost limitless repertoire of potential antigen binding specificities [63]. A representation of V(D)J recombination process is given in (Figure 6) [65].

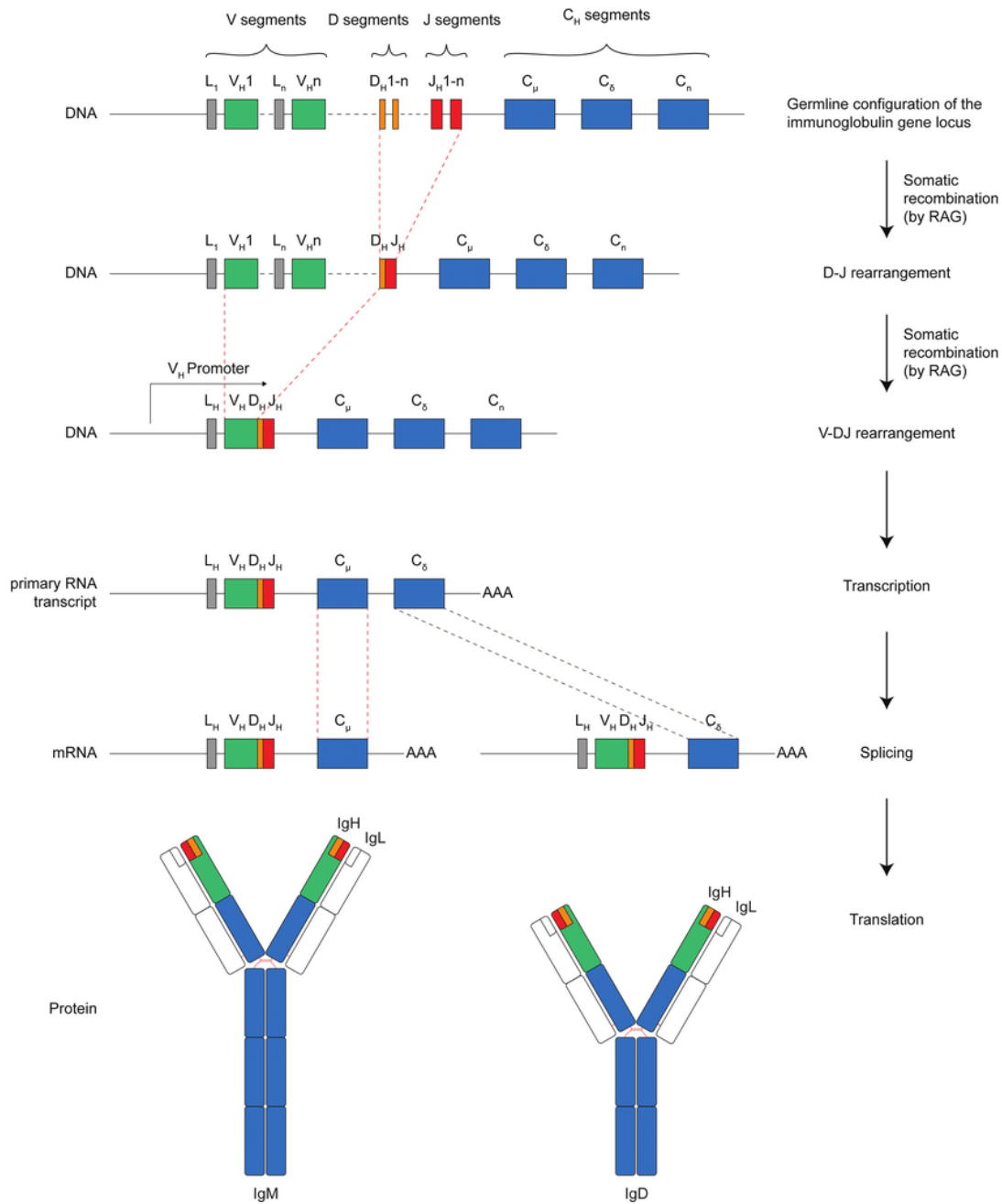


Figure 6:

V(D)J recombination of the heavy chain immunoglobulin (IgH) from germ line gene segments. The immunoglobulin locus is organized in gene segments: the variable (V), diversity (D), and joining (J) and constant (C) gene segment. The variable (V) region comprising the V, D, and J gene segments is generated by random recombination of these sequences. L = leader sequence. Figure published by Backhaus, "Generation of Antibody Diversity", 2018 [65].

During B-cell development, rearrangement of DNA occurs both in the VL/VH- and CH-region genes. As described before, V-region rearrangements take place at the pre-B cell stage and produce the complete V-region genes for the heavy and light chains which will permanently characterize an individual clone [66-68]. However, B cells undergo another step of BCR diversification, during GCs reactions, which is called somatic

hypermutation (SHM). This process is regulated by the activation-induced cytidine deaminase (AID). AID is a processive enzyme that binds single-stranded DNA and deaminates cytosines in DNA. Cytosine deamination generates highly mutagenic deoxy-uracil (U) in the DNA of both strands of the Ig loci. Mutagenic processing of the U by the DNA damage response generates the entire spectrum of base substitutions characterizing SHM at and around the initial U lesion [69]. SHM introduces single point mutations in the variable regions of the Ig loci (IgV), which can alter the antibody binding to its cognate antigen. Mutations that promote affinity for the antigen will be selected for, resulting in a progressive increase in the affinity of the antibody response [70]. CH-region diversity results from a set of CH genes corresponding to the different Ig isotypes and subclasses [71]. Class-switch recombination (CSR) is another diversification step initiated by AID, which consist in a process that replaces the immunoglobulin constant region during GCs reactions [72, 73]. Ig heavy chain class switching occurs rapidly after activation of mature naïve B cells, resulting in a switch from expressing IgM and IgD to expression of IgG, IgE, or IgA; this switch improves the ability of antibodies to remove the pathogen that induces the humoral immune response [74, 75]. Each isotype (represented in Figure 7) has a specific role and ability to be compartmentalized in different part of the body, in order to activate specific immune cells type and allow the immune system to neutralize pathogens with appropriate strategies. IgM is the first antibody isotype to appear during evolution, ontogeny and immune responses, and it not only serves as the first line of host defense against infections but also plays an important role in immune regulation and immunological tolerance [76-78]. The most abundant immunoglobulin in the blood is IgG, which is very potent in initiating proinflammatory pathways such as the activation of innate immune effector cells via cellular receptors specific for the antibody constant region (Fc receptors) and the activation of the complement pathway [79]. IgA is the most abundant immunoglobulin in mucosal areas, such as intestine and respiratory tract, and body fluids such as saliva and milk [80-83]. Although IgE concentration is around 1000 times lower than IgG, this isotype can initiate strong immune reaction that can have negative effects on the body itself, like allergy and anaphylactic shocks [84-86]. Although evolutionarily conserved, IgD role has been elucidated only recently, with studies showing its importance in helping peripheral accumulation of physiologically autoreactive B cells unclear and in enhancing mucosal homeostasis and immune surveillance [87]. The amount and variety of immunoglobulins produced by the body hint at the critically important roles played by those molecules. Indeed, antibodies are the key molecular effectors of adaptive immunity, during both pathogens clearance and prevention of new infections.

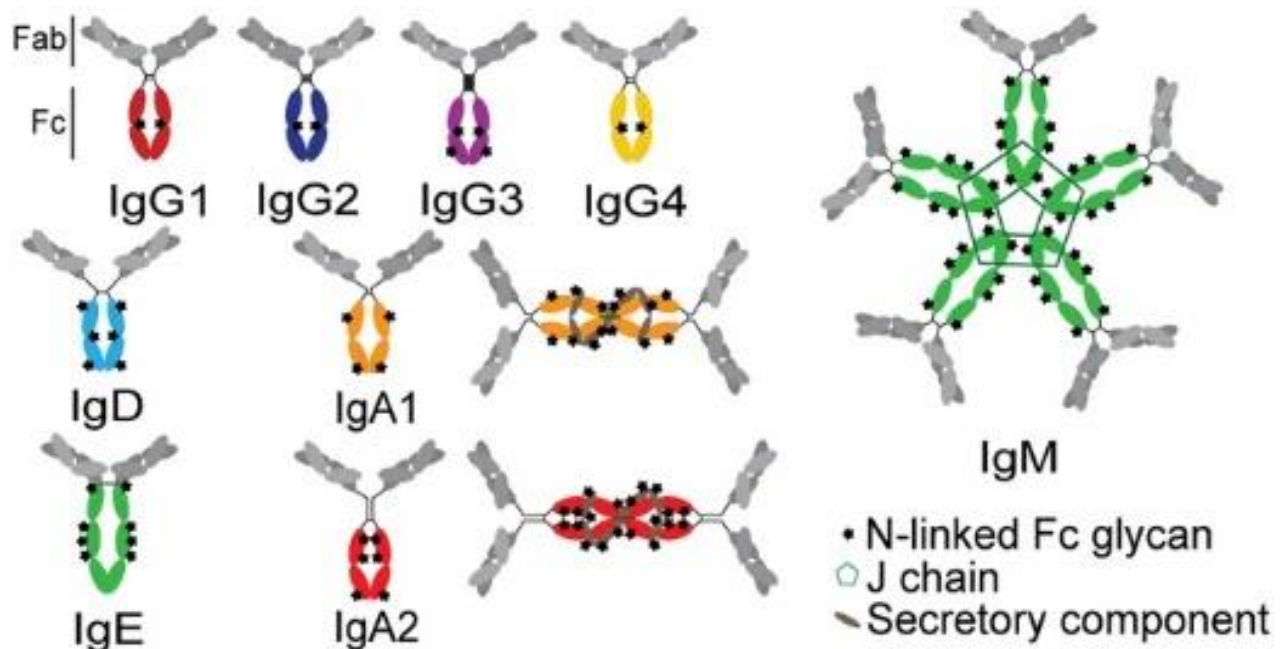


Figure 7:

Structures of antibody isotypes and subclasses. Fc domains are in color while Fab domains are in gray. Stars indicate N-linked Fc glycans. IgA isotypes are shown as both monomers (predominant in serum) and dimers (predominant at mucosal surfaces). Figure published by Boudreau et al, "Extra-Neutralizing FcR-Mediated Antibody Functions for a Universal Influenza Vaccine", *Front Immunol*, 2019 [88]

Cytokines

Cytokines are secreted proteins with growth, differentiation, and activation functions that regulate and determine the nature of immune responses and control immune cell trafficking and the cellular arrangement of immune organs [89, 90]. Which cytokines are produced in response to an immune insult determines initially whether an immune response develops and subsequently whether that response is cytotoxic, humoral, cell-mediated, or allergic (Figure 8). A cascade of responses can be seen in response to cytokines, and often several cytokines are required to synergize to express optimal function. An additional confounding variable in dissecting cytokine function is that each cytokine may have a completely different function, depending on the cellular source, target, and, most important, specific phase of the immune response during which it is presented [91, 92]. Numerous cytokines have both pro-inflammatory and anti-inflammatory potential; which activity is observed depends on the immune cells present and their state of responsiveness to the cytokine. Cytokines provide cells with the ability to communicate with one another and orchestrate complex multicellular behavior, in both homeostatic and inflammatory phenomena [93]. As described in the previous chapters regarding T and B cells, cytokines are fundamental in modulating the immune response by activating or suppressing the development and action of immune cells. Considering their critical role in initiating and maintaining inflammation and potentially autoimmune responses, cytokines and cytokines receptors have been the targets of therapeutic approaches in order to treat allergic and autoimmune diseases [94].

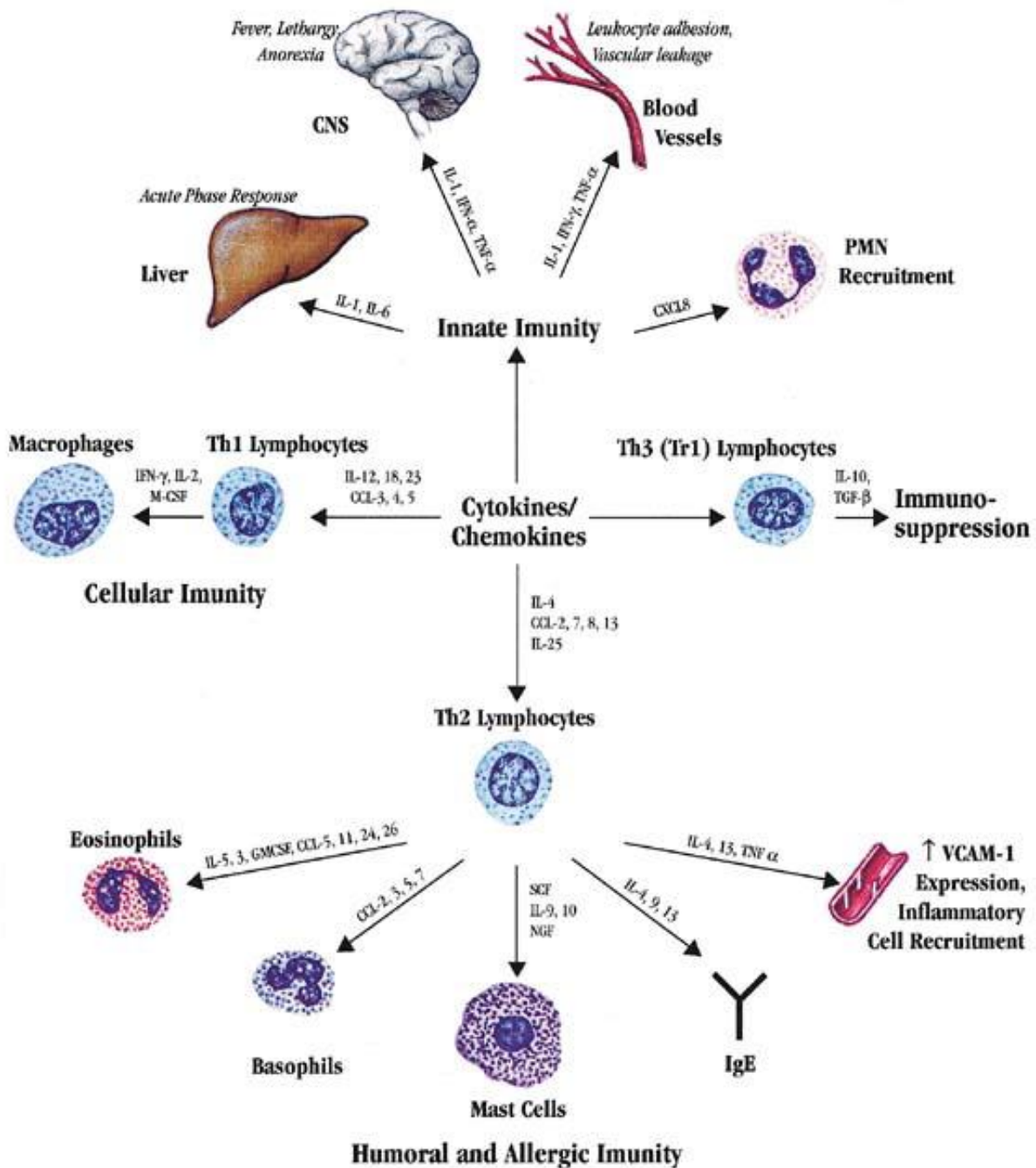


Figure 8:

Summary of actions of cytokines and chemokines. Cytokines derived predominantly from mononuclear phagocytic cells are uniquely important in innate immunity and both initiate immune responses and generate symptoms associated with infections and inflammatory disorders. Phenotype of the subsequent immune response is a function of the repertoire of cytokines produced by the responding T-helper lymphocytes. TH1-like lymphocytes are characterized by their production of IFN- γ and primarily contribute to cellular immunity. TH2-like lymphocytes are characterized by their production of IL-4, IL-5, IL-9, and IL-13 and contribute to humoral and allergic responses. TH3-like lymphocytes have immunosuppressive tendencies and are characterized by their production of IL-10 and TGF- β . Figure published by Borish et al, "Cytokines and chemokines", J Allergy Clin Immunol, 2003 [89].

For instance, anti-TNF α therapy was efficacious in treating several autoimmune diseases, such as Crohn's disease, Ulcerative Colitis (UC) and Rheumatoid Arthritis (RA), and tested in Hidradenitis Suppurativa (HS), Psoriasis, Psoriatic Arthritis [95-98]. Similarly, anti-IL17 therapy was successful in reducing symptoms of Psoriasis, PsA and Ankylosing Spondylitis (AS), and tested in HS [99-101]. Modulating the immune system by inhibiting one of its components (a specific cytokine) was proved to be a good therapeutic strategy.

Autoimmunity

As described in the previous chapters, the immune system is a complex cellular and molecular network whose role is to identify and eliminate external pathogens and aberrant molecular structures such as tumors. The immune system is subject to errors and malfunctions, just like any other component of our body. A lack of activity is of course deleterious, as pathogens can more easily infect the body and result in serious consequences or even death. However, an increased activity can also be deleterious, especially if the immune system targets self-molecules. The latter case is the definition of autoimmunity, which mainly happens when B and T cells target antigens from "self" and mount an immune response against them, leading to inflammation, cellular death and tissue damage.

Autoimmunity development

There are around 100 distinct autoimmune diseases that have been described, and their treatment is a challenge. The root causes of most of autoimmune diseases are not well known, but there are several molecular mechanisms that were proposed for the development of autoimmunity.

Hygiene hypothesis

Animals and plants have a complex and effective immune system that protect them from invading microorganisms [102]. Being able to resist to numerous pathogenic attacks is a critically important survival skill, especially for long-lived organisms. Such statement is even more relevant for species that migrate and are susceptible to enter in contact with an increased variety of microbes and of parasites. Humans, for instance, had only recently (around 13 000 years ago) changed from a nomad to a sedentary life-style after the invention of agriculture. Therefore, during the millions years-long human evolution, having an immune system able to rapidly react to different and potentially new pathogens was fundamental for survival [103]. Microbial pathogens repeatedly put our species under evolutionary pressure, with the most known and documented example being caused by *Yersinia pestis*. This bacterium was responsible for the plague, also called Black Death because of the typical bubonic symptoms, which reduced the world population from an estimated 475 million to 350–375 million in the 14th century, with death rates going up to 60-80% in some cities of Italy [104, 105]. The immune system evolved to perfect its performance in protecting us from most common pathogens and allow us to survive, at population level, new lethal pandemics. Our immune system evolved also by mixing with other hominids species, which resulted in introgressions selected because of the increased immune system performances. *Homo sapiens* developed around 200 000 years ago, and migrated outside of Africa around 50 000 years ago, slowly expanding in the entire world [106]. During

these migrations, *Homo sapiens* encountered other hominids that inhabited Europe and Asia, and replaced them over time. Although extinct, these hominids species mixed with *Homo sapiens* and, as a result, our genome contains traces of other hominids genetic material. Around 2% of modern day non-African human genome derives from Neanderthal, particularly within European and Asian populations, with some contaminations of Denisovan genes in populations from Oceania [107, 108]. The study of introgressions from other hominids species is of particular interest for the understanding of our immune system and its evolution. Indeed, Neanderthal genetic influence is not randomly distributed along human genome, as natural selection tends to favor phenotypes increasing survival chances and to discard the ones that decrease survival fitness. Most of Neanderthal genetic traces were found in regions coding for adaptive immune system components, for instances human leukocyte antigen (HLA) genes [109]. Higher variability in this region allow for a wider spectrum of HLA molecules, which improves the targeting of pathogens antigens [110]. Other examples are a haplotype of STAT2 present in 5% of Europeans and 54% of Melanesians that was found to be introgressed from Neanderthals, and TLR genes carrying archaic haplotypes from Neanderthal and Denisovan [111]. These variants were initially neutral or advantageous for modern humans, as they increased the variability and response potential of the immune system, but some are today associated with disease phenotypes. For instances, some archaic introgressions were found to be associated with higher risk of Crohn's and celiac disease [112]. Indeed, a more aggressive immune system that was a survival advantage just a few centuries ago is now a potential source for autoimmunity development. The sudden (from an evolution time-line perspective) advancements in modern medicine, such as the use antibiotics and vaccines, the improved hygienic conditions of human society, from the use of soap to disinfectants, and the more sedentary life-style, drastically decreased the amount and variety of pathogens challenging our immune system. Numerous public health measures were taken after the industrial revolution by western countries to limit the spread of infections. These measures spread from the decontamination of the water supply, pasteurization and sterilization of milk and other food products, respect of the cold chain procedure, to the vaccination against common childhood infections and the wide use of antibiotics. The decline in infection was particularly clear for hepatitis A (HAV), childhood diarrhea and parasitic diseases. Interestingly, several countries that have eradicated those common infections saw the emergence of allergic and autoimmune diseases [113]. In the last 50 years, industrialized countries have been stricken by an epidemic increase in immune-mediated and inflammatory diseases, including hay fever, asthma, eczema, and food allergies. This sudden rise in allergic conditions has occurred during a major decrease in the incidence of infectious diseases around the world, driven by medical advances in vaccines, antimicrobials and hygiene practices [114]. Autoimmune diseases development seems to correlate with a decreased frequency of pathogens infections [115]. The incidence of autoimmune diseases has been steadily rising [116]. Concomitantly, the incidence of most infectious diseases has declined. This observation gave rise to the hygiene hypothesis, which postulates that a reduction in the frequency of infections contributes directly to the increase in the frequency of autoimmune and allergic diseases [117]. This hypothesis is supported by robust epidemiological data, but the underlying

mechanisms are unclear [118]. The role of pathogens in shaping the tolerance of our immune system is well known, as autoimmune disease development was prevented in various experimental models by infection with different bacteria, viruses and parasites [119]. Gut commensal bacteria also play an important role: dysbiosis of the gut flora is observed in patients with autoimmune diseases, although the causal relationship with the occurrence of autoimmune diseases has not been established yet [120]. Both pathogens and commensals act by stimulating immunoregulatory pathways [119, 121].

Molecular mimicry

Molecular mimicry is one of the leading mechanisms by which infectious or chemical agents may induce autoimmunity. It occurs when similarities between foreign and self-peptides favor an activation of autoreactive immunity by a foreign-derived antigen in a susceptible individual. Host genetics, exposure to microbiota and environmental chemicals are additional links to our understanding of molecular mimicry. [122]. Molecular mimicry has typically been characterized on an antibody or T cell level [123]. Cross-reactivity between self-antigens and microbial components originates from an incomplete negative selection of B and T cells [124]. A well-known example of autoimmunity caused by molecular mimicry is rheumatic fever, a group of diseases affecting the heart, brain, and joints, caused by group A streptococci infections [125]. Rheumatic fever onset is due to cross-reactive antibody and cellular immune responses that target antigens present in the heart, brain, joints and the group A streptococci. Molecular mimicry was proposed as possible cause for anti-nuclear antibodies development in SLE, as disease activity was associated with alterations of the gut commensals. Bacterial infections can release bacterial DNA associated with other bacterial molecules, which can be recognized by the immune system and provoke a humoral response potentially cross-reacting with human DNA and other nuclear antigens that are relevant in SLE [126]. *Cytomegalovirus* pp65 peptide-induced antibodies cross-reacted with TAF9 protein and induced lupus-like autoimmunity in a mouse model, suggesting another molecular mimicry-driven autoimmunity development model in SLE [127]. Human Endogenous Retroviruses (HERVs) were also proposed as potential mediators of autoimmunity caused by molecular mimicry, as HERV K-10 shares amino acid sequences with IgG1Fc, which is an antigen targeted by rheumatoid factor (RF) [128]. Molecular mimicry is a plausible mechanism for autoimmunity development, particularly when considering the variety and abundance of microbial antigens targeted by the immune system. Molecular mimicry is partially in contrast with hygiene hypothesis, which suggests that immune response to pathogens helps in building tolerance. Therefore, the consequences of interactions between immune system and microbial pathogens may be of difficult interpretation.

Epitope spreading

An epitope is an antigenic determinant, or a site on the surface of an antigenic molecule, to which a single antibody binds. Epitope spreading refers to the development of an immune response to epitopes distinct from, and non-cross-reactive with, the disease-causing epitope [129]. There are two different types of epitope spreading, intermolecular and intramolecular. The latter describes a type of spreading where the

immune response is directed against different epitopes of the same molecule, while the former is a diversification of the immune response against two or more different molecules [130]. Intramolecular epitope spreading is a form of immune response optimization, as targeting the same pathogenic antigen with different epitopes leads to a more efficient clearance of microbes or tumors. Intermolecular epitope spreading can lead to autoimmunity by initiating the targeting of self-antigens [131].

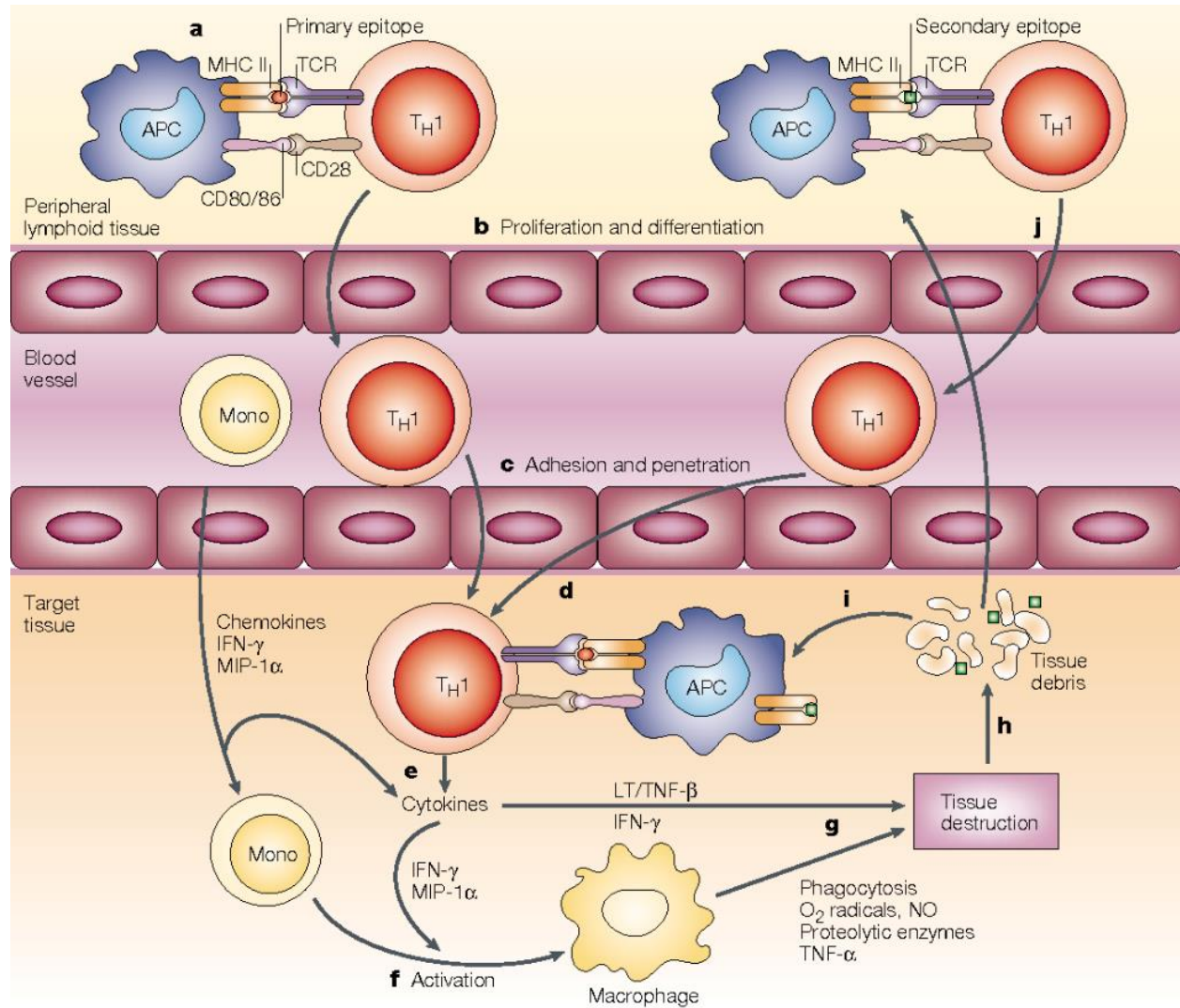


Figure 9:

Presentation of the primary epitope (the immunodominant self or viral epitope) occurs in peripheral lymphoid tissue (a), resulting in activation and differentiation of autoreactive TH1 cells (b). The activated TH1 cells migrate (c) into the target tissue, where they encounter antigen presented by resident APCs. (d). After antigen restimulation, the pathologic TH1 cells release a cascade of chemokines and cytokines (e), leading to recruitment of additional mononuclear phagocytes from the peripheral blood, which are activated along with resident APCs (f). Activated mononuclear cells then lead to bystander tissue destruction (g) via phagocytic mechanisms and release of TNF- α , proteolytic enzymes, NO and O₂ radicals. The tissue debris (h) is processed and presented on resident and peripheral APCs (i), leading to the activation and differentiation of a second wave of TH1 cells (j), which can re-enter the tissue and cause additional tissue destruction. Figure published by Vanderlugt et al, "Epitope spreading in immune-mediated diseases: implications for immunotherapy", *Nat Rev Immunol*, 2002 [132].

Evidence continues to accumulate supporting the hypothesis that tissue damage during an immune response can lead to the priming of self-reactive T and/or B lymphocytes, regardless of the specificity of the initial insult [132, 133]. This priming can lead to mounting a persistent inflammatory self-recognition process that ultimately leads to a chronic progressive disability that typically characterizes autoimmune diseases [134]. Systemic lupus erythematosus, multiple sclerosis, pemphigus, bullous pemphigoid and other autoimmune diseases, are all influenced by intermolecular and intramolecular B cell epitope spreading [135]. Endocytic processing, antigen presentation, and somatic hypermutation act as molecular mechanisms that assist in driving epitope spreading and broadening the immune response in autoimmune diseases [132]. Viral infections are thought to initiate epitope spreading in MS patients, which develop autoimmune responses to myelin proteins such as myelin basic protein (MBP), proteolipid protein (PLP), and myelin oligodendrocyte glycoprotein (MOG) [136]. In summary, epitope spreading was proven to be involved in autoimmunity development and chronicity in several diseases. However, epitope spreading can also mediate a down regulation of inflammation. Indeed, the induction of anti-inflammatory Th2 responses via epitope spreading may be an important intrinsic immunoregulatory mechanism geared to limit tissue destruction and promote re-establishment of tissue-specific immune tolerance [132]. Epitope spreading is tightly linked to immune reactions to infections and is overall a useful mechanism applied by the immune system in order to amplify T and B cells response. Similarly to mimicry, an incomplete negative selection in T and B cells development is potentially at the base of epitope spreading dysfunction and autoimmune side.

Bystander activation

Bystander activation is the activation of the immune system in an antigen-independent manner. It occurs because of infected cells alerting and instructing neighboring uninfected cells to produce inflammatory mediators. Thus, bystander activation can allow the immune system to overcome the ability of pathogens to disarm immune signaling in directly infected cells [137]. However, bystander activation can also cause autoimmunity. Indeed, bystander activation can activate B and T cells in an antigen-independent manner, through the production of pro-inflammatory cells, leading to the development of autoimmunity. This activation occurs due to a combination of an inflammatory milieu, co-signaling ligands, and interactions with neighboring cells [138]. For example, virus-specific T cells migrate to areas of virus infection/antigen such as the heart, pancreas, or CNS, where they encounter virus-infected cells that present viral peptides. The CD8⁺ T cells recognize these infected cells and release cytotoxic granules resulting in the killing or death of the infected cells. Under these circumstances the dying cells, the CD8⁺ T cells macrophages within the inflammatory focus release cytokines such as TNF, TNF- β , lymphotoxin (LT), and nitric oxide (NO), which can lead to bystander killing of the uninfected neighboring cells [139]. CD8⁺ T cells also mediate host injury by exerting cytotoxicity that is facilitated by natural killer cell-activating receptors, such as NKG2D, and cytolytic molecules, such as granzyme B [140]. An example of bystander activation is the autoimmune side of dengue fever. Indeed, the immune response of dengue fever/dengue hemorrhagic fever is a series of monocytes and macrophages-drive immunopathogenesis processes starting from viral infection and exacerbated by bystander activation [141]. Another example of autoimmunity caused through bystander

activation is liver injury associated with Hepatitis A infection. Hepatitis A virus (HAV)-infected cells produced IL-15 that induced TCR-independent activation of memory CD8+ T cells, which was associated with the severity of liver injuries [142]. Neutrophil extracellular traps (NETs) are considered to contribute to autoimmune inflammation and cause bystander tissue injury, but they have also been described to have potential immuno-regulatory action [143]. Overall, bystander activation can be considered as a weapon used by the immune system in case of infections by pathogens able to elude the immune system. Such immune response is intrinsically unspecific and designed to activate T cells in a TCR independent way, accepting autoimmunity as a trade-off for pathogens clearance.

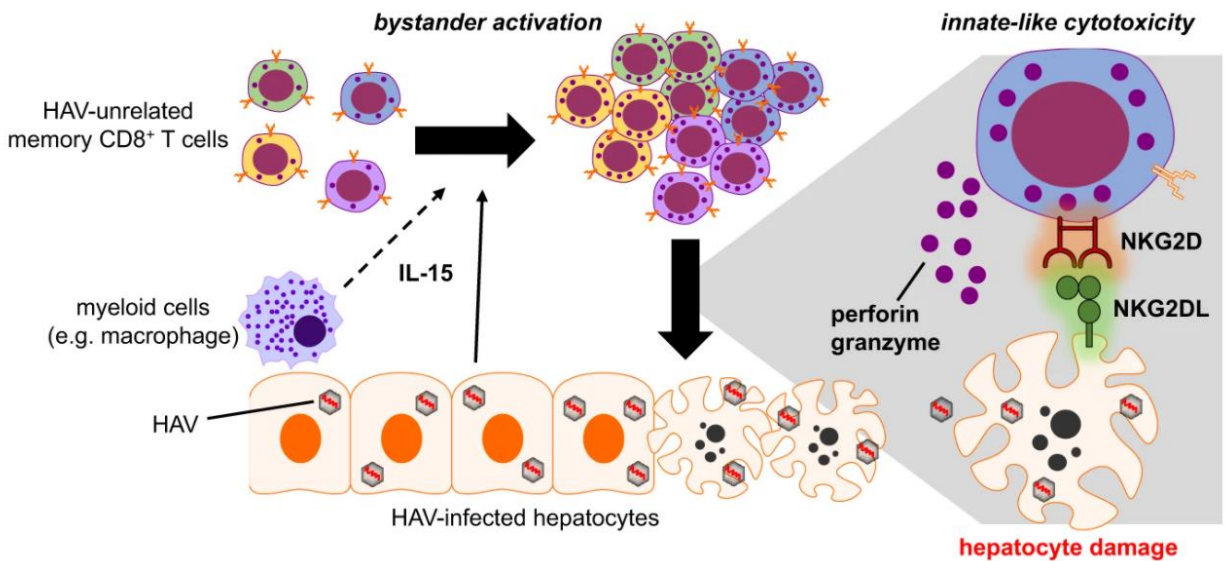


Figure 10:

*During acute hepatitis A, memory CD8+ T cells specific for HAV-unrelated viruses undergo IL-15-dependent bystander activation. IL-15 is produced by hepatocytes and possibly myeloid cells in the infected liver. These activated, HAV-unrelated CD8+ T cells exhibit “innate-like cytotoxicity” to hepatocytes, which is triggered by the ligation of natural killer cell-activating receptors (e.g., NKG2D) with their ligands. Figure published by Kim et al, “The activation of bystander CD8(+) T cells and their roles in viral infection”, *Exp Mol Med*, 2019 [140].*

Autoimmunity prevention

The prevention of autoimmunity is a major challenge for the adaptive immune system. An efficient immune system works on the edge between producing BCRs and TCRs able to recognize the highest possible number of antigens but without recognizing non-pathogenic self-molecules. Being too conservative on the negative selection process would reduce the diversity of BCRs and TCRs, which would result in a less agile immune system. Not being conservative enough with negative selection would bring the opposite result, leading to the development of B and T cells more prone to targeting self-antigens and initiating autoimmune processes. Throughout human evolution, the selective pressure of a wide spectrum of microbial pathogens resulted in the development of an immune system leaning more toward increasing its efficacy and ability to react against unknown or elusive pathogens. However, in most of today's societies such an efficacy has not been that crucial for the last 200 years and highly active immune systems are a risk factor for

autoimmunity development. Despite having evolved to target a variety of pathogens, the immune system also developed several tolerance mechanisms in order to minimize the risk of autoimmunity, particularly in T and B cells.

Autoimmunity prevention in T cells

The generation process of the TCR in individual thymocytes during thymic development may result in the generation of individual clones with the potential for autoreactivity [144]. T lymphocytes play a central role in regulation of the immune system. Both effector and regulatory T cells work in equilibrium to provide optimal immune response against foreign pathogens. Normally, T cells do not react against self-antigens because of the presence of central and peripheral immunogenic tolerance [145]. Central tolerance eliminates autoreactive naive T cells that develop in thymus by presenting them with self-antigens on the thymic cells, which correspond to the previously described negative selection. The autoreactive T cells that escape thymus are subjected to additional mechanisms such as clonal anergy, ignorance, and deletion. T cell anergy is a tolerance mechanism in which the lymphocyte is intrinsically functionally inactivated following an antigen encounter, but remains alive for an extended period of time in a hyporesponsive state [146]. T cell anergy is induced by TCR binding to peptides presented by APCs but with a lack of costimulatory signals. Anergy induction is not only important in preventing autoimmunity, but it also generates the precursors for peripheral Treg cell differentiation [147]. Clonal deletion in the peripheral T cells is achieved through activation-induced cell death (AICD), which happens after TCR binding and induced expression of Fas ligand [148]. Moreover, Tregs, specifically CD4⁺CD25⁺Foxp3⁺ Tregs, exert a tight control over autoreactive B and T cell responses in the periphery. Failure of any one of these checkpoints can cause uncontrolled expansion of these self-reactive T cells leading to the development of autoimmune diseases [149]. Clonal diversion of T cells leads to the differentiation in Tregs, which is another mechanism of immune tolerance [150].

Autoimmunity prevention in B cells

Similarly to T cells, also B cells present tolerance mechanisms aimed at minimizing the risk of autoimmunity development. During B cells development in the bone marrow, a negative selection is applied in order to discard or re-arrange BCRs showing autoimmune properties, which is defined as central B cells tolerance [151]. Peripheral tolerance mechanisms are also present and fundamental in avoid autoimmunity generated by lack an incomplete central negative selection. If a mature B cell recognizes autoantigens in peripheral tissues without specific helper T cell response, this cell may be functionally inactivated by anergy mechanisms or die by apoptosis [152]. Anergic B cells populate peripheral lymphoid organs and continue to express unoccupied antigen receptors yet are unresponsive to antigen stimulation [153]. A proposed mechanism for anergy induction in B cells is the permanent binding of BCR, which translates in the induction of inhibitory molecules expression inhibiting B cell activation [154]. Moreover, BCR binding is not enough for B cell activation, as cognate interactions with T cells are needed. If such interaction does not happen within a certain period of time, B cell become unresponsive [155]. Therefore, T cells activity can be

considered as a tolerance mechanism for B cells, as the latter cannot be activated without availability of the former. Self-reactive B cells generated by somatic mutations during GC reaction are also eliminated [156]. Moreover, Bregs also have an important regulatory and tolerance role, through the production of inhibitory cytokines such as IL10, preventing autoimmunity development [157].

Autoantibodies

Immunoglobulins are fundamental components of the immune system, as they are the base of adaptive immunity efficiency in not only performing pathogens clearance, but also in preventing future infections. Antibodies produced by freshly activated B cells are fundamental tools in the immune reaction against ongoing infections, as they can direct immune cells expressing immunoglobulins receptors toward foreign molecules or microbes. After infection's clearance, long-lived plasma cells continue producing antibodies that will circulate throughout the body and will effectively hinder or prevent new infections from already encountered pathogens. There is a plethora of potential targets for the adaptive immune system, which are not only external pathogens but also "internal". Indeed, the immune system is also trained to recognize tumors and to induce apoptosis in cancerous cells. Therefore, B cells are also selected to produce antibodies targeting self-antigens characterizing aberrant cellular states. Furthermore, the immune system role is not only to eliminate its targets, but also to maintain homeostasis with some of them. For instance, the immune system targets bacteria from the gut microbiome in order to maintain a state of permanent light inflammation that keeps their population under control. Considering the broad spectrum of roles that the immune system can cover, we can consider it as the "house-keeper" of our body, and antibodies are arguably the main molecular tool used. However, the specificity of the immune system is not perfect, as explained while describing the pathways potentially resulting in autoimmunity. Indeed, autoimmunity can arise under different circumstances and lead to the development of autoimmune diseases, which affect a significant part of population in developed countries. Antibodies clearly play an important role in autoimmunity, as they are abundantly present in patients with autoimmune diseases, such as SLE and RA. Antibodies targeting self-antigens are named autoantibodies, and are the main topic of this thesis. Autoantibodies' role within the immune system, although widely studied since several decades, is still partially unclear. Intuitively, autoantibodies would be associated with a pathogenic role, but an immunoregulatory and homeostatic purpose has been proposed as well [158]. Understanding the dualism between the two roles of autoantibodies is of great importance for the treatment of autoimmune diseases.

Autoantibodies dualism: pathogenicity and immune system regulation

Autoantibodies targeting specific antigens have been associated with autoimmune diseases since the beginning of the previous century, precisely from the "horror autotoxicus" definition given to autoantibodies by Ehrlich in 1902 [159]. Autoantibodies directed against intracellular antigens are typical of lupus-like diseases and, although their role is still not well understood, they are thought to participate in autoimmune diseases pathogenesis [160-162]. Pathogenic autoantibodies directed against secreted or membrane-associated autoantigens cause diseases mainly by disrupting the function of target proteins or by promoting

the destruction of cells expressing these cell-surface molecules [163]. Such autoantibodies are involved in the development of various type of autoimmune diseases, from systemic to organ-specific ones. For instance, antibodies directed against SSA and SSB antigens are abundantly present in around 30% of SLE and 70-90% of Sjögren Syndrome (SS) patients [164, 165]. Anti-IgG Fc antibodies, commonly called rheumatoid factor (RF), are expressed in the majority of patients suffering from arthritic diseases [166]. Around 25-40% of RA patients present anti-citrullinated protein antibodies (ACPA), while 44% present anti-carbamylated proteins (anti-CarP) antibodies [167]. Several neuropsychiatric diseases were recently linked to specific anti-neuronal autoantibodies targeting GABAergic and glycinergic synapses, which are directly pathogenic by down-regulating synaptic proteins, activating complement or antagonizing ligand binding [168]. ANAs, particularly anti-centromeres (CENP) and anti-Scl-70 (topoisomerase I) autoantibodies are used in the diagnosis of Systemic Sclerosis (SSc), while antibodies directed against non-nuclear and cell surface antigens such as anti-endothelial cell, antiplatelet-derived growth factor receptor, anti-AT1 receptor and interferon-inducible protein 16 are considered as functional in the development of SSc [169]. The development of autoantibodies to type IV collagen antigens expressed in the glomerular and alveolar basement membranes has been found to play a pathogenic role in anti-glomerular basement membrane (anti-GBM) disease [170]. Although the pathogenic capacity of autoantibodies is very well described in literature, there are also examples of non-pathogenic autoantibodies. For instance, IgM targeting phosphorylcholine can enhance clearance of damaged cells and induce intracellular blockade of inflammatory signaling cascades, showing a protective action from atherosclerosis and may downmodulate the severity of autoimmune disease [171]. IgM anti-DNA antibodies negatively correlated with SLE symptoms severity, suggesting that such autoantibodies may have a protective role in SLE [172]. Such hypothesis was reinforced by the finding that treatment with IgM anti-DNA resulted in an inhibition of SLE symptoms in a mouse model [173]. Anti-idiopathic antibodies are immunoglobulins targeting the Fab antigen-binding section of another immunoglobulin, with RF as most known example, and are thought to immuno-modulate the humoral response in order to prevent autoimmune pathogenicity [174, 175]. Presence of IgM RF in SLE sera was associated with a lower severity of symptoms, although IgA RF defined a high disease activity subpopulation [176]. Beneficial autoimmunity against pro-inflammatory cytokines has also been reported to play a role in the immuno-modulation of autoimmune diseases [177]. Moreover, protective autoantibodies also play an important role in detecting cancers. For instance, IgM antibodies bind to various tumor-antigens, induce apoptosis of malignant cells and, most importantly, they detect not only malignant cells but also their precursor stages [178]. Considering all the examples above, it is not possible to generalize on the role of autoantibodies. Targeted antigen, immunoglobulin isotype, disease state and affected pathways are all elements to take into account when investigating the role of a given autoantibody.

Natural Autoantibodies

As previously described, antibody production is linked to B cells development and activation through antigenic stimulation. However, a significant portion of antibodies is produced without any previous

immunization and targets a wide spectrum of antigens, from microbial to self-antigens. Those immunoglobulins were historically named natural autoantibodies (NAAs) [158]. NAAs are of IgG, IgM and IgA isotypes and target a variety of serum proteins, cell surface structures and intracellular molecular complexes and they are encoded by germline genes with no, or few, mutations [179]. B cells that produce NAAs comprise 15–20% of the circulating B cells in adults and 50% of the B cells in cord blood of newborns; and NAAs are evolutionarily conserved, as they have been found in all jawed vertebrates, from cartilaginous fish to amphibians, birds, and mammals [180]. The role of such antibodies is not clear, but they are most likely involved in homeostasis maintenance and may be a first barrier of defense, as a sort of innate humoral immunity [181, 182]. Clinically healthy volunteers also produce NAAs, which reinforces the hypothesis that such immunoglobulins are an endemic component of the immune system [183]. Interestingly, NAAs present overall low binding affinity but evolutionary preserved polyreactivity and avidity [184]. The ability of polyreactive natural antibodies to bind different antigens relies on two different types of recognition: identical epitopes present on different antigens or different epitopes from different antigens. Most natural polyreactive antibodies efficiently recognize antigens that are different in nature, such as proteins, nucleic acids, phospholipids and polysaccharides, and, therefore, are highly unlikely to share identical epitopes. This indicates that polyreactivity is a function of features inherent to the binding cleft of the antibody and not of structural features inherent to and shared by different antigens [185]. Polyreactive NAAs manifest the capacity to recognize three-dimensional structures and thus represent a fundamental feature of the immune system, which may explain why they have long been preserved during evolution [186]. Most of NAAs are of IgM isotype, which have been described to have beneficial effects in both tolerance and protection from microbial aggressions. IgM-NAAs regulate the inflammatory response to apoptotic cells to enhance their removal, bind to leukocytes to regulate their function and can prevent autoimmunity development [187]. NAAs reacting with either self or non-self antigens constitute a vast network of infinite interactions providing high complexity, stability and plasticity [186]. In healthy individuals, NAAs are of low prevalence and generally show low affinity to their respective antigens, whereas in autoimmune disease, their frequency and affinity toward specific antigens are in many cases increased [188]. It was also hypothesized that pathogenic autoantibody production may be explained as an expansion of naturally present autoreactive lymphocytic clones that, in genetically predisposed individuals, can induce cell or organ damage and thus development of autoimmune disorders [184]. Isotype switching of NAAs might be a mechanism involved in autoimmunity development. Indeed, IgM are overall associated with protective and homeostatic roles, while high-affinity, somatically mutated IgG and IgA autoantibodies reflect a pathologic process where homeostatic pathways related to cell clearance, antigen-receptor signaling or cell effector functions are disturbed [185, 189]. For instance, disease-associated IgG ANAs and ACPA have been shown to activate innate pattern recognition receptors leading to increased cell death and tissue injury, while a class of IgM autoantibodies targeting oxidation-associated neo-antigens can oppose these pathogenic effects through enhancing phagocytic clearance of apoptotic cells and inhibiting of TLRs agonists [190]. Oxidation-specific epitopes may be immunodominant targets of natural antibodies,

suggesting an important function for these antibodies in the host response to the consequences of oxidative stress [191]. Although their role is not fully understood, NAAs abundance and evolutionary conservation suggest that they are an important component of the molecular arm of the immune system, for both pathogens clearance and homeostasis maintenance, and can be considered as an adaptive immunity “contribution” to the innate immune system.

Biomarkers

Biomarker’s definition

The definition of a biomarker is simple and purposely broad, slightly different in the wording depending on the organization proposing it but mostly overlapping. For instance, the FDA considers a biomarker as “a defined characteristic that is measured as an indicator of normal biological processes, pathogenic processes or responses to an exposure or intervention” [192]. In other words, nearly any measure, from basic information such as patients’ weight or blood pressure to more sophisticated ones as genes expression or proteins levels, can be considered as a biomarker. Although broadly defined, in the context of clinical trials, the term biomarker is mostly used for cellular and molecular measurements on biological material collected from patients, performed with the aim of improving diseases understanding or clinical treatments. The broad definition of a biomarker reflects the variety of its uses. Depending on the timing and methodologies of measurement, biomarkers can be used as:

- **Predictive:** biomarkers measured at baseline (beginning of the treatment) or during the patients screening phase, used to predict the response or non-response to a given treatment. Such markers are at the base of precision medicine’s approaches, as they can direct caregivers toward treatments that are efficacious in a specific disease subpopulation. The use of predictive biomarkers ultimately leads to the pre-selection of patients to be treated and to increased treatment efficacy when compared to unselected patients.
- **Mechanistic:** biomarkers whose levels change after treatment in a pharmacodynamics manner. The change in concentration or level of such markers usually does not correlate with treatment response and their change is often dose-dependent. They are helpful in better understanding treatments effects and choosing optimal drug’s doses.
- **Diagnostic:** biomarkers used to help caregivers in the diagnosis of a specific disease. Symptoms and disease phenotypes do not always allow for a clear diagnosis, therefore cellular and molecular markers can help in narrowing down or ruling out diseases. Biomarkers with early diagnosis potential are extremely useful, as an early disease detection is associated with better treatments outcomes.
- **Prognostic:** biomarkers used to identify the likelihood of a clinical event, disease recurrence, or disease progression in patients with a disease or medical condition of interest, without taking into account any specific treatment [192, 193]. Such markers are useful in predicting the severity of

symptoms, which can help caregivers in tuning disease treatments in order to tackle future worsening or potential complications.

- **Efficacy:** biomarkers used to monitor the efficacy of a given treatment, which helps caregivers in following treatment effects. A rapid assessment of the beneficial effects of an ongoing treatment is of critical importance in order to prevent symptoms' worsening and to change or confirm a therapeutic approach.
- **Safety:** biomarkers able to predict the likelihood of adverse events appearance and treatment's toxicity [192]. Some treatments, particularly in oncology, can have heavy secondary effects and potentially endanger patient's survival. Following the functioning of organs and predicting any conditions worsening help caregivers in measuring the strain put on the body, and in adapting the treatments in order to prevent or at least limit the magnitude of adverse events.

The use of biomarkers, and in particular laboratory-measured biomarkers, in clinical research is relatively recent, and the best approaches to this practice are still being developed and refined [194]. Biomarkers assessments have to fulfill certain criteria before being applied in clinical trials or therapeutic use. Indeed, assays measuring biomarkers need to firstly be technically validated by proven robustness, reproducibility and accuracy. Secondly, the clinical utility of a given biomarker needs to be proven by its developers and approved by health authorities [195]. The validation process of a biomarker can be troublesome, which is due in part to the lack of a regulatory guidance connecting marker discovery with well-established methods for validation [196, 197]. However, personalized medicine's application and endotypes identification is nowadays increasingly more required in order to treat diseases with unmet clinical needs from oncology to autoimmunity, and biomarkers are the key to reach this goal. The most appropriate context to evaluate the value of a biomarker related to treatment efficacy is the clinical development, hence biomarkers should be explored during clinical trials.

Clinical trials

The development and approval of a drug is a lengthy, complex and heavily regulated process that usually lasts around 10-13 years and costs between hundreds of millions and few billions of dollars [198-202]. Before being marketed, a drug must be tested through several development phases in order to fulfill all regulatory criteria. This process is classically divided in discovery phase, pre-clinical development and clinical trials (Figure 11). After the identification and validation of a therapeutic target, new molecular and biological compounds are tested in order to investigate their in-vitro capacity to interact with the target in a potentially beneficial manner. This discovery phase is mostly based on screening assays and testing in animal models, with optimization steps aimed at increasing the binding capacity of the candidate drug to its target [203]. A few selected molecules are then tested in pre-clinical trials conducted in animals, mostly rodents and other mammals, in order to delineate the pharmacokinetic profile and general safety, as well as to identify toxicity patterns [204]. Compounds showing sufficiently good safety and pharmacokinetic profiles can start the clinical development phase, where they are tested in humans. The clinical

development process is further divided in three distinct phases, each of them designed to investigate different aspects of the application of the new drug. The phase I is typically conducted on a relatively small number of healthy volunteers, with exception of oncology where cancer patients are enrolled, and its aim is to verify the safety and pharmacokinetic profiles of the drug in humans [205, 206]. This phase is critical, as the safety of a drug is of utmost importance for its approval and commercialization. Furthermore, serious adverse events can have a deleterious impact on the reputation of the institution sponsoring the trial, reducing the trust of patients and caregivers. Drugs with sufficiently good safety profiles are then tested in phase II trials, where around 100-300 patients are enrolled in different treatment cohorts characterized by different doses of the drug or a placebo cohort used as control [207]. The aim of this phase is mainly to select the optimal treatment doses and to provide an initial assessment of its therapeutic efficacy in humans when compared to a placebo. The design of this phase is particularly complex, as the clinical teams often need to find a compromise between the number of tested doses and the number of patients per cohort. Spreading the enrolled patients over a large number of doses may result in a loss of statistical power leading to uncertain comparison with placebo or between cohorts, while not testing enough doses may lead to a poor optimization of the therapy. Indeed, considering the significant production cost of some drugs, particularly biologicals, it is fundamental to optimize the treatment doses in order to keep high rate of positive clinical outcome and reduce the treatment cost. Drugs successfully tested in the phase II are then tested in phase III clinical trials. Such trials are usually conducted on 300-3000 patients that are treated with one or two drug doses and compared to a placebo cohort [208, 209]. This is the final step necessary to obtain the approval from health authorities and those trials are designed and statistically powered in order to assess the treatment efficacy, which is quantified using one or several clinical parameters. Successful drugs undergo the approval process of health authorities, which analyze the results of the trials and decide whether a treatment can be commercialized. Once the drug is commercialized and provided to potentially hundreds of thousands or even millions of patients, the pharmaceutical companies monitor the appearance of adverse events. This post-marketing monitoring is often coupled with phase IV clinical trials, which are designed to explore new formulations, new indications, and other patentable innovations [210].

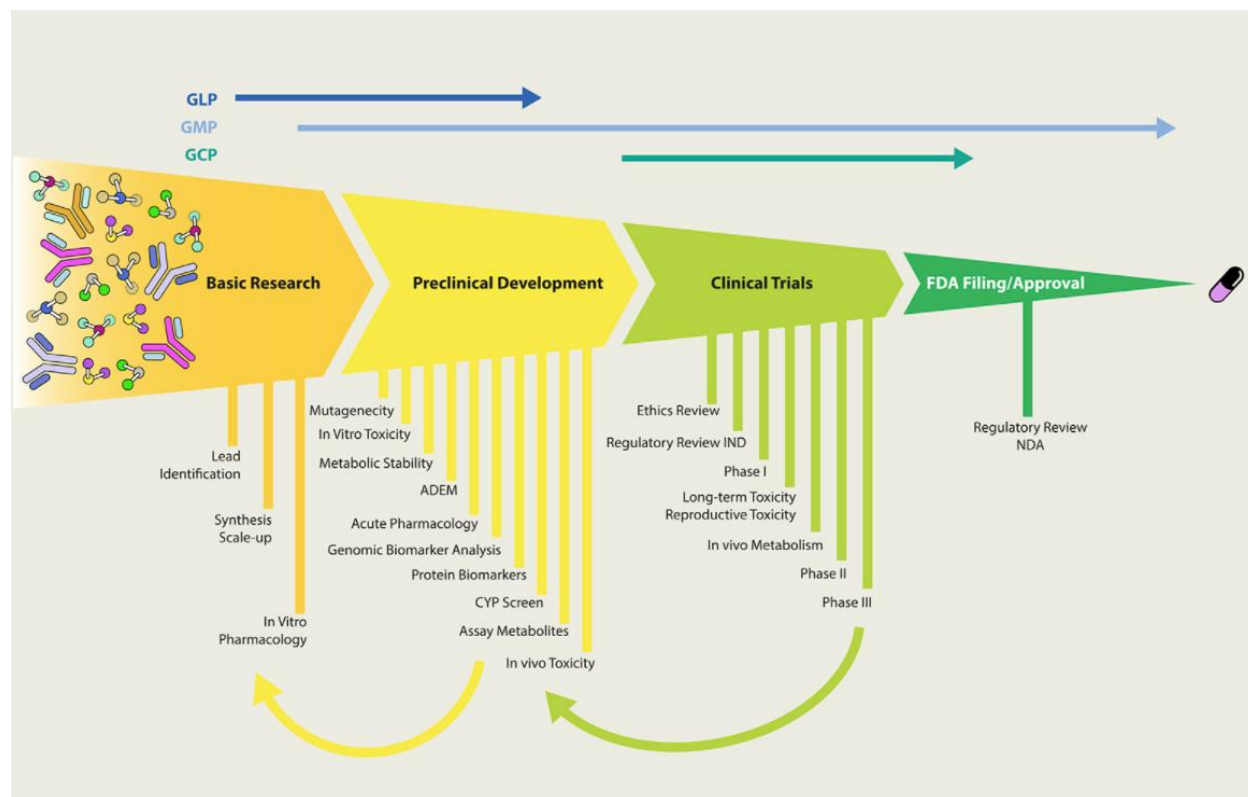


Figure 11:

A schematic of the activities involved in the drug discovery and development process. At the left are shown icons depicting small molecules (NMEs) and biological molecules (NBEs) being considered for development. At the top are the time lines for quality assurance guides governing the process; they are good laboratory practice (GLP), good manufacturing practice (GMP), and good clinical practice (GCP). Specific activities in the stages of development are shown at the bottom; they include studies of absorption, distribution, excretion and metabolism (ADEM), screening for activity at cytochrome P450 (CYP) liver enzymes, and regulatory filings for Investigational New Drug (IND) and New Drug Application (NDA). Abbreviations: NBE, New Biological Entity; NME, New Molecular Entity. Figure published by Mohs et al., "Drug discovery and development: Role of basic biological research", *Alzheimers Dement (N Y)*, 2017 [211].

The cost of drug development increased significantly during the last decades, while the number of approved drugs decreased, which is a serious challenge for the economy of pharmaceutical companies [212]. The structure of the clinical development phase has been changing lately, with the aim of reducing the cost of clinical development and the risk of rejections. For instance, phase I trials in oncology are often coupled with extension studies aimed at testing the efficacy of the treatment [213, 214]. Clinical teams leading phase II clinical trials also tend to optimize the trial design in order to have a better understanding of the potential clinical efficacy of a given treatment and to reduce the failure rate in the following phase III [215, 216]. Biomarkers can also increase the success rate of clinical trials, as they can inform on various aspect of treatments effects, from safety to clinical response. For instance, biomarkers are already widely applied in oncology in order to pre-select patients with highest chances of responding to specific treatments [217]. However, other disease areas have been slower in adopting the use of biomarkers. The financial pressure on pharmaceutical companies to optimize the development cost of new drugs is now a strong driver for an

increase in the exploration and use of biomarkers. This will be particularly relevant in disease areas where the use of biomarkers was considered as “nice to have” but not necessary, such as arthritic diseases.

Autoantibodies as biomarkers

Autoantibodies have been widely studied since a number of decades; however, their use as biomarkers has mostly been restricted to a few well-known examples.

Rheumatoid factor and anti-CCP antibodies

Autoantibodies are already used as diagnostic biomarkers in a number of autoimmune diseases. Some of the most well-known examples are Rheumatoid Factors (RF) and anticyclic citrullinated protein (CCP) antibodies detected to support the diagnosis of RA. RF is present in a large number of diseases and even in healthy elderly individuals, but can help in predicting the development of RA in the general population [218]. Anti-CCP are widely used in RA diagnosis, although present in only around 25-40% of the affected population, because of their high specificity and value in predicting aggressive joint erosion [219, 220]. In clinical practice, it is recommended to use both autoantibodies together because anti-CCP antibodies alone are only moderately sensitive, and the combination of the two markers improves diagnostic accuracy [221]. Increased levels of RF and anti-CCP antibodies were associated with disease severity, progression and morbidity, making them useful prognostic markers [220]. RF and anti-CCP antibodies were investigated as potential predictive markers for anti-TNF α therapy of RA patients, showing that only anti-CCP antibodies were partially useful in predicting clinical response after abatacept treatment [222]. The isotype switching of IgM to IgG and IgA of anti-CCP antibodies is also of particular interest, as the presence of IgG and IgA anti-CCP pre-dated the onset of RA symptoms by years [223]. Levels of anti-CCP antibodies and RF significantly decreased after anti-TNF α treatment, but without correlation to clinical response [224]. Overall, those two autoantibodies have been widely explored as biomarkers in RA and other arthritic diseases, which proved them as useful and robust diagnostic tools and prognostic markers. However, their utility in predicting clinical response was relatively poor, which may be due to the complex pathogenesis of RA and the poor efficacy of current treatments.

Antinuclear antibodies

Another well-known example of autoantibodies used as biomarkers are antinuclear antibodies (ANAs). The presence of ANAs in patients' blood is detected by using intracellular and nuclear antigens from human laryngeal carcinoma (HEp-2 cells), to which ANAs will bind and lead to fluorescent emission, whose patterns can be correlated with certain autoimmune diseases [225]. ANAs are present in 90-95% of Systemic Sclerosis (SSc) patients and are used to support SSc diagnosis [226]. Patients with Sjögren Syndrome (SS) express ANAs directed against a variety of autoantigens too [227]. ANAs are also present not only in most of SLE patients but in 20-30% of healthy individuals as well, therefore their specificity for autoimmune diseases is relatively low, similarly to RF for RA [228]. The biological role of ANAs is not entirely clear, as both pathogenic and protective functions were proposed [229]. ANAs have been applied

as entry criterion for SLE clinical trials enrollment, and patients positive to those autoantibodies have shown significantly better clinical response to belimumab, an anti-TNFSF13B monoclonal antibody [230]. ANAs detection is regularly performed in SLE and SS, which are two relatively similar diseases characterized by the presence of a variety and high concentrations of autoantibodies, mostly targeting nuclear antigens such as DNA, RNA, Histones and ribosomal proteins [231]. Some members of ANAs targeting ribonucleic proteins, such as SSA, SSB, RNP and Sm received a lot of scientific attention in the last few decades, particularly because of their high abundance and specificity, which makes them good diagnostic markers. Anti-SSA and SSB antibodies are detected in 50-90% (depending on cohorts and detection techniques applied) of SS patients and are already used in its diagnosis and stratification [232, 233]. Presence of those autoantibodies pre-dated the development of symptoms and correlated with younger age at diagnosis, longer disease duration and overall higher morbidity [234, 235]. Anti-SSA and SSB antibodies have also been detected in around 30-40% of SLE patient, but without correlation with disease activity [236]. SLE, pSS and overall expression of anti-SSA antibodies is a particularly risky condition during pregnancy, as fetuses run the risk to develop neonatal Lupus [237]. Indeed, maternal anti-SSA antibodies may be passed on to the fetus via transplacental passage and lead to the development of Lupus-like cutaneous symptoms and complete congenital heart block [238, 239]. Anti-Sm and RNP antibodies are also used in the diagnosis of SLE, as they are found respectively in 5-30% and 25-47% of patients [240]. Anti-RNP antibodies have also been associated with disease severity in SS, but their application as potential prognostic markers is still recent [241]. Although there are thousands of different proteins and in the nucleus of cells, only a few of them provoke a strong autoimmune reaction, particularly antigens complexed with DNA and RNA [242]. Those antigens can be “exposed” to the immune system via a number of biological processes, from apoptosis to neutrophil extracellular traps (NETs), and their targeting leads autoantibodies to triggering the complement cascade, penetrating into living cells, modulating gene expression, and even inducing profibrotic phenotypes of renal cells [243-245]. In summary, ANAs and other autoantibodies targeting certain nuclear antigens are widely used diagnostic and prognostic tools applied in the management of a number of autoimmune disease.

Autoantibodies in cancer

Autoantibodies are being explored as biomarkers also in oncology, where early diagnosis is critical for patients survival and potential prognostic or predictive markers might help in giving the right treatment to the right patient [246]. Oncologic diagnosis is mostly based on intrusive, time consuming and complicated examinations, while autoantibodies detection requires minimal intrusiveness (blood sampling) and can be performed in short times with simple ELISA assays. Furthermore, using specific autoantibodies to strengthen diagnosis and prognosis (similarly to RA, SLE and SSc) would help caregivers in selecting the most appropriate treatment and increasing patients' survival [247]. Cancer neoantigens could reflect tumorigenesis, but they are hardly detectable at the early stage, while autoantibodies are biologically amplified and hence may be measurable early on, making them promising biomarkers to discriminate cancerous cells from healthy tissue accurately [248]. Additionally, although current cancer screening

techniques are very efficient, a certain percentage of early cases still passes undetected. For instance, around 15% to 20% of breast cancers cannot be detected via image-based screening, thus autoantibodies filling this gap would be extremely useful in clinical practice [249]. The use of autoantibodies in oncology is still recent, but combinations of autoantibodies already showed good diagnostic potential for lung, breast and colon cancers [250-255]. Moreover, anti-ECPKA autoantibodies were found to be specific markers potentially involved in the development of numerous cancers, thus being a potential diagnostic marker of early phase tumors [256]. Increased levels of autoantibodies directed against tumor-associated antigens (TAAs) have been found in early stages of breast, lung, gastrointestinal, ovarian, colorectal, esophageal, hepatocellular and prostate cancers [257, 258]. A panel of anti-TAAs autoantibodies was tested for the diagnosis of breast cancer and ductal carcinoma in situ (DCIS), reaching 64% and 45% respectively of sensitivity and a specificity of 85% [259]. Overall, autoantibodies use as biomarkers in oncology is still at the exploratory/confirmatory phase but it has the potential to improve the precision of diagnosis and treatments. Interestingly, most studies confirmed that the use of single autoantibodies was not sufficient in achieving useful diagnostic performances, hence the need for the combination of several autoantibodies. The latter approach was applied in this thesis, particularly in the first part of the PhD.

Autoantibodies in neurodegenerative diseases

The field of neurodegenerative diseases is in critical need for biomarkers, from early diagnosis to prognosis, thus autoantibodies have been explored as biomarkers in several neurodegenerative diseases [260]. The interest in autoantibodies in CNS-related diseases derives from the involvement of autoimmunity, particularly B-cells, in their pathogenesis. Emerging evidence suggests that B cells also contribute to the pathogenesis of neurodegenerative diseases, including Alzheimer disease (AD) and Parkinson disease (PD) [261]. For instance, naturally occurring autoantibodies against ss-amyloid and alpha-synuclein have been detected in healthy persons and altered levels in patients were associated with particular neurodegenerative disorders [262]. The role of those NAAs is still not clear, as it was suggested that they may have a protective role [263-265]. In the case of PD, it was hypothesized that several autoantibodies directed at antigens associated with its pathogenesis may activate the immune system and lead to neuroinflammation, which would be the cause of symptoms development and disease progression [266, 267]. In AD, autoantibodies targeting amyloid peptides, protein Tau, neurotransmitter receptors, glial markers and oxidized low-density lipoproteins are thought to participate in the disease pathogenesis, particularly in neurons death [268, 269]. The use of autoantibodies profiling in neurodegenerative diseases is still at the exploratory phase, but it may improve disease understanding and clinical practices. Indeed, autoantibodies may pre-date symptoms by years, allowing an early diagnosis and a timely prevention of disease progression. Although of critical importance, autoantibodies with such potential have not been identified yet in neurodegenerative diseases.

Aim of the thesis

As presented throughout the introduction, the immune system plays a critical role in both homeostasis and disease pathogenesis. Therefore, components of the immune system have been targets for immunomodulatory therapies. Monoclonal antibodies targeting key components have been widely tested and their efficacy was proven in a number of diseases. However, a significant part of treated patients does not achieve a positive clinical response, particularly in autoimmune diseases with a heterogeneous pathogenesis. Identifying biomarkers able to predict which patients would positively respond or not to a given treatment would drastically improve the efficacy of therapeutic approaches. Indeed, pre-selecting patients with higher chances of achieving clinical response would allow for an improved tailoring of therapies. Such approach would be particularly useful in the context of complex autoimmune diseases, from arthritis to urticaria, and from systemic to skin or organ-specific conditions. The treatment of those diseases is particularly challenging, as several pathways might be involved in their pathogenesis and their symptomology can be wide and difficult to assess. Therefore, using biomarkers able to distinguish which therapeutic approaches are relevant, within a certain diseases for a given patient, would be a tremendous advancement toward precision medicine, which would translate in giving the right compound at the right dose to the right patient.

As already described in the corresponding section, autoantibodies are potentially useful biomarkers for the prediction of clinical response. They are easy to detect, since ELISA-like immunoassays are sensitive enough, and their testing is non-intrusive, as the main biological matrices used are serum and plasma.

The aim of this thesis was to apply autoantibodies profiling to clinical trials of three different diseases and treatments.

Autoantibodies profiling in an anti-IL17 clinical trial of Psoriatic Arthritis

Anti-IL17 treatment was proven to be efficacious in the treatment of Psoriatic Arthritis (PsA). However, only around 33% of patients achieved significant clinical response (ACR50), while around 80% of psoriasis patients achieved a clinical response (PASI scores) using the same drug. Finding markers able to identify responders or non-responders to anti-IL17 treatment at baseline would help in increasing treatment efficacy by pre-selecting patients. Hence, I performed autoantibodies profiling on baseline PsA serum samples from an anti-IL17 clinical trial with two purposes. Firstly, I attempted to find autoantibodies specifically present in ACR50 responders versus non-responders, with the final goal to build a panel of markers that may result in the development of a companion diagnostic for anti-IL17 treatment of PsA. The second purpose was to test a high number of autoantibodies in order to increase our technical knowledge in autoantibody detection and identify markers that might be relevant for other diseases.

Autoantibodies profiling in Hidradenitis Suppurativa

HS is a well-characterized disease but its etiology is still not well known, so there is a need for biomarkers able to improve our understanding of molecular and cellular pathways involved in its pathogenesis. B-cells

and aggressive immune system activation were observed in HS skin lesions. Therefore, the goal of autoantibodies profiling was to identify and characterize specific autoantibodies that might be linked to disease development and strengthen the hypothesis of B-cells involvement.

Anti-FcεR1a autoantibodies and sFcεR1a detection in Chronic Spontaneous Urticaria

Anti-FcεR1a autoantibodies are thought to initiate mast cells and basophils activation by cross-bridging with cell surface receptors, thus causing Urticaria symptoms. Patients expressing anti-FcεR1a autoantibodies would potentially not respond to an anti-IgE treatment, as they may activate mast cells and basophils in an IgE-free manner. The goal of this project was to investigate the possible correlation between anti-FcεR1a autoantibodies in sera from Chronic Spontaneous Urticaria (CSU) patients and their response to an anti-IgE treatment. Moreover, soluble FcεR1a (sFcεR1a) was tested as surrogate marker for cell-bound FcεR1a. It was observed that surface expression of FcεR1a on basophils decreased after anti-IgE treatment, thus cell-bound FcεR1a is considered as a relevant mechanistic marker for such treatment. However, the detection of cell-bound FcεR1a is of difficult application in large phase III clinical trials performed in numerous clinical sites. Indeed, its detection is based on a cellular assay using blood as sample matrix, which can be challenging from a logistic point of view. Blood needs to be quickly processed and delivered to central laboratories performing the biomarker assay, which can introduce a variability in the collection, storage and handling of samples that would also be reflected on the quality of the biomarker data. A soluble form of FcεR1a is detectable in serum, which is a matrix more easily handled in large clinical trials. I quantified sFcεR1a in CSU patients in order to verify whether the soluble form concentration would decrease after treatment, as described for the cell-bound form.

Results part I: Autoantibodies profiling in an anti-IL17 clinical trial of PsA

Introduction

Psoriatic arthritis (PsA) has been defined as an inflammatory arthritis associated with psoriasis, and it has been included in the group of spondyloarthropathies together with ankylosing spondylitis, reactive arthritis, inflammatory bowel disease associated spondyloarthritis and undifferentiated spondyloarthritis [270]. It has a prevalence of 2–4% in adults from Western countries, and 20–30% of psoriasis patients are at risk of developing psoriatic arthritis [271, 272]. The pathogenesis of PsA is complex and not well understood, with genetic and environmental factors involved together with immune-mediated inflammation [273, 274]. The complexity of its pathogenesis is reflected by the heterogeneity of PsA symptoms, including arthritis, enthesitis, dactylitis and axial as well as potential skin and nail involvement [275]. The correct diagnosis of PsA, particularly at an early stage, is critically important but it also represents a major challenge, as both psoriasis and PsA remain under recognized and undertreated in current clinical practice [276]. A delayed diagnosis of PsA is associated with long-term adverse outcomes, while an early detection of PsA development may prevent significant joint damage and associated disability [277]. The overlapping symptomology of psoriasis and PsA forces both rheumatologists and dermatologists to collaborate and perform complex differential diagnosis supported by the use of questionnaires for PsA development risk and recent imaging techniques [278, 279]. Similarly to its diagnosis, PsA treatment is challenging as well. PsA patients are typically treated with a combination or alternation of methotrexate (MTX), nonsteroidal anti-inflammatory drugs (NSAIDs), disease-modifying antirheumatic drug (DMARD) or anti-TNF agents, with the latter being the most effective in slowing down or stopping the radiographic progression of joint damage [280-282]. The most used clinical endpoints for evaluation of PsA treatments are ACR20, 50 and 70, which correspond to a decrease of 20, 50 and 70% respectively of arthritic symptoms [283]. Although highly effective, TNF antagonists fail to induce a response in 25-33% of patients, with ACR20 achieved in around 40% of treated patients [284]. Recently approved treatments of PsA are based on the inhibition of IL12/23, IL17, JAK, and CTLA-4, which achieved similar or slightly higher ACR20 response rates to TNF inhibitors but showed better safety profiles [284, 285]. Although PsA treatment improved significantly in the last decade thanks to the use of new therapies, there are still gaps that need to be bridged in early diagnosis and prediction of treatment efficacy. In the last years, many different kind of biomarkers were explored in PsA, with the aim of supporting diagnosis, prognosis and treatment outcome prediction [286]. Although several markers were associated with favorable PsA treatment outcome, none is currently applied in clinical practice [287, 288]. Autoantibodies have been widely explored as biomarkers in RA, but PsA and psoriasis have been considered as seronegative diseases and, consequently, there is a small number of published studies on autoreactive immunoglobulin as potentially useful markers in PsA [289-293]. In the context of anti-IL17 treatment of PsA, we hypothesized that autoantibodies may be useful markers for the prediction of treatment non-response. Such hypothesis was based on the dichotomy of PsA, which present both psoriatic and arthritic components. Anti-IL17 therapy was approved for the treatment of both psoriasis and PsA, and it reduced disease activity in RA, but a clear difference in clinical response rates was observed.

Indeed, 35.2% of RA patients achieved ACR20 after 24 weeks of anti-IL17 treatment, while ACR20 response rate was of 50-60% in PsA and psoriasis-specific clinical endpoint PASI75 (Psoriasis Area Surface Index 75, refers to decrease of 75% of skin surface affected by psoriasis) was achieved in 80-90% of psoriasis treated patients [294-297]. Overall, anti-IL17 treatment resulted more efficacious in the treatment of psoriasis-related symptoms (PASI), when compared to arthritis-related symptoms decrease (ACR). As already mentioned, PsA and psoriasis patients are thought to express lower levels and variety of autoantibodies, when compared to RA. Therefore, the presence of specific autoantibodies in PsA patients may be representative of RA components and thus potentially correlate with a non-response, for ACR scores, to anti-IL17 treatment. In the context of my thesis, I performed autoantibodies profiling using the baseline samples of one of the anti-IL17 phase III clinical trials performed by Novartis, NCT01392326. The final goal of this project was to identify one or a group of autoantibodies that would discriminate between responders and non-responders, and potentially predict which patients would not respond, to anti-IL17 treatment.

Clinical trial description and samples selection

NCT01392326 was a randomized, double-blind, placebo-controlled, multicenter study of secukinumab (Cosentyx, an anti-IL17 humanized antibody) to demonstrate the efficacy at 24 weeks and to assess the long term safety, tolerability and efficacy up to 2 years in patients with active psoriatic arthritis. The study population consisted of a representative group of both RF and anti-cyclic citrullinated peptides (CCP) negative subjects of at least 18 years of age and with active PsA. More information on the patients inclusion and exclusion criteria used in this study can be found in the methods section. Figure 12, published by Mease et al, is a schematic representation of the study's structure [298].

Considering the aim of the autoantibodies profiling approach, which was to find biomarkers that can discriminate clinical non-responders from responders and potentially predict which PsA patients would not respond to anti-IL17 treatment, only baseline samples from all treatment groups and placebo arm, with valid ICF for exploratory biomarkers activities, were selected and used. 566 samples were finally selected and used in the autoantibodies profiling experiments.

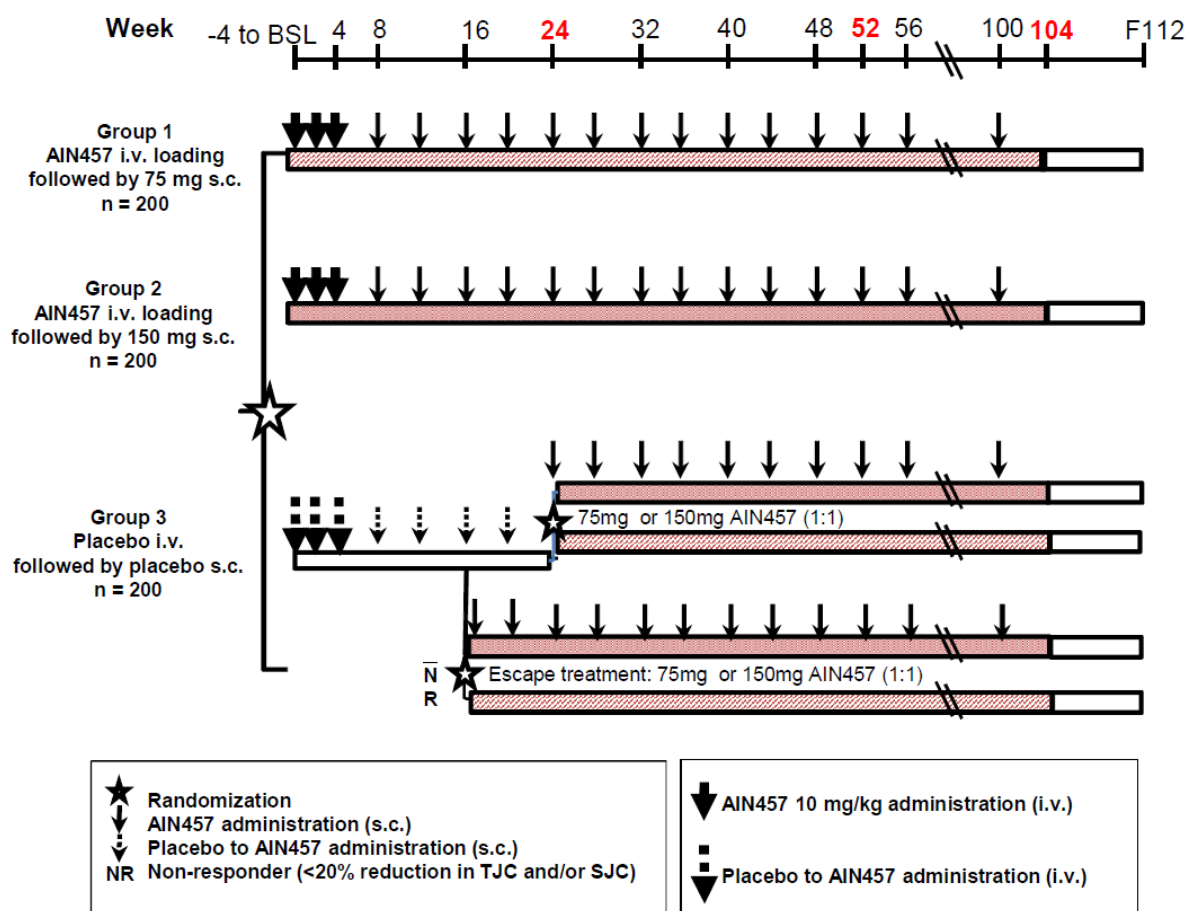


Figure 12:

Scheme representing the structure of the clinical trial NCT01392326. After recruitment, patients were randomized in either placebo, 75 mg s.c. or 150 mg s.c. dose of anti-IL17 (AIN457). At week 16, ACR20 non-responders in placebo cohort were treated with either 75 mg or 150 mg of anti-IL17. At week 24, ACR20 responders in the placebo cohort were treated with either 75 mg or 150 mg of anti-IL17. Published by Mease et al, "Secukinumab Inhibition of Interleukin-17A in Patients with Psoriatic Arthritis", *N Engl J Med*, 2015 [298].

Antigens selection

PsA being a complex disease, with several pathways potentially involved in the pathogenesis and in the progression of the disease, the panel of antigens used in the autoantibodies profiling needed to reflect this diversity. Therefore, I selected 208 antigens covering numerous proteins and post-translational modification families, of both self and microbial origin. The complete list of antigens is available in the methods section. Some of the most relevant antigens groups were:

- Linked to cells and tissues structures such as Collagen I, II, III, IV, V, VI and Myosin.
- Previously described to be specific of anti-TNFa non-responders RA samples (COG4, PPP2R1A, KPNB1, RAB11B) [299].
- Nuclear antigens such as SSA, SSB, Sm, RNPs, Histone, DNA, RNA.

- Viral antigens: EBV (*Epstein-Barr Virus*), CMV (*Cytomegalovirus*) and HBV (*Hepatitis-B virus*) proteins.
- Bacterial antigens: Flagellin-BSA, *Lachnospiraceae*, *Helicobacterium*, *Streptococcus pyogenes*, *Prevotella*.
- Fungal antigens from *Candida albicans* and *Saccharomyces cerevisiae*.
- Circulating proteins such as Fibrinogen, Immunoglobulins, Apolipoprotein E (ApoE), Prothrombin.
- Post-translational modifications such as Advanced Glycation Events (AGEs), Citrullinated BSA, Trimethyllysine-BSA, Glycated-BSA.
- Cytokines and cytokines receptors, such as IL1b, IL6, IL17A, IL17F, IL23, IL17R, IL21R, IL22R, IL23R.
- Thyroid proteins: TPO and Thyroglobulin.

Clinical endpoint selection

The clinical parameter used as endpoint to evaluate the performance of the anti-IL17 treatment in this clinical trial was ACR20 after 24 weeks of treatment. ACR20 is a composite score defined as both improvement of 20% in the number of tender and number of swollen joints, and a 20% improvement in three of the following five criteria: patient global assessment, physician global assessment, functional ability measure, visual analog pain scale and erythrocyte sedimentation rate or C-reactive protein (CRP) [300]. ACR50 and ACR70 have the same definition as ACR20, but with an improvement of 50% and 70% respectively. Table1 shows that by using ACR20 as response criteria, around 50% of PsA patients were classified as responders to the anti-IL17 treatment. ACR50 and ACR70 responders in the treatment arms were respectively 30.7-34.7% and 16.8-18.8%. Another response criteria monitored during the study was the PASI score. Similarly to ACR, PASI (Psoriasis Area and Severity Index) is a composite score taking into account the surface and severity of psoriatic lesions on the patients skin [301]. PASI75 and PASI90 indicate a reduction of the PASI score from baseline of 75% and 90% respectively.

Treatment	ACR20	ACR50	ACR70	PASI75	PASI90
150 mg/kg	50%	34.7%	18.8%	61.1%	45.4%
75 mg/kg	50.5%	30.7%	16.8%	64.8%	49.1%
Placebo	17.3%	7.4%	2%	8.3%	3.7%

Table 1:

Summary of ACR20, ACR50, ACR70, PASI75 and PASI90 responders' rate at week 24 for each patients' cohort in the study NCT01392326. Data published by Mease et al, "Secukinumab Inhibition of Interleukin-17A in Patients with Psoriatic Arthritis", *N Engl J Med*, 2015 [298].

The choice of which response criteria should be preferred for the statistical analysis was critical and driven by 3 factors: confounding placebo effect, clinical relevance and samples size. As shown in Table 1, ACR20 was achieved in 17.3% of patients receiving placebo, while 7.4% achieved ACR50 and 2% achieved ACR70. Although a clear difference between treatment and placebo arms in the response ratio for ACR20, we estimated that the confounding placebo effect was too high and would potentially pollute the results of

the statistical analysis of autoantibodies profiles. Furthermore, ACR50 and ACR70 were considered as stricter response criteria. Therefore, ACR20 was not considered as the preferred clinical endpoint for our analysis. PASI scores were also considered less relevant, as they are skin-related while PsA most critical burden is represented by its arthritis symptoms. ACR50 was preferred to ACR70, as the number of ACR70 responders was estimated too low to have enough statistical power in order to significantly discriminate them from non-responders.

ACR scores were assessed throughout the entire clinical trial, but only week 24 was considered as the time-point to be used to evaluate clinical treatment efficacy. This decision was taken after discussion with the clinical team, which considered previous and later time-points as less informative. Moreover, the efficacy of secukinumab was assessed based on response rates at week 24. Earlier time points were disregarded as response rates were not stabilized before week 16 (Figure 13), which was not taken into account together with week 20 as considered too close to week 24. Later time-points were disregarded as well, as considered less clinically relevant when compared to week 24.

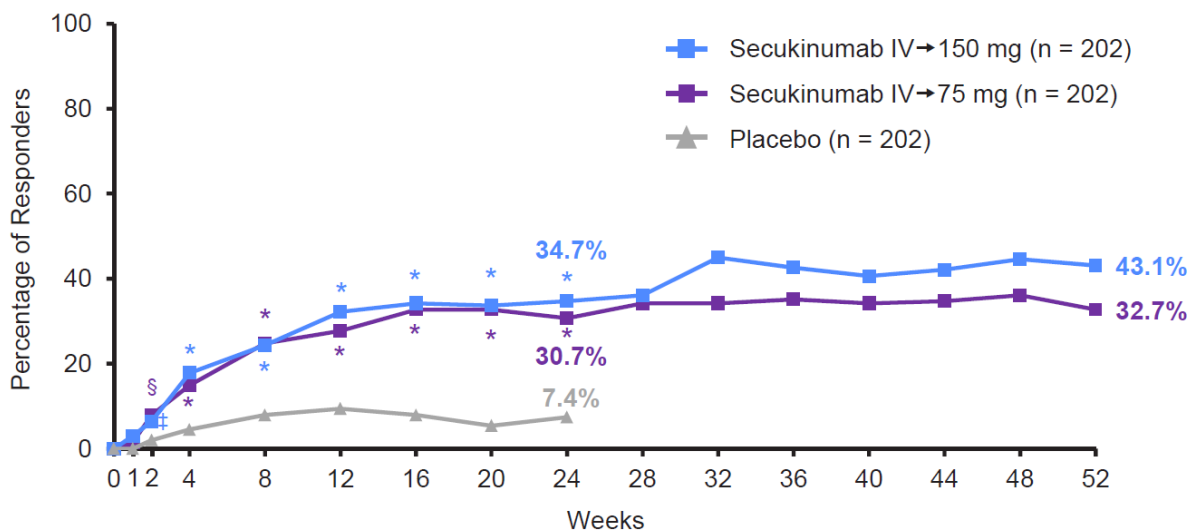


Figure 13:

The proportion of patients with at least a 50% improvement in American College of Rheumatology response criteria (ACR50) through the 52 weeks of treatment is shown. P-values for ACR50 response at week 24 were tested as part of the statistical hierarchy and adjusted for multiplicity. * p-value <0.001, § p-value <0.01, ‡ p-value <0.05 versus placebo. Figure published by Mease et al, "Secukinumab Inhibition of Interleukin-17A in Patients with Psoriatic Arthritis", *N Engl J Med*, 2015 [298].

Sensitivity and specificity parameters

Sensitivity, or true positives rate, is defined as the proportion of correctly detected positives. In the case of this project the aim was to detect ACR50 non-responders, hence the sensitivity corresponds to the proportion of ACR50 non-responders correctly identified as non-responders. Specificity, or true negatives

rate, is defined as the proportion of correctly identified negatives. In the case of this project, the “negatives” correspond to ACR50 responders, therefore the specificity is defined as the proportion of ACR50 responders correctly identified as responders. The minimum levels required for sensitivity and specificity were discussed together with secukinumab clinical team. The highest priority was given to the specificity of the differentiation between responders and non-responders. Indeed, there should be no risk of not giving the drug to a patient that would actually respond positively to the treatment. This translated in fixing a specificity of 100% when detecting ACR50 non-responders, which means that all ACR50 responders would be identified as responders. Another suggestion from the clinical team was to achieve a sensitivity of at least 70% when detecting ACR50 non-responders, which was considered as a minimum threshold to represent a commercial interest for a potential companion diagnostic. In order to avoid a risk of data overfitting during the predictive model building phase, it was decided that the number of markers selected to discriminate ACR50 non-responders from responders should not be higher than 20. Therefore, the minimum requirements for a successful discrimination between ACR50 non-responders and responders were 70% sensitivity, 100% specificity and not using more than 20 markers.

Results

Higher autoantibodies levels in ACR50 non-responders

566 baseline serum samples from CSU patients of the clinical study NCT01392326 were analyzed by autoantibody profiling assay based on Luminex (details in methods section) in order to detect IgG, IgM and IgA autoantibodies targeting 208 different antigens. The dataset obtained counted more than 355000 data points (Figure 14A). This dataset was mined to investigate the presence of autoantibodies that could discriminate between ACR50 responders and non-responders. The volcano plot in Figure 14B shows that none of the autoantibodies could be considered as significantly over- or under-expressed between ACR50 responders and non-responders when considering both p-value and average fold change. Hence, I focused the analysis on the autoantibodies presenting at least a significant p-value after T-test to compare levels in ACR50 responders and non-responders. Indeed, when considering only the p-value some autoantibodies, such as IgG anti-Lachnospiraceae, IgG and IgM anti-ssDNA and IgG anti-Annexin 2, were significantly more expressed in ACR50 non-responders, although the fold change would be classically judged as non-significant. Figure 14B also shows that most differentially expressed autoantibodies have higher signal in ACR50 non-responders, compared to ACR50 responders. Such result was expected and in line with previous findings with the hypothesis that anti-IL17 treatment efficacy might be lower in PsA patients with higher levels of autoantibodies, hence with a possibly more RA-driven PsA.

Autoantibodies signals distribution and positivity rates

Autoantibodies signal distribution is fundamentally different when compared to other markers such as proteins or RNA. Indeed, except for rare cases, most samples have a “negative” (background level, 100-

300 MFI) or mildly positive (300-1000 MFI) signal for a given autoantibody, with only a “tail” of samples being positive (>1000 MFI) or highly positive (>5000 MFI).

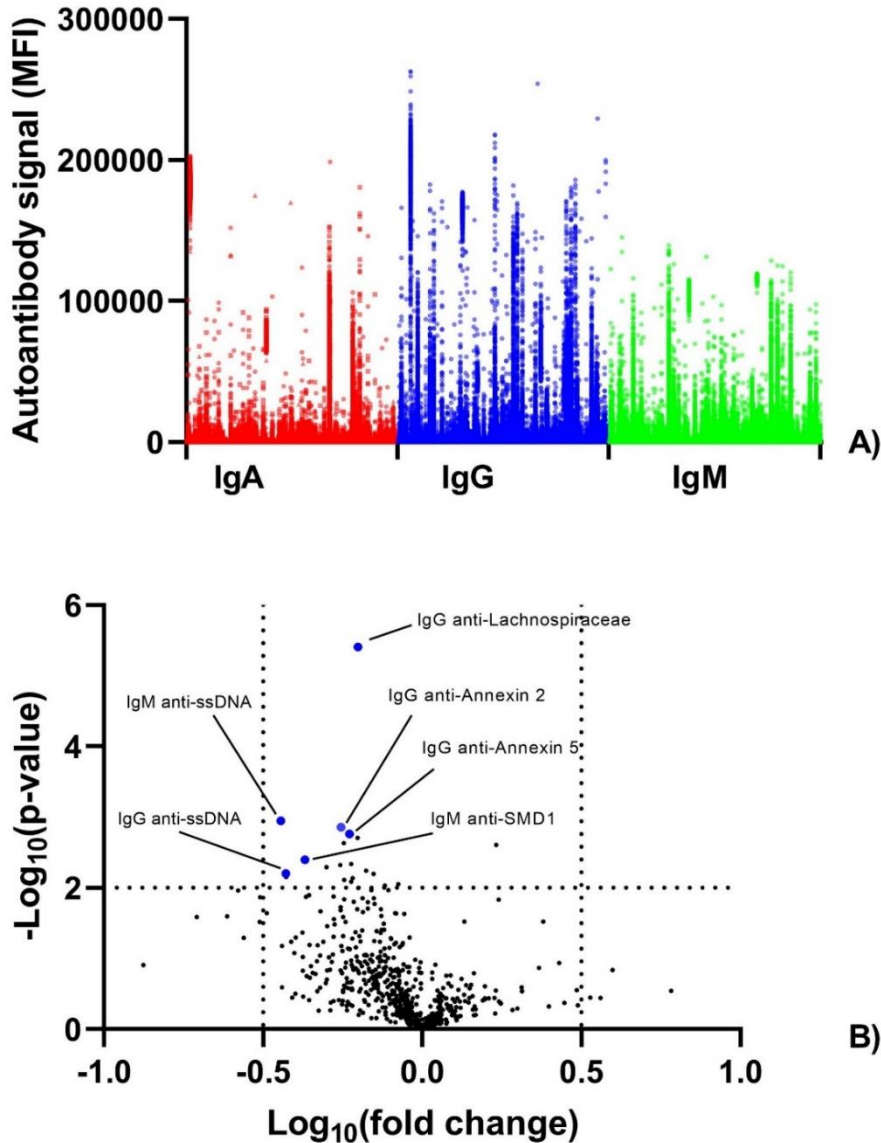


Figure 14:

A) Scatter plot showing the totality of IgA (red), IgG (blue) and IgM (green) signals (expressed in MFI, Median Fluorescence Index) obtained measuring autoantibodies directed against 208 different antigens (details in methods section) using serum samples from 566 CSU patients from the clinical trial NCT01392326. Data obtained by autoantibody profiling assay based on Luminex; $n=188$ for patient from 150 mg treatment group; $n=188$ for patients from 75 mg treatment group; $n=190$ for patients from placebo group. B) Volcano plot showing the difference in autoantibodies levels at baseline between ACR50 responders vs non-responders in the 150 mg ($n=188$) and 75 mg ($n=188$) treatment arms of the study NCT01392326. The fold change for each autoantibody was calculated by dividing the mean levels of ACR50 responders by the mean levels of ACR50 non-responders. Data obtained by autoantibody profiling assay based on Luminex. P-values were calculated with unpaired, double tailed, T-test.

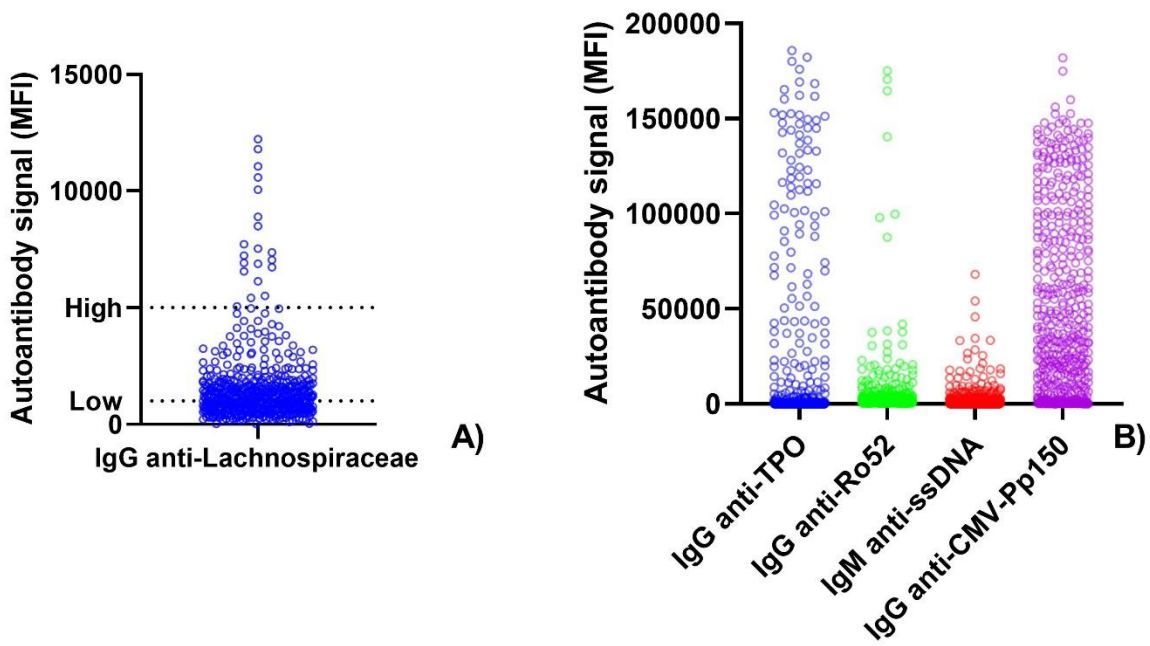


Figure 15:

A) IgG anti-Lachnospiraceae signals (measured by autoantibody profiling assay based on Luminex) distribution for all samples from NCT01392326. High positivity threshold set at 5000 MFI, low positivity threshold level set at 1000 MFI, $n=566$. B) Signals distributions of IgG anti-TPO (Thyroid Peroxidase, blue), IgG anti-Ro52 (Sjogren Syndrome antigen 52, green), IgM anti-ssDNA (single strand DNA, red), IgG anti-CMV-Pp150 (Cytomegalovirus Pp150, purple), $n=566$ for all autoantibodies. Data obtained by autoantibody profiling assay based on Luminex.

Some examples of autoantibody signals distribution are shown in Figure 15. Figure 15A shows the distribution of IgG anti-Lachnospiraceae, which can be considered as a usual autoantibody signals distribution. The tail of positive signals is the “interesting” part of the data set, as those are the ones that can be differentiated from the rest of the population and harbor the potential for endotyping. Figure 15B shows the distributions of autoantibodies targeting different kind of autoantibodies. IgG anti-TPO is a well known autoantibody present in a number of diseases, but also in healthy volunteers. A cloud of negative samples and a uniform distribution of positive and highly positive samples characterize its distribution. IgG anti-Ro52 and IgM anti-ssDNA distributions are characterized by fewer highly positive samples and larger negative cloud. IgG anti-CMV-Pp150, an antibody directed against an antigen from *Cytomegalovirus*, presents a uniform distribution with a relatively small negative cloud and most of samples above the high positivity threshold. It is clear that each antigen is targeted differently by the immune system, with anti-nuclear antigens (Ro52 and ssDNA) autoantibodies being present in a relatively small portion of samples population while anti-viral (CMV) antibodies are present in the majority of samples. The rate of positivity,

defined as the percentage of samples with signals above the positivity threshold of 1000 MFI, varied significantly between antigens.

Positivity rate thresholds (%)	Number and percentage of IgA antibodies	Number and percentage of IgG antibodies	Number and percentage of IgM antibodies
>70	25; 12%	46; 22%	31; 14.9%
>50	36; 17%	66; 31.7%	56; 26.9%
>30	59; 28.4%	87; 41.8%	72; 34.6%
>20	70; 33.7%	101; 48.6%	85; 40.8%
>10	89; 42.8%	123; 59.1%	104; 50%
>5	111; 53.4%	138; 66.3%	124; 59.6%
<5	97; 46.6%	70; 33.7%	84; 40.4%

Table 2:

Summary of numbers and percentages of autoantibodies with positivity rates (percentage of samples with signal above 1000 MFI) above several thresholds, divided per isotype. This table gives an overview of the abundance of autoantibodies for each isotype. The percentages were calculated by dividing the number of autoantibodies with positivity rate above specific thresholds by the total number of autoantibodies per isotype (n=208). Autoantibodies data from all samples (n=566) were used for this analysis.

Autoantibodies with positivity rate below 5% have a low potential for discriminating between samples categories. Even if all positive samples belonged to a specific group, the low positivity rate and hence low sensitivity would bring a high risk of data overfitting. As shown in Table 2, 46.6% of IgA, 33.7% of IgG and 40.4% of IgM autoantibodies was characterized by a positivity rate below 5%.

The 20 “best hits” of autoantibodies most differentially expressed between ACR50 non-responders and responders, ordered by ascending p-value, are listed in Table 3. Within this list, 19 autoantibodies were overexpressed in ACR50 non-responders, while only IgG anti-*Shigella* showed higher signals in responders. Interestingly, most of the listed antigens are located in the cell nucleus, such as single and double strand DNA, Ro52 and SMD1. Anti-nuclear antibodies (ANAs) are linked to inflammation and cell necrosis [302-304], suggesting that such phenomena might be more important in the tissues of ACR50 non-responders. IgM anti-IL17R is listed as well (with IgG anti-IL17R being slightly overexpressed in ACR50 non-responders too), which is particularly relevant in a clinical trial of an anti-IL17 drug. Such result would suggest that the immune system is already targeting the IL17 pathway and possibly inhibiting it. Therefore, an anti-IL17 treatment might be less efficacious in such patients, as it may be a redundant inhibitory action. The antibody showing the highest difference between ACR50 responders and non-responders was IgG anti-Lachnospiraceae, which is a commensal bacterium. This result was particularly interesting, as PsA development is linked to microbiome alteration, and Lachnospiraceae is a core member of the gut microbiome [305, 306].

Antibody	p-value	Overexpressed in	Antigen family
IgG anti-Lachnospiraceae	3.9*10 ⁻⁶	Non-responders	Commensal bacteria
IgM anti-ssDNA	1.1*10 ⁻³	Non-responders	Nuclear
IgG anti-Annexin 2	1.3*10 ⁻³	Non-responders	Circulating protein
IgG anti-Annexin 5	1.7*10 ⁻³	Non-responders	Circulating protein
IgG anti-Alpha Actinin	1.9*10 ⁻³	Non-responders	Structural protein
IgM anti-IL21	2.3*10 ⁻³	Non-responders	Circulating protein
IgG anti-Shigella	2.4*10 ⁻³	Responders	Deleterious bacteria
IgM anti-SMD1	3.9*10 ⁻³	Non-responders	Nuclear
IgG anti-dsDNA	4.5*10 ⁻³	Non-responders	Nuclear
IgA anti-HSP65	4.7*10 ⁻³	Non-responders	Intracellular
IgM anti-Ro52	5.7*10 ⁻³	Non-responders	Nuclear
IgG anti-ssDNA	6.2*10 ⁻³	Non-responders	Nuclear
IgA anti-Intrinsic Factor	6.3*10 ⁻³	Non-responders	Glycoprotein
IgG anti-S100B	7.0*10 ⁻³	Non-responders	Nuclear
IgM anti-PL7	7.7*10 ⁻³	Non-responders	Nuclear
IgG anti-Hemoglobin A2	8.8*10 ⁻³	Non-responders	Circulating protein
IgM anti-Cytokeratin 18	9.2*10 ⁻³	Non-responders	Structural protein
IgG anti-IL26	1.0*10 ⁻²	Non-responders	Circulating protein
IgM anti-Trimethyllysine-BSA	1.1*10 ⁻²	Non-responders	Post-translational modification
IgM anti-IL17R	1.1*10 ⁻²	Non-responders	Membrane protein

Table 3:

List of the 20 autoantibodies most differentially expressed between ACR50 responders and non-responders, ordered by ascending p-value after unpaired, double-tailed T-test; n ACR50 non-responders = 249; n ACR50 responders = 127. Only samples from the 150 mg (n=188) and 75 mg (n=188) treatment cohorts were considered for this analysis. For each antigen it is specified whether the corresponding autoantibody was overexpressed in ACR50 responders or non-responders, as well as the antigen family.

Hypothetically, an increased production of IgG targeting Lachnospiraceae might be linked to an alteration of gut microbiome and a different endotype of PsA. Another interesting finding was the overexpression of IgM anti-IL21 in ACR50 non-responders. IL21 is associated with psoriasis severity and with an imbalance in Th17 and T-reg cells [307, 308], suggesting that the production of anti-IL21 autoantibodies by the immune system might be a form of autoregulation or homeostasis maintenance. Autoantibodies targeting Alpha Actinin might also have a role in the pathogenesis of arthritic diseases by being linked to the signaling pathway of TNF α and IL1 [309]. Although the overexpressed autoantibodies in ACR50 non-responders could be linked to PsA pathogenesis and IL17 pathway, only a subset of samples showed increased signals for a given marker. As shown in Figure 16, when considering single antibodies, only a fraction of highly positive ACR50 non-responders samples could be clearly discriminated from ACR50 responders.

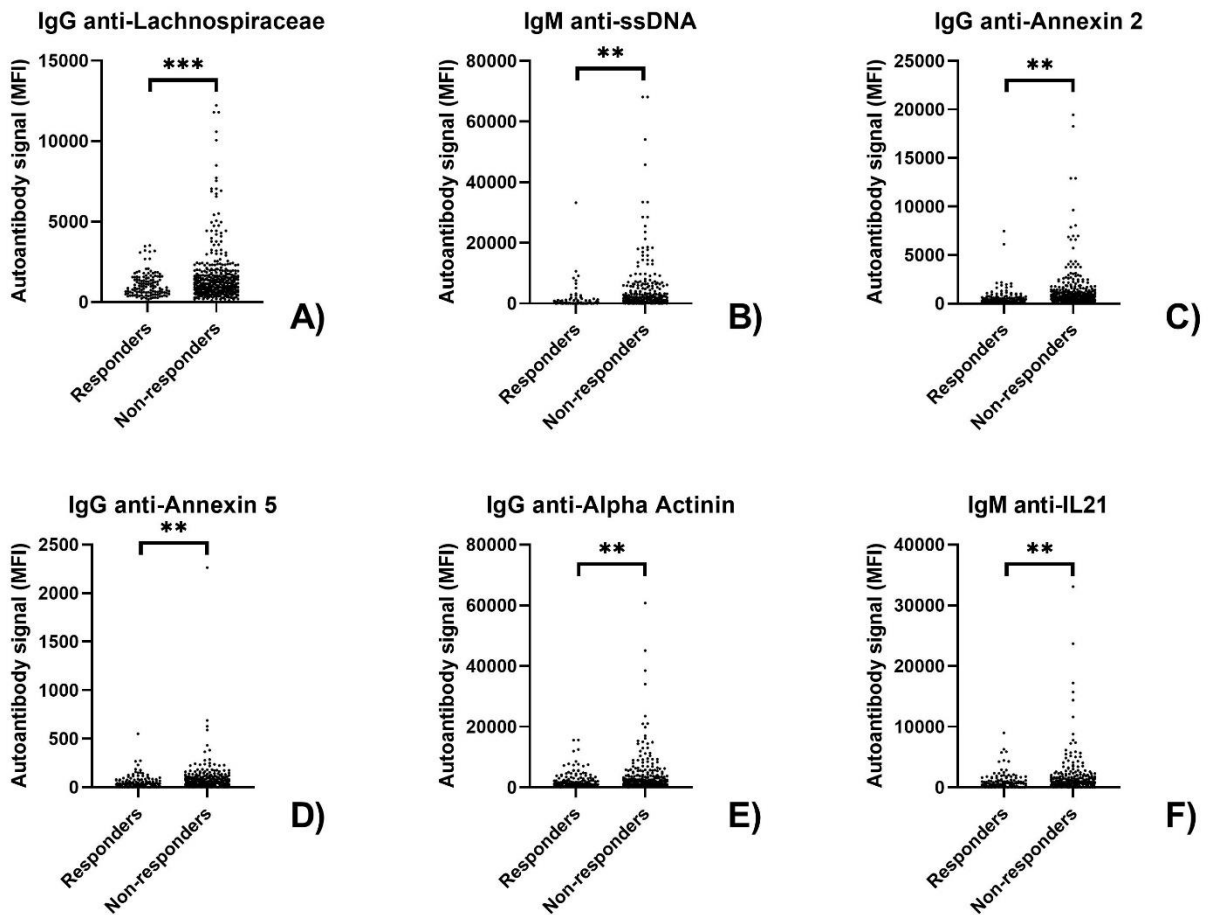


Figure 16:

Autoantibody profiles of A) IgG anti-Lachnospiraceae; B) IgM anti-ssDNA; C) IgG anti-Annexin 2; D) IgG anti-Annexin 5; E) IgG anti-Alpha Actinin; F) IgM anti-IL21. For all autoantibodies, n ACR50 non-responders = 249, n ACR50 responders = 127. All data obtained by autoantibody profiling assay based on Luminex. Only samples from the 150 mg ($n=188$) and 75 mg ($n=188$) treatment cohorts were considered for this analysis. Autoantibodies levels of ACR50 responders and non-responders were compared with Mann-Whitney test.

Such poor discrimination between responders and non-responders while using a single autoantibody was expected. Indeed, positivity rates for autoantibodies are rarely above 20-30%. Moreover, autoantibodies specifically present in a clinically selected population subset of a complex disease such as PsA have even less chances of being abundant. Additionally, the patients selected to participate in the clinical study NCT01392326 were screened as RF and anti-CCP negative before enrolment, hence they did not express the most common autoantibody in arthritic diseases.

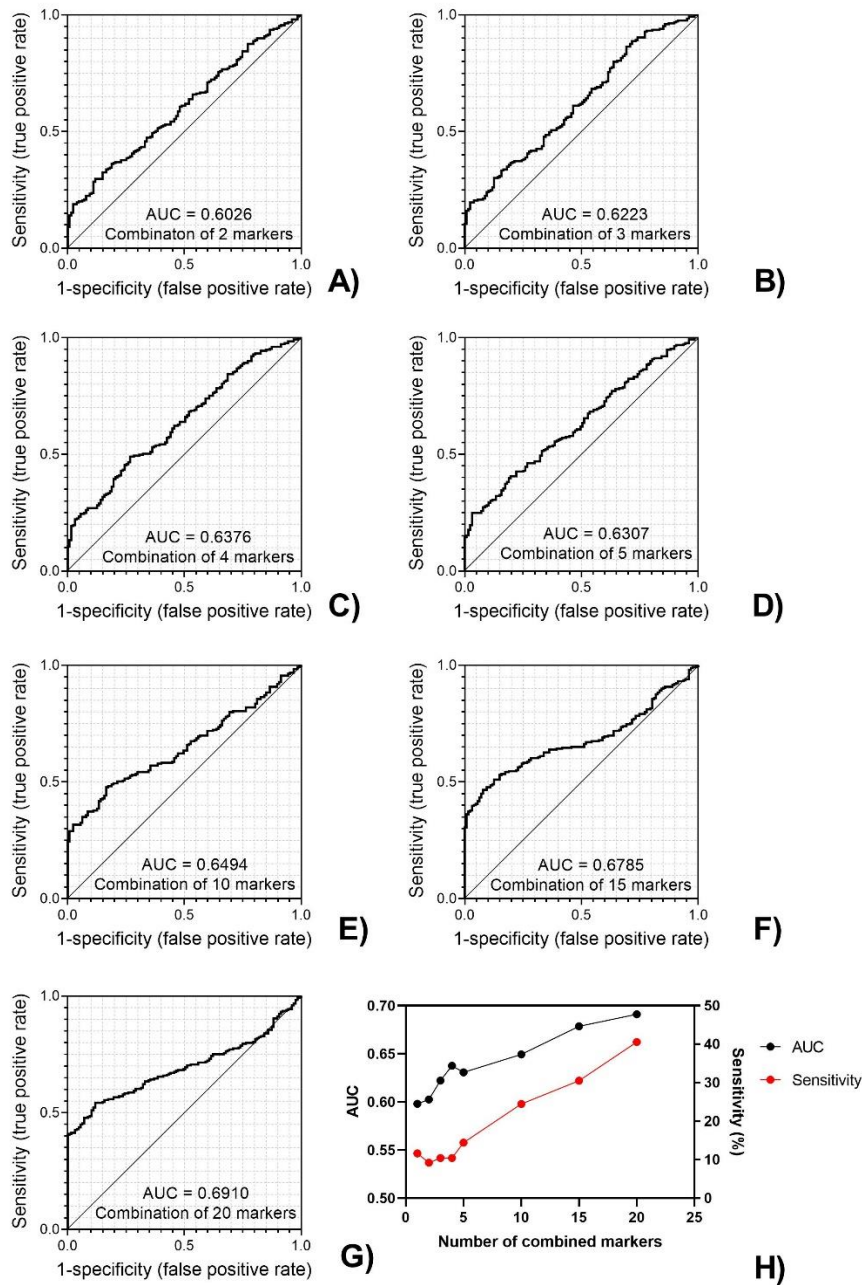


Figure 17:

Receiver operating characteristic (ROC) curve showing the performance (expressed in AUC, area under the curve), in discriminating ACR50 non-responders from responders, of linear combinations (details in method section) of autoantibodies when increasing the number of markers used in the combination. A) $n=2$, autoantibodies used: IgG anti-Lachnospiraceae and IgM anti-ss-DNA. B) $n=3$, autoantibody added: IgG anti-Annexin 2. C) $n=4$, autoantibody added: IgG anti-Annexin 5. D) $n=5$, autoantibody added: IgG anti-Alpha Actinin. E) $n=10$, autoantibodies added: IgM anti-IL21, IgM anti-SMD1, IgG anti-dsDNA, IgA anti-HSP65 and IgM anti-Ro52. F) $n=15$, autoantibodies added: IgG anti-ssDNA, IgA anti-Intrinsic Factor, IgG anti-S100B, IgM anti-PL7 and IgG anti-Hemoglobin A2. G) $n=20$, autoantibodies added: IgM anti-Cytokeratin 18, IgG anti-IL26, IgM anti-Trimethyllysine-BSA, IgM anti-IL17R and IgG anti-RNP/Sm. H) Variation of AUC and sensitivity of the discrimination between ACR50 non-responders ($n=249$) and responders ($n=127$) with number of markers used in the linear combination. Only samples from the 150 mg ($n=188$) and 75 mg ($n=188$) treatment cohorts were considered for this analysis.

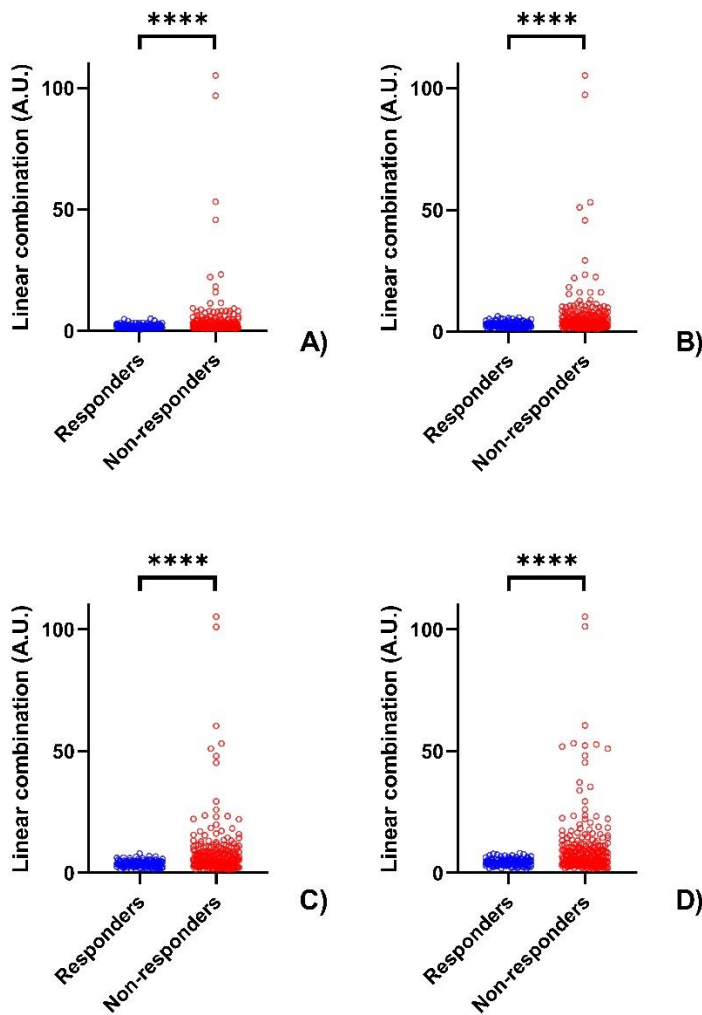


Figure 18:

Scatter plots showing the distribution in ACR50 non-responders (red) and responders (blue) of linear combinations (details in the methods section) using different number of markers. A) $n=5$, autoantibodies used: IgG anti-Lachnospiraceae, IgM anti-ss-DNA, IgG anti-Annexin 2, IgG anti-Annexin 5 and IgG anti-Alpha Actinin. B) $n=10$, autoantibodies added: IgM anti-IL21, IgM anti-SMD1, IgG anti-dsDNA, IgA anti-HSP65 and IgM anti-Ro52. C) $n=15$, autoantibodies added: : IgG anti-ssDNA, IgA anti-Intrinsic Factor, IgG anti-S100B, IgM anti-PL7 and IgG anti-Hemoglobin A2. D) $n=20$, autoantibodies added: IgM anti-Cytokeratin 18, IgG anti-IL26, IgM anti-Trimethyllysine-BSA, IgM anti-IL17R and IgG anti-RNP/Sm. Values of linear combinations are expressed in arbitrary units (A.U.). P-values calculated with Mann-Whitney test: all p-values < 0.0001 .

Although a single autoantibody could not discriminate sufficiently well between non-responders and responders to ACR50, a combination of autoantibodies would improve such differentiation. There are several options to combine and use multiple parameters to discriminate between population subsets. As the aim of this project was to find autoantibodies that could discriminate between non-responders and responders to ACR50 and to ultimately build the bases for the development of a companion diagnostic, the best way to combine the analyzed markers would be a linear combination. Indeed, non-linear combination methods (such as Forest tree or Bayesian statistics) would be difficult to potentially translate in a companion

diagnostic. A linear combination of different antibodies levels would be easier to implement in a companion diagnostic.

Linear combination methods would be more easily applied to a potential companion diagnostic, as it would be possible to simply mix antigens together during an ELISA plate coating and measure serum positivity for autoantibodies targeting the antigens mix. The linear method chosen for the combination was quite simple: Euclidean distance after data standardization by average (further details in methods section). The selection of antibodies used in the combination based on the list of antigens showed in Table 3, with the addition of IgG anti-RNP/Sm (autoantibody with 21st lowest p-value in the comparison of ACR50 non-responders and responders), while IgG anti-*Shigella* were not included in the combination as more elevated in ACR50 responders. As shown in Figure 17 and 18, increasing the number of autoantibodies combined improved the discrimination between ACR50 non-responders and responders.

However, even when using a linear combination of 20 markers, the AUC increased from 0.6026 (when combining two markers) to 0.6910, which was considered too low to be used as a base for the development of a companion diagnostic. The sensitivity, at specificity 100%, increased from 10% to 40%. Although such result can be considered as encouraging, the amount of needed markers in order to reach it was considered too high. Indeed, using 20 markers was judged to present a high risk of data over-fitting. Thus, considering the initial goal of reaching a sensitivity of 70%, while having a specificity of 100%, the result provided did not meet the criteria to pursue the development of a companion diagnostic.

Discussion

PsA is a complex disease with a poorly known pathogenesis and its treatment is a challenge for pharmaceutical companies. Potentially identifying non-responders to a given treatment, by using specific biomarkers, would help increasing the success rates of treatments. Indeed, pre-selecting patients based on their chances of responding positively to a specific treatment would allow doctors to not waste time on long-term treatments that might not control PsA symptoms. Such pre-selection approach, although theoretically ideal for patients, doctors and pharmaceutical companies, is of difficult introduction in some disease areas. Pre-selection of patients by assessing several biomarkers is widely used in oncology and critical in the identification of the best treatment to be given to the right patient [310, 311]. Biomarkers studies and use in oncology are particularly important, as caregivers need to quickly identify the best treatment options in order to maximize the chances of patient survival. Such pressure is not present in the area of arthritic diseases, where patients have symptoms for years and standards of care can mitigate their worsening. PsA is usually treated with anti-TNF α therapy, which has a success rate of around 40% in achieving ACR20. Anti-drug antibodies (ADAs) start developing after anti-TNF α treatment and have a neutralizing effect toward the drug, which forces caregivers to switch toward a different TNF α inhibitor [312]. The new generation therapy targeting IL17 with secukinumab resulted more efficacious when compared to TNF α inhibitors, as it achieved ACR20 after 24 weeks of treatment in around 50% of PsA patients [313].

In this thesis project, we aimed at using a wide panel of antigens, comprising structural proteins, nuclear antigens, microbial molecules, ribonucleic structures and post-translational modifications, with the aim of detecting autoantibodies that may discriminate between non-responders and responders to ACR50. Overall, autoantibodies of 3 isotypes (IgG, IgM and IgA) targeting 208 different antigens were screened using serum samples of 566 PsA patients (baselines from the NCT01392326 clinical trial).

As shown in the results section, the discrimination between responders and non-responders to ACR50 was not sufficient to continue toward the development of a companion diagnostic based on autoantibodies detection. The minimum performance criteria agreed upon with the clinical team were 100% specificity and 70% sensitivity when detecting non-responders to ACR50. Even by linearly combining 20 autoantibodies, when considering a specificity of 100%, the sensitivity obtained was around 40%, hence not sufficient to meet the criteria requested by the clinical team. However, the results obtained were still particularly interesting and potentially relevant to have a new insight in the autoimmunity within PsA.

Firstly, the hypothesis that ACR50 non-responders may present more autoantibodies, when compared to ACR50 responders, appeared to be correct. Indeed, as shown in the result section, 19/20 most differentially expressed antibodies between the two samples populations were overexpressed in ACR50 non-responders. This result suggests the presence of a potential RA-driven endotype within PsA. Anti-IL17 treatment is more efficacious in resolving psoriasis symptoms rather than RA ones [294-297], thus PsA patients not responding to anti-IL17 treatment may present a pathogenesis closer to RA, which may be reflected by an overall higher expression of autoantibodies. Secondly, the antibodies with highest overexpression in ACR50 non-responders were linked to IL17 pathway or to RA pathogenesis. Although this result could not be applied in the development of a companion diagnostic, it may be interesting for better understanding some autoimmune phenomena that may interfere with the anti-IL17 treatment of PsA. Hereby I discuss the potential origins and roles of antibodies overexpressed in ACR50 non-responders.

Some of the autoantibodies more expressed in ACR50 non-responders were directed against nuclear antigens. Specifically, autoantibodies targeting DNA, SMD1, S100B and Ro52 were among the 20 best “hits” that were overexpressed in ACR50 non-responders. Anti-nuclear autoantibodies are associated with inflammation, apoptosis and necrosis of cells [314]. Indeed, it is during such biological processes that antigens present in the nucleus of the cell are exposed to the immune system and may become a target of immune responses [302, 315]. Anti-nuclear autoantibodies are also associated with neutrophils activity, specifically with presence of neutrophils extracellular traps (NETs) [316]. Neutrophils release their intracellular and nuclear content to form web-like chromatin structures, whose role is to trap and clear microbial pathogens [317, 318]. Although efficient, such phenomena expose nuclear content such as Histones, DNA and ribonucleoproteins to the immune system, provoking the expression of anti-nuclear autoantibodies. Overall, anti-nuclear antibodies are more present in RA when compared to psoriasis, with around 50% and 5% positivity rates respectively [319, 320]. Therefore, the presence of anti-nuclear autoantibodies in PsA could be linked to neutrophilic activity and/or a more aggressive inflammatory state

leading to ANAs production. IL17 promotes neutrophils neutrophil-mediated immunity and abundant presence of neutrophils is specific of psoriatic skin lesions [321, 322]. Anti-IL17 treatment in PsA patients with elevated neutrophils activity would theoretically be efficacious, hence anti-nuclear antibodies present in ACR50 non-responders are probably not linked to NETs. Such autoantibodies may then originate from different inflammatory phenomena independent from IL17. Considering the difference between ANAs presence in psoriasis, PsA and RA, those autoantibodies should be further explored not only for PsA endotyping but also for early differential diagnosis of PsA, which would help in preventing severe joint damage and in increasing treatment efficacy.

The antibody showing the most discrimination between ACR50 non-responders and responders was IgG anti-Lachnospiraceae. The target of this autoantibody is a commensal bacteria, and a core member of gut microbiome [306]. Arthritis development has been associated with alteration of gut microbiome [323, 324]. The relationship between our body and the commensal bacteria, particularly the gut microbiota, is of critical importance for our health. The gut microbiota performs some basic functions in the immunological, metabolic, structural and neurological landscapes of the human body, and it exerts a significant influence on both physical and mental health of an individual [325]. The composition of commensal bacteria populations is dynamic and one of its core roles is to help maintaining immune homeostasis within the body [326]. A dysbiosis between gut microbiota and host may lead to the development of autoimmunity, through a deregulation and loss of tolerance of the immune system [327-329]. For instance, molecular mimicry links the microbiota with autoimmune pancreatitis [330]. The presence of higher levels of antibodies targeting a commensal bacterium such as Lachnospiraceae, in ACR50 non-responders, would suggest that gut microbiota alteration might play a role in the pathogenesis of PsA in these patients. Gut microbiota plays an important role in regulating the production of IL17 [331, 332], and a link between antibodies targeting a commensal bacteria and anti-IL17 treatment response is intriguing. It is unclear why a subpopulation of ACR50 non-responders in an anti-IL17 trial would express higher levels of IgG anti-Lachnospiraceae, but such finding is in line with the fundamental role of gut microbiota in the development of autoimmunity and production of IL17.

Another interesting finding was the presence of higher levels of anti-Alpha Actinin autoantibodies in some of the ACR50 non-responders. Alpha Actinin might play a role in the pathogenesis of PsA, as it was described to be a mediator in the activation of the TNFa pathway [309]. Anti-Alpha Actinin autoantibodies may be a homeostatic attempt from the body to downregulate the TNFa activation. IL17 and TNFa pathways partially overlap, as some inflammatory genes are regulated by both cytokines [333, 334]. Although it is not clear which biological role anti-Alpha Actinin autoantibodies may have, we can hypothesize that they may partially reduce TNFa signaling efficiency. Therefore, as those autoantibodies could potentially downregulate the TNFa pathway and considering the overlapping of genes activated by TNFa and IL17, this subgroup of patients might be more resilient to anti-IL17 treatment.

The easiest result to interpret is the presence of IgG and IgM anti-IL17R in PsA patients classified as ACR50 non-responders. The presence of those autoantibodies would suggest a homeostatic effort from the immune system, with the aim of downregulating the activation of IL17 pathway. Indeed, those autoantibodies would potentially inhibit the binding of IL17 to its receptor, hence preventing or slowing down the activation of IL17 pathway. Although remote, another possibility that should be taken into account is that anti-IL17R autoantibodies might activate the receptor in an IL17-independent manner, hence simulating the molecular cascade of IL17 activation. Regardless of the exact role of those autoantibodies, PsA patients expressing them might be more resilient to anti-IL17 treatment. Indeed, if those autoantibodies downregulate the IL17 pathway, then an anti-IL17 treatment would be redundant with the homeostatic process put in place by the immune system and thus result less efficient. If anti-IL17R antibodies were able to activate the IL17 pathway, then anti-IL17 treatment would be less efficacious, as the pathway would be activated in an IL17 independent manner.

A subgroup of PsA patients classified as ACR50 non-responders showed higher levels of anti-IL21 when compared to ACR50 responders. IL21 is associated with psoriasis severity and it is linked to unbalance in Th17-reg cells [307, 308]. Therefore, the presence of anti-IL21 autoantibodies could be interpreted as an attempt of the immune system to downregulate the activation of Th17-reg. Similarly to anti-IL17R autoantibodies, the PsA patients expressing such autoantibodies might theoretically be more resilient to anti-IL17 treatment. Indeed, in this group of patients, the IL17 pathway would be already partially downregulated, thus the action of an anti-IL17 monoclonal antibody would result redundant and potentially less efficacious.

The higher levels of anti Annexin 2 and 5 in a subgroup of ACR50 non-responders was intriguing. There is little evidence in the literature connecting Annexin 2 and 5 to IL17 and PsA. In a 1994 study, anti-Annexins IgG and IgM were detected in patients from various skin disorders and a healthy control group, to investigate whether such autoantibodies could be potential diagnostic markers [335]. The result of this study showed a homogenous presence of anti-Annexins autoantibodies in diseases and control groups, hence dismissing any diagnostic potential. Annexin 2 was described to upregulate the production of ROS and IL17 in a mouse model, suggesting an immuno-regulatory role [336]. Taking this information into account, an inhibition of Annexin 2 might decrease the activation of IL17 pathway. Autoantibodies targeting Annexin 2 might be the result of an effort from the body to inhibit the IL17 pathway. Under such circumstances, PsA patients expressing anti-Annexin 2 autoantibodies might be more resistant to anti-IL17 treatment, as the latter would be redundant with the homeostatic action of autoantibodies. Annexin 5 was more difficult to link to IL17 and PsA. Annexin 5 post-chemotherapy administration was recently described as a promising immune checkpoint inhibitor for cancer treatment, as it binds with high affinity to phosphatidylserine (PS) externalized by apoptotic cells, thereby hindering their interaction with immune cells [337]. Annexin 5 may also play a role in blood coagulation, apoptosis, phagocytosis and formation of plasma membrane-derived microparticles [338]. Moreover, anti-Annexin 5 autoantibodies were found more elevated in sera from RA

patients when compared to a control group [339]. Those pieces of information suggest an immunoregulatory role of Annexin 5 and a potential link to RA. Anti-Annexin 5 autoantibodies in PsA and RA patients could be the result of a homeostatic effort from the body to modulate the activity of the immune system. The fact that such autoantibodies were already found in RA could suggest that anti-Annexin 5 autoantibodies may be a sign of a RA-driven PsA pathogenesis in a subgroup of patients, which would explain a loss of response to anti-IL17 treatment. However, before accepting such a conclusion, anti-Annexin 5 autoantibodies should be detected in psoriatic patients as well and assessed to be less elevated when compared to RA patients.

Autoantibodies targeting Intrinsic factor were found more elevated in a subgroup of ACR50 non-responders. Intrinsic factor was described to promote Th17 inflammation in pernicious anemia patients [340]. Although not described in arthritic diseases, in the scope of PsA patients the role of such autoantibodies may be to partially inhibit the activation of IL17 pathway. Under such circumstances, anti-IL17 treatment would be less efficacious, as IL17 pathway might be already downregulated by autoantibodies directed against Intrinsic Factor.

Although autoantibodies profiling showed several potentially relevant findings, their performance in discriminating ACR50 non-responders from responders was relatively low, as each autoantibody was present only in a subgroup of ACR50 non-responders samples. Even after linearly combining the 20 best hits discriminating ACR50 non-responders from responders, the obtained sensitivity was around 40%, which was judged as not sufficient for further steps toward the development of a companion diagnostic. Overall, the results obtained with autoantibodies profiling were interesting and provided some new insight into the biological diversity of autoimmune response within PsA patients. The number of antigens used in the autoantibodies profiling in this project was relatively small if compared to the several thousands of different proteins present in the human body. The custom-made approach of this project could not allow a significantly higher amount of antigens; nevertheless, it allowed a high flexibility in the building of the antigens panel. Indeed, one of the most interesting aspects of this project was the possibility to test numerous antigens for which autoantibodies were not already described in literature as relevant in PsA. This project enabled an increase the technical expertise in autoantibodies profiling in my department. Of particular interest were antigens such as protein Tau (critical in Alzheimer's research), for which we detected high levels of IgG and IgM. Such information is particularly relevant when considering the importance that pharmaceutical research is giving to the detection of protein Tau in plasma. Indeed, autoantibodies directed against protein Tau would interfere with immunoassay-based detection methods. Moreover, such autoantibodies could be of clinical relevance in Alzheimer's patients, as potential markers for either early diagnostic or therapeutic endotyping. Post-translational modifications is another extremely interesting set of antigens that was tested in this project. Results obtained with advanced glycation events (AGEs) modified bovine serum albumin (BSA) were of critical importance for the rest of the PhD project, particularly for the Hidradenitis Suppurativa autoantibodies profiling. Indeed, the autoantibodies profiling

performed with PsA patients allowed us to identify numerous autoantibodies that were never tested within my department and to include them in more targeted autoantibodies profiling approaches that were applied to other projects. Anti-CEL-BSA autoantibodies, the most interesting finding of this PhD project, were detected in our PsA autoantibodies profiling (more details in the Hidradenitis Suppurativa section).

Another aspect that should be considered when analyzing the results of autoantibodies profiling in PsA is the heterogeneity of the disease. As stated numerous times, PsA is a complex disease and its complexity reflected well in the variety of autoantibodies detected. When exploring autoantibodies data in order to discriminate ACR50 non-responders from responders, many markers were more elevated in one group or the other, but such differences were relatively small. For instance, even IgG anti-Lachnspiraceae, the marker that discriminated the most between non-responders and responders, showed a sensitivity of 12% (with a specificity of 100%). Many autoantibodies targeted antigens of the same family, like anti-nuclear antibodies, or with similar role toward IL17 pathway, like IL21 or Annexin 2. Finding one or just a few markers, in this case autoantibodies, able to discriminate at least 70% of ACR50 non-responders from non-responders in PsA was unlikely. The disease heterogeneity within PsA is indeed probably too important to find a single or a combinations of few markers that may define relevant endotypes. A possible way to overcome such difficulty would be to combine different kind of datasets. For instance, combining transcriptomic and proteomics data with autoantibodies would allow a more comprehensive understanding of the disease and higher chances to identify relevant markers for diagnostic or prognostic purposes. Such approach might be needed in future in order to increase the success rate of PsA treatment. Indeed, a better molecular understanding of the different sides of PsA will allow for an improvement in treatment strategies and early diagnosis, which are critical aspects for PsA management. Such approach would of course be relevant in other complex or not well understood diseases, such as Alzheimer's, Ankylosing Spondylitis (AS), RA and Parkinson's.

In conclusion, autoantibody profiling results obtained in PsA were not considered sufficiently good to start the development of a companion diagnostic. However, the results obtained showed a clear interest and relevance of autoantibodies in better understanding the biological diversity of PsA and in identifying potential homeostatic processes put in place by the immune system in this disease and that may interfere with anti-IL17 treatment. The approach used in this project could potentially be adopted in more clinical trials, in order to identify endotyping markers that could support the therapeutic strategies put in place, thus the advance of precision medicine.

Results Part II: Manuscript Hidradenitis Suppurativa

This result section consists of the manuscript “Disease Association of Anti–Carboxyethyl Lysine Autoantibodies in Hidradenitis Suppurativa”, published on February 2023 in the Journal of Investigative Dermatology.

Disease Association of Anti-Carboxyethyl Lysine Autoantibodies in Hidradenitis Suppurativa



JID Open

Giulio Macchiarella^{1,2}, Vanessa Cornacchione³, Celine Cojean⁴, Julia Riker⁴, Yichen Wang⁴, Helene Te⁴, Melanie Ceci⁴, Johann E. Gudjonsson⁵, Swann Gaulis⁴, Jean François Goetschy⁴, Audrey Wollschlegel⁴, Stephanie K. Gass⁶, Sofia Oetliker-Contin⁶, Barbara Wettstein-Ling⁶, Dirk J. Schaefer⁶, Pascale Meschberger⁷, Roland de Roche⁸, Rik Osinga^{6,8}, Grazyna Wieczorek⁴, Ulrike Naumann⁹, Joachim C.U. Lehmann⁴, Anna Schubart⁴, Andreas Hofmann¹⁰, Lukas Roth⁴, Edwin F. Florencia¹¹, Christian Loesche¹², Elisabetta Traggiai³, Alexandre Avrameas¹, Errol P. Prens¹¹, Till A. Röhn^{4,13} and Ben Roediger^{4,13}

Hidradenitis suppurativa (HS) is a chronic inflammatory skin disease characterized by recurring suppurating lesions of the intertriginous areas, resulting in a substantial impact on patients' QOL. HS pathogenesis remains poorly understood. An autoimmune component has been proposed, but disease-specific autoantibodies, autoantigens, or autoreactive T cells have yet to be described. In this study, we identify a high prevalence of IgM, IgG, and IgA antibodies directed against Nε-carboxyethyl lysine (CEL), a methylglyoxal-induced advanced glycation end-product, in the sera of patients with HS. Titers of anti-CEL IgG and IgA antibodies were highly elevated in HS compared with those in healthy controls and individuals with other inflammatory skin diseases. Strikingly, the majority of anti-CEL IgG was of the IgG2 subclass and correlated independently with both disease severity and duration. Both CEL and anti-CEL-producing plasmablasts could be isolated directly from HS skin lesions, further confirming the disease relevance of this autoimmune response. Our data point to an aberration of the methylglyoxal pathway in HS and support an autoimmune axis in the pathogenesis of this debilitating disease.

Journal of Investigative Dermatology (2023) **143**, 273–283; doi:10.1016/j.jid.2022.08.051

INTRODUCTION

Hidradenitis suppurativa (HS) is a chronic inflammatory skin disease characterized by painful and recurrent nodules and

abscesses, primarily affecting inverse body regions (Prens and Deckers, 2015). HS pathogenesis is clinically well-characterized, but its etiology remains poorly understood.

The association with inflammasome components, particularly IL-1β, has led to the growing consensus that HS is, at least in part, an autoinflammatory disease. The prominence of neutrophils in HS lesions, the association of HS with monogenic autoinflammatory syndromes (Figueras-Nart et al., 2019), and the responsiveness of patients with HS to anti-TNF antibodies and the IL-1 receptor antagonist contribute to this hypothesis (Savage et al., 2019; Tzanetakou et al., 2016). More recently, the possibility that HS also comprises an autoimmune (adaptive) component has emerged (Constantinou et al., 2019). The prominence of T cells, B cells, and plasma cells within HS lesions (Byrd et al., 2019; Gudjonsson et al., 2020; Musilova et al., 2020), together with emerging evidence that IL-17 inhibition may be beneficial in patients with HS (Fletcher et al., 2020), support the notion of adaptive immune cell involvement in this disease. HS has also been associated with other autoimmune diseases, particularly Crohn's disease, ulcerative colitis (UC), and spondyloarthropathies (Chen and Chi, 2019; Richette et al., 2014). Nevertheless, the role of the adaptive immune system in HS remains unclear.

Autoantibodies are a common feature in several autoimmune diseases, and their detection is used for a wide range of clinical applications, including for diagnostic and prognostic

¹Biomarker Development (BMD), Novartis Institutes for BioMedical Research, Novartis Pharma AG, Basel, Switzerland; ²Biozentrum, Faculty of Sciences, University of Basel, Basel, Switzerland; ³NIBR Biologics Center (NBC), Novartis Institutes for BioMedical Research, Novartis Pharma AG, Basel, Switzerland; ⁴Autoimmunity, Transplantation and Inflammation (ATI) Disease Area, Novartis Institutes for BioMedical Research, Novartis Pharma AG, Basel, Switzerland; ⁵Department of Dermatology, University of Michigan, Ann Arbor, Michigan, USA; ⁶Department of Plastic, Reconstructive & Aesthetic Surgery and Hand Surgery, University Hospital, University of Basel, Switzerland; ⁷Department of Surgery, Kantonsspital Baselland, Liestal, Switzerland; ⁸Praxis beim Merian Iselin, Basel, Switzerland; ⁹Chemical Biology and Therapeutics (CBT), Novartis Institutes for BioMedical Research, Novartis Pharma AG, Basel, Switzerland; ¹⁰Biotherapeutic and Analytical Technologies, Novartis Institutes for BioMedical Research, Novartis Pharma AG, Basel, Switzerland; ¹¹Department of Dermatology, Erasmus University Medical Centre, Rotterdam, the Netherlands; and ¹²Translational Medicine, Novartis Institutes for BioMedical Research, Novartis Pharma AG, Basel, Switzerland

¹³These authors contributed equally to this work.

Correspondence: Ben Roediger, Autoimmunity, Transplantation & Inflammation Disease Area, Novartis Institutes for BioMedical Research, Basel CH-4056, Switzerland. E-mail: ben.roediger@novartis.com

Abbreviations: CEL, carboxyethyl lysine; CML, carboxy-methyl-lysine; HS, hidradenitis suppurativa; UC, ulcerative colitis

Received 9 March 2022; revised 1 August 2022; accepted 5 August 2022; accepted manuscript published online 16 September 2022; corrected proof published online 23 November 2022

purposes as well as for monitoring disease progression and treatment response. The target antigens of autoantibodies also provide insights into the underlying mechanisms of disease pathogenesis. These may include organ-specific self-proteins, for example, thyroid peroxidase in Hashimoto's disease, but also chemically modified antigens, such as deamidated peptides in coeliac disease and citrullinated peptides in rheumatoid arthritis. Elevated titers of antibodies against nuclear antigens and citrullinated peptides have also been observed in HS (Byrd et al., 2019; Mulani et al., 2018). However, to date, no disease-specific autoantigens have been identified in HS.

The metabolite methylglyoxal is produced nonenzymatically during glycolysis, specifically from glyceraldehyde-3-phosphate and dihydroxyacetone phosphate. Because methylglyoxal has cytotoxic activity, it is usually inactivated by the glyoxalase system. However, when produced in excess, methylglyoxal acts as a major precursor in the formation of advanced glycation end-products, pathogenic and proinflammatory modifications of proteins and lipids (Vistoli et al., 2013). Although methylglyoxal is produced as part of normal cellular metabolism, its production is elevated in metabolic and inflammatory diseases.

In this study, we identify antibodies against N ϵ -carboxyethyl lysine (CEL), a stable adduct generated by methylglyoxal, as highly prevalent and highly abundant in patients with HS. Anti-CEL IgG and IgA autoantibodies were specifically elevated in HS compared with those in healthy volunteers and individuals suffering from other inflammatory skin and autoimmune diseases, and anti-CEL IgG titers independently correlated with HS disease severity and duration. Our data lend support for an autoimmune etiology in HS and provide, to the best of our knowledge, several unreported avenues for future investigation into the pathogenesis, assessment, and treatment of this debilitating disease.

RESULTS

To identify potential autoantibodies in HS, sera from 61 patients (Hurley stages 2–3) and 22 healthy volunteers (cohort 1) were screened for the presence of autoreactive IgG, IgA, and IgM against a custom panel of 51 antigens (Figure 1a), comprising endogenous, nuclear, and microbial antigens commonly associated with inflammatory and autoimmune disease (Supplementary Table S1). The panel also included a selection of commercially available, post-translationally modified BSA, namely carboxymethyl-lysine (CML), CEL, and carbamyl-lysine, along with glycolaldehyde- and malondialdehyde-modified BSA. Of all 51 antigens assessed, only CEL showed differential Ig reactivity compared with those in healthy volunteers, particularly of the IgG and IgA isotypes (Figure 1a and b and Supplementary Figure S1a and b). Anti-CEL IgM was also significantly elevated in HS sera, but the fold change was less pronounced owing to the presence of high titers of anti-CEL IgM in healthy individuals (Supplementary Figure S1c). The fold difference in anti-CEL IgG between HS and healthy control was both substantial (9.4-fold) and robust, with ~90% of patients with HS exhibiting greater titers than the average titer of the healthy donors (Figure 1c).

We applied receiver operating characteristic curves to evaluate the capability of anti-CEL IgG to distinguish HS sera from healthy sera, using the standard area under the curve as readout, in which a perfect classifier has an area under the curve of 1, and a random classifier gives a value of 0.5 (Søreide, 2009). Anti-CEL IgG gave an area under the curve of 0.9136 ($P < 0.0001$), which increased to 0.9367 when anti-CEL IgA was included in the classification (Figure 1d and Supplementary Figure S1d).

To assess whether anti-CEL autoantibodies are present in other inflammatory skin or autoimmune diseases, we assessed anti-CEL Ig in the sera of patients with atopic dermatitis ($n = 30$), acne ($n = 31$), UC ($n = 25$), and Crohn's disease ($n = 13$). Acne was chosen as a common comorbidity of HS (Hua et al., 2021), which has been associated with plasma cell infiltration into the skin (Carlavan et al., 2018), whereas AD is an unrelated inflammatory skin disease that nevertheless accompanies lymphadenopathy (Spergel and Paller, 2003) and changes in the B cell compartment (Czarnowicki et al., 2016). Anti-CEL titers were not significantly upregulated in acne or atopic dermatitis, although intermediate levels of anti-CEL IgG antibodies were observed in Crohn's disease and UC (Figure 1e). We conclude that anti-CEL IgG is highly prevalent and highly elevated in patients with HS.

Next, we sought to understand the relevance of CEL in HS. Carboxylethyl modifications to lysine are one of many types of advanced glycation end-products, which are collectively associated with several physiological but also pathological processes. Several other advanced glycation end-product-modified antigens were included in our original autoantibody screen, the most chemically similar to CEL being CML (Figure 2a), which elicited a modest but statistically insignificant binding in some HS sera (Figure 1a and Supplementary Figure S1a–c). We therefore assessed the specificity of the anti-CEL autoantibodies in HS in contrast to that of CML as well as octopine, a carboxylethyl modification of arginine (Figure 2a). Preincubation of HS sera with CML and octopine had minimal effect on CEL binding (Figure 2b), indicating that the autoantibodies in HS sera are specific for CEL, not CML, nor a nonlysine-associated carboxylethyl motif.

CEL but not CML is typically formed by the metabolite methylglyoxal, a glycolytic by-product that reacts with specific amino acid residues through the Maillard reaction to form stable adducts. We therefore tested the capability of methylglyoxal to induce changes to histone that might render it reactive to HS sera. We chose histone not only because of its susceptibility to methylglyoxal but also because methylglyoxal-induced post-translational adductions to histones are common in cellular metabolism (Galligan et al., 2018) and therefore represent a potential endogenous target. Recombinant human histone A2 was chemically modified by incubation with pyruvate and cyanoborohydride and was then assessed for HS sera binding by Luminex. As shown in Figure 2c, HS sera bound to modified but not unmodified histone. Because methylglyoxal can also induce modifications to arginine, particularly in histones, we also assessed the CEL specificity of this reaction by preincubating the sera in CEL. CEL preincubation completely abrogated HS

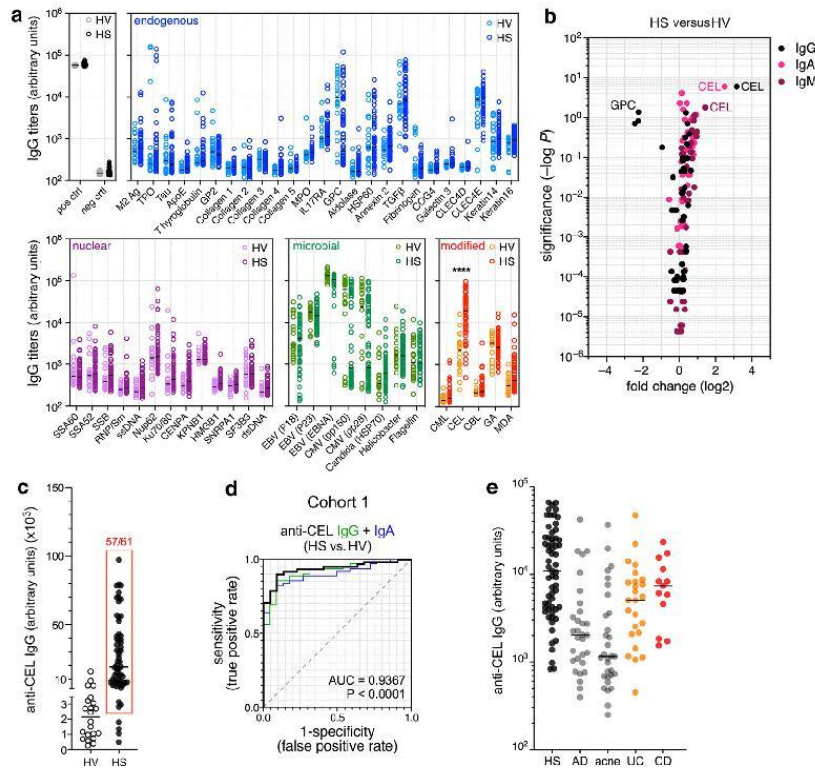


Figure 1. Identification of anti-CEL autoantibodies in HS sera. (a) Distribution of log-normalized titers of IgG antibodies (arbitrary units) detected in the sera of patients with HS (n = 61; cohort 1) and HV (n = 22) targeting indicated antigens, subdivided in five groups: negative/positive controls (gray/black), endogenous antigens (blue), nuclear antigens (pink/purple), microbial antigens (green), and post-translational modifications (orange/red). See [Supplementary Table S1](#) for abbreviations. **** $P < 0.0001$ (students *t*-test). (b) Volcano plot depicting fold change in autoantibody titers in HS (n = 61) versus healthy (n = 22) sera; black for IgG, purple for IgM, and pink for IgA. Each dot represents a single antigen shown in a. Significance was calculated by *t*-test (Bonferroni corrected). (c) Linear scale titers of IgG anti-CEL antibodies (arbitrary units) in HS (n = 61) versus healthy (n = 22) sera. The red box identifies the number of HS samples with titers higher than the average of healthy values. (d) Receiver operator characteristic analysis distinguishing patients with HS from HVs on the basis of IgG (green), IgA (blue), and IgG + IgA (black) anti-CEL titers. AUC for IgG + IgA is shown. (e) Log distribution of IgG anti-CEL titers (arbitrary units) in serum samples from patients with indicated conditions. HS, n = 61; AD, n = 30; acne vulgaris, n = 31; CD, n = 13. UC, n = 25. AD, atopic dermatitis; ApoE, apolipoprotein E; AUC, area under the curve; CD, Crohn's disease; CEL, carboxyethyl lysine; dsDNA, double-stranded DNA; EBV, Epstein-Barr virus; GA, Glycoaldehyde; GPC, gastric parietal cell antigen; HS, hidradenitis suppurativa; HV, healthy volunteers; MDA, malondialdehyde; MPO, myeloperoxidase; neg ctrl, negative control; pos ctrl, positive control; ssDNA, single-stranded DNA; TPO, thyroid peroxidase; UC, ulcerative colitis.

sera reactivity to methylglyoxal-modified histone (Figure 2d). These data strongly imply that anti-CEL autoantibodies bind to CEL independently of the modified protein.

We then sought to detect CEL directly in healthy and HS lesional skin. Resected tissue from patients with Hurley stages 2 and 3 (n = 12) undergoing surgery were biopsied, and the tissue was snap frozen and lysed before assessment for and quantification of CEL by simple ELISA. Nonlesional as well as healthy donor skin was included as controls. CEL was detected in all samples, but in 3 of 12 lesional samples, CEL was especially abundant, ~3-fold greater than in control samples (Figure 2e). We conclude that autoantibodies against CEL in HS are highly CEL specific and that CEL modifications are likely present in healthy skin and may be abundant in some HS lesions.

To understand the clinical relevance of anti-CEL autoantibodies in HS, we repeated these measurements in plasma samples from a second, clinically well-validated cohort of 40 patients with HS (cohort 2), which included patients across the entire severity spectrum (i.e., Hurley stages 1–3) and in which additional clinical data, including refined Hurley score and age of onset, were known. Patient characteristics for both cohorts are summarized in [Supplementary Table S2](#). We confirmed the high titers of anti-CEL IgG and IgA in patients with HS in cohort 2 (Figure 3a and b and data not shown), although the magnitude of the effect was smaller in the second cohort (3.85-fold), possibly owing to increased variability of control plasma compared with that of serum. The receiver operating characteristic curve comparing anti-CEL in HS with that in healthy plasma gave an area under

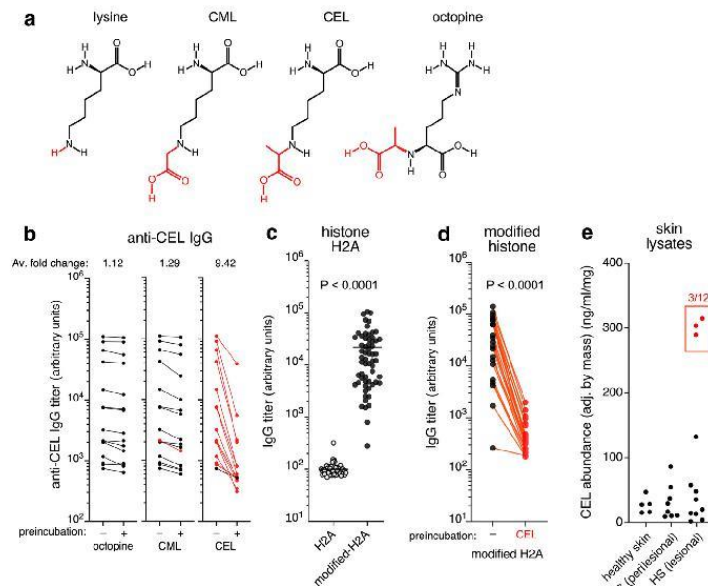


Figure 2. Specificity of anti-CEL autoantibodies in HS sera. (a) Chemical structures of lysine, CML, CEL, and octopine. (b) Titers (arbitrary units) of IgG anti-CEL in HS plasma samples (n = 15) with and without preincubation with octopine, CML, or CEL. Data points connected by a line belong to the same patient. Red connections represent a decrease of greater than 1.5-fold in anti-CEL BSA signal after sample preincubation. (c, d) Titers of IgG against recombinant human histone A2 and histone that was chemically modified by incubation with pyruvate and cyanoborohydride in HS serum samples (n = 61) (c) without or (d) after preincubation with CEL. Data points connected by a line belong to the same patient. **** $P < 0.0001$ (Mann-Whitney U test). (e) Levels of CEL detected in healthy (n = 5), perilesional HS (n = 8), and lesional HS (n = 12) skin by direct ELISA. The red box identifies 3 of 12 lesional HS samples, with CEL levels markedly higher than those of healthy skin. Av, average; CEL, carboxyethyl lysine; CML, carboxy-methyl-lysine; HS, hidradenitis suppurativa.

the curve of 0.7037 ($P = 0.0027$) for IgG, which increased to 0.7404 when anti-CEL IgA was included in the classification (Figure 3c and Supplementary Figure S2a). Importantly, these data enabled us to perform correlation analyses of anti-CEL against relevant clinical parameters.

We did not observe any relationship between anti-CEL IgG titer and sex, body mass index, smoking status, or age in either cohort (data not shown). In contrast, we observed a weak correlation between anti-CEL IgG titers and disease severity (refined Hurley stage) ($r = 0.3173$, $P = 0.0461$) and a stronger correlation with disease duration ($r = 0.3528$, $P = 0.0114$) in cohort 2 (Figure 3d and e). We did not observe a correlation between disease duration and disease severity in cohort 2 (Figure 3f), consistent with previous reports indicating that patients with HS generally reach their maximum disease activity shortly after disease onset, after which their status remains relatively stable (Kromann et al., 2014; Vanlaerhoven et al., 2018; von der Werth and Williams, 2000). Thus, anti-CEL IgG titers appeared to independently correlate with disease severity and duration. When we binned patients into five disease-severity subgroups, anti-CEL IgG titers were lowest in patients with mild, recently acquired disease and highest in patients with severe, long-lasting disease (Figure 3g). Consistent with this, we saw a good correlation between anti-CEL IgG and a combination of severity and duration ($r = 0.4550$, $P = 0.0012$) (Figure 3h and Supplementary Figure S2a–f and see Materials and Methods

for details). Interestingly, anti-CEL IgA titers did not correlate with severity, disease duration, or the combination of the two (Figure 3i and data not shown). Similarly, anti-CEL IgM titers did not correlate with severity, disease duration, or the combination, but interestingly, anti-CEL IgM titers were lower in patients treated with antibiotics (Supplementary Figure S2g and h). We conclude that anti-CEL IgG but not anti-CEL IgA or IgM independently correlates with disease severity and duration in patients with HS.

Several groups have identified the presence of B cells and plasma cells within affected skin of patients with HS, with one study suggesting the existence of pseudo lymphoid follicles (van der Zee et al., 2012). This raised the possibility that the anti-CEL autoantibodies were being generated within the skin. To assess this potentiality, we first confirmed the presence of B cells in HS lesions by immunostaining for the B cell-specific marker CD20. B cells were present in all tissues examined, where they were either loosely organized in the dermis in association with abscesses or tunnels (Figure 4a and Supplementary Figure S3a) or more tightly ordered in smaller lymphoid clusters, many of which were associated with CD21⁺ follicular dendritic cells, indicative of germinal center-like structures (Figure 4b). Many follicular-type clusters were observed adjacent to subcutaneous adipose tissue (Figure 4c–e), which are relevant because adipocytes have been implicated in tertiary lymphoid organ formation in Crohn's disease (Guedj et al., 2019). Spatial RNA profiling of

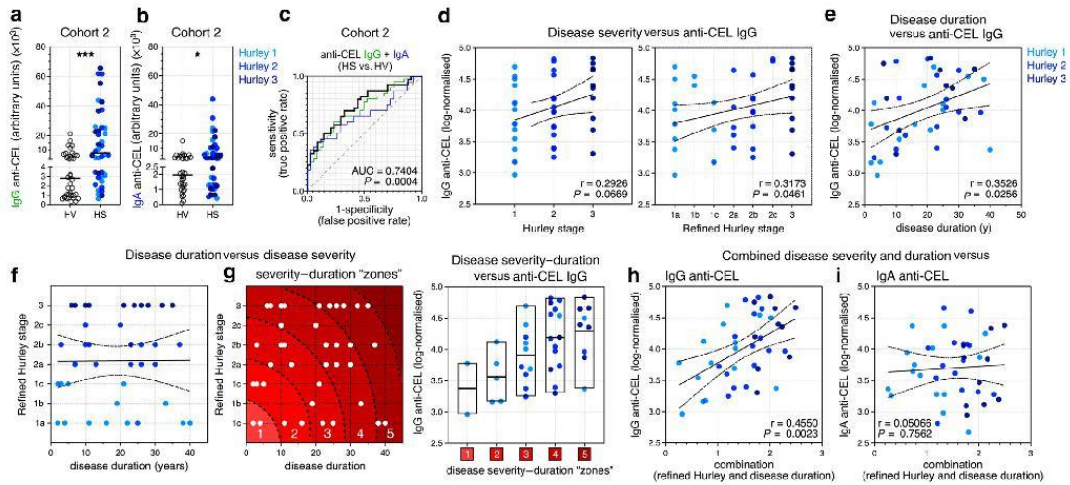


Figure 3. Anti-CEL IgG correlates with disease duration and severity in patients with HS. (a, b) Linear distribution of (a) IgG and (b) IgA anti-CEL titers in plasma samples of healthy volunteers (n=38) and HS patients (n = 40; cohort 2). *** $P = 0.0001$ (IgG) and * $P = 0.0265$ (IgA) (Man-Whitney U test). (c) Receiver operator characteristic analysis distinguishing patients with HS (n = 40) from healthy volunteers (n = 38) on the basis of IgG (green), IgA (blue), and IgG + IgA (black) anti-CEL titers. AUC for IgG + IgA is shown. (d) Scatter plot depicting the modest positive correlation between log-normalized IgG anti-CEL titers in HS plasma samples from cohort 2 (n = 40) versus Hurley score (left) and refined Hurley score (right) (Spearman test). (e) Scatter plot showing the positive correlation between log-normalized IgG anti-CEL titers in HS plasma samples and disease duration ($P = 0.0256$; Spearman test). (f) Scatter plot showing the lack of correlation between disease duration and refined Hurley score in patients with HS ($P = 0.7628$; Spearman test). (g) Left: Demarcation of disease duration–severity zones based on refined Hurley score and disease duration (see also Supplementary Figure S2). Right: Log-normalized IgG anti-CEL titers in indicated HS groups. (h) Scatter plot showing the positive correlation between log-normalized IgG anti-CEL titers in HS plasma samples and a linear combination (Euclidean distance) of refined Hurley score and disease duration ($P = 0.0023$; Spearman test). (i) Scatter plot showing the lack of correlation between log-normalized IgA anti-CEL titers in HS plasma samples and a linear combination of refined Hurley score and disease duration ($P = 0.7562$; Spearman test). AUC, area under the curve; CEL, carboxyethyl lysine; HS, hidradenitis suppurativa.

HS sections comparing diffuse regions of B cells with follicular-type clusters confirmed the enrichment of germinal center-associated transcripts, including *C3*, *CR2* (encoding CD21), and *FDCSP* (Figure 4f–h and Supplementary Figure S3b and c and Supplementary Table S3), although other germinal center-associated transcripts, including *AICDA* and *IL21*, were not readily detected on this platform. Finally, a retrospective analysis of our previously published transcriptomics data (Penno et al., 2020) confirmed the association between B cell-associated transcripts and lesional but not nonlesional tissue (Figure 4i), where we also observed an association between *CR2* expression and *CXCL13*, *FDCSP*, and *CR1* (encoding CD35) (Figure 4j), markers of follicular dendritic cells. We conclude that B cells are prominent in HS lesional tissue and that some but not all HS lesions contain ectopic germinal centers and follicular dendritic cells.

To verify the presence of plasma cells in HS lesions, we used flow cytometry. Resected tissue from patients with Hurley stages 2–3 (n = 7) was subjected to enzymatic digestion, single cell isolation, and subsequent antibody staining and assessment by flow cytometry. (Non-naïve) B cells were identified as CD45⁺ CD19⁺ IgD[−] CD20^{hi} HLA-DR⁺ cells, whereas plasmablasts were identified as CD19⁺ CD20^{lo} CD38^{hi}. Bona fide plasma cells were identified on the basis of CD27 expression within the CD38^{hi} plasmablast population (Figure 5a). In these experiments, we also

included CD86, a B cell activation marker, and CD63, which we identified as a plasma cell-enriched surface molecule in a single-cell RNA-sequencing dataset from HS skin (Supplementary Figure S4a and b). Both B cells and plasmablasts were abundant in lesional HS skin, consistent with previous studies. Of note, we also observed CD86 expression by a subpopulation of B cells and a transitory CD63⁺ population bridging the B cells to the plasma cells (Figure 5a–d), suggestive of in situ differentiation of HLA-DR⁺ CD63[−] B cells into CD63^{hi} CD38^{hi} plasmablasts. We also observed an HLA-DR[−] CD38^{hi} CD63^{hi} CD27⁺ population that lacked CD19 (Figure 5e), consistent with the phenotype of long-lived plasma cells (Halliley et al., 2015).

Phenotyping of these cells for surface IgG, IgM, and IgA subclasses revealed a predominance of IgG1⁺ and IgA1⁺ subclasses in both B cells and plasmablasts (Figure 5f and g and Supplementary Figure S4c and d). IgG2⁺ cells were consistently observed in both subsets, albeit at a reduced frequency. IgG3⁺ and IgG4⁺ cells were rare, as were IgM⁺ cells. Relative to B cells, IgA⁺ cells were markedly reduced in plasmablasts and plasma cells (Figure 5f and g and Supplementary Figure S4e), suggesting a potential selection bias limiting IgA-producing cells from entering the plasmablast/plasma cell compartment. Collectively, we identify a spectrum of B cells, plasmablasts, and plasma cells in varying states of activation and differentiation, consistent with dynamic B cell activity within lesional HS skin.

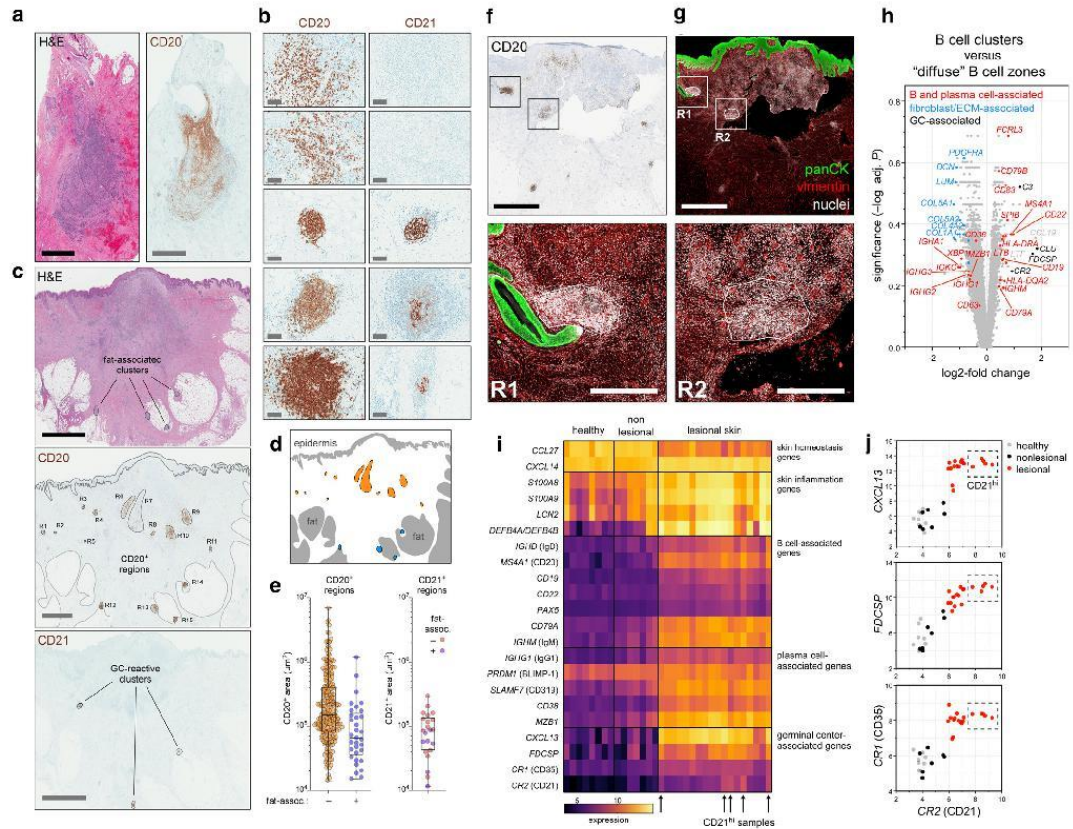


Figure 4. Detection of B cells and germinal center-like structures in HS skin. (a) Representative H&E (left) and CD20 staining (right) of HS skin. Each bar = 2 mm. (b) Representative staining of CD20⁺ B cells (left) and CD21⁺ germinal center-like structures (right) in HS skin. B cells were either diffusely distributed (top two panels) or densely organized in lymphoid follicles (bottom three panels), which often but not always accompanied CD21 expression. Each bar = 100 μ m. (c) Representative H&E (top; bar = 3 mm), and CD20 (middle; bar = 2 mm), and CD21 (bottom; bar = 3 mm) staining of HS skin, showing fat associated and CD21⁺ follicles. (d) Schematic of demarcating epidermis and fat (gray) and fat-associated (blue) and non-fat-associated (orange) CD20⁺ regions. (e) Quantification of CD20⁺ (left) and CD21⁺ (right) areas (in μ m²), stratified according to their association with fat. Collectively, these data represent 269 ROIs across 10 HS patient samples. (f) Representative CD20 and (g) immunofluorescence staining of serial sections of a skin sample of patients with HS (each bar = 2 mm), identifying a B cell cluster (R1) and a diffuse B cell zone (R2). Each bar in R1 and R2 = 0.5 mm. See also [Supplementary Figure S3c](#). (h) Comparison of gene expression in B cell clusters (nine ROIs) versus diffuse B cell zones (11 ROIs) by volcano plot (n = 4 patients), as measured by NanoString Digital Spatial Profiling. Selected genes expressed by B cells and plasma cells are marked in red, fibroblast-associated genes are marked in blue, and GC-implicated genes are marked in black. See also [Supplementary Table S3](#). (i) Heatmap depicting the expression of indicated genes in mRNA expression data (microarray; (Penno CA et al., 2020)) from healthy (n = 8), nonlesional HS (n = 7), and lesional HS (n = 18) skin. Arrows indicate five HS samples with an enriched expression of CR2 (encoding CD21) in lesional skin. (j) Scatter plots of selected GC-associated genes from [i](#). CD21^{hi} samples (boxed) are associated with concomitant expression of CR1, CXCL13, and FDCSP. GC, germinal center; HS, hidradenitis suppurativa; PanCK, pan-cytokeratin; ROI, region of interest.

To assess the capacity of skin B cells and plasmablasts to produce anti-CEL autoantibodies, we performed enzyme-linked immunosorbent spots on sorted populations from three patients with HS in which adequate cell numbers could be obtained for such functional analyses. Specifically, CD45⁺ CD3⁻ CD19⁺ IgD⁻ CD20^{hi} CD38^{lo} (non-naïve) B cells and CD20^{lo} CD38^{hi} plasmablasts were sorted to high purity and plated on CEL BSA-coated membranes in tissue culture media and assessed for IgG and IgA secretion the following day (Figure 5h and [Supplementary Figure S5a](#)). Global IgA and IgG secretion was also assessed and observed in both B

cells and plasmablasts ([Supplementary Figure S5b](#)). CEL-specific Ig was infrequently observed from sorted B cells (Figure 5i and data not shown), but CEL-specific IgG and IgA were readily detected in plates incubated with plasmablasts sorted from all the three patients, without the need for further stimulation in vitro, a hallmark of plasmablasts/plasma cells (Figure 5j and data not shown). We conclude that anti-CEL-specific plasmablasts are present in lesional skin of patients with HS and produce anti-CEL antibodies in situ.

Finally, we were interested in the functional consequences of the anti-CEL Igs. Our initial examination of HS sera from

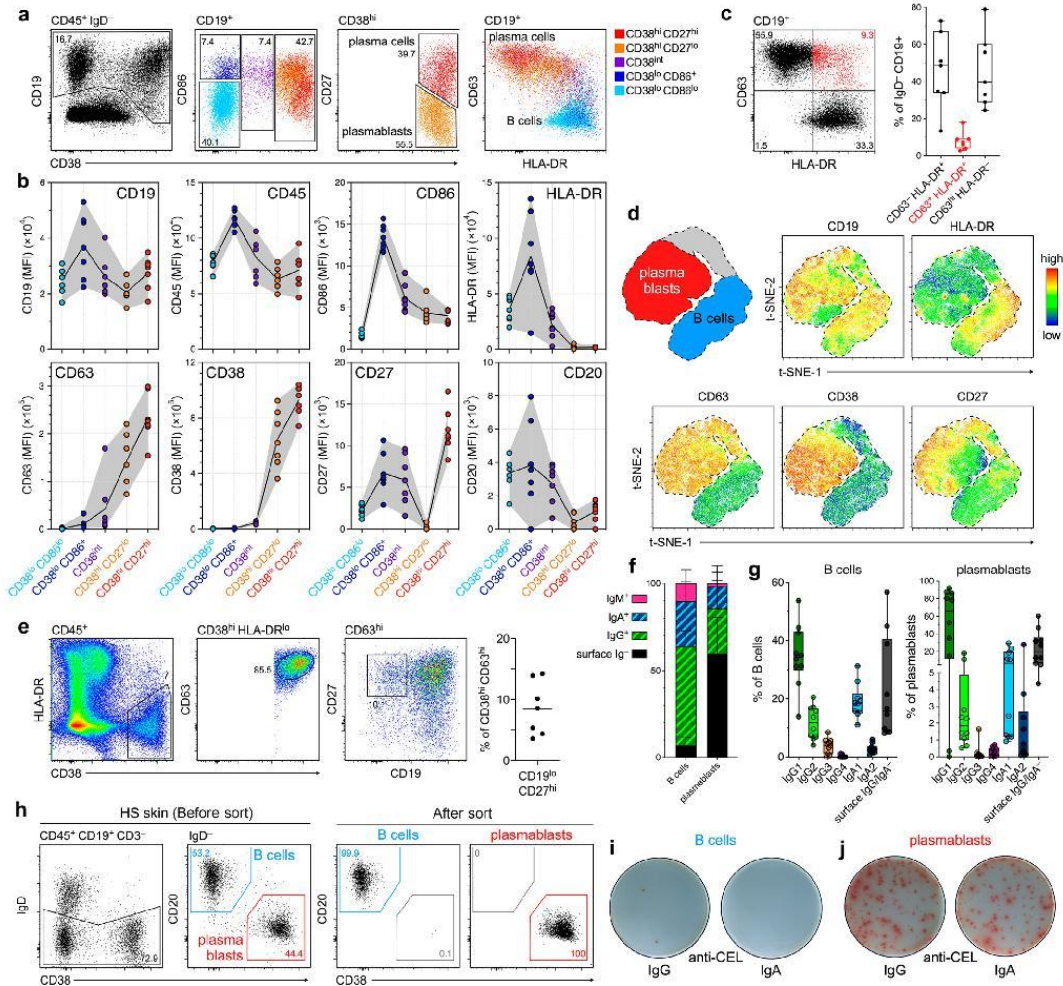


Figure 5. Detection of anti-CEL antibody-producing plasmablasts in HS skin. (a) Representative flow cytometry dotplots of (non-naïve) B cells ($CD45^{+} IgD^{-} CD19^{+} CD38^{lo}$), plasmablasts ($CD38^{hi}$), and plasma cells ($CD38^{hi} CD27^{+}$) in lesional HS skin. (b) MFI values for indicated surface markers across the five B- and plasma cell populations identified in a ($n = 7$). (c) Representative flow cytometry dotplot (left) and frequencies (right) of HLA-DR $^{+} CD63^{+}$ B cells, HLA-DR $^{-} CD63^{hi}$ plasmablasts, and HLA-DR $^{+} CD63^{+}$ (transitional) cells (red) in lesional HS skin. (d) t-SNE plots of flow cytometry data from $CD19^{+}$ cells isolated from HS skin. Top left: Schematic defining the location of B cells (blue), plasmablasts (red), and transitional cells (gray) in the accompanying t-SNE plots. (e) Identification of $CD38^{hi} CD63^{hi} CD19^{lo} CD27^{+}$ cells resembling long-lived plasma cells in lesional HS skin ($n = 7$). (f) The proportion of B cells and plasmablasts expressing surface IgM (pink), IgA (blue), and IgG (green) in HS skin samples ($n = 7$). (g) The proportion of surface Ig $^{-}$ cells is shown in black. (h) Representative flow cytometry dotplots of (non-naïve) $CD20^{hi} CD38^{lo}$ B cells (blue) and $CD20^{lo} CD38^{hi}$ plasmablasts (red) in lesional HS skin before (left) and after (right) sorting for ELISPOT readouts. (i, j) Representative ELISPOT plates of sorted B cells and plasmablasts (2.5×10^4 cells per well) isolated from HS skin, identifying the presence of CEL-specific antibody-secreting cells. Data are representative of three independent experiments. CEL, carboxyethyl lysine; ELISPOT, enzyme-linked immunosorbent spot; HS, hidradenitis suppurativa; MFI, mean fluorescence intensity; t-SNE, t-distributed stochastic neighbor embedding.

cohort 1 indicated the presence of anti-CEL IgM, IgG, and IgA and that all the three subclasses could compete equally for CEL binding in vitro (data not shown), but we had not identified the IgG subclasses nor performed any functional assays. We therefore reassessed the plasma samples from cohort 2 for IgG isotype specificity. Strikingly, the vast majority of anti-

CEL IgG was IgG2 (Supplementary Figure S6a). Consistent with this, anti-CEL IgG2 titers correlated near perfectly with total anti-CEL IgG titers, and deviations from this correlation were explained by the presence of additional IgG1 and IgG3 subclasses in a subset of patients (Supplementary Figure S6b and c). IgG2 is typically associated with bacterial capsular

polysaccharide antigens and is weakly capable of activating complement and Fc receptor cross-linking. We assessed both *in vitro*, using CEL BSA as a model antigen. For complement activation, we used the plasma from cohort 2, which contained variable titers of anti-CEL IgG1, IgG2, IgG3, IgM, and IgA. Plates were coated with CEL BSA before the addition of HS or healthy control plasma, washed, and then provided excessive complement from healthy serum and incubated for 1 hour at 37 °C. Soluble C5b-9 was used as a readout of complement activation. Half of the sample of patients with HS exhibited complement activation above that seen in healthy controls (Supplementary Figure S6d). Soluble C5b-9 correlated weakly with individual anti-CEL IgG and IgM titers but very strongly with a combination of both IgG and IgM (Supplementary Figure S6e–g), suggesting that both IgG and IgM subclasses contributed to complement activation in this assay.

For the Fc receptor activation experiments, we used locally and commercially obtained serum from patients with HS, together with *in vitro* generated macrophages. We stimulated macrophages with a mixture of CEL BSA and HS serum, measuring TNF secretion as readout. Macrophages treated with CEL BSA alone or CEL BSA with healthy serum were negative (data not shown), whereas HS serum alone similarly induced negligible TNF secretion across the seven donors assessed (Supplementary Figure S6h). In contrast, serum from 2 of 7 donors with HS induced robust TNF production in combination with CEL BSA, which correlated with IgG2 titers (Supplementary Figure S6h and data not shown). We conclude that anti-CEL autoantibodies are capable of activating complement and macrophages *in vitro*.

DISCUSSION

In this study, we identify anti-CEL IgGs as highly prevalent and highly abundant autoantibodies in patients with HS. Anti-CEL-producing plasmablasts were detectable within lesional skin, and anti-CEL IgG titers correlated with both disease duration and severity of patients with HS. Although autoantibodies have been previously identified in HS, for example, antinuclear antibodies and anticyclic citrullinated peptide (Byrd et al., 2019; Carmona-Rivera et al., 2022; Mulani et al., 2018), they have all been associated more markedly with other autoimmune diseases (i.e., systemic lupus erythematosus and rheumatoid arthritis, respectively). To the best of our knowledge, this study identifies a hitherto unknown association between anti-CEL autoantibodies and HS that demonstrate a high degree of disease specificity. Nevertheless, anti-CEL IgG is not a conventional autoantibody, being mainly of the IgG2 subtype. This observation was striking and unexpected because most pathogenic antibodies are IgG1 or IgG4, whereas natural (non-IgM) autoantibodies are believed to favor the IgG3 subclass (Lobo, 2016). IgG2 plays an important role against encapsulated bacteria (Vidarsson et al., 2014), but the relevance of the anti-CEL IgG2 in HS remains unclear. Although our data do not provide a formal demonstration for a potential pathogenic role of anti-CEL autoantibodies in HS, *in vitro*, anti-CEL IgG could activate both complement and macrophages and is thus theoretically capable of proinflammatory functions.

Alternatively, anti-CEL IgG may serve counter-inflammatory and/or protective functions, as has been theorized for other autoantibodies (Pisetsky, 2012).

A second finding around this target relates to the high titers of anti-CEL IgM antibodies in healthy subjects, which is consistent with the previously reported presence of natural autoantibodies against advanced glycation end products and other naturally occurring adducts in healthy individuals and patients with diabetes (Shibayama et al., 1999; Turk et al., 2001; Wang et al., 2013). Indeed, CEL is a common modification in mammalian physiology and is readily detectable within the serum of healthy individuals, which aligns with the function of natural autoantibodies in homeostatic maintenance. However and notably, few healthy individuals exhibited concordantly high anti-CEL IgG and rarely to the levels seen in patients with HS. Thus, it is not the presence of anti-CEL autoantibodies that appears to be disease defining but rather the conversion to IgG- and IgA-producing subclasses. How, when, and where such class switching occurs remains unknown, but we speculate on the basis of our results that the inflammatory skin lesions themselves may serve as a site of IgG and IgA plasma cell generation.

The predominance of anti-CEL IgG2 may reflect the chronic nature of HS, as might be explained by the temporal model, which predicts the emergence of IgG2 later in immune responses (Collins and Jackson, 2013). Alternatively, this may reflect qualitative features of the microenvironment during class switching, for example, the presence of IFN- γ (Kitani and Strober, 1993). It is also possible that the anti-CEL IgG2 reflects the nature of T cell help or lack thereof. The potential role of T cells in anti-CEL generation was not investigated in our study and remains an important avenue for future investigation. However, it should be noted that T-cell recognition of methyl-lysines has been recently reported (Corbière et al., 2020), raising the possibility that patients with HS may uniquely harbor T cells specific for carboxyethyl-lysine. The origins and effector functions of autoreactive CEL-specific T cells within patients with HS, presuming that they exist, remain completely unknown and require future investigation.

The selective detection of CEL- but not CML-specific autoantibodies in HS strongly implicates a role for methylglyoxal in the etiology of the disease. Dysregulation of the methylglyoxal pathway has been identified and extensively investigated in the context of type 2 diabetes and metabolic disorders (Maessen et al., 2015; Schalkwijk and Stehouwer, 2020; Shamsaldeen et al., 2016), both common comorbidities in HS. It is therefore tempting to speculate that there exists an interplay between global metabolic changes and the immune recognition of the associated protein modifications. However, the lack of association between anti-CEL titers and body mass index undermines this concept, and there exist more proximal explanations. For example, methylglyoxal is a byproduct of glycolysis, a driver of inflammation (Soto-Herederó et al., 2020). Indeed, a recent report suggests that myeloid cells utilize methylglyoxal as part of an anti-inflammatory mechanism (Baumann et al., 2020). Thus, it is likely that HS lesions are abundant in methylglyoxal, which may modify the abundance and/or distribution of CEL-modified proteins in HS lesional skin.

The relationship between anti-CEL IgG titers with both disease severity and duration is suggestive of a disease process in which CEL-reactive B cells are generated and/or expanded proportionally to disease severity and that these cells also persist for several years. On the basis of our flow cytometry and enzyme-linked immunosorbent spot experiments with HS skin, we speculate that this process involves the in situ generation of CEL-specific plasmablasts, some of which may persist into long-lived plasma cells. Increased plasma cells have been observed in the blood of patients with HS (Musilova et al., 2020), which would be consistent with the trafficking of skin-derived plasma cells to the bone marrow. An important consequence of this interpretation is the prediction that anti-CEL IgG titers can be expected to accumulate throughout life and serve as a permanent record of global disease burden. If true, anti-CEL IgG may hold important prognostic value, particularly in epidemiological studies. Anti-CEL autoantibodies may additionally hold potential as diagnostic and/or severity biomarkers in HS (Der Sarkissian et al., 2022).

Finally, the presence of anti-CEL autoantibodies in patients with Crohn's and UC (albeit at lower titers than in HS) adds to an intriguing list of commonalities between HS and inflammatory bowel disease. Inflammatory bowel disease, particularly Crohn's, but also UC is more common in patients with HS than in the general population (Chen and Chi, 2019). Both Crohn's disease and UC lesions are similarly characterized by B cell infiltrates (Defendenti et al., 2012). HS also shares other histopathological features with Crohn's, particularly the perirectal ulceration and granulomatous cutaneous inflammation (Principi et al., 2016), and all the three diseases respond to anti-TNF therapy. Together, these data suggest that methylglyoxal and anti-CEL autoantibodies may also play a role in inflammatory bowel disease and adds weight to the notion that there exist several shared pathological pathways between HS and inflammatory bowel disease.

In conclusion, our data define a hitherto unappreciated and unconventional pathway of autoantibody production in HS, which raises several questions but also opportunities for better understanding and management of this devastating disease.

MATERIALS AND METHODS

Serum and plasma samples from patients with HS

The sera of patients in cohort 1 were taken from patients with HS during their baseline visit as part of a proof-of-concept, phase 2 randomized clinical trial of CJM112, a human anti-IL-17A/IL-17AF high-affinity IgG1κ mAb in HS (NCT02421171). Only baseline samples (i.e., untreated at the time of collection) from patients who signed written informed consent for exploratory biomarker analysis were used. Patient characteristics collected as part of the study are summarized in Supplementary Table S2. The plasma of patients in cohort 2 was collected from 40 patients with HS recruited through the HS outpatient clinic of the Department of Dermatology, Erasmus University Medical Center (Rotterdam, The Netherlands). All samples were obtained with written informed consent from the participants in accordance with the Declaration of Helsinki principles, the Swiss Human Research Act, and the approval of the responsible ethics committee (Ethikkommission Nordwest- und Zentralschweiz).

HS skin samples

Skin from patients with HS undergoing surgical excision was received from the Department of Plastic, Reconstructive, Aesthetic and Hand Surgery of the University Hospital Basel (Basel, Switzerland); from the Clinic for General, Visceral, Vascular and Thoracic Surgery, Cantonal Hospital Baselland (Liestal, Switzerland); or from Praxis beim Merian Iselin (Basel, Switzerland), or the patients were recruited from the HS outpatient clinic of the Department of Dermatology, Erasmus University Medical Center. All patients provided written informed consent, and the study was conducted in accordance with the ethical principles originating in the Declaration of Helsinki and approved by the Institutional Review Board of the Erasmus University Medical Center.

Autoantibody profiling

Autoantibodies were detected using a custom-made Luminex assay on the basis of magnetic beads. All washing steps of magnetic beads in tubes and plates were performed with the support of magnetic separation plates.

Quantification and statistical analyses

The statistical details and tests used, the number and representation of *n*, and any other forms of quantification present are specified in the respective figure legends and results section.

Additional details of the data and approaches are available in the Supplementary Materials and Methods.

Data availability statement

The authors confirm that the data supporting the findings of this study are available within the article and its supplementary materials. Datasets related to this article can be found at <https://www.ncbi.nlm.nih.gov/geo/query/acc.cgi?acc=GSE148027>, hosted at the Gene Expression Omnibus, GSE148027.

ORCIDs

Giulio Macchiarella: <http://orcid.org/0000-0001-9959-3675>
Vanessa Cornacchione: <http://orcid.org/0000-0002-4551-5193>
Celine Cojean: <http://orcid.org/0000-0003-2399-9833>
Julia Riker: <http://orcid.org/0000-0001-5024-6170>
Yichen Wang: <http://orcid.org/0000-0003-1955-2318>
Helene Te: <http://orcid.org/0000-0002-2872-2430>
Melanie Ceci: <http://orcid.org/0000-0003-1830-8057>
Johann E. Gudjonsson: <http://orcid.org/0000-0002-0080-0812>
Swann Gaulis: <http://orcid.org/0000-0001-8319-7723>
Jean François Goetschy: <http://orcid.org/0000-0002-8077-9725>
Audrey Wollschlegel: <http://orcid.org/0000-0002-3408-1190>
Stephanie K. Gass: <http://orcid.org/0000-0002-0181-161X>
Sofia Oetliker-Contin: <http://orcid.org/0000-0002-4419-8480>
Barbara Wettstein-Ling: <http://orcid.org/0000-0002-8718-7351>
Dirk J. Schaefer: <http://orcid.org/0000-0002-9619-8650>
Pascale Meschberger: <http://orcid.org/0000-0003-1871-1145>
Roland de Roche: <http://orcid.org/0000-0003-3001-0544>
Rik Osinga: <http://orcid.org/0000-0002-3333-0757>
Grazyna Wiecek: <http://orcid.org/0000-0001-9212-7858>
Ulrike Naumann: <http://orcid.org/0000-0001-7783-7675>
Joachim C.U. Lehmann: <http://orcid.org/0000-0001-6554-1885>
Anna Schubart: <http://orcid.org/0000-0003-4253-0600>
Andreas Hofmann: <http://orcid.org/0000-0001-5450-6267>
Lukas Roth: <http://orcid.org/0000-0001-9270-1936>
Edwin F. Florencia: <http://orcid.org/0000-0001-9005-4464>
Christian Loesche: <http://orcid.org/0000-0001-6505-0349>
Elisabetta Traggiai: <http://orcid.org/0000-0002-0616-6285>
Alexandre Avrameas: <http://orcid.org/0000-0003-4094-5829>
Errol P. Prens: <http://orcid.org/0000-0002-8158-660X>
Till A. Röhn: <http://orcid.org/0000-0002-2448-3110>
Ben Roediger: <http://orcid.org/0000-0002-4593-091X>

CONFLICT OF INTEREST

AA, AH, AS, AW, BR, CC, CL, ET, GW, HT, JCUL, JFG, JR, LR, MC, SG, TAR, UN, VC, and YW are current or former employees of and hold company stocks or stock options with Novartis Pharma AG.

ACKNOWLEDGMENTS

We thank Annette Begrich, Matthias Jecklin, Mateusz Piksa, and Paul Schroeder for the coordination of human tissue acquisition. We thank Astrid Jullion for assistance with the clinical data. We thank Friedrich Raulf, Corine Vedrine, Elena Degl Innocenti, and Siwar Garmatou for reagents and technical assistance. We also acknowledge the flow cytometry assistance of Cyril Allard, Emeline Thevenon, Matthias Wrobel, Martine Marchant, and Elodie Riquet. We thank the team at NanoString Technologies, particularly Jennifer Hart and Jingjing Gong. We thank Georg Martiny-Baron, Feriel Hacini-Rachinel, Julian Störin, Rainer Hillenbrand, Catherine Regnier, Sandro Bruno, Pascal Forrer, Frank Kolbinger, Stephen Oliver, Peter Gergely, Tobias Junt, and Isabelle Isnardi for useful discussions. We are grateful to Jonas Zierer and Lucia Csepregi for their helpful comments. We thank the following principal investigators in the hidradenitis suppurativa study (NCT02421171): Gregor Jenec, Christos C. Zouboulis, Falk G. Bechara, Matthew Zook, Lars French, Robert Hunger, Barbara Hováth, Sylke Schneider-Burns, James A. Solomon, Michael H. Gold, Howard Sofen, Joel Schlessinger, Benjamin N. Lockshin, Kenneth W. Dawes, Jan Mekkes, and Christian Vestergaard. We also thank Izabela Rozenberg, Philip Jarvis, and Thomas Peters for their respective roles in hidradenitis suppurativa study (NCT02421171). This work was supported by Novartis Institutes for BioMedical Research.

AUTHOR CONTRIBUTIONS

Conceptualization: AA, BR, CL, ET, TAR, VC; Formal Analysis: AA, AS, BR, ET, GM, GW, JCUL, LR, SG, VC, YW; Investigation: AA, AH, AS, AW, BR, CC, EPP, ET, GM, GW, HT, JCUL, JFG, JR, LR, MC, TAR, UN, VC, YW; Methodology: AA, AS, AW, BR, CC, ET, GM, GW, HT, JCUL, JEG, JFG, JR, LR, MC, UN, YW; Resources: BWL, DJS, EFF, EPP, JEG, PM, RDR, RO, SKG, SOC; Supervision: AA, AS, BR, EPP, ET, GW, JCUL, LR, TAR; Writing – Original Draft Preparation: BR, GM, TAR; Writing – Review and Editing: AA, BR, EFF, EPP, ET, GM, JEG, LR, TAR, VC

SUPPLEMENTARY MATERIAL

Supplementary material is linked to the online version of the paper at www.jidonline.org, and at <https://doi.org/10.1016/j.jid.2022.08.051>

REFERENCES

Baumann T, Dunkel A, Schmid C, Schmitt S, Hiltensperger M, Lohr K, et al. Regulatory myeloid cells paralyze T cells through cell-cell transfer of the metabolite methylglyoxal. *Nat Immunol* 2020;21:555–66.

Byrd AS, Carmona-Rivera C, O'Neil LJ, Carlucci PM, Cisar C, Rosenberg AZ, et al. Neutrophil extracellular traps, B cells, and type I interferons contribute to immune dysregulation in hidradenitis suppurativa. *Sci Transl Med* 2019;11:eaav5908.

Carlavan I, Bertino B, Rivier M, Martel P, Bourdes V, Motte M, et al. Atrophic scar formation in patients with acne involves long-acting immune responses with plasma cells and alteration of sebaceous glands. *Br J Dermatol* 2018;179:906–17.

Carmona-Rivera C, O'Neil LJ, Patino-Martinez E, Shipman WD, Zhu C, Li QZ, et al. Autoantibodies present in hidradenitis suppurativa correlate with disease severity and promote the release of proinflammatory cytokines in macrophages. *J Invest Dermatol* 2022;142:924–35.

Chen WT, Chi CC. Association of hidradenitis suppurativa with inflammatory bowel disease: A systematic review and meta-analysis. *JAMA Dermatol* 2019;155:1022–7.

Collins AM, Jackson KJ. A temporal model of human IgE and IgG antibody function. *Front Immunol* 2013;4:235.

Constantinou CA, Fragoulis GE, Nikiphorou E. Hidradenitis suppurativa: infection, autoimmunity, or both? *Ther Adv Musculoskelet Dis* 2019;11:1759720X19895488.

Corbière V, Segers J, Desmet R, Lecher S, Loyens M, Petit E, et al. Natural T cell epitope containing methyl lysines on mycobacterial heparin-binding hemagglutinin. *J Immunol* 2020;204:1715–23.

Czarnowicki T, Gonzalez J, Bonifacio KM, Shemer A, Xiangyu P, Kunjavia N, et al. Diverse activation and differentiation of multiple B-cell subsets in patients with atopic dermatitis but not in patients with psoriasis. *J Allergy Clin Immunol* 2016;137:118–29.e5.

Defendenti C, Grosso S, Atzeni F, Croce A, Senesi O, Saibeni S, et al. Unusual B cell morphology in inflammatory bowel disease. *Pathol Res Pract* 2012;208:387–91.

Der Sarkissian S, Hessian S, Kirby JS, Lowes MA, Mintoff D, Naik HB, et al. Identification of biomarkers and critical evaluation of biomarkers validation in hidradenitis suppurativa: a systematic review [published correction appears in *JAM Dermatol* 2022;158:590]. *JAMA Dermatol* 2022;158:300–13.

Figueras-Nart I, Mascaró JM Jr, Solanich X, Hernández-Rodríguez J. Dermatologic and dermatopathologic features of monogenic autoinflammatory diseases. *Front Immunol* 2019;10:2448.

Fletcher JM, Moran B, Petrasca A, Smith CM. IL-17 in inflammatory skin diseases psoriasis and hidradenitis suppurativa. *Clin Exp Immunol* 2020;201:121–34.

Galligan JJ, Wepy JA, Streeter MD, Kingsley PJ, Mitchener MM, Wauchope OR, et al. Methylglyoxal-derived posttranslational arginine modifications are abundant histone marks. *Proc Natl Acad Sci USA* 2018;115:9228–33.

Gudjonsson JE, Tsoi LC, Ma F, Billi AC, van Straalen KR, Vossen ARJV, et al. Contribution of plasma cells and B cells to hidradenitis suppurativa pathogenesis. *JCI Insight* 2020;5.

Guedj K, Abitbol Y, Cazals-Hatem D, Morvan M, Maggioli L, Panis Y, et al. Adipocytes orchestrate the formation of tertiary lymphoid organs in the creeping fat of Crohn's disease affected mesentery. *J Autoimmun* 2019;103:102281.

Halliley JL, Tipton CM, Liesveld J, Rosenberg AF, Darce J, Gregoretti IV, et al. Long-lived plasma cells are contained within the CD19(-)CD38(hi)CD138(+) subset in human bone marrow. *Immunity* 2015;43:132–45.

Hua VJ, Kilgour JM, Cho HG, Li S, Sarin KY. Characterization of comorbidity heterogeneity among 13,667 patients with hidradenitis suppurativa. *JCI Insight* 2021;6:e151872.

Kitani A, Strober W. Regulation of C gamma subclass germ-line transcripts in human peripheral blood B cells. *J Immunol* 1993;151:3478–88.

Kromann CB, Deckers IE, Esmann S, Boer J, Prens EP, Jemec GB. Risk factors, clinical course and long-term prognosis in hidradenitis suppurativa: a cross-sectional study. *Br J Dermatol* 2014;171:819–24.

Lobo PI. Role of natural autoantibodies and natural IgM anti-leucocyte autoantibodies in health and disease. *Front Immunol* 2016;7:198.

Maessen DE, Stehouwer CD, Schalkwijk CG. The role of methylglyoxal and the glyoxalase system in diabetes and other age-related diseases. *Clin Sci (Lond)* 2015;128:839–61.

Mulani S, McNish S, Jones D, Shanmugam VK. Prevalence of antinuclear antibodies in hidradenitis suppurativa. *Int J Rheum Dis* 2018;21:1018–22.

Musilova J, Moran B, Sweeney CM, Malara A, Zaborowski A, Hughes R, et al. Enrichment of plasma cells in the peripheral blood and skin of patients with hidradenitis suppurativa. *J Invest Dermatol* 2020;140:1091–4.e2.

Penno CA, Jäger P, Laguerre C, Hasler F, Hofmann A, Cass SK, et al. Lipidomics profiling of hidradenitis suppurativa skin lesions reveals lipooxygenase pathway dysregulation and accumulation of proinflammatory leukotriene B4. *J Invest Dermatol* 2020;140:2421–32. e10.

Pisetsky DS. Antinuclear antibodies in rheumatic disease: a proposal for a function-based classification. *Scand J Immunol* 2012;76:223–8.

Prens E, Deckers I. Pathophysiology of hidradenitis suppurativa: an update. *J Am Acad Dermatol* 2015;73:S8–11.

Principi M, Cassano N, Contaldo A, Iannone A, Losurdo G, Barone M, et al. Hidradenitis suppurativa and inflammatory bowel disease: an unusual, but existing association. *World J Gastroenterol* 2016;22:4802–11.

Richette P, Molto A, Viguier M, Dawidowicz K, Hayem G, Nassif A, et al. Hidradenitis suppurativa associated with spondyloarthritis – results from a multicenter national prospective study. *J Rheumatol* 2014;41:490–4.

Savage KT, Flood KS, Porter ML, Kimball AB. TNF- α inhibitors in the treatment of hidradenitis suppurativa. *Ther Adv Chronic Dis* 2019;10:2040622319851640.

Schalkwijk CG, Stehouwer CDA. Methylglyoxal, a highly reactive dicarbonyl compound, in diabetes, its vascular complications, and other age-related diseases. *Physiol Rev* 2020;100:407–61.

Shamsaldeen YA, Mackenzie LS, Lione LA, Benham CD. Methylglyoxal, A metabolite increased in diabetes is associated with insulin resistance,

- vascular dysfunction and neuropathies. *Curr Drug Metab* 2016;17:359–67.
- Shibayama R, Araki N, Nagai R, Horiuchi S. Autoantibody against N(epsilon)-(carboxymethyl)lysine: an advanced glycation end product of the Maillard reaction. *Diabetes* 1999;48:1842–9.
- Soreide K. Receiver-operating characteristic curve analysis in diagnostic, prognostic and predictive biomarker research. *J Clin Pathol* 2009;62:1–5.
- Soto-Herederó G, Gómez de Las Heras MM, Gabandé-Rodríguez E, Oller J, Mittelbrunn M. Glycolysis - a key player in the inflammatory response. *FEBS Journal* 2020;287:3350–69.
- Spergel JM, Paller AS. Atopic dermatitis and the atopic march. *J Allergy Clin Immunol* 2003;112:S118–27.
- Turk Z, Ljubic S, Turk N, Benko B. Detection of autoantibodies against advanced glycation endproducts and AGE-immune complexes in serum of patients with diabetes mellitus. *Clin Chim Acta* 2001;303:105–15.
- Tzanetakou V, Kanni T, Gitrakou S, Katoulis A, Papadavid E, Netea MG, et al. Safety and efficacy of anakinra in severe hidradenitis suppurativa: a randomized clinical trial [published correction appears in *JAM Dermatol* 2017;153:950]. *JAMA Dermatol* 2016;152:52–9.
- van der Zee HH, de Ruyter L, Boer J, van den Broecke DG, den Hollander JC, Laman JD, et al. Alterations in leucocyte subsets and histomorphology in normal-appearing perilesional skin and early and chronic hidradenitis suppurativa lesions. *Br J Dermatol* 2012;166:98–106.
- Vanlaerhoven AMJD, Ardon CB, van Straalen KR, Vossen ARJV, Prens EP, van der Zee HH. Hurley III hidradenitis suppurativa has an aggressive disease course. *Dermatology* 2018;234:232–3.
- Vidarsson G, Dekkers G, Rispens T. IgG subclasses and allotypes: from structure to effector functions. *Front Immunol* 2014;5:520.
- Vistoli G, De Maddis D, Cipak A, Zarkovic N, Carini M, Aldini G. Advanced glycoxidation and lipoxidation end products (AGEs and ALEs): an overview of their mechanisms of formation. *Free Radic Res* 2013;47(Suppl. 1):3–27.
- von der Werth JM, Williams HC. The natural history of hidradenitis suppurativa. *J Eur Acad Dermatol Venereol* 2000;14:389–92.
- Wang C, Turunen SP, Kumm O, Veneskoski M, Lehtimäki J, Nissinen AE, et al. Natural antibodies of newborns recognize oxidative stress-related malondialdehyde acetaldehyde adducts on apoptotic cells and atherosclerotic plaques. *Int Immunol* 2013;25:575–87.



This work is licensed under a Creative Commons Attribution-NonCommercial-NoDerivatives 4.0 International License. To view a copy of this license, visit <http://creativecommons.org/licenses/by-nc-nd/4.0/>

SUPPLEMENTARY MATERIALS AND METHODS

Serum samples from patients with hidradenitis suppurativa

The sera of patients in cohort 1 were taken from patients with hidradenitis suppurativa (HS) during their baseline visit as part of a proof-of-concept, phase 2 randomized clinical trial of CJM112, a human anti-IL-17A/IL-17AF high-affinity IgG1κ mAb in HS (NCT02421171). Briefly, all patients were adults aged between 18 and 65 years with chronic moderate-to-severe HS for at least 1 year before screening and who had previously undergone antibiotic therapy. Moderate-to-severe HS was defined as having an HS Physician's Global Assessment score of at least moderate severity (score ≥ 3) and with at least four abscesses and/or nodules. Additional inclusion criteria required patients to have HS lesions in at least two anatomical areas, and at least one area had to be minimally Hurley stage 2. Patients receiving systemic treatment (including retinoids and immunomodulatory therapies) or antibiotics were required to stop treatment at least 4 weeks before randomization. Patients previously treated with IL-17 pathway inhibitors, including secukinumab, ixekizumab, and brodalumab, were excluded from the study. Adequate wash-out periods were applied for patients treated with biologics; no wash-out period was requested for treatment with topicals. A further list of inclusion and exclusion criteria can be found at clinicaltrials.gov (Identifier: NCT02421172). Only baseline samples (i.e., untreated at the time of collection) from patients who signed written informed consent for exploratory biomarker analysis were used. Patient characteristics collected as part of the study are summarized in [Supplementary Table S2](#).

Serum samples from patients without HS

The sera of patients with acne were taken from patients during their baseline visit as part of a proof-of-concept, phase 2 randomized clinical trial of CJM112 in acne vulgaris (NCT02998671). Only baseline samples (i.e., untreated at the time of collection) from patients who signed written informed consent for exploratory biomarker analysis were used.

Serum samples from patients with atopic dermatitis, ulcerative colitis, and Crohn's disease were purchased from BioIVT (Westbury, NY). As per recruiting proceeding, all patients donating human material to BioIVT signed an informed consent accepting the use of such material for exploratory research.

Plasma samples from patients with HS

The plasma from patients in cohort 2 was collected from 40 patients with HS recruited through the HS outpatient clinic of the Department of Dermatology, Erasmus University Medical Center (Rotterdam, The Netherlands). Briefly, all patients were adults aged between 18 and 62 years with a clinical diagnosis of HS for at least 1 year before sample collection. No exclusions were made regarding severity or previous or ongoing treatment. All samples were obtained with written informed consent from the participants in accordance with the Declaration of Helsinki principles. The study protocol was approved by the Institutional Review Board of the Erasmus University Medical Center (MEC-2016-426). The patient characteristics are listed in [Supplementary Table S2](#).

Serum and plasma samples from healthy volunteers

Healthy volunteer (HV) serum controls (n = 22; aged 28–70 years, mean = 50 years, median = 52 years; three males [14%], 19 females [86%]), used in [Figure 1](#) and [Supplementary Figure S1](#), were purchased from BioIVT. As per recruiting proceeding, all patients donating human material to BioIVT signed an informed consent accepting the use of such material for exploratory research.

Plasma from HVs (n = 34; aged 25–80 years, mean = 36–46 years, median = 37–47 years; 19 males [56%], 15 females [44%]), as used in [Figure 3](#) and [Supplementary Figures S2](#) and [S6](#), was obtained under written informed consent either through the Novartis Tissue Donor Program (TRI0128; 2017-00271) or from the University Hospital Basel (Basel, Switzerland), as part of noninterventional biomarker study BASICHR0043 (2019-02188). Both are in accordance with the Swiss Human Research Act and approval of the responsible ethics committee (Ethikkommission Nordwest-und Zentralschweiz number: 329/13).

Specific details of healthy control samples are listed in [Supplementary Table S4](#). Note that to ensure confidentiality, the ages of Novartis Tissue Donor Program donors are only provided as range data.

HS skin samples from Basel and Baselland, Switzerland

Skin from patients with HS undergoing surgical excision was received from the Department of Plastic, Reconstructive, Aesthetic and Hand Surgery of University Hospital Basel (Basel, Switzerland); from the Clinic for General, Visceral, Vascular and Thoracic surgery, Cantonal Hospital Baselland (Liestal, Switzerland); or from Praxis beim Merian Iselin (Basel, Switzerland) as part of noninterventional biomarker studies TRI1270397 and BASICHR0043. All patients provided written informed consent, and the study was conducted in accordance with the ethical principles originating in the Declaration of Helsinki and was approved by the local Ethics Committee (EKNZ 2016-01204; EKNZ 2019-02188). The anatomical sites of excisions were inconsistently recorded and are not tracked in this manuscript.

HS skin samples from Rotterdam, Netherlands

Patients with moderate-to-severe HS undergoing surgery were recruited from the HS outpatient clinic of the Department of Dermatology, Erasmus University Medical Center. Patients had ceased any previous topical or systemic treatment at least 2 weeks before enrollment. Biopsies from lesional skin were collected from resected tissue after routine surgery. Lesional tissue was defined on the basis of the presence of nodules/abscesses and/or tunnels. Lesional tissue was not differentially segregated on the basis of the presence or absence of tunnels. The study protocol was approved by the Institutional Review Board of the Erasmus University Medical Center (MEC-2013-337) and was conducted in accordance with the ethical principles originating in the Declaration of Helsinki. The anatomical sites of excisions were inconsistently recorded and are not tracked in this manuscript.

Autoantigens

All autoantigens screened in this study were obtained from commercial sources, except for flagellin, which was

conjugated to BSA internally (see the paragraph below). The list of autoantigens, the commercial vendors, and catalog numbers as well as the rationale for their inclusion are summarized in [Supplementary Table S1](#).

BSA-conjugated flagellin modification

Flagellin (catalog number TLRL-BSFLA, Invivogen, San Diego, CA) was reconstituted by reverse pipetting with LAL water (catalog number H2OLAL-1.5, Invivogen) to obtain a solution at 1 mg/ml. A 1 g of BSA (catalog number 001-000-162, Jackson ImmunoResearch, West Grove, PA) was dissolved in 50 ml of demineralized water to obtain a stock solution at 20 mg/ml. A total of 100 mg of N-(3-Dimethylaminopropyl)-N'-ethylcarbodiimide hydrochloride (catalog number E1769-5g, Sigma-Aldrich, St. Louis, MO) were dissolved in 2 ml of demineralized water to obtain a stock solution at 50 mg/ml. A total of 50 µl of flagellin at 1 mg/ml were mixed in a micronic tube (32022-MIC, Vitaris, Baar, Switzerland) with 2.5 µl of BSA at 20 mg/ml and 10 µl of N-(3-Dimethylaminopropyl)-N'-ethylcarbodiimide hydrochloride at 50 mg/ml. The solution was incubated overnight at +4 °C with slow agitation on a rotor to allow the coupling of flagellin on BSA. The purification of BSA-conjugated flagellin was performed through dialysis. Dialysis units (Slide-A-Lyser Mini Dialysis Units [10,000 MWCO, 0.1 ml]) (catalog number 69570, Thermo Fisher Scientific, Waltham, MA) with the buoys (catalog number 69588, Thermo Fisher Scientific) were put for 10 minutes into 2 l of dialysis buffer (PBS) (catalog number 14733200, Roche, Basel, Switzerland). The solution containing BSA-conjugated flagellin was added to the dialysis unit and dialyzed for 1 hour at room temperature. The dialysis buffer was changed every hour three times. The purified solution of BSA-conjugated flagellin, with a final concentration of 800 µg/ml, was then stored at -20 °C.

Autoantibody profiling

Autoantibodies were detected using a custom-made Luminex assay on the basis of magnetic beads. All washing steps of magnetic beads in tubes and plates were performed with the support of magnetic separation plates. Briefly, 100 µl of stock solution of Luminex magnetic beads were prewashed twice with 200 µl of Tris-buffered saline (TBS) (T9039, Sigma-Aldrich) in micronic tubes (Vitaris, 32022-MIC) and then resuspended in 200 µl of coating solution containing antigens at 20 µg/ml in TBS. After overnight incubation at +4 °C with continuous rolling and cover from light, beads were washed twice with 200 µl of 0.05% TBS-Tween (T9039, Sigma-Aldrich) and then blocked with 400 µl of blocking solution for 2 hours at room temperature, with continuous rolling and cover from light. The blocking solution was composed of TBS with non-fat milk (T8793, Sigma-Aldrich) at 3%, fetal bovine serum (FBS) (10082-147, Gibco, Waltham, CA) at 10%, and Proclin300 (48912U, Sigma-Aldrich) at 0.1%. Before plate loading, Luminex beads were mixed and washed once with 1 ml of 0.05% TBS-Tween and Proclin300 at 0.1% and then resuspended with 10.4 ml of 0.05% TBS-Tween and Proclin300 at 0.1%. Before being loaded on plates, serum or plasma samples were diluted at 1:100 in

0.05% TBS Tween, 10% FBS, 1% non-fat milk, and 0.1% BSA (001-000-162, Jackson ImmunoResearch). A total of 100 µl/well of diluted serum were loaded on a black polystyrene plate (3915, Costar, Corning, New York, NY) together with 25 µl/well of prepared magnetic beads. After 1 hour of incubation at room temperature with stirring at 750 r.p.m. and cover from light, the plate was washed twice with 300 µl/well of 0.05% TBS-Tween using an automatic washer (Elx405UM, Biotek, Winooski, VT) combined with a magnetic separation plate and 3 minutes of waiting time before and after the first wash. After washing, 100 µl/well of phycoerythrin-tagged detection antibody targeting IgG, IgG1, IgG2, IgG3, IgG4, IgM, or IgA (2040-09, 9054-09, 9070-09, 9210-09, 9190-09, 2020-09, 2050-09, Southern Biotech, Birmingham, AL), respectively, at 0.5 µg/ml and 1 µg/ml for IgG subclasses and 0.2 µg/ml and 1 µg/ml in 0.05% TBS-Tween were added and incubated on plate for 1 hour at room temperature with stirring at 750 r.p.m. and cover from light. The plate was then washed twice with 300 µl/well of 0.05% TBS-Tween using an automatic washer coupled with a magnetic separation plate and 3 minutes of waiting time before and after the first wash. A total of 120 µl/well of TBS, 0.5% BSA, and 0.1% Proclin300 were then added to the plate. After 3 minutes of incubation at room temperature with a stirring of 750 r.p.m. and cover from light to resuspend the beads, the plate was read using the Flexmap3D reader. Results were reported using the median fluorescence index as the unit of measure.

Incubation with carboxyethyl lysine, carboxy-methyl-lysine, and octopine before autoantibodies profiling assay

To test the specificity of anti-carboxyethyl lysine (CEL) autoantibodies, plasma samples were diluted at 1:100 with dilution buffer (0.05% TBS-Tween, 10% FBS, 1% non-fat milk, 0.1% BSA, 0.1% Proclin300) containing 50 µg/ml of either CEL (25333, Cayman Chemical, Ann Arbor, MI), carboxy-methyl-lysine (16483, Cayman Chemical), or octopine (MBS6045660, MyBiosource, San Diego, CA). The samples were incubated for 30 minutes at room temperature before proceeding with the autoantibodies assay. Control samples diluted with a buffer not containing CEL, carboxy-methyl-lysine, or octopine were also incubated for 30 minutes at room temperature before proceeding with the autoantibodies assay.

Methylglyoxal modification of histone

Methylglyoxal-modified histone was prepared using a protocol described by [Srey et al. \(2010\)](#). Recombinant human histone H2A was dialyzed against PBS before the Methylglyoxal-modification reaction. Specifically, histone H2A (H2042, Sigma-Aldrich) at 0.1 mg/ml was mixed with sodium pyruvate (S8636, Sigma-Aldrich) (17.14 mM) and sodium cyanoborohydride (156159, Sigma-Aldrich) (25.71 mM) in PBS (11666789001, Sigma-Aldrich) (0.1 M, pH 7.0). The solution was incubated at 37 °C for 24 hours and then abundantly dialyzed against PBS. A control was also prepared using the same conditions but with the omission of sodium pyruvate.

CEL detection by direct ELISA

A total of 2-mm punch biopsies of lesional HS skin were immersed in liquid nitrogen using Covaris tissue tubes TT05 (520071, Covaris, Woburn, MA) and crushed with a CP02 cryoPREP Automated Dry Pulverizer (500001, Covaris). The fragments of skin were collected and weighted and then resuspended with 50 µl of 0.05% TBS-Tween Triton 1% X-100 (T8787, Sigma-Aldrich). These solutions were then sonicated five times for 30 seconds and vortexed between each sonication. Skin lysates were then diluted at 1:10 in PBS (11666789001, Sigma-Aldrich). A total of 50 µl/well of diluted skin lysates and standards (CEL BSA from Cell Biolabs, San Diego, CA, STA-302, at different concentrations in PBS) were loaded on an ELISA plate and incubated overnight at 4 °C with stirring at 400 r.p.m. and cover from light. The plate was then washed four times with 300 µl/well of 0.05% PBS Tween (P3563, Sigma-Aldrich) and blotted against a tissue. The plate was blocked with 150 µl/well of 3% PBS BSA (BSA from Roche, 10735078001) for 1 hour at room temperature, with stirring at 500 r.p.m. and cover from light. The plate was then washed four times with 300 µl/well of 0.05% PBS Tween and blotted against a tissue. A total of 100 µl/

Disease duration was expressed in years and calculated as follows:

$$\text{Disease duration} = \text{Patient's age} - \text{age at disease onset}$$

Both numerical disease severity and disease duration for each patient were then standardized by dividing by the average, as follows:

$$\text{Std disease severity (patient n)} = \frac{\text{disease severity (patient n)}}{\text{disease severity average}}$$

$$\text{Std disease duration (patient n)} = \frac{\text{disease duration (patient n)}}{\text{disease duration average}}$$

Standardized values were then combined by Euclidean distance, which was calculated using Pythagoras:

$$\text{Combination} = \sqrt{(\text{Std severity})^2 + (\text{Std duration})^2}$$

The overall formula used to calculate the linear combination of disease severity and duration is then as follows:

$$\text{Combination (patient n)} = \sqrt{\left(\frac{\text{disease severity (patient n)}}{\text{disease severity average}}\right)^2 + \left(\frac{\text{disease duration (patient n)}}{\text{disease duration average}}\right)^2}$$

well of biotinylated anti-CEL mAb (clone KNH30, MAB6594, Abnova, Taipei, Taiwan) diluted at 1:250 in 0.05% PBS Tween were loaded on the plate and incubated for 2 hours at room temperature, with stirring at 500 r.p.m. and cover from light. The plate was then washed four times with 300 µl/well of 0.05% PBS Tween and blotted against a tissue. A total of 100 µl/well of Streptavidin-horseradish peroxidase (DY998, R&D System, Minneapolis, MN) diluted at 1:200 were loaded on the plate and incubated for 30 minutes at room temperature, with stirring at 500 r.p.m. and cover from light. The plate was then washed four times with 300 µl/well of 0.05% PBS Tween and blotted against a tissue. A total of 100 µl/well of Ultra TMB (34028, Thermo Fisher Scientific) were loaded on the plate and incubated for 1 hour at room temperature. Finally, 100 µl/well of Sulfuric acid (38291, Fluka, Buchs, Switzerland) at 1 M was added, and plate optic deviance was read at 450 nm.

Linear combination of disease severity and disease duration

We used a refined Hurley score to define disease severity, and we transformed the seven categories (1a, 1b, 1c, 2a, 2b, 2c, and 3) into numerical values from 1 to 7.

See also [Supplementary Figure S2b–e](#) for a graphical depiction of this calculation.

HS skin digestion

Overnight digestion protocol (Basel, Switzerland). Fresh HS skin discards were processed within 3 hours after surgery. After removal of the fat layer, the skin was cut into small pieces, washed multiple times with wash buffer (RPMI1640 Glutamax medium, 25 mM 4-[2-hydroxyethyl]-1-piperazineethanesulfonic acid, 100 U/100 µg penicillin/streptomycin, 50 µg/ml gentamicin), and digested overnight with wash buffer supplemented with 100 µg/ml collagenase P (Roche), 3 µM calcium chloride (Fluka), and 10% fetal calf serum (PAALaboratories, Cölbe, Germany). After digestion, 1 mg/ml DNase1 (Sigma-Aldrich) was added and incubated for a further 30 minutes at 37 °C. The digested cell suspension was filtered through cell strainers (Corning, Corning, NY), and erythrocytes were lysed by incubating the suspension in erythrocyte lysis buffer Buffer EL (number 79217, Qiagen, Hilden, Germany) at room temperature for 5 minutes. Cells were then washed and counted using a Countess II Automated Cell Counter (Life Technologies, Carlsbad, CA), and the single-cell suspension was then frozen in 10% DMSO and 90% fetal calf serum at 50–100 × 10⁶ cells/vial aliquots

and stored for 1–2 days at -80°C before transfer into liquid nitrogen.

Short digestion protocol (Rotterdam, Netherlands). Samples were sourced from surgically excised lesional skin derived from patients with severe HS. Prepared on ice, samples were extensively minced using surgical scissors and subsequently incubated for 1.5 hours in $50\ \mu\text{g}/\text{ml}$ ($328.3\ \text{U}/\text{ml}$) LiberaseTM (Roche) in RPMI1640 (Lonza, BioWhittaker, Walkersville, MD) at 37°C , followed by a 10-minute incubation in $100\ \mu\text{g}/\text{ml}$ DNase I (Roche). Samples were then washed with 5% FBS (Life Technologies) in RPMI and strained through a $70\text{-}\mu\text{m}$ mesh (Corning). The resultant single-cell suspension was then frozen down in 10% DMSO (Merck, Kenilworth, NJ) and 90% FBS (Life Technologies).

Flow cytometry sorting experiments

Cells were thawed at 37°C and washed in PBS. Cell suspensions were resuspended in PBS containing LIVE/DEAD Fixable Aqua Dead Cell Stain (L34957, Thermo Fisher Scientific) for 15 minutes according to the manufacturer's instructions for the exclusion of dead cells. Cell suspensions were then washed twice in phenol red-free tissue culture media (RPMI 1640 Medium, no phenol red [Gibco by Life Technologies], 10% fetal calf serum [GE Healthcare, Chicago, IL], penicillin-streptomycin $10,000\ \text{U}/\text{ml}$ [Gibco by Life Technologies]) before the cells were resuspended in phenol red-free tissue culture media containing antibody cocktail for 1 hour at 4°C . Cells were then washed twice more in phenol red-free tissue culture media and filtered through $70\text{-}\mu\text{m}$ cell strainers (Corning). Cells were sorted using a FACSCanto II (BD Biosciences, San Jose, CA) (see [Supplementary Figure S5a](#)). Purity checks were routinely run after sorting to assess the fidelity of the sort.

Flow cytometry acquisition experiments

Cells were thawed at 37°C and washed in running buffer (PBS [Gibco], 1% fetal calf serum [GE Healthcare], EDTA [Gibco], and 0.05% sodium azide [Sigma-Aldrich]). Cell suspensions were resuspended and antibody stained in running buffer for 1 hour at 4°C . Cells were washed, filtered, and analyzed on either a 5-laser LSRFortessa (BD Biosciences) or a 5-laser. Cytek Aurora spectral flow cytometer using SpectroFlo software (Cytek Biosciences, Fremont, CA). Flow cytometry data were analyzed using FlowJo software (version 10.6.0, BD Biosciences).

Flow cytometry antibodies

The antibodies used in this study for flow cytometry (acquisition and sorting) were CD3 allophycocyanin (APC) (clone SK7, Thermo Fischer Scientific), CD3 BUV737 (clone SK7, BD Biosciences), CD19 BV711 (clone SJ25-C1, BD Biosciences), CD19 BV785 (clone HIB19, BioLegend, San Diego, CA), CD20 BV421 (clone 2H7, BD Biosciences), CD20 BV421 (clone Clone 2H7, BD Biosciences), CD20 BV650 (clone 2H7, BioLegend), CD27 V450 (clone M-T271, BD Biosciences), CD38 APC-Cy7 (clone HIT2, BioLegend), CD38 PE-Cy7 (clone HIT2, BD Biosciences), CD38 PE-Cy7 (clone HIT2, BioLegend), CD45 APC-Cy7 (clone 2D1, BD Biosciences), CD45 BUV395 (clone HI30, BD Biosciences), CD86 BUV737 (clone 2331 [FUN-1], BD Biosciences), CD63 Alexa Fluor 647 (clone H5C6, BD Biosciences), CD138 APC (clone MI15,

BioLegend), HLA-DR PerCP-Cy5.5 (clone L243, BioLegend), IgA FITC (polyclonal antibody, Jackson ImmunoResearch), IgA1 APC (clone SAA1, Cytogenos, Salamanca, Spain), IgA1 PerCP/Cy5.5 (clone SAA1, Cytogenos), IgA2 PerCP/Cy5.5 (clone SAA2, Cytogenos), IgD APC/Cy7 (clone IA6-2, BioLegend), IgD PE (clone IA6-2, BD Biosciences), IgD PE-Cy7 (clone IA6-2, BioLegend), IgG Alexa Fluor 647 (polyclonal antibody, Jackson ImmunoResearch), IgG1 PE (clone SAG1, Cytogenos), IgG2 FITC (clone SAG2, Cytogenos), IgG2 PE (clone SAG2, Cytogenos), IgG3 FITC (clone SAG3, Cytogenos), IgG4 APC (clone SAG4, Cytogenos), and IgM PE (polyclonal antibody, Jackson ImmunoResearch).

Antigen-specific and total Ig detection by enzyme-linked immunosorbent spot

For antigen-specific and total Ig-secreting cell detection, 96-well enzyme-linked immunosorbent spot plates (Millipore MSIPS4510 Sterile, hydrophobic high protein binding immobilized-P membrane) were coated with $1\ \mu\text{g}/\text{ml}$ purified unlabeled goat anti-human IgG or IgA or IgM (2040-01, 2050-01, and 2020-01, respectively, Southern Biotech) or $5\ \mu\text{g}/\text{ml}$ CEL antigen (25333, Cayman Chemical) for 2 hours at room temperature. After washing with PBS solution, the plates were blocked with 1% BSA in PBS and incubated for 30 minutes at 37°C . B cells and plasmablasts sorted from HS skin were added in a final volume of $200\ \mu\text{l}$ of basic medium prepared using RPMI 1640 (number 11875-093, Gibco) supplemented with 10% fetal bovine serum (number SH3007.03, HyClone, Thermo Fisher Scientific), $1\ \text{mM}$ sodium pyruvate (number 11360-070, Gibco), MEM nonessential amino acids ($100\ \mu\text{M}$ each, number 11140-050, Gibco), $50\ \mu\text{M}$ b-mercaptoethanol (number 31350-010, Gibco), penicillin/streptomycin (number P4333, Sigma-Aldrich), and kanamycin ($100\ \mu\text{g}/\text{ml}$, Gibco, Life Technologies) and incubated overnight at 37°C . Next, the plates were washed three times with 0.25% PBS Tween 20 and four times with PBS and incubated for 2 hours at room temperature with Ig-specific, biotin-conjugated secondary antibody (2043-08, 2050-08, 2020-08, Southern Biotech). After washing, avidin-peroxidase (A3151, Sigma-Aldrich) was added and left for 1 hour at room temperature. The assay was developed with AEC (A6926, Sigma-Aldrich). For quantification of antibody-secreting cells, plates were acquired, counted, and quality controlled using an enzyme-linked immunosorbent spot reader and ImmunoSpot 5.1 software (CTL Europe, Bonn, Germany).

Complement activation assay

For the complement activation experiments ([Supplementary Figure S6](#)), a 96-well high binding plate (655061, Greiner Bio-One, Monroe, NC) was first coated overnight at 4°C with $10\ \mu\text{g}/\text{ml}$ CEL BSA (STA-302, Cell Biolabs). The plate was then washed three times with PBS with 0.05% Tween 20 (524653-1EA, Calbiochem, San Diego, CA) and blocked with blocking buffer (37539, Thermo Fisher Scientific) for 1 hour at room temperature, followed by washing three times with PBS with 0.05% Tween 20. Plasma from patients with HS or HVs was diluted at 1:10 in PBS before loading on the plate. After 30 minutes of incubation at room temperature, the plate was washed twice with PBS Tween and once with PBS (10010-015, Gibco). The complement-preserved serum pool

of healthy donors was collected through the Basel Tissue Donor Program in accordance with the ethical principles originating in the Declaration of Helsinki, and was added to the plate and incubated for 1 hour at 37 °C. As an indication of the complement activation, the level of terminal complement complex sC5b-9 in each sample was quantified with ELISA (A020, QuidelOrtho, San Diego, CA) according to the manufacturer's instructions.

Single-cell RNA-sequencing data

The single-cell RNA-sequencing data from lesional HS skin was previously described (Gudjonsson et al., 2020). The candidate plasma cell markers were obtained by contrasting the plasma cells to the B cells with the findMarkers function from the scran (Lun et al., 2016) R package (1.18.5). The test type was set to t-test, and the blocking level was set to the donor identifications. The resultant volcano plot (Supplementary Figure S4a) was created using GraphPad Prism, version 9 (GraphPad Software, La Jolla, CA). The dot plots of cell clusters displaying the average gene expression and frequency of positive cells (Supplementary Figure S4b) were generated using R package ggplot2 (Wickham, 2016). All R calculations were run with R-4.0.3.

Affymetrix data

The generation of the RNA expression data from healthy, lesional HS, and nonlesional HS skin (Figure 4i) has previously been described (Penno et al., 2020) (dataset available through the Gene Expression Omnibus, GSE148027). Data shown in Figure 4i are robust multichip average-normalized expression values of Affymetrix data. The heatmap shown in Figure 4i was created using GraphPad Prism, version 9.

Conventional histology

To assess HS pathology, large (1–2 cm²) tissue fragments were cut from resected HS skin and fixed in 10% v/v neutral phosphate-buffered formalin solution (J.T. Baker, catalog number 3933.9010, Avantor, Radnor Township, PA) for 24 hours at room temperature and then transferred to 50% ethanol and 50% dihydrogen oxide and stored at 4 °C until processing. Fixed skin samples were dehydrated through a graded series of ethanol concentrations (50–100%), cleared with xylene, and infiltrated with paraffin overnight using the vacuum infiltration tissue processor (Leica ASP200S, Leica Biosystems, Muttens, Switzerland). On the following day, the tissue was embedded in paraffin blocks. HS tissue was sectioned (3 µm) and stained with H&E by MC or CC at Autoimmunity, Transplantation and Inflammation (ATI) Disease Area, Novartis Institutes for BioMedical Research, Novartis Pharma AG (Basel, Switzerland). Samples were imaged using a ScanScope XT slide scanner (Aperio, Leica Biosystems) at ×40 magnification.

Chromogenic immunohistochemistry

Automated immunohistochemical stainings for CD20 and CD21 were performed using a Ventana Discovery XT automated stainer (Roche) by MC or CC at Autoimmunity, Transplantation and Inflammation (ATI) Disease Area, Novartis Institutes for BioMedical Research, Novartis Pharma AG. Specific isotype controls were used as negative controls. Samples were digitalized using an Aperio ScanScope XT slide scanner (Leica Biosystems). Exemplary images in JPEG format

were taken using the Aperio ImageScope software, version 12.3.2.8013 (Leica Biosystems).

Spatial transcriptomics

Fluorescent labeling and spatial transcriptomics (Merritt et al., 2020) were performed by NanoString Technologies through the Technology Access Program (NanoString Technologies, Seattle, WA). Specifically, formalin-fixed, paraffin-embedded blocks from discarded tissue of patients with HS were pre-selected and sectioned, and adjacent control sections were obtained for CD20 (see histology methods) at Autoimmunity, Transplantation and Inflammation (ATI) Disease Area, Novartis Institutes for BioMedical Research, Novartis Pharma AG for spatial transcriptomic profiling using the HuWTA (Human Whole Transcriptome Atlas). Sections were processed according to NanoString GeoMx DSP (Digital Spatial Profiling) guidelines. Briefly, after deparaffinization and antigen retrieval procedures, sections were incubated with Whole Transcriptome Atlas probes overnight at 37 °C. On the next day, the slides were washed and stained with fluorescently labeled antibodies against pan-cytokeratin (Alexa Fluor 647, clone AE1+AE3, number NBP2-33200AF647, Novus Biologicals, Littleton, CO), CD20 (Alexa Fluor 594, clone IGEL/773, number NBP2-47840DL594, Novus Biologicals), and Vimentin (Alexa Fluor 488, clone E-5, number sc-373717, Santa Cruz Biotechnology, Dallas, TX) to visualize nuclei morphological features of the HS tissue. Sections were counterstained with SYTO-83 Orange Fluorescent Nucleic Acid Stain (number S11364, Thermo Fisher Scientific) to visualize nuclei.

After staining, HS sections were scanned using a GeoMx™ Digital Spatial Profiler to generate digital fluorescent images. CD20⁺ B cell regions of interest (ROIs) were preidentified on the basis of CD20 staining of serial sections (see Figure 4f and Supplementary Figure S3b and c), and final ROIs were manually defined from the fluorescent images through the GeoMx profiler.

To cleave the photocleavable oligos from each selected region, UV light was directed through a programmable digital micromirror device, and resultant samples were collected through microcapillary and dispensed into a 96-well plate. Gene expression values for each ROI were quantified by the GeoMx DSP platform. Gene expression values were normalized using the third quartile of all counts from each area of interest and subsequently log₂ transformed before further analysis.

ROI annotation and differential gene expression analysis were done through the GeoMx profiler software (the DE plots in the data report PPT were calculated using the linear mix model with Benjamini–Hochberg correction).

Antibodies for immunohistochemistry

List of antibodies used for Chromogenic Immunohistochemistry and Nanostring (including secondary antibodies) were mouse IgG2ak anti-human CD20cy (clone L26, M0755, Dako Deutschland, Hamburg, Germany), goat anti-mouse biotinylated (polyclonal antibody, BA-9200, Vector Laboratories, Burlingame, CA), rabbit anti-human CD21 (clone EP3093, ab75985, Abcam), goat anti-rabbit biotinylated (polyclonal antibody, 111-065-144, Jackson ImmunoResearch), monoclonal rabbit isotype control (ab172730,

Abcam), mouse IgG2ak isotype Control eFluor 660 (50-4724, eBioscience, San Diego, CA), mouse IgG1ak anti-human pan-cytokeratin Alexa Fluor 647 (clone AE1+AE3, NBP2-33200AF647, Novus Biologicals), mouse IgG2ak anti-human CD20 Alexa Fluor 594 (clone IGEL/773, number NBP2-47840DL594, Novus Biologicals), and mouse IgG1ak anti-human vimentin (Alexa Fluor 488, clone E-5, number sc-373717, Santa Cruz Biotechnology).

Image analysis

CD20⁺ and CD21⁺ ROIs in chromogenically stained HS skin were identified and outlined manually using the Aperio Imagescope pathology slide viewing software (Leica Microsystems). The association of B cell clusters with fat was assessed and annotated manually. Areas (in μm^2) of CD20⁺ and CD21⁺ ROIs were calculated using ImageJ software (National Institutes of Health, Bethesda, MD) and Microsoft Excel.

TNF secretion assay

Monocyte isolation and M1 differentiation. Anonymized buffy coats were received from HVs through the Interregionale Blutspende of the Swiss Red Cross in Bern, Switzerland. The blood was provided under informed consent and collected through the Novartis Tissue Donor Program (TRI0128) in accordance with the Swiss Human Research Act and approval of the responsible ethic committee (Ethikkommission Nordwest- und Zentralschweiz number: 329/13). PBMCs from human peripheral blood were isolated by density gradient centrifugation (Ficoll-Plaque, number 17-1440-03, GE Healthcare) followed by erythrocyte lysis (Buffer EL, number 79217, Qiagen). Human monocytes were then obtained by magnetic isolation (Human Monocyte Isolation Kit, number 19059, Stem Cell Technologies, Vancouver, Canada) according to the manufacturer's instructions. Subsequently, monocytes were cultured for 6 days in RPMI1640 Glutamax (number 72400-021, Gibco, distributed by Thermo Fisher Scientific) supplemented with 10% heat-inactivated fetal bovine serum (number A15-152, PAA laboratories, Toronto, Canada), 1% of sodium pyruvate (number 11360-039, Gibco), 1% penicillin and streptomycin (number 15140, Gibco), 25 mM 4-(2-hydroxyethyl)-1-piperazineethanesulfonic acid buffer (number 15630, Gibco), and 50 μM mercaptoethanol (number 31350-010, Gibco) in the presence of 40 ng/ml colony-stimulating factor 1 (number 216-MC, R&D Systems) and 50 ng/ml IFN- γ (number 285-IF, R&D Systems) at 37 °C and 5% carbon dioxide to differentiate M1 macrophages.

Activation of M1 macrophages with CEL/autoantibody immune complexes.

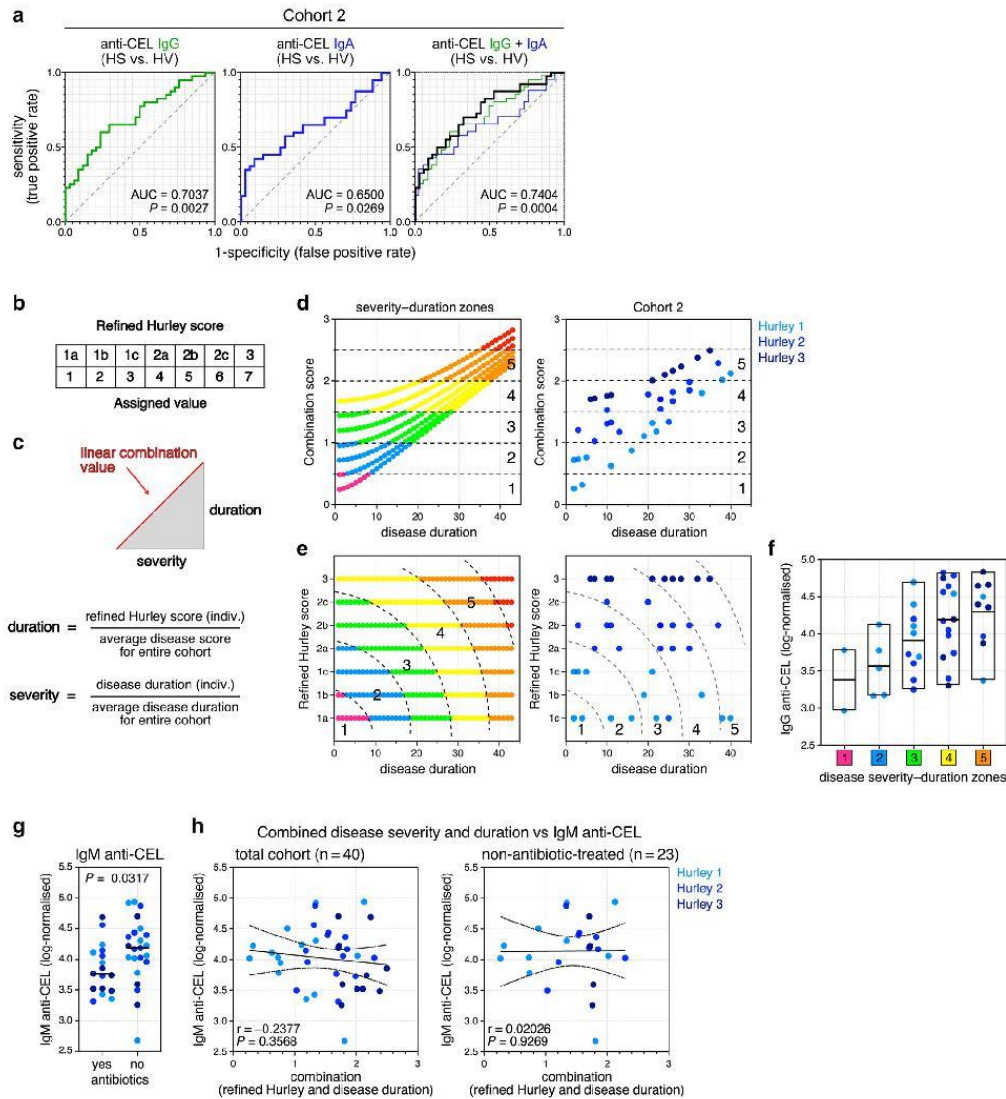
After harvest and wash, M1 macrophages were plated (100K per well at 2×10^6 cells/ml) in a complete RPMI1640 medium without the addition of colony-stimulating factor 1 and IFN- γ in 96-well plates. In parallel, we prepared master mixes of carboxy-methyl-lysine BSA or CEL BSA (number STA-314 and number STA-302, Cell Biolabs, distributed by LubioSciences, Zürich, Switzerland) with either HV or HS sera and incubated for 30 minutes at 37 °C to let the immune complexes form. Whereas HV sera (number S4190-500) were obtained from LabForce (Muttentz, Switzerland), HS sera were obtained from either BioIVT or our internal clinical collaboration. Afterward, 20 μl of the respective master mixture was added to the M1 macrophages (final concentrations for carboxy-methyl-lysine BSA or CEL BSA of 30 $\mu\text{g/ml}$ with HV and HS sera at 1:100) and incubated at 37 °C and 5% carbon dioxide. After 6 hours of incubation, we harvested the supernatants and determined the amount of secreted TNF by homogeneous time-resolved fluorescence (number 62HTNFAPEH, CysBio, Codolet, France).

Quantification and statistical analyses

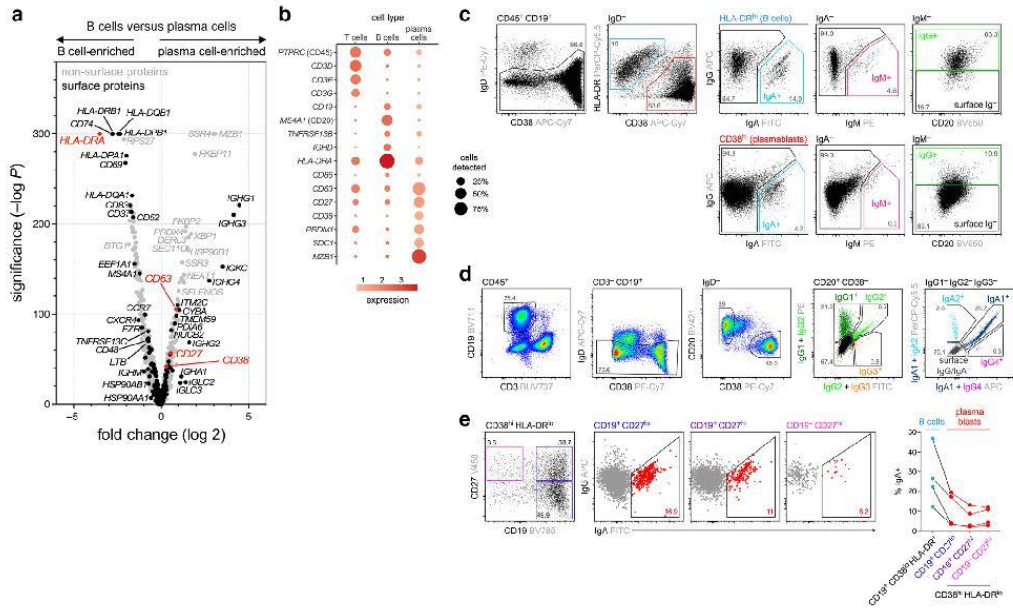
The statistical details and tests used, the number and representation of n, and any other forms of quantification present are specified in the respective figure legends and results section. All statistical analyses in this study were performed using the Prism 9 software (GraphPad Software).

SUPPLEMENTARY REFERENCES

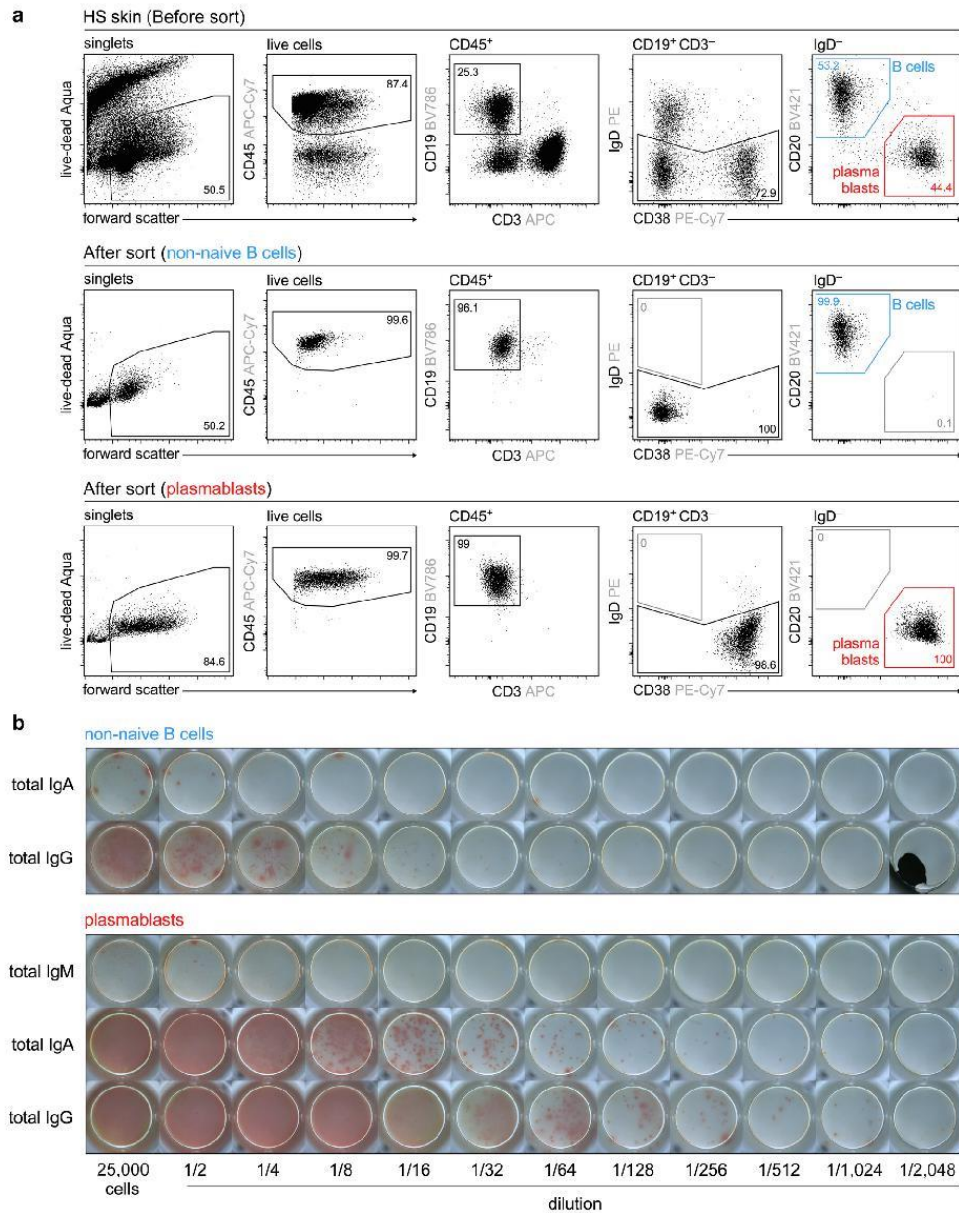
- Gudjonsson JE, Tsoi LC, Ma F, Billi AC, van Straalen KR, Vossen ARJV, et al. Contribution of plasma cells and B cells to hidradenitis suppurativa pathogenesis. *JCI Insight* 2020;5:e139930.
- Lun AT, McCarthy DJ, Marioni JC. A step-by-step workflow for low-level analysis of single-cell RNA-seq data with Bioconductor. *F1000Res* 2016;5:2122.
- Merritt CR, Ong GT, Church SE, Barker K, Danaher P, Geiss G, et al. Multiplex digital spatial profiling of proteins and RNA in fixed tissue. *Nat Biotechnol* 2020;38:586–99.
- Penno CA, Jäger P, Laguerre C, Hasler F, Hofmann A, Gass SK, et al. Lipidomics profiling of hidradenitis suppurativa skin lesions reveals lipooxygenase pathway dysregulation and accumulation of proinflammatory leukotriene B4. *J Invest Dermatol* 2020;140:2421–32. e10.
- Srey C, Hull GL, Connolly L, Elliott CT, del Castillo MD, Ames JM. Effect of inhibitor compounds on N^ε-(carboxymethyl)lysine (CML) and N^ε-(carboxyethyl)lysine (CEL) formation in model foods. *J Agric Food Chem* 2010;58:12036–41.
- Wickham H. *ggplot2: Elegant graphics for data analysis*. 2nd ed. New York, NY: Springer International Publishing; 2016.



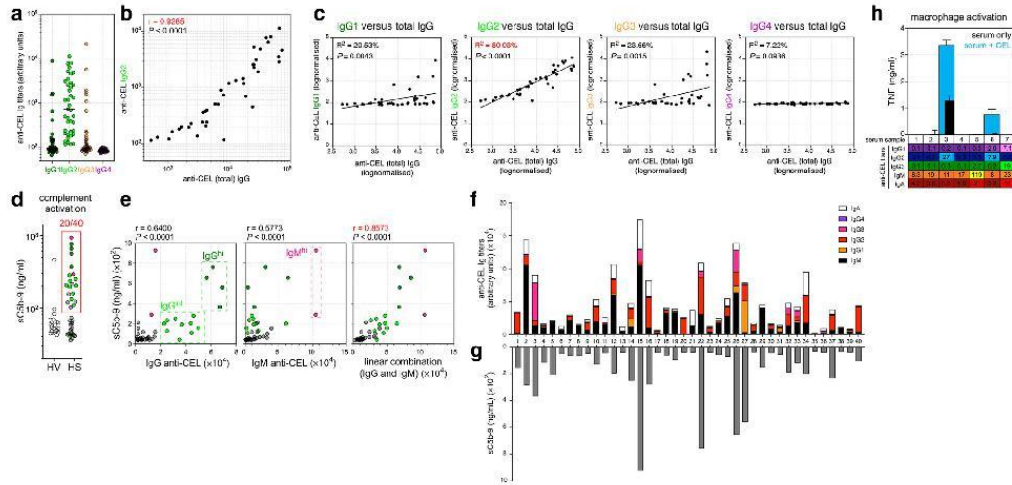
Supplementary Figure S2. Relationship between anti-CEL autoantibodies and clinical parameters in HS. (a) Receiver operator characteristic analysis distinguishing patients with HS (n = 40; cohort 2) from healthy volunteers (n = 38) on the basis of IgG (green, left), IgA (blue, middle), and IgG + IgA (black, right) anti-CEL titers. (b, c) Calculation of linear combination of severity and duration. (b) Refined Hurley scores (1a, 1b, 1c, 2a, 2b, 2c, and 3) were assigned integer values 1–7. Individual values for severity and disease duration (in years) were then normalized against the averages of the entire dataset to equalize the relative contribution of duration and severity. (c) Duration–severity combination was calculated using the Pythagorean equation. (d, e) Relationship between the combination value, disease duration, and refined Hurley score. Left: All hypothetical values on the left (up to a disease duration of 43 years). Colors indicate linear combination scores of 0–0.5 (zone 1; magenta), 0.5–1.0 (zone 2; blue), 1.5–2.0 (zone 3; green), 2.0–2.5 (zone 4; yellow), 2.5–3.0 (zone 5; orange), and >3.0 (red). Right: Distribution of patient samples (n = 40). (f) Log-normalized IgG anti-CEL titers in indicated HS groups. Disease severity–duration zones in e and f are identical to that shown in Figure 3f. (g) Log-normalized distribution of IgM anti-CEL titers in the plasma samples of patients with HS (n = 40; cohort 2), stratified according to whether patients were undergoing treatment with antibiotics (left; n = 17) or not (right; n = 23). $P = 0.0317$ (Mann–Whitney *U* test). (h) Scatter plots showing the lack of correlation (Spearman test) between log-normalized IgM anti-CEL titers and the combination of refined Hurley score and disease duration, for the total cohort (left; n = 40) and excluding patients taking antibiotics (right; n = 23). AUC, Area under the curve; CEL, carboxyethyl lysine; HS, hidradenitis suppurativa.



Supplementary Figure S4. Characterization of B cells and plasma cells in HS skin. (a) Comparison of gene expression in B cells versus plasma cells by volcano plot from single-cell RNA-sequencing data of HS lesional skin (Gudjonsson et al., 2020). Genes encoding proteins expressed on the cell surface are marked in black. Selected genes encoding cell surface proteins used in flow cytometry experiments in this study are marked in red. (b) Dot plots of pooled T-, B-, and plasma cell clusters in single-cell RNA-sequencing data of HS lesional skin (Gudjonsson et al., 2020), displaying the average gene expression (red intensity) and frequency of positive cells (circle size) of indicated markers. (c, d) Representative flow cytometry dotplots showing the gating strategy for identifying Ig isotypes (c) and subclasses (d) on the surface of CD20^{hi} HLA-DR⁺ CD38^{lo} B cells and CD20^{lo} HLA-DR^{lo} CD38^{hi} plasmablasts in lesional HS skin. (e) Left: Representative flow cytometry dotplots depicting surface IgA expression by indicated subpopulations of HLA-DR^{lo} CD38^{hi} plasmablasts isolated from lesional HS skin. Right: Frequency of surface IgA⁺ B cells (blue) and indicated subpopulations of HLA-DR^{lo} CD38^{hi} plasmablasts (red) isolated from lesional HS skin (n = 4). HS, hidradenitis suppurativa.



Supplementary Figure S5. ELISPOTS of sorted B cells and plasmablasts from HS skin. (a) Representative flow cytometry dotplots showing the gating strategy for identifying (non-naïve) CD20^{hi} CD38^{lo} B cells (blue box) and CD20^{lo} CD38^{hi} plasmablasts (red box) in lesional HS skin before (top panel) and after (bottom two panels) sorting for ELISPOT readouts. (b) Representative ELISPOT plates of B cells (top) and plasmablasts (bottom) sorted from HS skin, identifying the presence of (total) IgA and IgG antibody-secreting cells. Data are representative of three independent experiments and show a dilution series, starting from 2.5×10^4 cells per well. ELISPOT, enzyme-linked immunosorbent spot; HS, hidradenitis suppurativa.



Supplementary Figure S6. Isotype and functional capabilities of anti-CEL autoantibodies in patients with HS. (a) Log distribution of IgG1, IgG2, IgG3, and IgG4 anti-CEL titers in HS plasma samples (n = 40; cohort 2). (b) Scatter plot depicting the correlation between total IgG anti-CEL and IgG2 anti-CEL in HS plasma samples from cohort 2 (n = 40). $P < 0.0001$ (Spearman test). (c) Linear regression analyses of log normalized (total) IgG anti-CEL versus IgG1, IgG2, IgG3, and IgG4 anti-CEL titers in the cohort 2 HS plasma samples (n = 40). (d) Detection of sC5b-9 complex in the plasma of HVs (n = 20) and patients with HS (n = 40) after 1-h incubation in CEL BSA-coated plates in the presence of excessive complement from healthy serum. (e) Scatter plots depicting the correlation between sC5b-9 and IgG (left), IgM (middle), and IgG + IgM (right) anti-CEL titers in HS plasma samples (n = 40) (Spearman test). Individual samples have been colored on the basis of whether they exhibited high anti-CEL IgM (pink) or IgG (green) titers. (f) Cumulative abundance of IgM, IgA, IgG1, IgG2, IgG3, and IgG4 anti-CEL titers within the plasma of individual patients with HS (HS1–HS40). (g) Detection of sC5b-9 complex in plasma from indicated patients with HS (n = 40) after 1-h incubation in CEL BSA-coated plates in the presence of excessive complement from healthy serum. (h) TNF secretion by in vitro generated macrophages 6 h after incubation with commercially obtained serum from patients with HS (n = 7) in the presence (blue bars) or absence (black bars) of CEL BSA. Titers of indicated Ig isotypes and subclasses of anti-CEL (arbitrary units [$\times 10^3$]) in each of the seven serum samples are indicated in the bottom panel. CEL, carboxyethyl lysine; h, hour; HS, hidradenitis suppurativa; HV, healthy volunteer; sC5b-9, soluble complement 5b-9.

Results part III: Autoantibodies and sFceR1a in Chronic Urticaria

Introduction

Chronic Spontaneous Urticaria (CSU) is a skin disease defined as presence of urticaria for more than 6 weeks that is initiated independently of any exogenous stimulus [341]. Indeed, the absence of a clear trigger of urticaria symptoms is the defining trait of this disease, hence the “spontaneous” attribute. The pathogenesis of CSU revolves around the activation of IgE pathway within basophils and mast cells, with histamine release, mast cells degranulation and expression of pro-inflammatory cytokines such as IL4 and IL13, which ultimately provokes the common symptoms of CSU: wheals and angioedema [341, 342]. CSU treatment is based on the use of H1 antihistamines as first line of therapies, followed as omalizumab (anti-IgE monoclonal antibody) as second choice for patients with uncontrolled symptoms, and cyclosporine as third therapeutic level for patients not responding to anti-IgE treatment [343]. The root causes of CSU triggering are still not well understood, but the efficacy of anti-IgE treatment and the observed activation of immune cells expressing FceR1a point toward an over-sensitivity of IgE pathway. The observation that around 50% of sera from CSU patients could activate basophils and mast cells suggests the existence of an autoimmune component in CSU pathogenesis [344-346]. Anti-IgE treatment was shown to be efficacious in completely clearing CSU symptoms in around 40% of patients treated with ligelizumab (a second generation anti-IgE monoclonal antibody) and 26% in patients treated with omalizumab [347]. The observation that CSU symptoms were still active in around 50% of patients after anti-IgE treatment was in line with the hypothesis of IgE-independent autoimmunity as pathologic agent in a subset of CSU population. Moreover, autoantibodies targeting IgE and FceR1a were detected in CSU sera, supporting the hypothesis of autoimmunity involvement in disease pathogenesis [345]. It was hypothesized that anti-FceR1a IgG autoantibodies might lead to triggering of CSU symptoms and could be specifically present in patients unresponsive to anti-IgE treatment [348]. Indeed, patients expressing anti-FceR1a autoantibodies could potentially not respond to anti-IgE treatment, as their CSU trigger would not be IgE. For this reason, the Novartis clinical team leading ligelizumab development was interested in detecting anti-FceR1a autoantibodies in CSU patients. As stated above, ligelizumab showed greater control of symptoms compared with omalizumab in patients with CSU inadequately controlled by standard of care. Therefore, the first goal of this project was to investigate the possible correlation between anti-FceR1a autoantibodies and non-response to ligelizumab treatment. As described above, FceR1a is central in CSU pathogenesis and symptoms triggering, and a decrease of surface FceR1a was observed in basophils after anti-IgE treatment [349]. This observation was particularly interesting in the context of CSU, as it showed that inhibiting the binding of IgE to FceR1a decreased the expression of the receptor on the cells surface, potentially reducing the readiness of basophils to respond to IgE binding (Figure 20). Anti-IgE treatment may not only inhibit the current activation of IgE pathway, but also decrease future triggering of the pathway. Cell surface levels of FceR1a could then be a mechanistic and potentially efficacy marker. Such marker would be extremely useful in anti-IgE clinical trials, in order to follow the efficacy of the treatment in inhibiting the IgE-FceR1a binding. However, the detection of cell-bound FceR1a is performed using whole blood,

which is a challenging matrix for large multi-centers clinical trials. Indeed, whole blood collection in large clinical trials can introduce technical bias in samples collection and treatment in different clinical centers, particularly regarding shipment conditions. A surrogate marker for cell-bound FcεR1a detectable in serum or plasma would be more convenient and applicable in large clinical trials, as those matrices can be frozen and easily shipped to central labs for biomarker analysis. The soluble form of FcεR1a (sFcεR1a), cleaved from cells surface, is detectable in serum and may be a surrogate marker for cell-bound FcεR1a. The second aim of this project was then to detect the soluble form of FcεR1a (sFcεR1a) at different time-points of ligelizumab treatment, using serum samples from CSU patients from NCT02477332, in order to investigate a potential decrease of this marker after treatment and evaluate it as surrogate for cell-bound FcεR1a.

Clinical trial description and samples selection

The clinical trial NCT02477332 was composed of several treatment arms, as described in Figure 19 (published by Maurer et al [347]). Four cohorts were treated with different doses of ligelizumab (QGE031): 240 mg, 72 mg or 24 mg every 4 weeks for a total of 20 weeks, or 120 mg single dose at day 1. One cohort received a placebo every 4 weeks for 20 weeks. The last cohort was treated with the highest approved dose of omalizumab (300 mg) for CSU treatment every 4 weeks for 20 weeks.

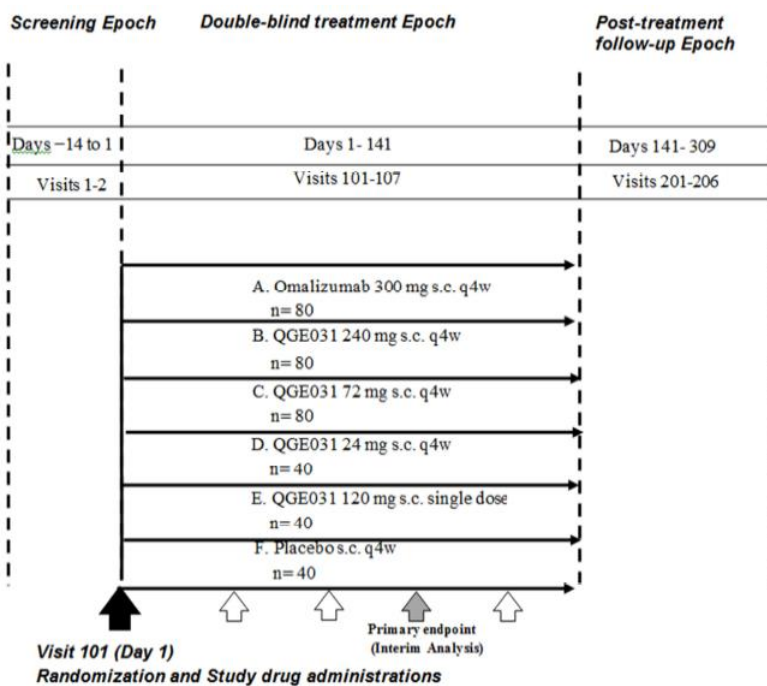


Figure 19:

Structure of clinical trial NCT02477332. Patients were divided in 6 cohorts: a) 300 mg of omalizumab every 4 weeks; b) 240 mg of ligelizumab every 4 weeks; c) 72 mg of ligelizumab every 4 weeks; d) 24 mg of ligelizumab every 4 weeks; e) 120 mg of ligelizumab, single dose; f) placebo every 4 weeks. Published by Maurer et al, "Ligelizumab for Chronic Spontaneous Urticaria", *N Engl J Med*, 2019 [347].

The purpose of the last cohort was to compare the performance of ligelizumab to an already approved drug, in order to investigate whether ligelizumab could have a better performance in CSU. The clinical endpoint used to classify the patients as responders or non-responders was UAS7, a score counting the number of CSU symptoms affecting the patient during the last 7 days. A patient was considered responder if the score UAS7 was equal to 0, meaning that during the last 7 days the patient didn't have any CSU symptom. Although UAS7=0 is a strict clinical endpoint, around 40-50% of patients in the highest treatment doses (ligelizumab 240 mg and 72 mg) achieved it.

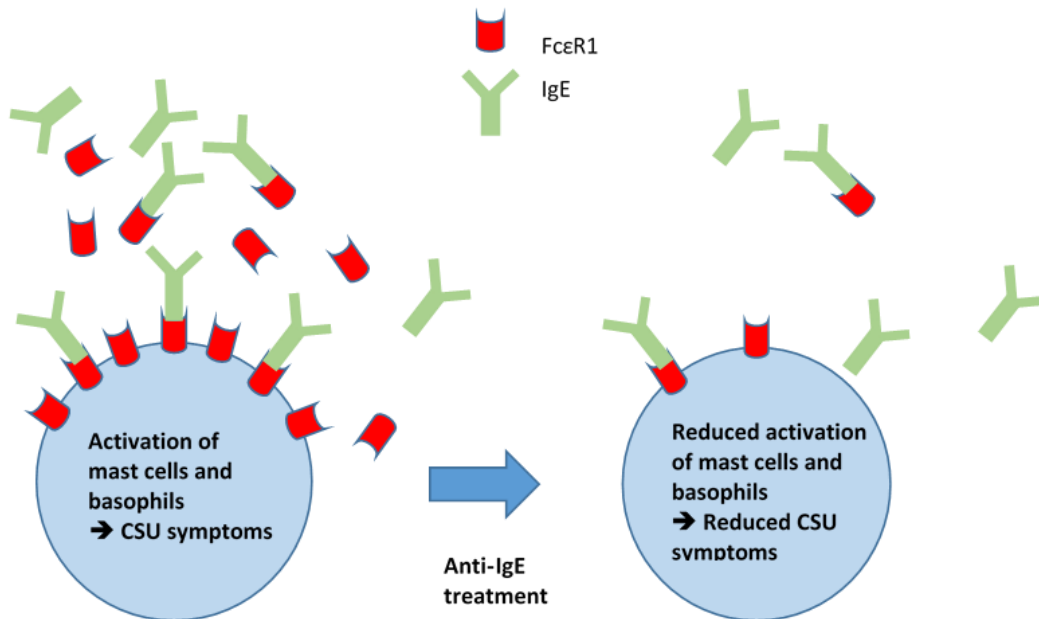


Figure 20:

Representation of anti-IgE treatment effect on expression of FcεR1 on mast cells and basophils surface. After anti-IgE treatment, there is a decrease in the expression of cell-bound FcεR1, which is linked to a reduced activation of mast cells and basophils. As shown by our results, the levels of sFcεR1a are also decreased after anti-IgE treatment.

Results

Anti-FcεR1a autoantibodies did not correlate with anti-IgE treatment response

Anti-FcεR1a autoantibodies were detected by applying the same Luminex-based autoantibodies profiling assay previously used in the others projects of this thesis. IgG, IgM and IgA anti-FcεR1a were detected in 240 baseline samples from NCT02477332. Figure 21 shows the distributions of anti-FcεR1a autoantibodies in UAS7=0 responders compared to non-responders in cohorts with highest treatment doses (ligelizumab 240 mg, 72 mg and omalizumab 300 mg). In summary, anti-FcεR1a autoantibodies of IgG, IgM and IgA isotype did not correlate with treatment response in any of the tested cohorts. The same lack of correlation between anti-FcεR1a autoantibodies and UAS7=0 was observed when mixing data from omalizumab, ligelizumab 240 mg and 72 mg cohorts (Figure 22).

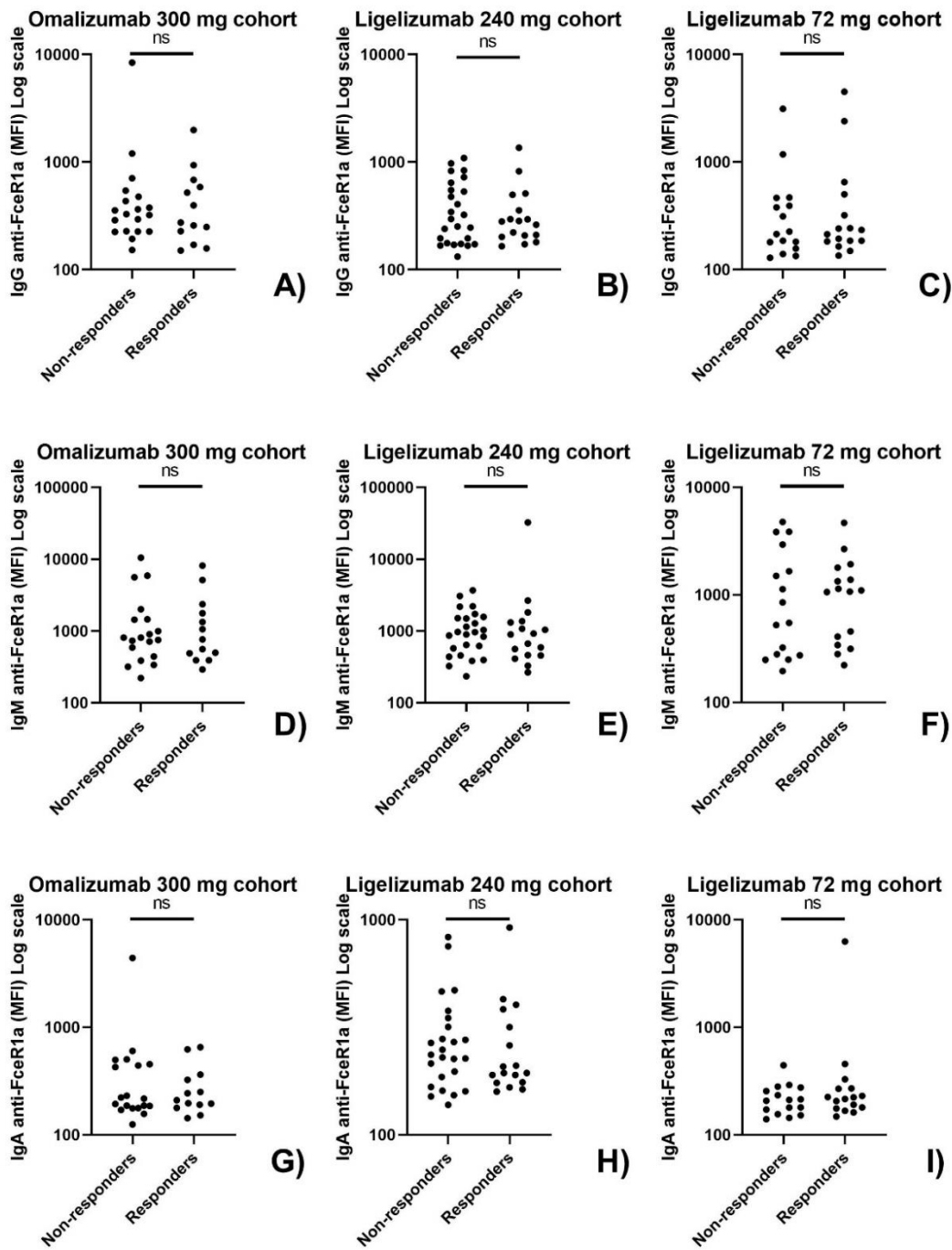


Figure 21:

Scatter plots showing the distributions of anti-FcεR1a autoantibodies in different treatment cohorts from NCT02477332: omalizumab 300 mg in A, D and G, ligelizumab 240 mg in B, E and H, ligelizumab 72 mg in C, F and I. IgG data in A, B, C; IgM data in D, E, F; IgA data in G, H, I. For omalizumab 300 mg *n* non-responders = 19, *n* responders = 13. For ligelizumab 240 mg *n* non-responders = 25, *n* responders = 17. For ligelizumab 72 mg *n* non-responders = 16, *n* responders = 16. Mann-Whitney test used to compare responders and non-responders values in each cohort. *P*-values obtained: A) *p*-value = 0.92; B) *p*-value = 0.81; C) *p*-value = 0.73; D) *p*-value = 0.99; E) *p*-value = 0.70; F) *p*-value = 0.75; G) *p*-value = 0.94; H) *p*-value = 0.56; I) *p*-value = 0.50.

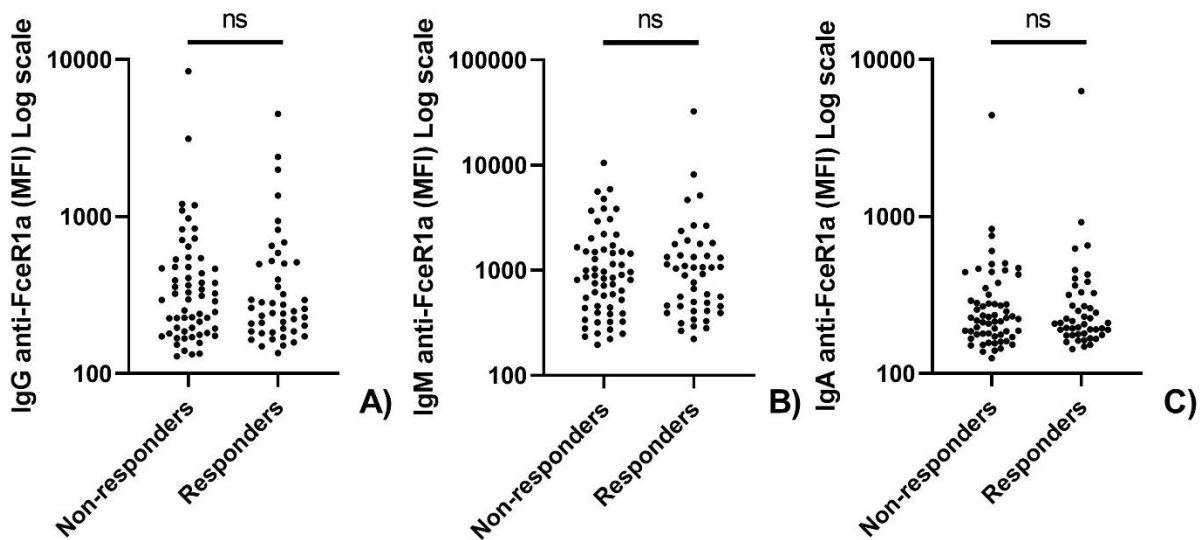


Figure 22:

Scatter plots showing distributions of anti-FceR1a autoantibodies values (expressed in MFI) in UAS7=0 responders and non-responders, for IgG (A), IgM (B) and IgA (C) isotypes, from the cohorts omalizumab 300 mg, ligelizumab 240 mg and ligelizumab 72 mg. N non-responders = 60, n responders = 46, ns = non significant p -value. P -values obtained with Mann-Whitney test: IgG, p -value = 0.62; IgM, p -value: 0.92; IgA, p -value = 0.83.

The results obtained did not confirm the initial hypothesis that non-responders to anti-IgE treatment would be positive to anti-FceR1a autoantibodies, while responders would not express such immunoglobulins.

Soluble FceR1a concentration dose-dependent decrease after anti-IgE treatment

The secondary aim of this project was to investigate the potential of soluble FceR1a (sFceR1a) as surrogate biomarker of cell-bound FceR1a. As already stated, it was shown that anti-IgE treatment decreased the expression of FceR1a on the surface of basophils, suggesting a reduction in basophils readiness to activate IgE pathway. Although extremely interesting, cell-bound FceR1a is a biomarker of difficult application in large phase III clinical trials. Therefore, we developed an assay to detect sFceR1a in serum and we applied it on samples from NCT02477332. The serum samples tested were from 226 different patients across all cohorts and for each patient we tested different 7 time-points: baseline, week 1, week 4, week 12, week 20, week 32 and week 44. The results (Figure 23) showed a dose dependent decrease of sFceR1a after anti-IgE treatment.

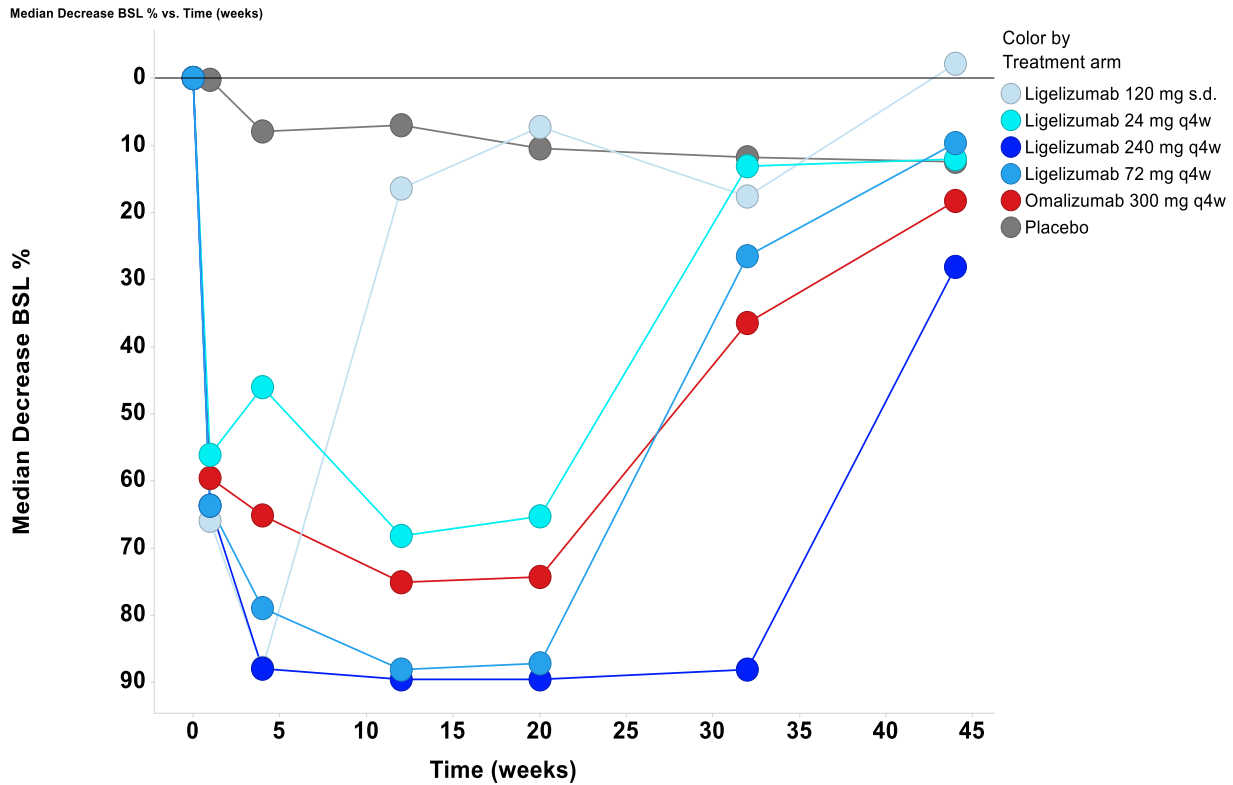


Figure 23:

Dose-dependent decrease (median decrease from baseline expressed in %) of soluble FcεR1α. Number of subjects per cohort was between 30 and 50, for a total of about 220 samples per visit except for week 32 (15-25 samples per cohort).

1 week after a single administration, the median decrease from baseline was 64% for ligelizumab 240 mg, 59% for omalizumab 300 mg, and 1% for placebo. 4 weeks after a single administration of ligelizumab 240 and 120 mg, both treatments showed a marked FcεR1α decrease of 88%, compared to 65% with omalizumab 300 mg. After 12 weeks of treatment, the median decreases from baseline with ligelizumab 240 mg, omalizumab 300 mg, and placebo were 90%, 75%, and 7%, respectively. After 12 and 24 weeks of washout (weeks 32 and 44), the median decreases were 88% and 28% for ligelizumab 240 mg, 36% and 18% for omalizumab 300 mg, and 11% and 12% for placebo (Figure 23), respectively. Considering the results obtained, sFceR1a could potentially be a surrogate biomarker for cell bound FceR1a. Unfortunately, the lack of cell bound FceR1a data for this clinical trial did not allow for a comparison between the concentrations of the two markers. A correlation between baseline IgE and FceR1α levels was also found ($p < 0.001$, $r = 0.645$, Pearson's test) (Figure 24), suggesting a possible link between the concentration of circulating IgE and the expression of sFceR1a.

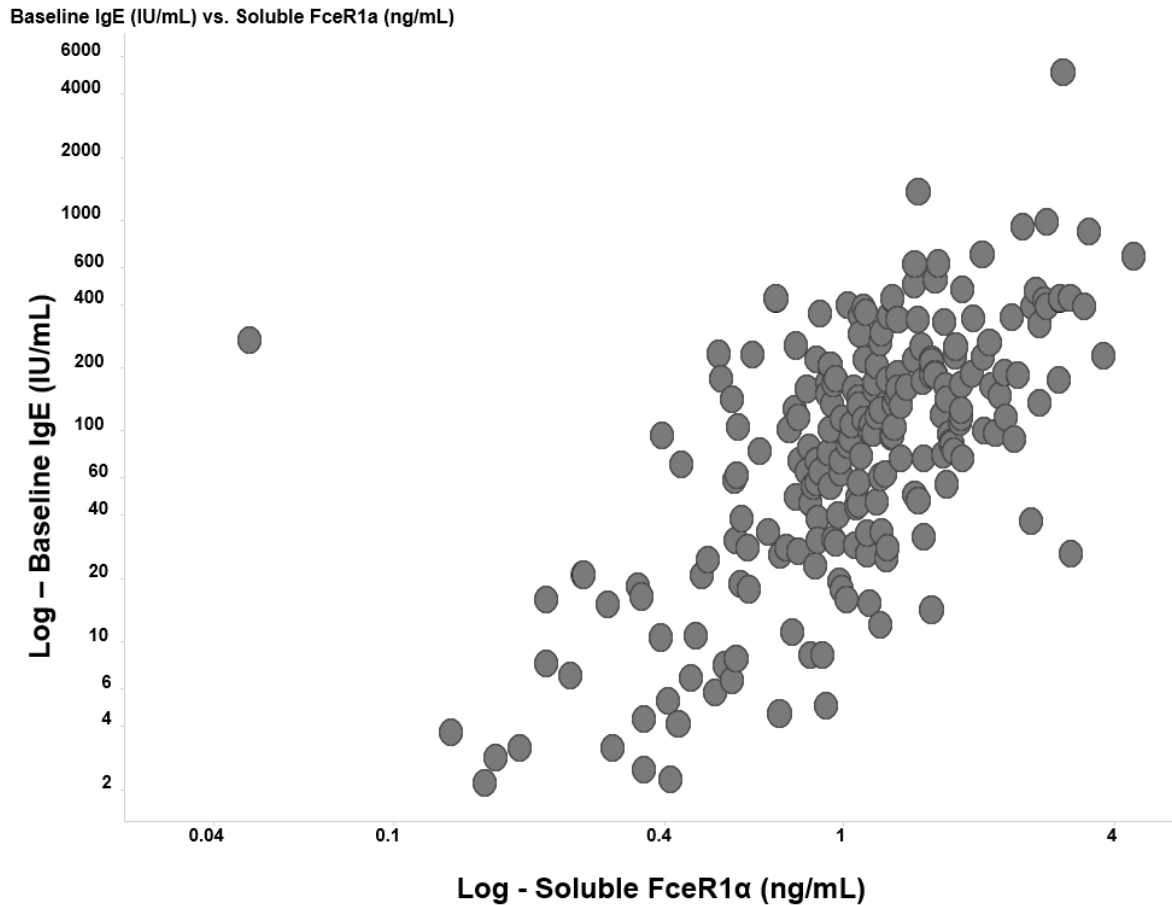


Figure 24:

Correlation between baseline IgE and soluble FcεR1α at baseline. Pearson's test results: p value < 0.001, $r=0.645$. 226 samples were tested.

Discussion

Anti-FcεR1a autoantibodies did not correlate with UAS7=0 response, suggesting that such immunoglobulins do not play a significant role in the triggering of CSU. As already described, it was suggested that anti-FcεR1a, particularly the IgG isotype, might trigger CSU symptoms by autoimmunity and in an IgE-free manner [348]. Although intriguing, such hypothesis did not take into account the different roles of autoantibodies. Although autoantibodies are usually considered pathogenic, there is decades-long debate about the duality of their role. Indeed, autoantibodies can also have a protective or homeostatic action, particularly so in the case of natural autoantibodies (NAAs). Such immunoglobulins would inhibit the activation of certain pro-inflammatory pathways, rather than activating them. In the specific case of CSU and anti-FcεR1a autoantibodies, their role could be of both IgE pathway activators or inhibitors. For instance, anti-FcεR1a autoantibodies could reduce the binding capacity of the receptor to IgE, thus inhibiting the activation of IgE pathway, without initiating an autoimmune reaction. In accordance with this hypothesis, an anti-FcεR1a monoclonal antibodies was tested as inhibitor of IgE binding on FcεR1a expressed on cells surface, and it successfully inhibited histamine, β-hexosaminidase and Ca²⁺ release in

a concentration-dependent manner in hFcεRI-expressing cells [350]. Our anti-FcεR1a autoantibodies data do not allow to propose a specific role for autoimmunity in CSU pathogenesis, as they are present in both UAS7=0 responders and non-responders after anti-IgE treatment. Performing functional assays on those autoantibodies may help in better understanding their biological role, particularly for mast cells degranulation, basophils activation and histamine release. In summary, only a combination of assays detecting the presence and the functionality of anti-FcεR1a autoantibodies may shed some light on their biological role in the pathogenesis of CSU.

The most interesting finding of this project was the decrease of sFcεR1a after anti-IgE treatment. Indeed, we showed that ligelizumab and omalizumab treatment decreased soluble FcεR1α concentrations in serum of CSU patients in a dose-dependent manner, similarly to that previously reported for the cell surface form of FcεR1, indicating a potential biological correlation between these two forms. Interestingly, the level of sFcεR1a increased back to baseline levels during the wash out period after treatment discontinuation in again a dose-dependent manner. Furthermore, ligelizumab 240 mg was more potent than omalizumab 300 mg in decreasing soluble FcεR1α levels in CSU patients as early as week 4 and maintaining this suppression well into the wash out period until about week 32. Such result is particularly relevant, especially when considering the difference in epitopes targeted by ligelizumab and omalizumab [351]. Indeed, although both antibodies target the same molecule, they bind IgE in slightly different epitopes. Both epitopes partially overlap with the binding sites between IgE and its receptors (CD23 and FcεR1a), but the inhibition efficacy is not the same between the two antibodies. When considering the inhibition of IgE binding to CD23, omalizumab was more effective than ligelizumab. However, when considering the inhibition of IgE binding to FcεR1a, ligelizumab was more effective than omalizumab [351]. This second result was reflected by our data, as sFcεR1a decrease after treatment was stronger for ligelizumab 240 mg and 72 mg when compared to omalizumab 300 mg. It is plausible to think that a more effective inhibition of IgE-FcεR1a binding would reflect on a stronger decrease of sFcεR1a expression.

In addition, baseline levels of soluble FcεR1α correlated with serum baseline IgE concentrations. This finding was particularly interesting, as it suggested a biological correlation between the two molecules. The authors that first published the detection of a human form of sFcεR1a suggested that sFcεR1a production might derive from IgE-FcεR1a binding [352]. Such hypothesis is in line with the observations of sFcεR1a and cell-bound FcεR1a decrease after anti-IgE treatment. Indeed, higher concentrations of circulating IgE would translate in higher binding with FcεR1a, which would result in higher sFcεR1a expression.

In summary, we showed the potential of sFcεR1a to be a surrogate marker for cell-bound FcεR1a. However, in order to validate this finding, the detection of both sFcεR1a and cell-bound FcεR1a in same patients receiving anti-IgE treatment is needed. Only with such data it would be possible to assess whether sFcεR1a decrease after anti-IgE treatment is a reflection of cell-bound FcεR1a decrease. The biomarker strategy for the next pivotal clinical trial of ligelizumab in CSU will include the detection of both FcεR1a forms, so that sFcεR1a value as a mechanistic marker for anti-IgE treatment will be fully assessed.

Monitoring sFceR1a in CSU patients undergoing ligelizumab treatment might allow following the effects of anti-IgE therapy at molecular level, in order to verify whether the drug is having the intended action in decreasing IgE pathway activation. Following the levels of sFceR1a after treatment discontinuation could also potentially allow predicting when the CSU symptoms may come back. Indeed, an increase in sFceR1a may be linked to cell-bound FceR1a levels increased expression on basophils and mast cells surface, thus being a marker of immune system readiness to activate IgE pathway. Considering the results obtained in this project and the data that will be collected in the next future, measuring sFceR1a levels may become a routine measure for the monitoring of clinical efficacy of anti-IgE treatment of CSU.

Discussion

As stated numerous times, the use of biomarkers able to increase the knowledge about a specific disease and/or inform on treatment efficacy would greatly improve the treatment approaches to autoimmune diseases. Indeed, the biological diversity within most autoimmune diseases is such that finding one single treatment with significant clinical efficacy in more than 30-50% of treated patients is a pending challenge. Arthritic diseases, such as RA, PsA and AS, represent some of the best examples. Although well-known and affecting a non-negligible portion of population, the treatments currently available for such diseases only allow for a control or slight improvement of symptoms in around half of the population. The pharmaceutical industry is in need for biomarkers able to distinguish between responders and non-responders to specific treatments, in order to support the approval of new drugs that might be efficacious in a small portion of patients. In other words, there is a possibility that the next advancement in the treatment of most autoimmune diseases may come from the identification of endotypes informing on which patient would respond to which treatment, rather than from new therapeutic targets. For some other diseases, such as Hidradenitis Suppurativa, the scientific community simply lacks information about all the pathogenic pathways activated, thus Universities and pharmaceutical companies are in the position of looking for a treatment while possessing limited knowledge on the disease. Most of the molecular biomarkers studies performed in the above-mentioned disease areas were based on proteomics and transcriptomic approaches. Although extremely useful in obtaining large datasets and in monitoring markers specific for disease symptoms and immune cells activations, such approaches neglect a fundamental physiological but also potentially pathological component of our body: immunoglobulins. Indeed, our immune system plays a critical role in our body and has been described as the main culprit in autoimmune diseases, with immunoglobulins being one of the pathogenic agents. Although immune cells can be considered as the most visible actors of immune system activity, antibodies are fundamental components as well. With average concentrations ranging between 10-30 mg/mL in the serum of healthy subjects, immunoglobulins are some of the most highly abundant proteins produced by our body. Monitoring the antigens targeted by the immune system can help in further understanding the pathogenesis and the homeostatic efforts taking place within a disease. Autoantibodies profiling may then be a missing piece of the molecular puzzle of autoimmune diseases biomarkers. Having a complete molecular understanding of a given disease population would facilitate the use of a more refined treatment strategy. Although the use of some autoantibodies, such as anti-SSA and SSB or RF, is of routine in several diseases, a profiling approach is still rare.

The results obtained throughout this thesis showed the potential of autoantibodies profiling applied to clinical trials. For instance, autoantibodies profiling performed in an anti-IL17 clinical trial in PsA allowed the identification of potential disease endotypes. Indeed, ACR50 non-responders were found positive for the expression of autoantibodies directed against components of IL17 pathway, gut microbiota and antigens linked to RA development. Such result suggested that anti-IL17 treatment might not be ideal in patients

already immuno-regulating the IL17 pathway or presenting RA-like autoantibodies. Such patients would be more resilient to anti-IL17 treatment, as shown by poorer performance of such treatment in RA, and could potentially be pre-identified as non-responders before receiving the treatment. Such pre-selection would support caregivers in selecting treatments that are more suitable and in reducing the risk of symptoms' deterioration. Furthermore, pre-selecting patients would also increase the overall efficacy of the treatment, increasing the chances of it being positively reviewed by health authorities and being applied on patients. A more efficacious treatment would then allow a better market penetration and increased sales for pharmaceutical companies. Under such circumstances, a pre-selection of patients before treatment would benefit all entities involved, from the patient to the caregivers and the producers.

On a more technical perspective, the results obtained with autoantibodies profiling in PsA patients proved to be critically helpful in the advancement of other projects of the thesis. Indeed, it was possible to test numerous antigens that were not previously described in literature as meaningful or that were never tested on such high number of samples. For instance, the selection of antigens for the profiling experiments performed with Hidradenitis Suppurativa samples was based on the results obtained in PsA. CEL-BSA was chosen because of the autoantibodies values obtained with PsA samples, which suggested a specific targeting of this small post-translational modification by the immune system in a subgroup of patients. Anti-CEL-BSA autoantibodies were then identified as a specific biomarkers in HS when compared to other diseases. Anti-CEL-BSA autoantibodies suggested a role of oxidative stress and of methylglyoxal in the pathogenesis of HS, favoring the hypothesis that HS development might have an autoimmune component. This result has the potential to start new research approaches on HS that may elucidate the pathogenesis of this complex disease. Ultimately, through autoantibodies profiling, a new potentially pathogenic pathway of HS was revealed, which would have been difficult to identify with other profiling approaches such as transcriptomics and proteomics.

Furthermore, the autoantibodies profiling assay used throughout the thesis was applied to Chronic Spontaneous Urticaria samples. The aim of the test was to verify whether patients classified as non-responders to an anti-IgE treatment would express anti-FcεR1a autoantibodies. The obtained results suggested that such hypothesis was not correct. Indeed, it was hypothesized that anti-FcεR1a autoantibodies could activate IgE pathway in IgE-free manner through direct targeting of the receptor. However, our results suggested that the sole presence of autoantibodies does not correlate with anti-IgE treatment non-response. FcεR1a is a central molecule in the IgE pathway and it certainly plays a role in the clinical response to anti-IgE treatment. Indeed, the monitoring of sFcεR1a, the soluble form of the cell-bound receptor, at several time-points along the treatment and follow-up period showed a dose-dependent decrease. Such finding was similar to the result published on the decrease of FcεR1a on basophils surface following anti-IgE treatment. This result needs to be confirmed with the monitoring of both FcεR1a bound on cells surface and sFcεR1a after anti-IgE treatment. A correlation between the two forms of the receptor would be particularly interesting, as the level of FcεR1a bound on cells surface can be considered as a

marker for cells readiness to activate the IgE pathway. Therefore, if sFceR1a level correlated with the cell-bound form, sFceR1a would also be a marker for IgE pathway readiness. sFceR1a may potentially be used as a mechanistic and efficacy marker for anti-IgE treatment of CSU. Monitoring the level of sFceR1a during the treatment may provide information on the molecular efficacy of the anti-IgE treatment. Monitoring of sFceR1a during the post-treatment follow-up period could potentially provide indications on when the readiness of immune cells to activate IgE pathway would rise again, informing on when treating the patient again. Those hypotheses will be tested in the next pivotal phase III clinical trial planned for ligelizumab in CSU.

Although compelling, the autoantibodies results obtained during this thesis showed some limitations of this biomarkers data. Firstly, the abundance of each autoantibody was relatively low. 2/3 of detected autoantibodies targeting a specific antigen were present in less than 30% of the samples population, while slightly less than half autoantibodies were present in less than 5% of the population (Table 2). Such data distribution is particularly different when compared to other types of profiling data sets, such as transcriptomics or proteomics, where a given marker is present in the majority of samples. The latter distribution makes the statistical comparison between two or more populations simpler. Furthermore, the low abundance of autoantibodies would allow the identification of only small endotypes, which would be difficult to translate in the development of a companion diagnostic.

Another limitation of autoantibodies profiling was the lack of a functional component of the collected data. The simple detection of autoantibodies did not inform on their role, as it could not distinguish between natural, homeostatic or pathogenic autoantibodies. Obtaining such an information together with the detection of autoantibodies would greatly help in better understanding the immune process in which such immunoglobulins are involved. For instance, the presence of anti-IL17R autoantibodies in PsA samples was, although compelling, of unclear meaning. Anti-IL17R autoantibodies could have a protective and homeostatic role by partially inhibiting the overexpressed IL17 pathway. However, they could also have a pathogenic role, as they could initiate the IL17 pathway in an IL17-free manner, similarly to what was proposed for anti-FceR1a autoantibodies role in CSU. Considering the complexity of functional assays for antibodies, such an approach is of difficult application together with large profiling experiments. Alternatively, functional assays could be used to validate or further explore the most interesting autoantibodies findings. Such approach was used with anti-CEL autoantibodies in Hidradenitis Suppurativa, when we showed that HS samples expressing higher levels of IgG anti-CEL would induce higher activation of macrophages and complement pathway, and that B-cells present in HS lesional skin produced anti-CEL immunoglobulins.

The autoantibodies profiling approach used in this thesis was based on the detection of 3 isotypes (IgG, IgM and IgA) targeting 208 antigens. The number of antigens used is extremely small when compared to the totality of antigens that our immune system can interact with. When considering only human proteins and without taking into account post-translational modifications, there are more than 10000 antigens that

could potentially be targeted by the immune system. It is difficult to calculate an approximate number of antigens when considering microbial (bacterial, viral and fungal), food, pollen and post-translational modifications. Therefore, this thesis can be considered as a first step toward showing the potential for autoantibodies profiling, but it is just a very small step in an extremely variegated and large field. Increasing the number of detected autoantibodies is of critical importance for a profiling approach, together with maintaining high standards of specificity. There are already other platforms with the potential to use more antigens for autoantibodies detection. For instance, Protagen is a company using a similar Luminex immunoassay to detect autoantibodies targeting up to 8000 human proteins, which is highly focused in autoantibodies profiling of cancer and autoimmune diseases. Microarrays technologies, such as the Protoarray from Thermo Fisher, also allow for the coating of several thousands of antigens and for the detection of the corresponding autoantibodies. The most common limitation of these platforms is the lack of a wide range of post-translational modifications. As shown with the results obtained in Hidradenitis Suppurativa and considering well known examples such as anti-CCP and anti-carbamylated peptides antibodies, post-translational modifications are particularly relevant antigens to be explored when performing autoantibodies profiling. Antigens such as Advanced Glycation Events (AGEs) have been studied since decades, but mostly CEL and CML were used for autoantibodies detection in diseases where oxidative stress is known for playing a pathogenic role. For instance, IgM anti-CEL autoantibodies were detected in Alzheimer's patients, while anti-CML autoantibodies were detected in diabetes [353, 354]. Although widely present even in healthy subjects, post-translational modification such as AGEs might be relevant markers in a number of diseases presenting inflammation and immune cells infiltrations, such as Crohn's disease and Ulcerative Colitis where AGEs receptor (RAGE) levels may play a role in their pathogenesis, but also in oncology [355-357]. Moreover, the levels of IgG anti-CEL found in Crohn and Ulcerative Colitis during this thesis were relatively high when compared to HS and healthy volunteers (HS manuscript, figure 1.e), which reinforced the hypothesis that oxidative stress may play an important role in the pathogenesis of those diseases. Ultimately, current autoantibodies profiling approaches should include post-translational modification in their antigens panel, as the corresponding autoantibodies have been so far relatively poorly explored and could potentially unveil novel biological pathways involved in the tested diseases.

Another common limitation of autoantibodies profiling studies found in literature is the focus toward detecting only the most abundant isotype in serum, which is IgG, while the detection of IgM, IgA or IgE is relatively rare. However, IgM and IgA antibodies are easily detectable in serum and have biologically relevant roles. IgM is considered the protective autoantibodies isotype, while IgA is the most abundant immunoglobulin in secretions and has a critical role in the regulation of the gut microbiota. Autoantibodies from both isotypes can be useful biomarkers in finding diseases endotypes, as they can inform on which pathways may be under homeostatic control by IgM or which antigens may be targeted by IgA in the gut or in secretions. IgA might be particularly relevant for autoimmunity development, as the microbiota plays a critical role in the immune homeostasis and tolerance [358]. Moreover, a dysbiosis between microbiota and

host has been linked to the development of several autoimmune diseases [359]. Additionally, monitoring the levels of the three most abundant isotypes (IgG, IgM and IgA) allows a better understanding of the immune response targeting a specific antigen. Detecting IgG subclasses can also potentially provide a deeper understanding of the autoantibodies' role, as different subclasses bind to different cellular receptors and thus activate different immune pathways [360]. The data collected during this thesis on IgG subclasses targeting CEL are a clear example. Most of IgG anti-CEL belonged to the IgG2 isotype, which is mostly associated with bacterial antigens and considered as anti-inflammatory and to dampen down the immune response [361]. This finding, coupled with the correlation between IgG2 and disease duration (while IgG1 and IgG3 anti-CEL correlated with disease severity, data not shown), showed the diversity within IgG antibodies and in the immune response against a given CEL. IgE results should be analyzed carefully, especially if detected in serum, as the levels of this immunoglobulin are between 1 thousand and 1 million times lower than IgG [362]. Such a difference in concentrations can be a source of artifacts when using an anti-IgE detection antibody with a slight cross-reactivity for IgG or other abundant isotypes. Moreover, when detecting autoantibodies in serum, all isotypes are in competition for binding with the coated antigens, which means that IgE have the lowest chances of binding to an antigen if IgG, IgM or IgA autoantibodies are targeting the same molecule. Therefore, although having a fundamental role in activating relevant immune cells such as basophils and mast cells, and thus being potentially interesting biomarkers, IgE autoantibodies' detection would require an attentive experimental setting aiming at minimizing any competition or any potential cross-reactivity with other isotypes. In conclusion, autoantibodies profiling should be performed by detecting at least IgG, IgM and IgA, with IgG subclasses potentially providing interesting information on the role of autoantibodies, while IgE should be measured with a carefully validated experimental setting.

Ultimately, autoantibodies profiling has the potential to improve our understanding of autoimmune diseases, by revealing which antigens are targeted by the immune system. Knowing which molecular pathways or families of antigens are regulated, with a pathogenic or homeostatic outcome, through autoantibodies binding could unveil new possibilities for endotyping a given disease or for discovering new potential therapeutic targets. Considering the variety of antigens that may be recognized by the immune system, any exploratory autoantibodies approach should be based on a panel of antigens of diverse nature and containing not only human but also microbial proteins and post-translational modifications. Current high-throughput technologies used for autoantibodies profiling are mostly based on human proteins panels, which represent only a fraction of the antigens possibly targeted by the immune system. Furthermore, coupling autoantibodies profiling with large antigens panels and multi-isotype detection with other large datasets like transcriptomic and proteomics would result in a more complete molecular figure of a patient or set of patients. Such diverse datasets would allow for a better understanding of the disease which would translate in higher chances to improve treatment strategies and potentially discover new therapeutic targets. The results presented in this thesis, although limited to a few diseases and relatively low amount of biomarkers, represent a step toward precision medicine.

Methods

Serum samples of Psoriatic Arthritis patients from the trial NCT01392326

Serum samples from PsA patients were collected during the clinical trial NCT01392326. Only baseline samples from patients having signed an informed consent for exploratory biomarkers analysis were used for the experiments presented in this manuscript. More information on the inclusion and exclusion criteria of these patients can be found in the clinical protocol already published by Mease et al [298].

Serum samples of Chronic Spontaneous Urticaria patients from the trial NCT02477332

Serum samples from CSU patients were collected during the clinical trial NCT02477332. Only samples from patients having provided an informed consent for exploratory biomarkers analysis were used during the experiments described in this manuscript. More information on the inclusion and exclusion criteria can be found in the clinical protocol already published by Maurer et al [347].

Serum samples of inflammatory Acne patients from NCT02998671

Serum samples of inflammatory Acne samples were collected during the clinical study NCT02998671. Only baseline samples from patients having signed an informed consent for exploratory biomarkers analysis were used.

Inclusion and exclusion criteria applied to selected patients for the study NCT02998671 [361]:

Inclusion criteria:

- Male and female subjects aged 18 to 45 years of age included, and otherwise in good health as determined by medical history, physical examination, vital signs, ECGs and laboratory tests at screening.
- Body weight between 50 and 120 kg, inclusive at screening.
- Patients with papulo-pustular acne vulgaris with between 25 and 100 facial inflammatory lesions (papules, pustules and nodules), and presence of non-inflammatory lesions (open and closed comedones) in the face at screening and baseline, who have failed systemic therapy for inflammatory acne.
- No more than 5 facial inflammatory nodules at screening and baseline.
- Investigator's Global assessment (IGA) score of at least moderate (3) acne severity on the face at screening and baseline.

Exclusion criteria:

- Appropriate wash out periods are required for investigational drugs, any oral/systemic treatment for acne, systemic or lesional injected (for acne) corticosteroids or systemic immunomodulators,

any systemic hormonal treatments, previous treatment with biologics, oral retinoids (in particular isotretinoin) and any topical anti-acne treatment.

- Use of facial medium depth chemical peels (excluding home regimens) within 3 months prior to baseline.
- Any live vaccines (this includes nasal-spray flu vaccine) starting from 6 weeks before baseline.
- Any other forms of acne
- Any severe, progressive or uncontrolled medical or psychiatric condition or other factors at randomization that in the judgment of the investigator prevents the patient from participating in the study.
- History of hypersensitivity or allergy to the investigational compound/compound class being used in this study.
- Active systemic infections (other than common cold) during the 2 weeks prior to baseline.
- History of severe systemic Candida infections or evidence of Candidiasis in the 2 weeks prior to baseline.
- Evidence of active tuberculosis at screening. All patients will be tested for tuberculosis status using a blood test (QuantiFERON®-TB (Tuberculosis) Gold In-Tube). Patients with evidence of tuberculosis may enter the trial after adequate treatment has been started according to local regulations.
- Patients with known active Crohn's disease
- History of immunodeficiency diseases, including a positive HIV (ELISA and Western blot) test result at screening.
- A positive Hepatitis B surface antigen or Hepatitis C test result at screening
- Pregnant or nursing (lactating) women, where pregnancy is defined as the state of a female after conception and until the termination of gestation, confirmed by a positive Human chorionic gonadotropin (HCG) laboratory test.
- WOCBP, defined as all women physiologically capable of becoming pregnant, unless they are using highly effective methods of contraception during dosing and for 13 weeks after stopping medication.

Cohorts of HS samples for HS manuscript

Cohort 1: serum samples of HS patients were collected during the clinical study NCT02421172. Only baseline samples from patients having signed an informed consent for exploratory biomarkers analysis were used.

Inclusion and exclusion criteria applied to selected patients for the study NCT02421172 (cohort 1) [364]:

Inclusion criteria:

- Male and female patients 18 to 65 years of age with clinically diagnosed chronic HS for at least 1 year (prior to screening) who have undergone previous antibiotic therapy
- Weight between 50 kg and 150 kg
- HS-PGA score of at least moderate severity at the time of inclusion with at least 4 abscesses and/or nodules. HS lesions must be present in at least two distinct anatomical areas, and at least one area must be minimally Hurley Stage II (moderate)

Exclusion criteria:

- Use of previous biologics or other specified concomitant medications
- Use of any systemic treatment for HS in the last 4 weeks prior to randomization
- Presence of more than 25 draining fistulae.
- Surgical treatment for HS in the last 4 weeks prior to randomization/first treatment.
- Women of child-bearing potential and sexually active males unwilling to use a condom during intercourse while taking drug and for 15 weeks after stopping investigational medication.
- Evidence of active tuberculosis at screening
- History of severe systemic Candida infections or evidence of Candidiasis in the last two weeks
- Active systemic or skin infections (other than common cold or HS related) during the two weeks before randomization/first treatment
- Any live vaccines (including nasal spray flu vaccine) starting from 6 weeks before randomization.

Cohort 2: plasma samples of HS patients collected by the Department of Dermatology of the Erasmus Medical Centre in Rotterdam. All participants signed an informed consent to allow the use of samples for exploratory research. No available inclusion and exclusion criteria.

Cohort 3: serum samples from HS patients collected by the University Hospital Basel, Department of Plastic, Reconstructive, Aesthetic and Hand Surgery in Basel, Switzerland. All participants signed an informed consent to allow the use of samples for exploratory research. No available inclusion and exclusion criteria.

Cohort 4: serum of HS patients collected by Bioreclamation IVT and commercially purchased. As per recruiting proceeding, all patients donating human material to Bioreclamation IVT signed an informed consent accepting the use of such material for exploratory research. No available inclusion and exclusion criteria.

Commercial serum samples

Serum samples from HS, Asthma, RA, Sjogren, SLE, IPF, Atopic dermatitis, Ulcerative colitis, Crohn's disease, Cystic Fibrosis and healthy volunteers were purchased from Bioreclamation IVT. As per recruiting proceeding, all patients donating human material to Bioreclamation IVT signed an informed consent accepting the use of such material for exploratory research. No available inclusion and exclusion criteria.

Plasma samples from healthy volunteers

The plasma of healthy volunteers was collected via the Basel Tissue Donor Program (BTDP) supported by Novartis. All patients donating human material through this program signed an informed consent accepting the use of such material for exploratory research. No available inclusion and exclusion criteria.

Skin samples

Skin sections from HS patients undergoing surgical removal of their lesions and skin of healthy volunteers were received from the University Hospital Basel, Department of Plastic, Reconstructive, Aesthetic and Hand Surgery in Basel, Switzerland as part of a non-interventional biomarker study TRI1270397. Patients provided written informed consent and the study was conducted in accordance with the ethical principles originating in the Declaration of Helsinki and approved by the local Ethics Committee. No available inclusion and exclusion criteria.

Autoantibodies profiling assay

Autoantibodies were detected using a custom-made Luminex assay based on magnetic beads. All washing steps of magnetic beads in tubes and plates were performed with the support of magnetic separation plates. Briefly, 100 μ L of stock solution of Luminex magnetic beads were pre-washed twice with 200 μ L of TBS (Sigma, T9039) in micronic tubes (Vitaris, 32022-MIC), then re-suspended in 200 μ L of coating solution containing antigens at 20 μ g/mL in TBS. After over-night incubation at +4°C with continuous rolling and cover from light, beads were washed twice with 200 μ L of TBS Tween 0.05% (Sigma, T9039), then blocked with 400 μ L of blocking solution for 2 hours at room temperature, with continuous rolling and cover from light. The blocking solution was composed of TBS with non-fat milk (Sigma, T8793) at 3%, FBS (Gibco, 10082-147) at 10% and Proclin300 (Sigma, 48912U) at 0.1%. Before plate loading, Luminex beads were mixed together and washed once with 1 mL of TBS Tween 0.05% Proclin300 0.1%, then re-suspended with 10.4 mL of TBS Tween 0.05% Proclin300 0.1%. Before being loaded on plates, serum or plasma samples were diluted 1:100 in TBS Tween 0.05% FBS 10% non-fat milk 1% BSA (Jackson ImmunoResearch, 001-000-162) 0.1%. 100 μ L/well of diluted serum were loaded on a black polystyrene plate (Costar, 3915) together with 25 μ L/well of prepared magnetic beads. After one hour of incubation at room temperature, with stirring at 750 rpm and cover from light, the plate was washed twice with 300 μ L/well of TBS Tween 0.05% using an automatic washer (Biotek, Elx405UM) combined with a magnetic separation plate and 3 minutes of waiting time before and after the first wash. After washing, 100 μ L/well of PE-tagged detection antibody targeting IgG, IgG1, IgG2, IgG3, IgG4, IgM or IgA (Southern Biotech, 2040-09, 9054-09, 9070-09, 9210-09, 9190-09, 2020-09, 2050-09), respectively at 0.5 μ g/mL, 1 μ g/mL for IgG subclasses, 0.2 μ g/mL and 1 μ g/mL in TBS Tween 0.05%, were added and incubated on plate for one hour at room temperature with stirring at 750 rpm and cover from light. The plate was then washed twice with 300 μ L/well of TBS Tween 0.05% using an automatic washer coupled with a magnetic separation plate and 3 minutes of waiting time before and after the first wash. 120 μ L/well of TBS BSA 0.5% Proclin300 0.1% were then

added on plate. After 3 minutes of incubation at room temperature with a stirring of 750 rpm and cover from light to re-suspend the beads, the plate was read using the Flexmap3D reader. Results were reported using the median fluorescence index (MFI) as unit of measure.

Incubation with CEL, CML and Octopine before autoantibodies profiling assay

To test the specificity of anti-CEL autoantibodies, plasma samples were diluted 1:100 with dilution buffer (TBS Tween 0.05% FBS 10% non-fat milk 1% BSA 0.1% Proclin300 0.1%) containing either CEL (Cayman Chemical, 25333), CML (Cayman Chemical, 16483) or Octopine (MyBiosource MBS6045660). The samples were incubated for 30 minutes at room temperature before proceeding with the autoantibodies assay. Control samples diluted with a buffer not containing CEL, CML or Octopine were also incubated 30 minutes at room temperature before proceeding with the autoantibodies assay.

CEL modification on Histone

CEL-Histone was prepared using a protocol described by Srey et al [365]. Histone H2A was dialyzed against PBS before the CEL-modification reaction. Briefly, Histone H2A (Sigma, H2042) at 0.1 mg/mL was mixed with sodium pyruvate (Sigma, S8636) (17.14 mM), and sodium cyanoborohydride (Sigma, 156159) (25.71 mM) in PBS (Sigma, 11666789001) (0.1 M, pH 7.0). The solution was incubated at 37 °C for 24 hours, then abundantly dialyzed against PBS. A control was also prepared using the same conditions but with the omission of sodium pyruvate. Dialysis units (Slide-A-Lyser® Mini Dialysis Units (10,000 MWCO, 0.1 mL)) (Thermo Fisher, cat#69570) with the buoys were put for 10 minutes into 2 L of dialysis buffer (PBS) (Roche, cat#14733200). The solution containing CEL-Histone was added to the dialysis units and dialyzed for one hour at room temperature. The dialysis buffer was changed every hour for three times. The purified solution of CEL-Histone, with final concentration of 800 µg/mL was then stored at -20°C.

Autoantibodies detection in HS skin

2 mm punch biopsies of lesional HS skin were immersed in liquid nitrogen using Covaris tissue tubes TT05 (Covaris, 520071) and crushed with a CP02 cryoPREP Automated Dry Pulverizer (Covaris, 500001). The fragments of skin were collected and weighted, and then re-suspended with 50 µL of TBS Tween 0.05% Triton X-100 (Sigma, T8787) 1%. These solutions were then sonicated five times for 30 seconds and vortexed between each sonication. Skin lysates were then diluted in 1:10 in TBS Tween 0.05% FBS 10% non-fat milk 1% Proclin300 0.1%. Autoantibodies detection protocol was then performed as the one described for serum and plasma samples.

CEL detection by direct ELISA

2 mm punch biopsies of lesional HS skin were immersed in liquid nitrogen using Covaris tissue tubes TT05 (Covaris, 520071) and crushed with a CP02 cryoPREP Automated Dry Pulverizer (Covaris, 500001). The fragments of skin were collected and weighted, and then re-suspended with 50 µL of TBS Tween 0.05% Triton X-100 (Sigma, T8787) 1%. These solutions were then sonicated five times for 30 seconds and

vortexed between each sonication. Skin lysates were then diluted 1:10 in PBS (Sigma, 11666789001). 50 μ L/well of diluted skin lysates and standards (CEL-BSA from CellBiolabs, STA-302, at different concentrations in PBS) were loaded on an ELISA plate and incubated over-night at 4°C with stirring at 400 rpm and cover from light. The plate was then washed 4 times with 300 μ L/well of PBS Tween 0.05% (Sigma, P3563) and blotted against a tissue. The plate was blocked with 150 μ L/well of PBS BSA 3% (BSA from Roche, 10735078001) for one hour at room temperature, with stirring at 500 rpm and cover from light. The plate was then washed 4 times with 300 μ L/well of PBS Tween 0.05% and blotted against a tissue. 100 μ L/well of biotinylated anti-CEL monoclonal antibody (Abnova, clone KNH30, MAB6594) diluted 1:250 in PBS Tween 0.05% were loaded on the plate and incubated for two hours at room temperature, with stirring at 500 rpm and cover from light. The plate was then washed 4 times with 300 μ L/well of PBS Tween 0.05% and blotted against a tissue. 100 μ L/well of Streptavidin-HRP (R&D, DY998) diluted 1:200 were loaded on plate and incubated for 30 minutes at room temperature, with stirring at 500 rpm and cover from light. The plate was then washed 4 times with 300 μ L/well of PBS Tween 0.05% and blotted against a tissue. 100 μ L/well of Ultra TMB (Thermo Fisher, 34028) were loaded on the plate and incubated for one hour at room temperature. Finally, 100 μ L/well of Sulfuric acid (Fluka, 38291) at 1 M were added and plate optic deviance (OD) was read at 450 nm.

FceR1a detection assay

MSD plate (MSD, cat#L15XA-3) were coated with 50 μ L/well of 1 μ g/mL of anti-FceR1a (Invitrogen, cat#14-5899-82) in PBS (Roche, cat#1666789001) over-night with incubation protected from light and with 500 rpm stirring at 4°C. Plate was washed 3 times with 150 μ L/well of PBS Tween20 (Sigma, cat#P3563), then blocked with 100 μ L/well of FBS (Gibco, cat#10082-147) 10% in PBS, for 2 hours at RT, protected from light and with 500 rpm stirring. Plate was washed 3 times with 150 μ L/well of PBS T and then 50 μ L/well of samples and standards were added for 90 minutes protected from light, at 23°C and stirring at 800 rpm. Plate was washed 3 times with 150 μ L/well of PBS T. 50 μ L/well of recombinant human IgE (Abcam, cat#Ab65866) was added to the plate and incubated for 30 minutes protected from light, at 23°C and stirring at 800 rpm. Plate was washed 3 times with 150 μ L/well of PBS T. 50 μ L/well of 1 μ g/mL of biotinylated anti-human IgE detection antibody (Novartis, clone 669-6-7, custom biotinylation) in PBS T was added and incubated for 1 hour in a mixer with 23°C and 800 rpm. Plate was washed 3 times with 150 μ L/well of PBS T. 50 μ L/well of Streptavidin-Sulfo Tag (MSD, cat#R32AD-1) diluted at 1:2000 in PBS T were added to the plate and incubated for 30 minutes protected from light, with stirring at 850 rpm and temperature at 23°C. Plate was washed 3 times with 150 μ L/well of PBS T. Read buffer (MSD, cat#R92TC-1) was diluted by 2 with demineralized water and 250 μ L/well were added to the plate. After 2 minutes of incubation in a mixer with stirring at 400 rpm and temperature at 23°C, the plate was read using an MSD Imager 600.

Biotinylation of anti-IgE antibody

Anti-human IgE antibody (Novartis, clone 669-6-7) at 1 mg/mL was extensively dialyzed in PBS (Roche, cat#1666789001). Slide-A-Lyser Mini Dialysis Units (10,000 MWCO) (Thermo Fisher, cat#69570) were pre-

incubated in PBS using a buoy system. 100 μ L of anti-human IgE antibody were added to each dialysis unit and dialyzed against 2 liters of PBS for 2 hours. Dialysis PBS was changed and anti-human IgE antibody was dialyzed for additional 2 hours against 2 liters of PBS. After dialysis, 100 μ L of anti-human IgE antibody were mixed with 0.7 μ L of NHS-PEG4-Biotin (Thermo Scientific, cat#21329) at 20 mM, in a 1.5 mL micronic tube. Such quantities correspond to an antibody/biotin ratio of 1:20. NHS-PEG4-Biotin solution was prepared by solubilizing 2 mg of lyophilized NHS-PEG4-Biotin in 170 μ L of demineralized water. The micronic tube containing the biotin and antibody mic was covered with aluminum foil and strapped on a roller for a 1-hour incubation at RT. After 1-hour incubation, 100 μ L of anti-human IgE conjugated with biotin were added to dialysis units for a 2 hours long dialysis against 2 liters of PBS. A second dialysis was performed using fresh PBS and an over-night incubation. Biotinylated anti-human IgE was then stored at 4°C.

Protocol Flagellin-BSA modification

Flagellin (Invivogen, cat# TLRL-BSFLA) was reconstituted by reverse pipetting with LAL water (Invivogen, cat# H2OLAL-1.5) to obtain a solution at 1 mg/mL. 1 g of BSA (Jackson Immunoresearch, cat#001-000-162) was dissolved in 50 mL of demineralized water in order to obtain a stock solution at 20 mg/mL. 100 mg of N-(3-Dimethylaminopropyl)-N'-ethylcarbodiimide hydrochloride (EDC) (Sigma, cat#E1769-5g) were dissolved in 2 mL of demineralized water in order to obtain a stock solution at 50 mg/mL. 50 μ L of Flagellin at 1 mg/mL were mixed in a micronic tube (Vitaris, 32022-MIC) with 2.5 μ L of BSA at 20 mg/mL and 10 μ L of EDC at 50 mg/mL. The solution was incubated over night at +4°C with slow agitation on a rotor, to allow the coupling of Flagellin on BSA. The purification of Flagellin-BSA was performed through dialysis. Dialysis unit (Slide-A-Lyser® Mini Dialysis Units (10,000 MWCO, 0.1 mL)) (Thermo Fisher, cat#69570) with the buoys were put for 10 minutes into 2 L of dialysis buffer (PBS) (Roche, cat#14733200). The solution containing Flagellin-BSA was added to the dialysis unit and dialyzed for one hour at room temperature. The dialysis buffer was changed every hour for three times. The purified solution of Flagellin-BSA, with final concentration of 800 μ g/mL was then stored at -20°C.

Statistical methods

Data were analyzed and graphs were created using Tibco Spotfire (version 10.3.3) and GraphPad Prism (version 8.1.2), with the support of Excel 2016 for the organization and storage of data and samples information. Autoantibodies data in the results section I were also analyzed by using RStudio for explorative analysis. Anova, T-test and Mann-Whitney were used to compare biomarkers levels between different samples populations, depending on the specific data analysis to be performed. Linear regression, Spearman and Pearson's tests were used to investigate the correlation levels between numerical data, depending on the specific data analysis to be performed. Statistical tests performed are specified in the legends of the corresponding figures.

ROC curves were prepared and corresponding AUC were calculated using GraphPad Prism. True positive rate and false positive rate used for ROC curves were calculated using Excel 2016. True positive rate was defined as the proportion of correctly identified positives. False positive rate was defined as the proportion of negatives incorrectly identified as positives.

Linear combination of disease severity and disease duration

We used refined Hurley score to define disease severity and we transformed the seven categories (1a, 1b, 1c, 2a, 2b, 2c and 3) in numerical values from 1 to 7. Disease duration was expressed in years and calculated in as follows:

$$Disease\ duration = Patient's\ age - age\ at\ disease\ onset$$

Both numerical disease severity and disease duration for each patient were then standardized by dividing by the average, as follows:

$$Std\ disease\ severity\ (patient\ n) = \frac{disease\ severity\ (patient\ n)}{disease\ severity\ average}$$

$$Std\ disease\ duration\ (patient\ n) = \frac{disease\ duration\ (patient\ n)}{disease\ duration\ average}$$

Standardized values were then combined by Euclidean distance, which was calculated using Pythagoras:

$$Combination = \sqrt{(Std\ severity)^2 + (Std\ duration)^2}$$

The overall formula used to calculate the linear combination of disease severity and duration is then as follows:

$$Combination\ (patient\ n) = \sqrt{\left(\frac{disease\ severity\ (patient\ n)}{disease\ severity\ average}\right)^2 + \left(\frac{disease\ duration\ (patient\ n)}{disease\ duration\ average}\right)^2}$$

Linear combination of autoantibodies data

As described in the results section I, a linear combination of autoantibodies values was performed in order to combine data from single autoantibodies and improve the discrimination between ACR50 non-responders and responders.

Values obtained for each autoantibody can be used as coordinates in a space, with two, three or more dimensions and distance from axis origin can be calculated. For example, distance in a seven-dimension space was calculated with the following steps:

- For each autoantibody separately, values were standardized by dividing each value by the mean of values.
- For each samples seven-dimension distance was calculated with the following formula:

$$7D = \sqrt{a^2 + b^2 + c^2 + d^2 + e^2 + f^2 + g^2}$$

With a, b, c, d, e, f and g as standardized coordinates calculated from values obtained by Luminex immunoassay. This linear combination was used with up to 20 different autoantibodies.

List of antigens used in PsA autoantibodies profiling

Antigen	Supplier	Antigen group
BSA	Jackson ImmunoResearch	Albumin
Prealbumin	Sigma	Albumin
Apolipoprotein B	Millipore	Apolipoprotein
Apolipoprotein E	Millipore	Apolipoprotein
Apolipoprotein E4	Sigma	Apolipoprotein
B2 glycoprotein	Diarect	Apolipoprotein
<i>Akkermansia</i>	Bioclone	Bacterial antigen
<i>Faecalibacterium</i> allergen	Bioclone	Bacterial antigen
Flagellin-BSA	Custom-made	Bacterial antigen
<i>Helicobacterium</i>	Bioclone	Bacterial antigen
<i>Klebsiella</i> surface antigen	Bioclone	Bacterial antigen
<i>Lachnospiraceae</i>	Bioclone	Bacterial antigen
LPS-BSA	Custom-made	Bacterial antigen
<i>Porphyromas gingivalis</i>	Bioclone	Bacterial antigen
<i>Prevotella</i>	Bioclone	Bacterial antigen
Protein A	Bioclone	Bacterial antigen
rIpaC <i>Shigella</i>	Bioclone	Bacterial antigen
rSopC <i>Salmonella</i>	Bioclone	Bacterial antigen
<i>Ruminococcus</i>	Bioclone	Bacterial antigen
RuvB <i>E.coli</i>	Creative Diagnostic	Bacterial antigen
<i>Staphilococcus</i> Protein A	Creative Diagnostic	Bacterial antigen
<i>Streptococcus pyogenes</i> arcA	Diarect	Bacterial antigen
<i>Streptococcus pyogenes</i> tkt	Diarect	Bacterial antigen

Laminin	R&D Systems	Cell development
Spectrin alpha chain 1	Origene	Cell development
Tissue Transglutaminase	Diarect	Cell development
TPT1	Prospec	Cell development
Transforming growth factor, beta-induced	Mybiosource	Cell development
Glial fibrillary acidic protein	Novoprotein	CNS
Myelin Associated Glycoprotein	Life technologies	CNS
Myelin basic protein	MyBiosource	CNS
Myelin oligodendrocyte glycoprotein	Anaspec	CNS
S100B	R&D Systems	CNS
Tau-381	Millipore	CNS
IL-1 beta	Acro Biosystems	Cytokine
IL12	Peprtech	Cytokine
IL17A	R&D Systems	Cytokine
IL21	R&D Systems	Cytokine
IL23	Prospec	Cytokine
IL26	DiscoverX	Cytokine
IL33	Peprtech	Cytokine
IL6	R&D Systems	Cytokine
sRANKL	Prospec	Cytokine
TNFa	R&D Systems	Cytokine
<i>Aspergillus Restrictocin</i>	Creative Diagnostic	Fungal antigen
<i>Candida albicans bgl2</i>	Diarect	Fungal antigen
<i>Candida albicans Enolase</i>	Diarect	Fungal antigen
<i>Candida albicans HSP70</i>	Diarect	Fungal antigen
<i>Candida albicans Met6</i>	Diarect	Fungal antigen
Deamidated gliadin peptide	Zedira	Fungal antigen
GLC8 <i>Saccharomyces cerevisiae</i>	Creative Diagnostic	Fungal antigen
Gliadin	Diarect	Fungal antigen
Aldolase	Sigma	Glycolysis
Alpha Enolase	USBiological	Glycolysis
Pyruvate Kinase	Sigma	Glycolysis
Alpha-crystallin B chain	Origene	Heat shock protein
HSP 27	R&D Systems	Heat shock protein
HSP 60	Enzo Life Sciences	Heat shock protein
HSP65		Heat shock protein
HSP70	HyTest	Heat shock protein
HSP90	R&D Systems	Heat shock protein
Alkalin Phosphatase	MyBiosource	Immune system regulation
Alpha-1 antitrypsin	Sigma	Immune system regulation
Annexin 1	Prospec	Immune system regulation

Annexin 2	Prospec	Immune system regulation
Annexin 5	Prospec	Immune system regulation
Antichymotrypsin enzyme	Mybiosource	Immune system regulation
Concanavalin A	Sigma	Immune system regulation
Hemoglobin A1C	Mybiosource	Immune system regulation
Human Alkaline phoshatase	Novoprotein	Immune system regulation
IgA	Jackson ImmunoResearch	Immunoglobulin
IgG	Jackson ImmunoResearch	Immunoglobulin
IgM	Agrisera	Immunoglobulin
Bactericidal/permeability increasing protein	Arotec	Inflammation
Liver Cytosol type 1 antigen	Arotec	Inflammation
Mitochondrial antigen	Arotec	Inflammation
Parietal Cell antigen	Arotec	Inflammation
C5		Innate immune system
Eosinophil Peroxidase	Arotec	Innate immune system
Lingual antimicrobial peptide	R&D Systems	Innate immune system
COG4	Origene	Intracellular
KPNB1	Origene	Intracellular
PPP2R1A	Origene	Intracellular
RAB11B	Origene	Intracellular
Alpha-1-microglobulin/bikunin precursor	Prospec	Metabolism
Amyloid P	Millipore	Metabolism
Calmodulin	Sigma	Metabolism
Calreticulin	Mybiosource	Metabolism
Creatine Kinase	Lee Biosolutions	Metabolism
Cytochrome C	Sigma	Metabolism
Cytochrome P450	Diarect	Metabolism
Dermatan Sulfate	Millipore	Metabolism
Fibrinogen	Sigma	Metabolism
Glomerular Basement Membrane	Diarect	Metabolism
Glutamine synthetase	Mybiosource	Metabolism
Hemoglobin A2	Novus Bio	Metabolism
Insulin	R&D Systems	Metabolism
Intrinsic Factor	Diarect	Metabolism
Methylated Ubiquitin	R&D Systems	Metabolism
Mitochondrial 2-oxo acid dehydrogenase	Diarect	Metabolism
NADPH	Life technologies	Metabolism
Prothrombin	Thermo Fisher	Metabolism
Retinol Binding protein	Sigma	Metabolism

Retinol-binding protein 3	USCN	Metabolism
Ribulose-phosphate 3-epimerase	Prospec	Metabolism
Threonyl-tRNA synthetase	Diarect	Metabolism
Ubiquitin	Creative Diagnostic	Metabolism
Visfatin	Biolegend	Metabolism
Vitronectin	R&D Systems	Metabolism
Advanced Glyaction Event-BSA	Cellbiolabs	Modified Albumin
Albumin-DNP	Sigma	Modified Albumin
BSA-Chondroitin	Custom-made	Modified Albumin
Carbamylated-BSA	Home-made	Modified Albumin
Carboxyethyllysine-BSA	Cell Biolabs	Modified Albumin
Digoxin-BSA	Fitzgerald	Modified Albumin
DNP-Bovine Albumin	Millipore	Modified Albumin
DNP-BSA	Life Technologies	Modified Albumin
Glycated albumin	Sigma	Modified Albumin
Heparan-BSA	Custom-made	Modified Albumin
Malondialdehyde (MDA)-BSA	USBiological	Modified Albumin
Trimethyllysine BSA	Immunechem	Modified Albumin
Cathepsin G	Arotec	NETs
Myeloperoxidase	Arotec	NETs
Neutrophil Elastase	EastCoast Bio	NETs
Proteinase 3	Arotec	NETs
Glycoprotein 2	Diarect	Neutrophils activity
Alanyl-tRNA Synthase	Diarect	Nuclear antigen
CENP-A	Diarect	Nuclear antigen
CENP-B	Arotec	Nuclear antigen
Chromodomain-helicase-DNA-binding protein Mi-2	Diarect	Nuclear antigen
DNA human placenta	Sigma	Nuclear antigen
DNA polymerase beta	Prospec	Nuclear antigen
dsDNA	Diarect	Nuclear antigen
dsDNA plasmid	Diarect	Nuclear antigen
dsRNA	Biochain	Nuclear antigen
Histone	Sigma	Nuclear antigen
Histone antigen	Arotec	Nuclear antigen
Interleukin enhancer-binding factor 3	Mybiosource	Nuclear antigen
Jo-1	Diarect	Nuclear antigen
Ku 70/80	Diarect	Nuclear antigen
LA/SSB	Diarect	Nuclear antigen
Nucleoporin 210	Diarect	Nuclear antigen
Nucleosome antigen	Arotec	Nuclear antigen
Nup62	Diarect	Nuclear antigen
PCNA	Diarect	Nuclear antigen
PM/ScI100	Diarect	Nuclear antigen
Pm/ScI75	Diarect	Nuclear antigen

Ribosomal Phosphoprotein P0	Diarect	Nuclear antigen
Ribosomal Phosphoprotein P1	Diarect	Nuclear antigen
Ribosomal Phosphoprotein P2	Diarect	Nuclear antigen
RNA calf liver	Sigma	Nuclear antigen
RNP 68/70	Diarect	Nuclear antigen
RNP A	Diarect	Nuclear antigen
RNP C	Diarect	Nuclear antigen
RNP/Sm	Diarect	Nuclear antigen
RNPB	Diarect	Nuclear antigen
RO/SSA 52	Diarect	Nuclear antigen
Ro/SSA 60	Diarect	Nuclear antigen
Sci-70	Diarect	Nuclear antigen
Sm	Diarect	Nuclear antigen
SmD	Diarect	Nuclear antigen
SmD1	Diarect	Nuclear antigen
SmD2	Diarect	Nuclear antigen
Sp100	Diarect	Nuclear antigen
ssDNA	Sigma	Nuclear antigen
Glucan	Sigma	Polysaccharides-Fungal antigen
Mannan	Sigma	Polysaccharides-Fungal antigen
Elastase	Arotec	Protease
Decorin	Sigma	Proteoglycan
Heparan Sulfate ProteoGlycan	Cloud clone	Proteoglycan
Lumican	R&D Systems	Proteoglycan
CD36	Sigma	Receptor
CD74	R&D Systems	Receptor
FceR1a	R&D Systems	Receptor
IL17R	Acro Biosystems	Receptor
IL22 BP	R&D Systems	Receptor
IL36RN	Prospec	Receptor
Muscarinic acetylcholine receptor M3	MYBiosource	Receptor
TNFR1	Prospec	Receptor
Cardiolipin	Sigma	Structural lipid
Aggrecan	Sigma	Structural protein
Alpha actinin	Cytoskeleton	Structural protein
Beta Actin	Alpha Diagnostic	Structural protein
Collagen I	Millipore	Structural protein
Collagen II	Millipore	Structural protein
Collagen III	Prospec	Structural protein
Collagen IV	Millipore	Structural protein
Collagen V	Millipore	Structural protein
Collagen VI	Rockland	Structural protein

Cytokeratin 18	Thermo Fisher	Structural protein
Elastin	Sigma	Structural protein
Keratin 12	ARP	Structural protein
Myosin	Cytoskeleton	Structural protein
Myosin Heavy chain	Cytoskeleton	Structural protein
Vimentin	R&D Systems	Structural protein
Thyroglobulin	Diarect	Thyroid antigen
Thyroid Peroxidase	Diarect	Thyroid antigen
Cytomegalovirus G	Meridian	Viral antigen
Cytomegalovirus pp150	Prospec	Viral antigen
Cytomegalovirus pp28	Prospec	Viral antigen
Epstein-Barr Virus EBNA1 His Tag	Prospec	Viral antigen
Epstein-Barr Virus P18	Prospec	Viral antigen
Epstein-Barr Virus P23	Prospec	Viral antigen
Hepatitis B Virus	Prospec	Viral antigen
Respiratory Syncytial Virus	Meridian	Viral antigen

Table 4:

List of antigens used in autoantibodies profiling experiments. For each antigen, the provider and a general classification are specified.

Bibliography

1. Clark, R. and T. Kupper, *Old meets new: the interaction between innate and adaptive immunity*. J Invest Dermatol, 2005. 125(4): p. 629-37.
2. Janeway, C.A., Jr. and R. Medzhitov, *Innate immune recognition*. Annu Rev Immunol, 2002. 20(1): p. 197-216.
3. Hoffmann, J. and S. Akira, *Innate immunity*. Curr Opin Immunol, 2013. 25(1): p. 1-3.
4. Hoffmann, J.A., et al., *Phylogenetic perspectives in innate immunity*. Science, 1999. 284(5418): p. 1313-8.
5. Iriti, M. and F. Faoro, *Review of innate and specific immunity in plants and animals*. Mycopathologia, 2007. 164(2): p. 57-64.
6. Litman, G.W., J.P. Rast, and S.D. Fugmann, *The origins of vertebrate adaptive immunity*. Nat Rev Immunol, 2010. 10(8): p. 543-53.
7. Bonilla, F.A. and H.C. Oettgen, *Adaptive immunity*. J Allergy Clin Immunol, 2010. 125(2 Suppl 2): p. S33-40.
8. Kumar, B.V., T.J. Connors, and D.L. Farber, *Human T Cell Development, Localization, and Function throughout Life*. Immunity, 2018. 48(2): p. 202-213.
9. Wherry, E.J., *T cell exhaustion*. Nat Immunol, 2011. 12(6): p. 492-9.
10. Mousset, C.M., et al., *Comprehensive Phenotyping of T Cells Using Flow Cytometry*. Cytometry A, 2019. 95(6): p. 647-654.
11. Zuniga-Pflucker, J.C., *T-cell development made simple*. Nat Rev Immunol, 2004. 4(1): p. 67-72.
12. Kondo, K., I. Ohigashi, and Y. Takahama, *Thymus machinery for T-cell selection*. Int Immunol, 2019. 31(3): p. 119-125.
13. Starr, T.K., S.C. Jameson, and K.A. Hogquist, *Positive and negative selection of T cells*. Annu Rev Immunol, 2003. 21: p. 139-76.
14. Shah, D.K. and J.C. Zuniga-Pflucker, *An overview of the intrathymic intricacies of T cell development*. J Immunol, 2014. 192(9): p. 4017-23.
15. Sprent, J. and C.D. Surh, *Normal T cell homeostasis: the conversion of naive cells into memory-phenotype cells*. Nat Immunol, 2011. 12(6): p. 478-84.
16. Gourley, T.S., et al., *Generation and maintenance of immunological memory*. Semin Immunol, 2004. 16(5): p. 323-33.
17. Chapman, N.M., M.R. Boothby, and H. Chi, *Metabolic coordination of T cell quiescence and activation*. Nat Rev Immunol, 2020. 20(1): p. 55-70.
18. Zhu, J., *T Helper Cell Differentiation, Heterogeneity, and Plasticity*. Cold Spring Harb Perspect Biol, 2018. 10(10): p. a030338.
19. Romagnani, S., *Th1/Th2 cells*. Inflamm Bowel Dis, 1999. 5(4): p. 285-94.
20. Szabo, S.J., et al., *Molecular mechanisms regulating Th1 immune responses*. Annu Rev Immunol, 2003. 21: p. 713-58.
21. Charlton, B. and K.J. Lafferty, *The Th1/Th2 balance in autoimmunity*. Curr Opin Immunol, 1995. 7(6): p. 793-8.
22. Bedoya, S.K., et al., *Th17 cells in immunity and autoimmunity*. Clin Dev Immunol, 2013. 2013: p. 986789.
23. Park, H., et al., *A distinct lineage of CD4 T cells regulates tissue inflammation by producing interleukin 17*. Nat Immunol, 2005. 6(11): p. 1133-41.

24. Schmidt, M.E. and S.M. Varga, *The CD8 T Cell Response to Respiratory Virus Infections*. Front Immunol, 2018. 9: p. 678.
25. Reading, J.L., et al., *The function and dysfunction of memory CD8(+) T cells in tumor immunity*. Immunol Rev, 2018. 283(1): p. 194-212.
26. Mittrucker, H.W., A. Visekruna, and M. Huber, *Heterogeneity in the differentiation and function of CD8(+) T cells*. Arch Immunol Ther Exp (Warsz), 2014. 62(6): p. 449-58.
27. Kaech, S.M., E.J. Wherry, and R. Ahmed, *Effector and memory T-cell differentiation: implications for vaccine development*. Nat Rev Immunol, 2002. 2(4): p. 251-62.
28. Sakaguchi, S., *Regulatory T cells: history and perspective*. Methods Mol Biol, 2011. 707: p. 3-17.
29. La Cava, A., *Natural Tregs and autoimmunity*. Front Biosci (Landmark Ed), 2009. 14: p. 333-43.
30. Kawai, K., et al., *Regulatory T cells for tolerance*. Hum Immunol, 2018. 79(5): p. 294-303.
31. Oderup, C., et al., *Cytotoxic T lymphocyte antigen-4-dependent down-modulation of costimulatory molecules on dendritic cells in CD4+ CD25+ regulatory T-cell-mediated suppression*. Immunology, 2006. 118(2): p. 240-9.
32. Schmidt, A., N. Oberle, and P.H. Krammer, *Molecular mechanisms of treg-mediated T cell suppression*. Front Immunol, 2012. 3: p. 51.
33. Marie, J.C., et al., *TGF-beta 1 maintains suppressor function and Foxp3 expression in CD4+CD25+ regulatory T cells*. J Exp Med, 2005. 201(7): p. 1061-7.
34. Flippe, L., et al., *Future prospects for CD8(+) regulatory T cells in immune tolerance*. Immunol Rev, 2019. 292(1): p. 209-224.
35. Eibel, H., et al., *B cell biology: an overview*. Curr Allergy Asthma Rep, 2014. 14(5): p. 434.
36. Zhang, M., G. Srivastava, and L. Lu, *The pre-B cell receptor and its function during B cell development*. Cell Mol Immunol, 2004. 1(2): p. 89-94.
37. Hardy, R.R. and K. Hayakawa, *B cell development pathways*. Annu Rev Immunol, 2001. 19: p. 595-621.
38. Sandel, P.C. and J.G. Monroe, *Negative selection of immature B cells by receptor editing or deletion is determined by site of antigen encounter*. Immunity, 1999. 10(3): p. 289-99.
39. Melchers, F., *Checkpoints that control B cell development*. Journal of Clinical Investigation, 2015. 125(6): p. 2203-2210.
40. LeBien, T.W. and T.F. Tedder, *B lymphocytes: how they develop and function*. Blood, 2008. 112(5): p. 1570-80.
41. Katikaneni, D.S. and L. Jin, *B cell MHC class II signaling: A story of life and death*. Hum Immunol, 2019. 80(1): p. 37-43.
42. Scholl, P.R. and R.S. Geha, *MHC class II signaling in B-cell activation*. Immunol Today, 1994. 15(9): p. 418-22.
43. Mesin, L., J. Ersching, and G.D. Victora, *Germinal Center B Cell Dynamics*. Immunity, 2016. 45(3): p. 471-482.
44. Victora, G.D. and M.C. Nussenzweig, *Germinal centers*. Annu Rev Immunol, 2012. 30: p. 429-57.

45. Pieper, K., B. Grimbacher, and H. Eibel, *B-cell biology and development*. J Allergy Clin Immunol, 2013. 131(4): p. 959-71.
46. Zhang, Y., L. Garcia-Ibanez, and K.M. Toellner, *Regulation of germinal center B-cell differentiation*. Immunol Rev, 2016. 270(1): p. 8-19.
47. Suan, D., C. Sundling, and R. Brink, *Plasma cell and memory B cell differentiation from the germinal center*. Curr Opin Immunol, 2017. 45: p. 97-102.
48. Shapiro-Shelef, M. and K. Calame, *Regulation of plasma-cell development*. Nat Rev Immunol, 2005. 5(3): p. 230-42.
49. Nutt, S.L., et al., *The generation of antibody-secreting plasma cells*. Nat Rev Immunol, 2015. 15(3): p. 160-71.
50. Kurosaki, T., K. Kometani, and W. Ise, *Memory B cells*. Nat Rev Immunol, 2015. 15(3): p. 149-59.
51. Ahmed, R. and D. Gray, *Immunological memory and protective immunity: understanding their relation*. Science, 1996. 272(5258): p. 54-60.
52. Akkaya, M., K. Kwak, and S.K. Pierce, *B cell memory: building two walls of protection against pathogens*. Nat Rev Immunol, 2020. 20(4): p. 229-238.
53. Tedder, T.F., *B10 cells: a functionally defined regulatory B cell subset*. J Immunol, 2015. 194(4): p. 1395-401.
54. Lykken, J.M., K.M. Candando, and T.F. Tedder, *Regulatory B10 cell development and function*. Int Immunol, 2015. 27(10): p. 471-7.
55. Wang, L., Y. Fu, and Y. Chu, *Regulatory B Cells*. Adv Exp Med Biol, 2020. 1254: p. 87-103.
56. Kalampokis, I., A. Yoshizaki, and T.F. Tedder, *IL-10-producing regulatory B cells (B10 cells) in autoimmune disease*. Arthritis Res Ther, 2013. 15 Suppl 1(1): p. S1.
57. Bartram, C.R. and E. Kleihauer, *[Molecular mechanisms of antibody synthesis]*. Monatsschr Kinderheilkd, 1984. 132(10): p. 765-73.
58. Hwang, J.K., F.W. Alt, and L.S. Yeap, *Related Mechanisms of Antibody Somatic Hypermutation and Class Switch Recombination*. Microbiol Spectr, 2015. 3(1): p. MDNA3-0037-2014.
59. Di Noia, J.M. and M.S. Neuberger, *Molecular mechanisms of antibody somatic hypermutation*. Annu Rev Biochem, 2007. 76: p. 1-22.
60. Schatz, D.G. and Y. Ji, *Recombination centres and the orchestration of V(D)J recombination*. Nat Rev Immunol, 2011. 11(4): p. 251-63.
61. Chiu, M.L., et al., *Antibody Structure and Function: The Basis for Engineering Therapeutics*. Antibodies (Basel), 2019. 8(4): p. 55.
62. Tonegawa, S., *Somatic generation of antibody diversity*. Nature, 1983. 302(5909): p. 575-81.
63. Roth, D.B., *V(D)J Recombination: Mechanism, Errors, and Fidelity*. Microbiol Spectr, 2014. 2(6): p. 10.1128/microbiolspec.MDNA3-0041-2014.
64. Oettinger, M.A., et al., *RAG-1 and RAG-2, adjacent genes that synergistically activate V(D)J recombination*. Science, 1990. 248(4962): p. 1517-23.
65. Backhaus, O., *Generation of Antibody Diversity*. 2018.
66. Taussig, M.J., *Molecular genetics of immunoglobulins*. Immunol Suppl, 1988. 1: p. 7-15.
67. Xu, Z., et al., *Immunoglobulin class-switch DNA recombination: induction, targeting and beyond*. Nat Rev Immunol, 2012. 12(7): p. 517-31.

68. Chen, Z. and J.H. Wang, *Signaling control of antibody isotype switching*. *Adv Immunol*, 2019. 141: p. 105-164.
69. Pilzecker, B. and H. Jacobs, *Mutating for Good: DNA Damage Responses During Somatic Hypermutation*. *Front Immunol*, 2019. 10: p. 438.
70. Methot, S.P. and J.M. Di Noia, *Chapter Two - Molecular Mechanisms of Somatic Hypermutation and Class Switch Recombination*, in *Advances in Immunology*, F.W. Alt, Editor. 2017, Academic Press. p. 37-87.
71. Schroeder, H.W., Jr. and L. Cavacini, *Structure and function of immunoglobulins*. *J Allergy Clin Immunol*, 2010. 125(2 Suppl 2): p. S41-52.
72. Roco, J.A., et al., *Class-Switch Recombination Occurs Infrequently in Germinal Centers*. *Immunity*, 2019. 51(2): p. 337-350 e7.
73. Leeman-Neill, R.J., J. Lim, and U. Basu, *The Common Key to Class-Switch Recombination and Somatic Hypermutation: Discovery of AID and Its Role in Antibody Gene Diversification*. *J Immunol*, 2018. 201(9): p. 2527-2529.
74. Stavnezer, J. and C.E. Schrader, *IgH chain class switch recombination: mechanism and regulation*. *J Immunol*, 2014. 193(11): p. 5370-8.
75. Senger, K., et al., *Antibody Isotype Switching in Vertebrates*. *Results Probl Cell Differ*, 2015. 57: p. 295-324.
76. Liu, J., et al., *Role of the IgM Fc Receptor in Immunity and Tolerance*. *Front Immunol*, 2019. 10: p. 529.
77. Boes, M., *Role of natural and immune IgM antibodies in immune responses*. *Mol Immunol*, 2000. 37(18): p. 1141-9.
78. Weill, J.C. and C.A. Reynaud, *IgM memory B cells: specific effectors of innate-like and adaptive responses*. *Curr Opin Immunol*, 2020. 63: p. 1-6.
79. Lux, A., et al., *The pro and anti-inflammatory activities of immunoglobulin G*. *Ann Rheum Dis*, 2010. 69 Suppl 1: p. i92-96.
80. Woof, J.M. and M.A. Kerr, *The function of immunoglobulin A in immunity*. *J Pathol*, 2006. 208(2): p. 270-82.
81. Berbers, R.M., I.A. Franken, and H.L. Leavis, *Immunoglobulin A and microbiota in primary immunodeficiency diseases*. *Curr Opin Allergy Clin Immunol*, 2019. 19(6): p. 563-570.
82. Feller, L., et al., *Oral mucosal immunity*. *Oral Surg Oral Med Oral Pathol Oral Radiol*, 2013. 116(5): p. 576-83.
83. Dunne-Castagna, V.P., D.A. Mills, and B. Lonnerdal, *Effects of Milk Secretory Immunoglobulin A on the Commensal Microbiota*. *Nestle Nutr Inst Workshop Ser*, 2020. 94: p. 158-168.
84. Ribatti, D., *The discovery of immunoglobulin E*. *Immunol Lett*, 2016. 171: p. 1-4.
85. Rath, N., N. Raje, and L. Rosenwasser, *Immunoglobulin E as a Biomarker in Asthma*. *Immunol Allergy Clin North Am*, 2018. 38(4): p. 587-597.
86. LoVerde, D., et al., *Anaphylaxis*. *Chest*, 2018. 153(2): p. 528-543.
87. Gutzeit, C., K. Chen, and A. Cerutti, *The enigmatic function of IgD: some answers at last*. *Eur J Immunol*, 2018. 48(7): p. 1101-1113.
88. Boudreau, C.M. and G. Alter, *Extra-Neutralizing FcR-Mediated Antibody Functions for a Universal Influenza Vaccine*. *Front Immunol*, 2019. 10: p. 440.
89. Borish, L.C. and J.W. Steinke, *2. Cytokines and chemokines*. *J Allergy Clin Immunol*, 2003. 111(2 Suppl): p. S460-75.

90. Dinarello, C.A., *Historical insights into cytokines*. Eur J Immunol, 2007. 37 Suppl 1(Suppl 1): p. S34-45.
91. Toomer, K.H. and T.R. Malek, *Cytokine Signaling in the Development and Homeostasis of Regulatory T cells*. Cold Spring Harb Perspect Biol, 2018. 10(3).
92. Opal, S.M. and V.A. DePalo, *Anti-inflammatory cytokines*. Chest, 2000. 117(4): p. 1162-72.
93. Becher, B., S. Spath, and J. Goverman, *Cytokine networks in neuroinflammation*. Nat Rev Immunol, 2017. 17(1): p. 49-59.
94. Schreiber, G. and M.R. Walter, *Cytokine-receptor interactions as drug targets*. Curr Opin Chem Biol, 2010. 14(4): p. 511-9.
95. Monaco, C., et al., *Anti-TNF therapy: past, present and future*. Int Immunol, 2015. 27(1): p. 55-62.
96. Thukral, C., A. Cheifetz, and M.A. Peppercorn, *Anti-tumour necrosis factor therapy for ulcerative colitis: evidence to date*. Drugs, 2006. 66(16): p. 2059-65.
97. Yost, J. and J.E. Gudjonsson, *The role of TNF inhibitors in psoriasis therapy: new implications for associated comorbidities*. F1000 Med Rep, 2009. 1: p. 30.
98. Savage, K.T., et al., *TNF-alpha inhibitors in the treatment of hidradenitis suppurativa*. Ther Adv Chronic Dis, 2019. 10: p. 2040622319851640.
99. Silfvast-Kaiser, A., S.Y. Paek, and A. Menter, *Anti-IL17 therapies for psoriasis*. Expert Opin Biol Ther, 2019. 19(1): p. 45-54.
100. Wang, E.A., et al., *Targeting IL-17 in psoriatic arthritis*. Eur J Rheumatol, 2017. 4(4): p. 272-277.
101. Garcia-Montoya, L. and H. Marzo-Ortega, *The role of secukinumab in the treatment of psoriatic arthritis and ankylosing spondylitis*. Ther Adv Musculoskelet Dis, 2018. 10(9): p. 169-180.
102. Rodriguez, R.M., A. Lopez-Vazquez, and C. Lopez-Larrea, *Immune systems evolution*. Adv Exp Med Biol, 2012. 739: p. 237-51.
103. Dominguez-Andres, J. and M.G. Netea, *Impact of Historic Migrations and Evolutionary Processes on Human Immunity*. Trends Immunol, 2019. 40(12): p. 1105-1119.
104. Perry, R.D. and J.D. Fetherston, *Yersinia pestis--etiologic agent of plague*. Clin Microbiol Rev, 1997. 10(1): p. 35-66.
105. Benedictow, O.J., *The black death - The greatest catastrophe ever*. History Today, 2005. 55(3): p. 42-49.
106. Henry, J.P., *[Genetics and origin of Homo sapiens]*. Med Sci (Paris), 2019. 35(1): p. 39-45.
107. Sankararaman, S., et al., *The genomic landscape of Neanderthal ancestry in present-day humans*. Nature, 2014. 507(7492): p. 354-7.
108. Dannemann, M., A.M. Andres, and J. Kelso, *Introgression of Neandertal- and Denisovan-like Haplotypes Contributes to Adaptive Variation in Human Toll-like Receptors*. Am J Hum Genet, 2016. 98(1): p. 22-33.
109. Abi-Rached, L., et al., *The Shaping of Modern Human Immune Systems by Multiregional Admixture with Archaic Humans*. Science, 2011. 334(6052): p. 89-94.
110. Shiina, T., et al., *The HLA genomic loci map: expression, interaction, diversity and disease*. J Hum Genet, 2009. 54(1): p. 15-39.

111. Mendez, F.L., J.C. Watkins, and M.F. Hammer, *A Haplotype at STAT2 Introgressed from Neanderthals and Serves as a Candidate of Positive Selection in Papua New Guinea*. *American Journal of Human Genetics*, 2012. 91(2): p. 265-274.
112. Quach, H. and L. Quintana-Murci, *Living in an adaptive world: Genomic dissection of the genus Homo and its immune response*. *J Exp Med*, 2017. 214(4): p. 877-894.
113. Okada, H., et al., *The 'hygiene hypothesis' for autoimmune and allergic diseases: an update*. *Clin Exp Immunol*, 2010. 160(1): p. 1-9.
114. van Tilburg Bernardes, E. and M.C. Arrieta, *Hygiene Hypothesis in Asthma Development: Is Hygiene to Blame?* *Arch Med Res*, 2017. 48(8): p. 717-726.
115. Alexandre-Silva, G.M., et al., *The hygiene hypothesis at a glance: Early exposures, immune mechanism and novel therapies*. *Acta Trop*, 2018. 188: p. 16-26.
116. Lerner, A., P. Jeremias, and T. Matthias, *The World Incidence and Prevalence of Autoimmune Diseases is Increasing*. *International Journal of Celiac Disease*, 2016. 3(4): p. 151-155.
117. Wasko, N.J., F. Nichols, and R.B. Clark, *Multiple sclerosis, the microbiome, TLR2, and the hygiene hypothesis*. *Autoimmun Rev*, 2020. 19(1): p. 102430.
118. Leong, R.W., N. Mitrev, and Y. Ko, *Hygiene Hypothesis: Is the Evidence the Same All Over the World?* *Dig Dis*, 2016. 34(1-2): p. 35-42.
119. Bach, J.F., *The hygiene hypothesis in autoimmunity: the role of pathogens and commensals*. *Nat Rev Immunol*, 2018. 18(2): p. 105-120.
120. Shu, S.A., et al., *Microbiota and Food Allergy*. *Clin Rev Allergy Immunol*, 2019. 57(1): p. 83-97.
121. Taneja, V., *Arthritis susceptibility and the gut microbiome*. *FEBS Lett*, 2014. 588(22): p. 4244-9.
122. Rojas, M., et al., *Molecular mimicry and autoimmunity*. *J Autoimmun*, 2018. 95: p. 100-123.
123. Cusick, M.F., J.E. Libbey, and R.S. Fujinami, *Molecular mimicry as a mechanism of autoimmune disease*. *Clin Rev Allergy Immunol*, 2012. 42(1): p. 102-11.
124. Rose, N.R., *Negative selection, epitope mimicry and autoimmunity*. *Curr Opin Immunol*, 2017. 49: p. 51-55.
125. Cunningham, M.W., *Molecular Mimicry, Autoimmunity, and Infection: The Cross-Reactive Antigens of Group A Streptococci and their Sequelae*. *Microbiol Spectr*, 2019. 7(4).
126. Qiu, C.C., R. Caricchio, and S. Gallucci, *Triggers of Autoimmunity: The Role of Bacterial Infections in the Extracellular Exposure of Lupus Nuclear Autoantigens*. *Front Immunol*, 2019. 10: p. 2608.
127. Hsieh, A.H., et al., *Human cytomegalovirus pp65 peptide-induced autoantibodies cross-reacts with TAF9 protein and induces lupus-like autoimmunity in BALB/c mice*. *Sci Rep*, 2020. 10(1): p. 9662.
128. Trela, M., P.N. Nelson, and P.B. Rylance, *The role of molecular mimicry and other factors in the association of Human Endogenous Retroviruses and autoimmunity*. *APMIS*, 2016. 124(1-2): p. 88-104.
129. Powell, A.M. and M.M. Black, *Epitope spreading: protection from pathogens, but propagation of autoimmunity?* *Clin Exp Dermatol*, 2001. 26(5): p. 427-33.

130. Thrasyvoulides, A. and P. Lymberi, *Evidence for intramolecular B-cell epitope spreading during experimental immunization with an immunogenic thyroglobulin peptide*. Clin Exp Immunol, 2003. 132(3): p. 401-7.
131. Chan, L.S., et al., *Epitope spreading: lessons from autoimmune skin diseases*. J Invest Dermatol, 1998. 110(2): p. 103-9.
132. Vanderlugt, C.L. and S.D. Miller, *Epitope spreading in immune-mediated diseases: implications for immunotherapy*. Nat Rev Immunol, 2002. 2(2): p. 85-95.
133. Vanderlugt, C.J. and S.D. Miller, *Epitope spreading*. Curr Opin Immunol, 1996. 8(6): p. 831-6.
134. Tuohy, V.K. and R.P. Kinkel, *Epitope Spreading: A Mechanism for Progression of Autoimmune Disease*, in *Autoimmunity*, A. Górski, H. Krotkiewski, and M. Zimecki, Editors. 2001, Springer Netherlands: Dordrecht. p. 39-48.
135. Cornaby, C., et al., *B cell epitope spreading: mechanisms and contribution to autoimmune diseases*. Immunol Lett, 2015. 163(1): p. 56-68.
136. Miller, S.D. and T.N. Eagar, *Functional role of epitope spreading in the chronic pathogenesis of autoimmune and virus-induced demyelinating diseases*. Adv Exp Med Biol, 2001. 490: p. 99-107.
137. Holmgren, A.M., C.A. McConkey, and S. Shin, *Outrunning the Red Queen: bystander activation as a means of outpacing innate immune subversion by intracellular pathogens*. Cell Mol Immunol, 2017. 14(1): p. 14-21.
138. Pacheco, Y., et al., *Bystander activation and autoimmunity*. J Autoimmun, 2019. 103: p. 102301.
139. Fujinami, R.S., et al., *Molecular mimicry, bystander activation, or viral persistence: infections and autoimmune disease*. Clin Microbiol Rev, 2006. 19(1): p. 80-94.
140. Kim, T.S. and E.C. Shin, *The activation of bystander CD8(+) T cells and their roles in viral infection*. Exp Mol Med, 2019. 51(12): p. 1-9.
141. Lardo, S., et al., *The Autoimmune Mechanism in Dengue Hemorrhagic Fever*. Acta Med Indones, 2018. 50(1): p. 70-79.
142. Kim, J., et al., *Innate-like Cytotoxic Function of Bystander-Activated CD8(+) T Cells Is Associated with Liver Injury in Acute Hepatitis A*. Immunity, 2018. 48(1): p. 161-173 e5.
143. Euler, M. and M.H. Hoffmann, *The double-edged role of neutrophil extracellular traps in inflammation*. Biochem Soc Trans, 2019. 47(6): p. 1921-1930.
144. Cheng, M. and M.S. Anderson, *Thymic tolerance as a key brake on autoimmunity*. Nat Immunol, 2018. 19(7): p. 659-664.
145. Klein, L., E.A. Robey, and C.S. Hsieh, *Central CD4(+) T cell tolerance: deletion versus regulatory T cell differentiation*. Nat Rev Immunol, 2019. 19(1): p. 7-18.
146. Schwartz, R.H., *T cell anergy*. Annu Rev Immunol, 2003. 21: p. 305-34.
147. Kalekar, L.A., et al., *CD4(+) T cell anergy prevents autoimmunity and generates regulatory T cell precursors*. Nat Immunol, 2016. 17(3): p. 304-14.
148. Green, D.R., N. Droin, and M. Pinkoski, *Activation-induced cell death in T cells*. Immunol Rev, 2003. 193: p. 70-81.
149. Khan, U. and H. Ghazanfar, *T Lymphocytes and Autoimmunity*. Int Rev Cell Mol Biol, 2018. 341: p. 125-168.
150. Xing, Y. and K.A. Hogquist, *T-cell tolerance: central and peripheral*. Cold Spring Harb Perspect Biol, 2012. 4(6).

151. Nemazee, D., *Mechanisms of central tolerance for B cells*. Nat Rev Immunol, 2017. 17(5): p. 281-294.
152. Tobón, G.J., J.H. Izquierdo, and C.A. Cañas, *B Lymphocytes: Development, Tolerance, and Their Role in Autoimmunity—Focus on Systemic Lupus Erythematosus*. Autoimmune Diseases, 2013. 2013: p. 827254.
153. Yarkoni, Y., A. Getahun, and J.C. Cambier, *Molecular underpinning of B-cell anergy*. Immunol Rev, 2010. 237(1): p. 249-63.
154. Gauld, S.B., et al., *Maintenance of B cell anergy requires constant antigen receptor occupancy and signaling*. Nat Immunol, 2005. 6(11): p. 1160-7.
155. Fulcher, D.A., et al., *The fate of self-reactive B cells depends primarily on the degree of antigen receptor engagement and availability of T cell help*. J Exp Med, 1996. 183(5): p. 2313-28.
156. Tsubata, T., *B-cell tolerance and autoimmunity*. F1000Res, 2017. 6: p. 391.
157. van de Veen, W., et al., *Role of regulatory B cells in immune tolerance to allergens and beyond*. J Allergy Clin Immunol, 2016. 138(3): p. 654-665.
158. Avrameas, S., *Natural autoantibodies: from 'horror autotoxicus' to 'gnothi seauton'*. Immunol Today, 1991. 12(5): p. 154-9.
159. Ehrlich, P., *Verh Ges Dtsch Naturforsch*. 1902.
160. Nakamura, R.M. and E.M. Tan, *Recent progress in the study of autoantibodies to nuclear antigens*. Hum Pathol, 1978. 9(1): p. 85-91.
161. Routsias, J.G., P.G. Vlachoyiannopoulos, and A.G. Tzioufas, *Autoantibodies to intracellular autoantigens and their B-cell epitopes: molecular probes to study the autoimmune response*. Crit Rev Clin Lab Sci, 2006. 43(3): p. 203-48.
162. Tan, E.M., *Autoantibodies, autoimmune disease, and the birth of immune diagnostics*. J Clin Invest, 2012. 122(11): p. 3835-6.
163. Burbelo, P.D., J. Keller, and J.B. Kopp, *New horizons for human pathogenic autoantibodies*. Discov Med, 2015. 20(108): p. 17-25.
164. Wenzel, J., et al., *Antibodies targeting extractable nuclear antigens: historical development and current knowledge*. Br J Dermatol, 2001. 145(6): p. 859-67.
165. Cozzani, E., et al., *Serology of Lupus Erythematosus: Correlation between Immunopathological Features and Clinical Aspects*. Autoimmune Dis, 2014. 2014: p. 321359.
166. Scherer, H.U., T. Haupl, and G.R. Burmester, *The etiology of rheumatoid arthritis*. J Autoimmun, 2020. 110: p. 102400.
167. Derksen, V., T.W.J. Huizinga, and D. van der Woude, *The role of autoantibodies in the pathophysiology of rheumatoid arthritis*. Semin Immunopathol, 2017. 39(4): p. 437-446.
168. Pruss, H. and K. Kirmse, *Pathogenic role of autoantibodies against inhibitory synapses*. Brain Res, 2018. 1701: p. 146-152.
169. Choi, M.Y. and M.J. Fritzler, *Progress in understanding the diagnostic and pathogenic role of autoantibodies associated with systemic sclerosis*. Curr Opin Rheumatol, 2016. 28(6): p. 586-94.
170. McAdoo, S.P. and C.D. Pusey, *Antiglomerular Basement Membrane Disease*. Semin Respir Crit Care Med, 2018. 39(4): p. 494-503.

171. Silverman, G.J., *Protective natural autoantibodies to apoptotic cells: evidence of convergent selection of recurrent innate-like clones*. Ann N Y Acad Sci, 2015. 1362(1): p. 164-75.
172. Witte, T., *IgM antibodies against dsDNA in SLE*. Clin Rev Allergy Immunol, 2008. 34(3): p. 345-7.
173. Werwitzke, S., et al., *Inhibition of lupus disease by anti-double-stranded DNA antibodies of the IgM isotype in the (NZB x NZW)F1 mouse*. Arthritis Rheum, 2005. 52(11): p. 3629-38.
174. Rodkey, L.S., *Autoregulation of immune responses via idiotype network interactions*. Microbiol Rev, 1980. 44(4): p. 631-59.
175. Hampe, C.S., *Protective role of anti-idiotypic antibodies in autoimmunity--lessons for type 1 diabetes*. Autoimmunity, 2012. 45(4): p. 320-31.
176. Witte, T., et al., *Rheumatoid factors in systemic lupus erythematosus: association with clinical and laboratory parameters*. SLE study group. Rheumatol Int, 2000. 19(3): p. 107-11.
177. Shoenfeld, Y. and E. Toubi, *Protective autoantibodies: role in homeostasis, clinical importance, and therapeutic potential*. Arthritis Rheum, 2005. 52(9): p. 2599-606.
178. Toubi, E. and Y. Shoenfeld, *Protective autoimmunity in cancer (review)*. Oncol Rep, 2007. 17(1): p. 245-51.
179. Coutinho, A., M.D. Kazatchkine, and S. Avrameas, *Natural autoantibodies*. Curr Opin Immunol, 1995. 7(6): p. 812-8.
180. Mannoor, K., Y. Xu, and C. Chen, *Natural autoantibodies and associated B cells in immunity and autoimmunity*. Autoimmunity, 2013. 46(2): p. 138-47.
181. Dighiero, G., *Natural autoantibodies, tolerance, and autoimmunity*. Ann N Y Acad Sci, 1997. 815: p. 182-92.
182. Tomer, Y. and Y. Shoenfeld, *The significance of natural autoantibodies*. Immunol Invest, 1988. 17(5): p. 389-424.
183. Lacroix-Desmazes, S., et al., *Self-reactive antibodies (natural autoantibodies) in healthy individuals*. J Immunol Methods, 1998. 216(1-2): p. 117-37.
184. Avrameas, S., H. Alexopoulos, and H.M. Moutsopoulos, *Natural Autoantibodies: An Undersign Hero of the Immune System and Autoimmune Disorders-A Point of View*. Front Immunol, 2018. 9: p. 1320.
185. Elkon, K. and P. Casali, *Nature and functions of autoantibodies*. Nat Clin Pract Rheumatol, 2008. 4(9): p. 491-8.
186. Avrameas, S. and C. Selmi, *Natural autoantibodies in the physiology and pathophysiology of the immune system*. J Autoimmun, 2013. 41: p. 46-9.
187. Lobo, P.I., *Role of Natural IgM Autoantibodies (IgM-NAA) and IgM Anti-Leukocyte Antibodies (IgM-ALA) in Regulating Inflammation*. Curr Top Microbiol Immunol, 2017. 408: p. 89-117.
188. Meager, A., *Natural autoantibodies to interferons*. J Interferon Cytokine Res, 1997. 17 Suppl 1: p. S51-3.
189. Gronwall, C. and G.J. Silverman, *Natural IgM: beneficial autoantibodies for the control of inflammatory and autoimmune disease*. J Clin Immunol, 2014. 34 Suppl 1(0 1): p. S12-21.

190. Silverman, G.J., J. Vas, and C. Gronwall, *Protective autoantibodies in the rheumatic diseases: lessons for therapy*. Nat Rev Rheumatol, 2013. 9(5): p. 291-300.
191. Binder, C.J., et al., *The role of natural antibodies in atherogenesis*. J Lipid Res, 2005. 46(7): p. 1353-63.
192. Califf, R.M., *Biomarker definitions and their applications*. Exp Biol Med (Maywood), 2018. 243(3): p. 213-221.
193. Antoniou, M., A.L. Jorgensen, and R. Kolamunnage-Dona, *Biomarker-Guided Adaptive Trial Designs in Phase II and Phase III: A Methodological Review*. PLoS One, 2016. 11(2): p. e0149803.
194. Strimbu, K. and J.A. Tavel, *What are biomarkers?* Curr Opin HIV AIDS, 2010. 5(6): p. 463-6.
195. Hayes, D.F., *Biomarker validation and testing*. Mol Oncol, 2015. 9(5): p. 960-6.
196. Rifai, N., M.A. Gillette, and S.A. Carr, *Protein biomarker discovery and validation: the long and uncertain path to clinical utility*. Nat Biotechnol, 2006. 24(8): p. 971-83.
197. Allinson, J.L., *Clinical biomarker validation*. Bioanalysis, 2018. 10(12): p. 957-968.
198. Morgan, S., et al., *The cost of drug development: a systematic review*. Health Policy, 2011. 100(1): p. 4-17.
199. Van Norman, G.A., *Drugs, Devices, and the FDA: Part 1: An Overview of Approval Processes for Drugs*. JACC Basic Transl Sci, 2016. 1(3): p. 170-179.
200. Moore, T.J., et al., *Variation in the estimated costs of pivotal clinical benefit trials supporting the US approval of new therapeutic agents, 2015-2017: a cross-sectional study*. BMJ Open, 2020. 10(6): p. e038863.
201. Camilleri, M. and W.J. Tremaine, *Governance of clinical research*. Am J Gastroenterol, 2012. 107(3): p. 336-8.
202. DiMasi, J.A., H.G. Grabowski, and R.W. Hansen, *Innovation in the pharmaceutical industry: New estimates of R&D costs*. J Health Econ, 2016. 47: p. 20-33.
203. Hughes, J.P., et al., *Principles of early drug discovery*. Br J Pharmacol, 2011. 162(6): p. 1239-49.
204. Steinmetz, K.L. and E.G. Spack, *The basics of preclinical drug development for neurodegenerative disease indications*. BMC Neurol, 2009. 9 Suppl 1(Suppl 1): p. S2.
205. Muglia, J.J. and J.J. DiGiovanna, *Phase 1 clinical trials*. J Cutan Med Surg, 1998. 2(4): p. 236-41.
206. Salzberg, M., *First-in-Human Phase 1 Studies in Oncology: The New Challenge for Investigative Sites*. Rambam Maimonides Med J, 2012. 3(2): p. e0007.
207. Blass, B.E., *Chapter 9 - Basics of Clinical Trials*, in *Basic Principles of Drug Discovery and Development*, B.E. Blass, Editor. 2015, Academic Press: Boston. p. 383-413.
208. Curran, D., R.J. Sylvester, and G. Hoctin Boes, *Sample size estimation in phase III cancer clinical trials*. Eur J Surg Oncol, 1999. 25(3): p. 244-50.
209. Buyse, M., *Phase III design: principles*. Chin Clin Oncol, 2016. 5(1): p. 10.
210. Nell, G.K.H., *Chapter 24 - Phase IV Studies and Lifecycle Management*, in *Pharmaceutical Medicine and Translational Clinical Research*, D. Vohora and G. Singh, Editors. 2018, Academic Press: Boston. p. 383-391.

211. Mohs, R.C. and N.H. Greig, *Drug discovery and development: Role of basic biological research*. *Alzheimers Dement* (N Y), 2017. 3(4): p. 651-657.
212. May, M., *Clinical trial costs go under the microscope*. *Nature Medicine*, 2019.
213. Adashek, J.J., et al., *Phase I trials as valid therapeutic options for patients with cancer*. *Nat Rev Clin Oncol*, 2019. 16(12): p. 773-778.
214. Manji, A., et al., *Evolution of clinical trial design in early drug development: systematic review of expansion cohort use in single-agent phase I cancer trials*. *J Clin Oncol*, 2013. 31(33): p. 4260-7.
215. Cummings, J.L., *Optimizing phase II of drug development for disease-modifying compounds*. *Alzheimers Dement*, 2008. 4(1 Suppl 1): p. S15-20.
216. Van Norman, G.A., *Phase II Trials in Drug Development and Adaptive Trial Design*. *JACC Basic Transl Sci*, 2019. 4(3): p. 428-437.
217. Kalia, M., *Biomarkers for personalized oncology: recent advances and future challenges*. *Metabolism*, 2015. 64(3 Suppl 1): p. S16-21.
218. Onuora, S., *Rheumatoid arthritis: RF levels predict RA risk in the general population*. *Nat Rev Rheumatol*, 2012. 8(10): p. 562.
219. Braschi, E., K. Shojania, and G.M. Allan, *Anti-CCP: a truly helpful rheumatoid arthritis test? Can Fam Physician*, 2016. 62(3): p. 234.
220. Conigliaro, P., et al., *Autoantibodies in inflammatory arthritis*. *Autoimmun Rev*, 2016. 15(7): p. 673-83.
221. Ingegnoli, F., R. Castelli, and R. Gualtierotti, *Rheumatoid factors: clinical applications*. *Dis Markers*, 2013. 35(6): p. 727-34.
222. Atzeni, F., et al., *Biomarkers in Rheumatoid Arthritis*. *Isr Med Assoc J*, 2017. 19(8): p. 512-516.
223. Kokkonen, H., et al., *Antibodies of IgG, IgA and IgM isotypes against cyclic citrullinated peptide precede the development of rheumatoid arthritis*. *Arthritis Res Ther*, 2011. 13(1): p. R13.
224. Iannone, F., et al., *Changes in anti-cyclic citrullinated peptide antibodies and rheumatoid factor isotypes serum levels in patients with rheumatoid arthritis following treatment with different biological drugs*. *Clin Exp Rheumatol*, 2016. 34(3): p. 424-9.
225. Sur, L.M., et al., *Antinuclear Antibodies: Marker of Diagnosis and Evolution in Autoimmune Diseases*. *Lab Med*, 2018. 49(3): p. e62-e73.
226. Stochmal, A., et al., *Antinuclear Antibodies in Systemic Sclerosis: an Update*. *Clin Rev Allergy Immunol*, 2020. 58(1): p. 40-51.
227. Stefanski, A.L., et al., *The Diagnosis and Treatment of Sjogren's Syndrome*. *Dtsch Arztebl Int*, 2017. 114(20): p. 354-361.
228. Pisetsky, D.S., *Antinuclear antibody testing - misunderstood or misbegotten?* *Nat Rev Rheumatol*, 2017. 13(8): p. 495-502.
229. Pisetsky, D.S., *Antinuclear antibodies in rheumatic disease: a proposal for a function-based classification*. *Scand J Immunol*, 2012. 76(3): p. 223-8.
230. Pisetsky, D.S., B.H. Rovin, and P.E. Lipsky, *New Perspectives in Rheumatology: Biomarkers as Entry Criteria for Clinical Trials of New Therapies for Systemic Lupus Erythematosus: The Example of Antinuclear Antibodies and Anti-DNA*. *Arthritis Rheumatol*, 2017. 69(3): p. 487-493.

231. Dema, B. and N. Charles, *Autoantibodies in SLE: Specificities, Isotypes and Receptors*. Antibodies (Basel), 2016. 5(1).
232. Goeb, V., et al., *Clinical significance of autoantibodies recognizing Sjogren's syndrome A (SSA), SSB, calpastatin and alpha-fodrin in primary Sjogren's syndrome*. Clin Exp Immunol, 2007. 148(2): p. 281-7.
233. Brito-Zeron, P., et al., *Sjogren syndrome*. Nat Rev Dis Primers, 2016. 2: p. 16047.
234. Fayyaz, A., B.T. Kurien, and R.H. Scofield, *Autoantibodies in Sjogren's Syndrome*. Rheum Dis Clin North Am, 2016. 42(3): p. 419-34.
235. Baldini, C., et al., *Biomarkers for Sjogren's syndrome*. Biomark Med, 2018. 12(3): p. 275-286.
236. Pasoto, S.G., V. Adriano de Oliveira Martins, and E. Bonfa, *Sjogren's syndrome and systemic lupus erythematosus: links and risks*. Open Access Rheumatol, 2019. 11: p. 33-45.
237. Yokogawa, N., et al., *Neonatal lupus erythematosus*. Nihon Rinsho Meneki Gakkai Kaishi, 2017. 40(2): p. 124-130.
238. Izmirly, P.M., et al., *Clinical and pathologic implications of extending the spectrum of maternal autoantibodies reactive with ribonucleoproteins associated with cutaneous and now cardiac neonatal lupus from SSA/Ro and SSB/La to U1RNP*. Autoimmun Rev, 2017. 16(9): p. 980-983.
239. Zuppa, A.A., et al., *Neonatal lupus: Follow-up in infants with anti-SSA/Ro antibodies and review of the literature*. Autoimmun Rev, 2017. 16(4): p. 427-432.
240. Migliorini, P., et al., *Anti-Sm and anti-RNP antibodies*. Autoimmunity, 2005. 38(1): p. 47-54.
241. Abbara, S., et al., *Anti-RNP positivity in primary Sjogren's syndrome is associated with a more active disease and a more frequent muscular and pulmonary involvement*. RMD Open, 2019. 5(2): p. e001033.
242. Reeves, W., M. Satoh, and H. Richards, *Origins of antinuclear antibodies*. 2004. p. 401-431.
243. Wang, X. and Y. Xia, *Anti-double Stranded DNA Antibodies: Origin, Pathogenicity, and Targeted Therapies*. Front Immunol, 2019. 10: p. 1667.
244. Choi, Y., et al., *Neutrophil Extracellular DNA Traps Induce Autoantigen Production by Airway Epithelial Cells*. Mediators Inflamm, 2017. 2017: p. 5675029.
245. Colonna, L., C. Lood, and K.B. Elkon, *Beyond apoptosis in lupus*. Curr Opin Rheumatol, 2014. 26(5): p. 459-66.
246. Cho-Chung, Y.S., *Autoantibody biomarkers in the detection of cancer*. Biochim Biophys Acta, 2006. 1762(6): p. 587-91.
247. Dudas, S.P., M. Chatterjee, and M.A. Tainsky, *Usage of cancer associated autoantibodies in the detection of disease*. Cancer Biomark, 2010. 6(5-6): p. 257-70.
248. Qiu, J., et al., *Autoantibodies as Potential Biomarkers in Breast Cancer*. Biosensors (Basel), 2018. 8(3).
249. Rauf, F., K.S. Anderson, and J. LaBaer, *Autoantibodies in Early Detection of Breast Cancer*. Cancer Epidemiol Biomarkers Prev, 2020. 29(12): p. 2475-2485.
250. Yang, B., et al., *Autoantibodies as diagnostic biomarkers for lung cancer: A systematic review*. Cell Death Discov, 2019. 5(1): p. 126.

251. Tang, Z.M., et al., *Serum tumor-associated autoantibodies as diagnostic biomarkers for lung cancer: A systematic review and meta-analysis*. PLoS One, 2017. 12(7): p. e0182117.
252. Bassaro, L., et al., *Screening for Multiple Autoantibodies in Plasma of Patients with Breast Cancer*. Cancer Genomics Proteomics, 2017. 14(6): p. 427-435.
253. Pei, L., et al., *Discovering novel lung cancer associated antigens and the utilization of their autoantibodies in detection of lung cancer*. Immunobiology, 2020. 225(2): p. 151891.
254. Huang, H., et al., *The diagnostic efficiency of seven autoantibodies in lung cancer*. Eur J Cancer Prev, 2020. 29(4): p. 315-320.
255. Chen, M., et al., *Development of a panel of serum IgG and IgA autoantibodies for early diagnosis of colon cancer*. Int J Med Sci, 2020. 17(17): p. 2744-2750.
256. Nesterova, M., et al., *Autoantibody biomarker opens a new gateway for cancer diagnosis*. Biochim Biophys Acta, 2006. 1762(4): p. 398-403.
257. Yadav, S., et al., *Autoantibodies as diagnostic and prognostic cancer biomarker: Detection techniques and approaches*. Biosens Bioelectron, 2019. 139: p. 111315.
258. Macdonald, I.K., C.B. Parsy-Kowalska, and C.J. Chapman, *Autoantibodies: Opportunities for Early Cancer Detection*. Trends Cancer, 2017. 3(3): p. 198-213.
259. Chapman, C., et al., *Autoantibodies in breast cancer: their use as an aid to early diagnosis*. Ann Oncol, 2007. 18(5): p. 868-73.
260. DeMarshall, C., et al., *Utility of autoantibodies as biomarkers for diagnosis and staging of neurodegenerative diseases*. Int Rev Neurobiol, 2015. 122: p. 1-51.
261. Sabatino, J.J., Jr., A.K. Probstel, and S.S. Zamvil, *B cells in autoimmune and neurodegenerative central nervous system diseases*. Nat Rev Neurosci, 2019. 20(12): p. 728-745.
262. Neff, F., et al., *Immunotherapy and naturally occurring autoantibodies in neurodegenerative disorders*. Autoimmun Rev, 2008. 7(6): p. 501-7.
263. Albus, A., et al., *Encoding the Sequence of Specific Autoantibodies Against beta-Amyloid and alpha-Synuclein in Neurodegenerative Diseases*. Front Immunol, 2019. 10: p. 2033.
264. Roettger, Y., et al., *Prion peptide uptake in microglial cells--the effect of naturally occurring autoantibodies against prion protein*. PLoS One, 2013. 8(6): p. e67743.
265. Gold, M., et al., *Mechanisms of action of naturally occurring antibodies against beta-amyloid on microglia*. J Neuroinflammation, 2013. 10: p. 5.
266. De Virgilio, A., et al., *Parkinson's disease: Autoimmunity and neuroinflammation*. Autoimmun Rev, 2016. 15(10): p. 1005-11.
267. Tansey, M.G. and M. Romero-Ramos, *Immune system responses in Parkinson's disease: Early and dynamic*. Eur J Neurosci, 2019. 49(3): p. 364-383.
268. Wu, J. and L. Li, *Autoantibodies in Alzheimer's disease: potential biomarkers, pathogenic roles, and therapeutic implications*. J Biomed Res, 2016. 30(5): p. 361-372.
269. Colasanti, T., et al., *Autoantibodies in patients with Alzheimer's disease: pathogenetic role and potential use as biomarkers of disease progression*. Autoimmun Rev, 2010. 9(12): p. 807-11.
270. Cantini, F., et al., *Psoriatic arthritis: a systematic review*. Int J Rheum Dis, 2010. 13(4): p. 300-17.

271. Ocampo, D.V. and D. Gladman, *Psoriatic arthritis*. F1000Res, 2019. 8.
272. Scher, J.U., et al., *Preventing psoriatic arthritis: focusing on patients with psoriasis at increased risk of transition*. Nat Rev Rheumatol, 2019. 15(3): p. 153-166.
273. Generali, E., et al., *Biomarkers in psoriatic arthritis: a systematic literature review*. Expert Rev Clin Immunol, 2016. 12(6): p. 651-60.
274. Veale, D.J. and U. Fearon, *The pathogenesis of psoriatic arthritis*. Lancet, 2018. 391(10136): p. 2273-2284.
275. Coates, L.C. and P.S. Helliwell, *Psoriatic arthritis: state of the art review*. Clin Med (Lond), 2017. 17(1): p. 65-70.
276. Menter, A., *Psoriasis and psoriatic arthritis overview*. Am J Manag Care, 2016. 22(8 Suppl): p. s216-24.
277. McHugh, N.J., *Early Psoriatic Arthritis*. Rheum Dis Clin North Am, 2015. 41(4): p. 615-22.
278. Altomare, G. and F. Capsoni, *The diagnosis of early psoriatic arthritis*. G Ital Dermatol Venereol, 2013. 148(5): p. 501-4.
279. Napolitano, M., et al., *Psoriatic arthritis and psoriasis: differential diagnosis*. Clin Rheumatol, 2016. 35(8): p. 1893-1901.
280. Raychaudhuri, S.P., et al., *Management of psoriatic arthritis: Early diagnosis, monitoring of disease severity and cutting edge therapies*. J Autoimmun, 2017. 76: p. 21-37.
281. Menter, A., *Psoriasis and psoriatic arthritis treatment*. Am J Manag Care, 2016. 22(8 Suppl): p. s225-37.
282. Ogdie, A., L.C. Coates, and D.D. Gladman, *Treatment guidelines in psoriatic arthritis*. Rheumatology (Oxford), 2020. 59(Supplement_1): p. i37-i46.
283. American College of Rheumatology Committee to Reevaluate Improvement, C., *A proposed revision to the ACR20: the hybrid measure of American College of Rheumatology response*. Arthritis Rheum, 2007. 57(2): p. 193-202.
284. Schemoul, J., C. Poulain, and P. Claudepierre, *Treatment strategies for psoriatic arthritis*. Joint Bone Spine, 2018. 85(5): p. 537-544.
285. Singh, J.A., et al., *Special Article: 2018 American College of Rheumatology/National Psoriasis Foundation Guideline for the Treatment of Psoriatic Arthritis*. Arthritis Care Res (Hoboken), 2019. 71(1): p. 2-29.
286. Verheul, M.K., et al., *Biomarkers for rheumatoid and psoriatic arthritis*. Clin Immunol, 2015. 161(1): p. 2-10.
287. Pouw, J., et al., *Emerging molecular biomarkers for predicting therapy response in psoriatic arthritis: A review of literature*. Clin Immunol, 2020. 211: p. 108318.
288. Chandran, V. and J.U. Scher, *Biomarkers in psoriatic arthritis: recent progress*. Curr Rheumatol Rep, 2014. 16(11): p. 453.
289. Yuan, Y., et al., *Identification of Novel Autoantibodies Associated With Psoriatic Arthritis*. Arthritis Rheumatol, 2019. 71(6): p. 941-951.
290. Chimenti, M.S., et al., *Auto-reactions, autoimmunity and psoriatic arthritis*. Autoimmun Rev, 2015. 14(12): p. 1142-6.
291. Dolcino, M., et al., *Crossreactive autoantibodies directed against cutaneous and joint antigens are present in psoriatic arthritis*. PLoS One, 2014. 9(12): p. e115424.
292. Liu, Y., X. Liao, and G. Shi, *Autoantibodies in Spondyloarthritis, Focusing on Anti-CD74 Antibodies*. Front Immunol, 2019. 10: p. 5.

293. Baraliakos, X., et al., *High prevalence of anti-CD74 antibodies specific for the HLA class II-associated invariant chain peptide (CLIP) in patients with axial spondyloarthritis*. *Ann Rheum Dis*, 2014. 73(6): p. 1079-82.
294. Tahir, H., et al., *Secukinumab in Active Rheumatoid Arthritis after Anti-TNF α Therapy: A Randomized, Double-Blind Placebo-Controlled Phase 3 Study*. *Rheumatol Ther*, 2017. 4(2): p. 475-488.
295. Kavanaugh, A., et al., *Secukinumab for Long-Term Treatment of Psoriatic Arthritis: A Two-Year Followup From a Phase III, Randomized, Double-Blind Placebo-Controlled Study*. *Arthritis Care Res (Hoboken)*, 2017. 69(3): p. 347-355.
296. Mease, P., et al., *Secukinumab improves active psoriatic arthritis symptoms and inhibits radiographic progression: primary results from the randomised, double-blind, phase III FUTURE 5 study*. *Ann Rheum Dis*, 2018. 77(6): p. 890-897.
297. Yang, E.J., K.M. Beck, and W. Liao, *Secukinumab in the treatment of psoriasis: patient selection and perspectives*. *Psoriasis (Auckl)*, 2018. 8: p. 75-82.
298. Mease, P.J., et al., *Secukinumab Inhibition of Interleukin-17A in Patients with Psoriatic Arthritis*. *N Engl J Med*, 2015. 373(14): p. 1329-39.
299. Konthur, Z., et al., *Protein array screening reveals IgA autoantigenicity patterns predicting anti-TNF therapy response in rheumatoid arthritis patients*. *Annals of the Rheumatic Diseases*, 2011. 70(Suppl 2): p. A69-A70.
300. Felson, D.T., et al., *American College of Rheumatology. Preliminary definition of improvement in rheumatoid arthritis*. *Arthritis Rheum*, 1995. 38(6): p. 727-35.
301. Herrier, R.N., *Advances in the treatment of moderate-to-severe plaque psoriasis*. *Am J Health Syst Pharm*, 2011. 68(9): p. 795-806.
302. Herrera-vanOostdam, D.A., et al., *Apoptosis and necrosis increase antigenicity of proteins recognized by antinuclear antibodies*. *Reumatismo*, 2004. 56(3): p. 156-61.
303. Racanelli, V., et al., *Autoantibodies to intracellular antigens: generation and pathogenetic role*. *Autoimmun Rev*, 2011. 10(8): p. 503-8.
304. Grygiel-Gorniak, B., et al., *Antinuclear antibodies in autoimmune and allergic diseases*. *Reumatologia*, 2017. 55(6): p. 298-304.
305. Eppinga, H., et al., *The microbiome and psoriatic arthritis*. *Curr Rheumatol Rep*, 2014. 16(3): p. 407.
306. Vacca, M., et al., *The Controversial Role of Human Gut Lachnospiraceae*. *Microorganisms*, 2020. 8(4).
307. Wang, Y., et al., *Interleukin-21 is associated with the severity of psoriasis vulgaris through promoting CD4+ T cells to differentiate into Th17 cells*. *Am J Transl Res*, 2016. 8(7): p. 3188-96.
308. Shi, Y., et al., *IL-21 Induces an Imbalance of Th17/Treg Cells in Moderate-to-Severe Plaque Psoriasis Patients*. *Front Immunol*, 2019. 10(1865): p. 1865.
309. Huang, R.Y., Q.C. Huang, and B.M. Burgering, *Novel insight into the role of alpha-actinin-1 in rheumatoid arthritis*. *Discov Med*, 2014. 17(92): p. 75-80.
310. Ma, Y. and S. Gamagedara, *Biomarker analysis for oncology*. *Biomark Med*, 2015. 9(9): p. 845-50.
311. Smith, A.D., D. Roda, and T.A. Yap, *Strategies for modern biomarker and drug development in oncology*. *J Hematol Oncol*, 2014. 7: p. 70.

312. Ogric, M., et al., *Clinically important neutralizing anti-drug antibodies detected with an in-house competitive ELISA*. Clin Rheumatol, 2019. 38(2): p. 361-370.
313. Nash, P., et al., *Efficacy and safety of secukinumab administration by autoinjector in patients with psoriatic arthritis: results from a randomized, placebo-controlled trial (FUTURE 3)*. Arthritis Res Ther, 2018. 20(1): p. 47.
314. Bouts, Y.M., et al., *Apoptosis and NET formation in the pathogenesis of SLE*. Autoimmunity, 2012. 45(8): p. 597-601.
315. Smeenk, R.J., *Antinuclear antibodies: cause of disease or caused by disease?* Rheumatology (Oxford), 2000. 39(6): p. 581-4.
316. van der Linden, M., et al., *Neutrophil extracellular trap release is associated with antinuclear antibodies in systemic lupus erythematosus and anti-phospholipid syndrome*. Rheumatology (Oxford), 2018. 57(7): p. 1228-1234.
317. Ravindran, M., M.A. Khan, and N. Palaniyar, *Neutrophil Extracellular Trap Formation: Physiology, Pathology, and Pharmacology*. Biomolecules, 2019. 9(8).
318. Papayannopoulos, V., *Neutrophil extracellular traps in immunity and disease*. Nat Rev Immunol, 2018. 18(2): p. 134-147.
319. Steiner, G. and J. Smolen, *Autoantibodies in rheumatoid arthritis and their clinical significance*. Arthritis Res, 2002. 4 Suppl 2(Suppl 2): p. S1-5.
320. Janjumratsang, P., et al., *Positive direct immunofluorescence and autoantibody profiles in psoriasis patients*. J Dermatol, 2008. 35(8): p. 508-13.
321. Liu, R., et al., *IL-17 Promotes Neutrophil-Mediated Immunity by Activating Microvascular Pericytes and Not Endothelium*. J Immunol, 2016. 197(6): p. 2400-8.
322. Chiang, C.C., et al., *Neutrophils in Psoriasis*. Front Immunol, 2019. 10: p. 2376.
323. Stoll, M.L., et al., *Altered microbiota associated with abnormal humoral immune responses to commensal organisms in enthesitis-related arthritis*. Arthritis Res Ther, 2014. 16(6): p. 486.
324. Liu, X., et al., *Role of the Gut Microbiome in Modulating Arthritis Progression in Mice*. Sci Rep, 2016. 6: p. 30594.
325. Adak, A. and M.R. Khan, *An insight into gut microbiota and its functionalities*. Cell Mol Life Sci, 2019. 76(3): p. 473-493.
326. Wu, H.J. and E. Wu, *The role of gut microbiota in immune homeostasis and autoimmunity*. Gut Microbes, 2012. 3(1): p. 4-14.
327. Marchesi, J.R., et al., *The gut microbiota and host health: a new clinical frontier*. Gut, 2016. 65(2): p. 330-9.
328. Kim, D., S.A. Yoo, and W.U. Kim, *Gut microbiota in autoimmunity: potential for clinical applications*. Arch Pharm Res, 2016. 39(11): p. 1565-1576.
329. Lin, L. and J. Zhang, *Role of intestinal microbiota and metabolites on gut homeostasis and human diseases*. BMC Immunol, 2017. 18(1): p. 2.
330. Signoretti, M., et al., *Gut microbiota and pancreatic diseases*. Minerva Gastroenterol Dietol, 2017. 63(4): p. 399-410.
331. Douzandeh-Mobarrez, B. and A. Kariminik, *Gut Microbiota and IL-17A: Physiological and Pathological Responses*. Probiotics Antimicrob Proteins, 2019. 11(1): p. 1-10.

332. Calcinotto, A., et al., *Microbiota-driven interleukin-17-producing cells and eosinophils synergize to accelerate multiple myeloma progression*. Nat Commun, 2018. 9(1): p. 4832.
333. Zaba, L.C., et al., *Amelioration of epidermal hyperplasia by TNF inhibition is associated with reduced Th17 responses*. J Exp Med, 2007. 204(13): p. 3183-94.
334. Chiricozzi, A., et al., *Integrative responses to IL-17 and TNF-alpha in human keratinocytes account for key inflammatory pathogenic circuits in psoriasis*. J Invest Dermatol, 2011. 131(3): p. 677-87.
335. Bastian, B.C., et al., *Autoantibodies to annexins: a diagnostic marker for cutaneous disorders?* J Dermatol Sci, 1994. 8(3): p. 194-202.
336. He, S., et al., *Annexin A2 Modulates ROS and Impacts Inflammatory Response via IL-17 Signaling in Polymicrobial Sepsis Mice*. PLoS Pathog, 2016. 12(7): p. e1005743.
337. Kang, T.H., et al., *Annexin A5 as an immune checkpoint inhibitor and tumor-homing molecule for cancer treatment*. Nat Commun, 2020. 11(1): p. 1137.
338. van Genderen, H.O., et al., *Extracellular annexin A5: functions of phosphatidylserine-binding and two-dimensional crystallization*. Biochim Biophys Acta, 2008. 1783(6): p. 953-63.
339. Rodriguez-Garcia, M.I., et al., *Annexin V autoantibodies in rheumatoid arthritis*. Ann Rheum Dis, 1996. 55(12): p. 895-900.
340. Troilo, A., et al., *Intrinsic factor recognition promotes T helper 17/T helper 1 autoimmune gastric inflammation in patients with pernicious anemia*. Oncotarget, 2019. 10(30): p. 2921-2929.
341. Saini, S.S. and A.P. Kaplan, *Chronic Spontaneous Urticaria: The Devil's Itch*. J Allergy Clin Immunol Pract, 2018. 6(4): p. 1097-1106.
342. Jain, S., *Pathogenesis of chronic urticaria: an overview*. Dermatol Res Pract, 2014. 2014: p. 674709.
343. Hon, K.L., et al., *Chronic Urticaria: An Overview of Treatment and Recent Patents*. Recent Pat Inflamm Allergy Drug Discov, 2019. 13(1): p. 27-37.
344. Asero, R., et al., *Chronic urticaria: a focus on pathogenesis*. F1000Res, 2017. 6: p. 1095.
345. Bracken, S.J., S. Abraham, and A.S. MacLeod, *Autoimmune Theories of Chronic Spontaneous Urticaria*. Front Immunol, 2019. 10: p. 627.
346. Ferrer, M., *Immunological events in chronic spontaneous urticaria*. Clin Transl Allergy, 2015. 5(1): p. 30.
347. Maurer, M., et al., *Ligelizumab for Chronic Spontaneous Urticaria*. N Engl J Med, 2019. 381(14): p. 1321-1332.
348. Kolkhir, P., et al., *Autoimmune chronic spontaneous urticaria: What we know and what we do not know*. J Allergy Clin Immunol, 2017. 139(6): p. 1772-1781 e1.
349. Arm, J.P., et al., *Pharmacokinetics, pharmacodynamics and safety of QGE031 (ligelizumab), a novel high-affinity anti-IgE antibody, in atopic subjects*. Clin Exp Allergy, 2014. 44(11): p. 1371-85.
350. Hong, J.Y., et al., *Antibody to FcepsilonR1alpha Suppresses Immunoglobulin E Binding to High-Affinity Receptor I in Allergic Inflammation*. Yonsei Med J, 2016. 57(6): p. 1412-9.

351. Gasser, P., et al., *The mechanistic and functional profile of the therapeutic anti-IgE antibody ligelizumab differs from omalizumab*. Nat Commun, 2020. 11(1): p. 165.
352. Dehlink, E., et al., *A soluble form of the high affinity IgE receptor, Fc-epsilon-RI, circulates in human serum*. PLoS One, 2011. 6(4): p. e19098.
353. Vidarsson, G., G. Dekkers, and T. Rispens, *IgG subclasses and allotypes: from structure to effector functions*. Front Immunol, 2014. 5: p. 520.
354. Lin, C.Y., et al., *Elevated IgM against Nepsilon-(Carboxyethyl)lysine-modified Apolipoprotein A1 peptide 141-147 in Taiwanese with Alzheimer's disease*. Clin Biochem, 2018. 56: p. 75-82.
355. Ciccocioppo, R., et al., *Role of the advanced glycation end products receptor in Crohn's disease inflammation*. World J Gastroenterol, 2013. 19(45): p. 8269-81.
356. Yilmaz, Y., et al., *Serum levels of soluble receptor for advanced glycation endproducts (sRAGE) are higher in ulcerative colitis and correlate with disease activity*. J Crohns Colitis, 2011. 5(5): p. 402-6.
357. Schroter, D. and A. Hohn, *Role of Advanced Glycation End Products in Carcinogenesis and their Therapeutic Implications*. Curr Pharm Des, 2018. 24(44): p. 5245-5251.
358. Chervonsky, A.V., *Microbiota and autoimmunity*. Cold Spring Harb Perspect Biol, 2013. 5(3): p. a007294.
359. Giancchetti, E. and A. Fierabracci, *Recent Advances on Microbiota Involvement in the Pathogenesis of Autoimmunity*. Int J Mol Sci, 2019. 20(2): p. 283.
360. Vay, D., et al., *Antibodies against advanced glycation end product Nepsilon-(carboxymethyl)lysine in healthy controls and diabetic patients*. Diabetologia, 2000. 43(11): p. 1385-8.
361. Collins, A.M. and K.J. Jackson, *A Temporal Model of Human IgE and IgG Antibody Function*. Front Immunol, 2013. 4(235): p. 235.
362. Qiu, C., et al., *Cell-bound IgE and plasma IgE as a combined clinical diagnostic indicator for allergic patients*. Sci Rep, 2020. 10(1): p. 4700.
363. U.S. National Library of Medicine. *Study of Efficacy and Safety of CJM112 in Patients With Moderate to Severe Inflammatory Acne*. Available from: <https://clinicaltrials.gov/ct2/show/NCT02998671>.
364. U.S. National Library of Medicine. *Efficacy, Safety, and Pharmacokinetics Study of CJM112 in Hidradenitis Suppurativa Patients*. Available from: <https://clinicaltrials.gov/ct2/show/NCT02421172>.
365. Srey, C., et al., *Immunochemical and mass spectrometric analysis of Nepsilon-(carboxymethyl)lysine content of AGE-BSA systems prepared with and without selected antiglycation agents*. J Agric Food Chem, 2010. 58(22): p. 11955-61.

Curriculum Vitae Giulio Macchiarella

Education

- 2021 PhD, Autoantibodies as biomarkers in autoimmune diseases
Biozentrum University of Basel, Basel (CH)
Supervised by Dr. Alexandre Avrameas and Prof. Jean Pieters
- 2015 Master degree in Biochemical Engineering
Institut National des Sciences Appliquées (INSA) de Lyon, Lyon (FRA)
Thesis supervised by Dr. Alexandre Avrameas
- 2010 High School Diploma in Sciences
Liceo Scientifico Benedetto Croce, Palermo (ITA)

Employment

- From 2022 Group Lead, Associate Principle Scientist
Lonza, Basel (CH)
- 2021 Bioanalytical Scientist
Fresenius-Kabi, Nyon (CH)
- 2016-2020 PhD student, Autoantibodies as biomarkers in autoimmune diseases
Novartis Institute for Biomedical Research (NIBR) and Biozentrum University of Basel,
Basel (CH)
- 2015-2016 Scientific associate
Novartis Institute for Biomedical Research (NIBR), Basel (CH)